THE NOGGIN COVE FORMATION AND CARMANVILLE MELANGE: ISLAND ARC RIFTING IN NORTHEAST NEWFOUNDLAND

DENNIS HUGH JOHNSTON

The Noggin Cove Formation and Carmanville Melange: island arc rifting in northeast Newfoundland.

BY

Dennis Hugh Johnston

A thesis submitted to the School of Graduate Studies in partial fulfilment of the requirements for the degree of Master of Science

Department of Earth Science
Memorial University of Newfoundland
St. John's, Newfoundland

November 1992

ISBN 0-315-82650-9

Canada

Frontispiece

View from Noggin Hill looking out Hamilton Sound, August 1992. Woody Island is to the left; Rocky Point, White Island and Teakettle Point to the right. The town of Carmanville is in the foreground. Note the train of icebergs along the horizon. The Carmanville area is just west of the tectonic boundary between the Gander and Dunnage Zones.

The Noggin Cove Formation and Carmanville Melange: island arc rifting in northeast Newfoundland.

Abstract

The Noggin Cove Formation consists mainly of fragmental mafic volcanic rocks with subordinate pillowed basalt and black shale. Massive volcanic conglomerates and coarse sandstones, with lesser amounts of medium-bedded tuffs and lapilli breccias, dominate the fragmental rocks. Volcanic conglomerates and coarse-grained sandstones were predominantly deposited as subaqueous debris flows, some of which are spectacular in terms of their thickness and clast size.

The volume of fragmental rocks relative to basaltic lavas indicates an explosive volcanic source; ubiquitous vesicular clasts indicate shallow marine to subareal eruption. Debris flow conglomerates and sandstones dominate southern exposures but in the north they are subordinate to basaltic lavas and shallow marine deposits (highly calcareous tuffs and breccias). This distribution implies fragmental rocks were transported southward to form a marine volcaniclastic apron over pillow lavas, lava flows and basaltic dykes.

The Carmanville Melange consists mainly of sandstone, siltstone and mafic volcanic clasts and blocks in a black shale matrix. Melange is interbedded and interfolded with volcanic rocks of the underlying Noggin Cove Formation and with siltstones and sandstones of the overlying Woody Island Siltstone. In many cases, folded beds of siltstone can be seen within the black shale matrix. The melange is interpreted as olistostromal.

The Noggin Cove Formation and Carmanville Melange have undergone at least three stages of folding. D_2 deformation is the most intense, resulting in a very strong northeast trending cleavage which is axial planar to tight to isoclinal folds. Microprobe, SEM and textural analyses show that greenschist facies metamorphism and subsequent contact metamorphism have extensively altered the volcanic rocks of the Noggin Cove Formation.

Rifting is indicated by the debris flows of the Noggin Cove Formation and by olistostromes of the Carmanville Melange and Woody Island Siltstone. An arc to back-arc geochemical transition matches the stratigraphic record of rifting. The arc to back-arc succession is correlated with the Exploits and Wild Bight groups of the western Exploits Subzone.

Acknowledgements

Sincere thanks to my supervisor, Dr. Harold (Hank) Williams, for his academic guidance and financial support. His disciplined approach to geology, often tempered with a measure of music or humour, has been very instructive.

Dr. Kenneth Currie of the Geological Survey of Canada is thanked for help with amphibole classifications, providing financial and logistical support for field work and critically reviewing a paper on the Noggin Cove Formation. Dr. Toby Rivers and Dr. George Jenner were very helpful, offering academic guidance and critically reviewing my work on metamorphism and geochemistry (respectively). Dave van Everdingen and Jeroen van Gool are thanked for their "Quick Plot" program for structural data. Geoff Vienott is thanked for assistance on the microprobe, Caroline Emerson for assistance on the SEM, and Beverly Chapman for prompt return of geochemical results. Fellow graduate students are thanked for friendship, informative geology discussions and computer mini-courses.

A special thanks to the people of Carmanville, particularly Scott and Joan Hicks, and Gary, Ross and Roy Collins, for their great hospitality and humour.

Most important is a heartfelt thanks to my wife, Gretchen, for her unwavering and good-humoured support of an absentee husband.

CONTENTS

Tables

Figures

Chapter 1

Introduction

The research area is located along the southern shore of Hamilton Sound, northeast Newfoundland, centred around the towns of Noggin Cove and Carmanville (Figures 1.1 and 1.2). The highly indented shoreline affords extensive, wave-polished exposures of both the Noggin Cove Formation and the Carmanville Melange. Exposures of the Noggin Cove Formation occur inland to a maximum of approximately 4 Km (Figure 1.2). Access to these outcrops is facilitated by logging roads and All Terrain Vehicle (ATV) trails; off-road traversing is in places very difficult due to the dense spruce thicket that has grown up since the large forest fire of 1961.

1.1 Previous work in the Carmanville area.

The general format for the following section is to review how rocks of the Noggin Cove Formation and Carmanville Melange have been grouped in the past, finishing with the current classification. Until recently, these rocks have been included in groups with a northeast-southwest trend (eg. Gander Group, Davidsville Group). The significant departure in current studies is the inclusion of these units in an east-west trend

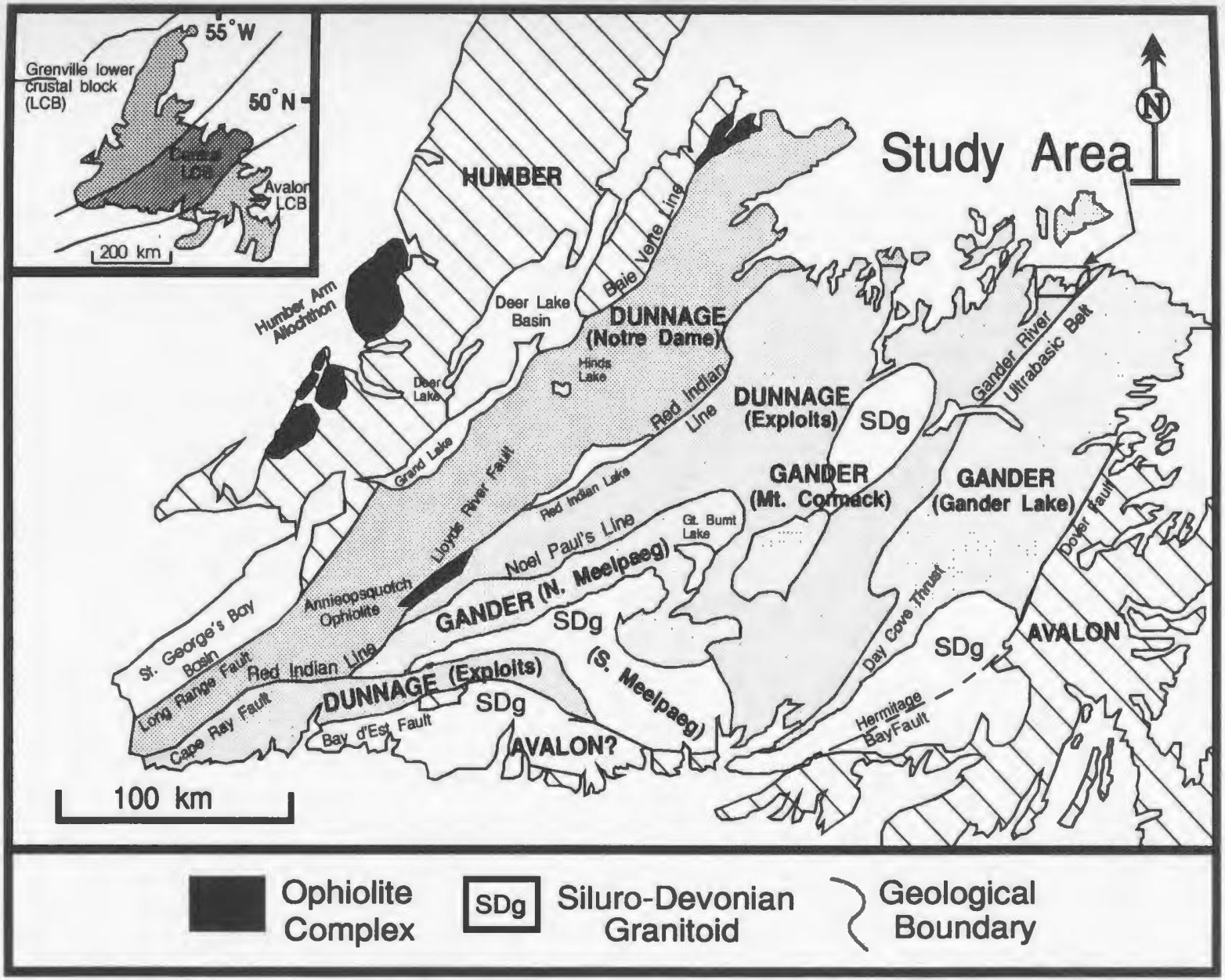

Figure 1.1: Tectonostratigraphic zones and subzones of Newfoundland. Modified from Williams et al., 1988 and Marillier et al., 1989.

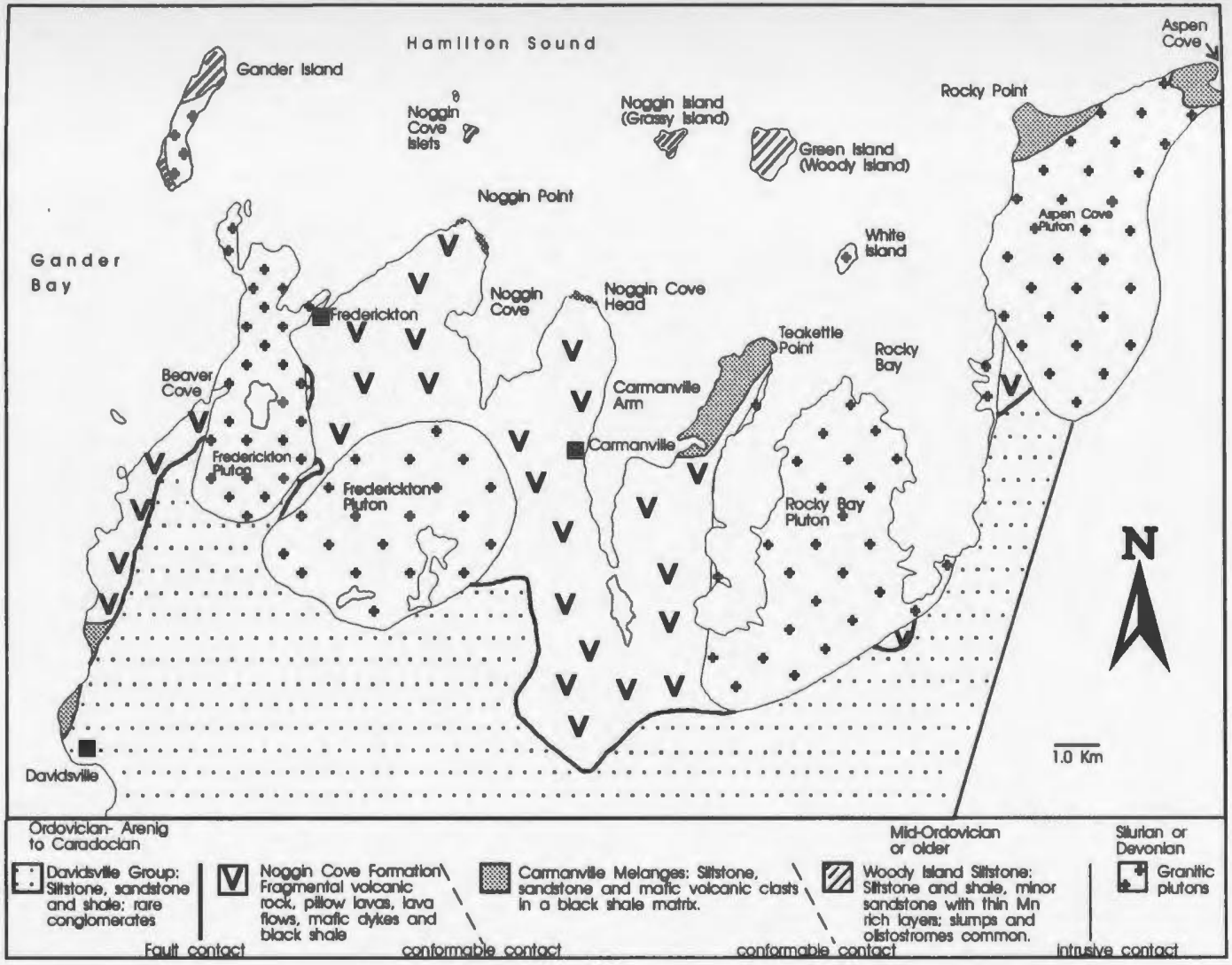

Figure 1.2: Geological sketch map of the Carmanville area. See Figure 1.1 for location.

across the northeast Exploits Subzone (Williams et al., 1991; Williams 1992; Currie 1992; Johnston 1992 and this study).

Gander Lake Series/Gander Lake Group

Following pioneer work by Jukes (1843) and Murray (1881), Twenhofel (1947) related phyllites, slates and quartzites exposed along Gander Lake (his "Gander Lake Series") to lithologically similar Silurian strata on the islands in Hamilton Sound. Jenness (1963) renamed the Gander Lake Series the Gander Lake Group, which included volcanic rock and large areas of sedimentary and metamorphic rock from Hare Bay in the east to Glenwood in the west. Jenness subdivided his Gander Lake Group into three broad lithological units: a lower unit of predominantly arenaceous rocks, a middle unit of intercalated sedimentary and volcanic rocks, and an upper unit of grey, green, red and black slates. Jenness interpreted the units as a conformable sequence that underwent eastward prograde metamorphism. Mid-Ordovician fossils were obtained from the middle and upper units. Jenness was the first to delineate the line of ultramafic lensoid bodies which extend northeast from Gander Lake to the coast, which he termed the Gander River ultrabasic belt (Jenness, 1958).

The Gander Lake Group was extended northward to the coast by Williams (1964, 1968) and included rocks from Gander Bay to the western side of Bonavista Bay. The volcanic rock and

melanges in the Carmanville area were assigned to Williams' unit 4 of the Gander Lake Group, equivalent to Jenness's middle unit (Williams, 1964; Jenness 1963).

Davidsville Group

Structural studies by Kennedy and McGonigal (1972) led to a revision of Jenness's subdivisions of the Gander Lake Group. These workers suggested the Gander Lake Group be subdivided into an eastern gneissic terrane, a central metasedimentary terrane and a western sedimentary and volcanic terrane. The Gander Lake Group was redefined to include only those rocks previously assigned to Jenness's lower unit, and excluded those rocks belonging to the gneissic terrane. The term Davidsville Group was proposed for the sedimentary and volcanic rocks overlying the redefined Gander Lake Group, equivalent to the middle and upper units of Jenness's (1963) Gander Lake Group. The volcanic rock and melanges in the Carmanville area were assigned to the lower part of the Davidsville Group. The name Gander Lake Group was changed to the Gander Group informally by McGonigal (1973), then formally proposed by Blackwood and Kennedy (1975), to address a contravention of the Code of Stratigraphic Nomenclature noted by Bruckner (1972).

Rocks of the Davidsville Group, with a single penetrative cleavage axial planar to folded beds, were separated from the

underlying polydeformed Gander Lake Group by an inferred major angular unconformity (Kennedy and McGonigal, 1972). Blocks in the Carmanville Melange more deformed than the host matrix were presumed to be derived from the underlying Gander Group, polydeformed during the Late Precambrian "Ganderian Orogeny". Incorporation of the polydeformed blocks was interpreted as the result of submarine gravity slides related to syndepositional faulting or due to overthrusting of unconsolidated sedimentary and volcanic rock (Kennedy, 1975).

Carmanville Ophiolitic Melange

Volcanic rocks and melange in the Carmanville area were interpreted as components of an ophiolitic melange in studies that stemmed from mapping of the Carmanville map sheet (2E/8; 1:50.000) by the Geological Survey of Canada in the late 1970's (Currie and Pajari, 1977; Pajari and Currie, 1978; Pickerill et al., 1978; Pajari et al., 1979). Currie and Pajari (1977) saw no evidence of Kennedy's structural contrast between the Gander and Davidsville Groups and according to these authors the Gander-Davidsville contact was conformable. Pickerill et al. (1978) recognized significant regional metamorphism in Davidsville Group rocks, comparable to that seen in Gander Group rocks; seeing no structural or metamorphic contrasts between the Gander and Davidsville Groups, these authors rejected the "Ganderian orogeny" of

Kennedy (1975). According to Pajari and Currie (1978), the polydeformed blocks in the Carmanville Melange (of Kennedy and McGonigal, 1972) were actually typical of a unit of the Davidsville Group, deformed by soft rock deformation.

Pajari et al. (1979) interpreted volcanic rocks in the Carmanville area and along the east shore of Gander Bay as kilometre scale rafts in an ophiolitic melange; the term Carmanville ophiolitic melange was introduced, its boundaries defined by the "geographic extent of the matrix horizons". Defined in this way, the research area for this study is entirely within the Carmanville ophiolitic melange. The melange consisted of sedimentary, mafic and ultramafic olistoliths in a matrix of black shale and silt. The Carmanville ophiolitic melange was interpreted to be the result of large submarine gravity slides as oceanic crust, obducted southeast onto the toe of the continental rise prism, became unstable and collapsed northwestward. This obduction and subsequent collapse only interrupted sedimentation locally (ie: where the ultramafic rocks are now present). Elsewhere, deposition of sediments, which included a distinctive quartz-rich continentally derived component, was continuous from pre-Ordovician through the Ordovician and possibly into the Silurian. These authors "tentatively" correlated the Carmanville Ophiolitic Melange with the Dunnage Melange to the west and related both to obduction of ocean floor and island

arc toward the southeast onto an accreting continental rise during the mid-Ordovician.

Pickerill et al. (1981) described the primary sedimentation history and depositional environment of the volcanic and volcaniclastic rocks in the Carmanville area. The volcanic rock was originally deposited on the slopes of an oceanic island. Four volcaniclastic facies were recognized, which represented resedimentation of shallow marine mafic fragmental rock into a deeper water environment characterized by massive and pillowed lavas, associated hyaloclastics, and minor carbonate. Resedimentation was by debris flows, turbidity currents and possibly fluidized sediment flows.

Karlstrom et al. (1982) described the structural features from New World Island in the west to the islands in Hamilton Sound in the east; this study also included observations from the east side of Gander Bay. These workers detailed three stages of folding. All deformations are recorded in rocks ranging in age from Ordovician to Middle Silurian (Llandoverian-Wenlockian). F_1 folds are recumbent, related to F_1 macroscopic thrust faulting. This macroscopic thrusting, in conjunction with Silurian-Devonian thrusting documented elsewhere in the Dunnage Zone, implied major portions of the Dunnage Zone may be allochthonous. The strong northeast trending cleavage that dips steeply to the southeast is axial planar to strongly asymmetric, en echelon, F_2 folds.

Repetition of rocks of low metamorphic grade and of the same formation across the area (eg. Caradocian shale), and the absence of rocks from deeper crustal levels, indicate the enveloping surface for the F_2 folds is relatively narrow and has a shallow dip. Hence, the Carmanville Melange can be correlated with the Dunnage Melange (in agreement with Pajari et al., 1979) and other melanges in the area. F_2 folds are offset by F_3-related high angle faults (eg Chanceport, Lukes Arm, Dildo, and Reach Faults). F_3 stuctures kink and fold the regional S_2 cleavage and are not important in the overall distribution of rock units in the area.

Williams (1983) examined the melange on Woody Island and concluded that the cleavage and associated folding in the melange were second generation structural features and are thus the product of hard rock deformation; this interpretation is at variance with an earlier interpretation (Pajari et al., 1979) which favored soft sediment deformation. Williams (1983) presents microstructural observations which show the S_2 cleavage post-dates peak metamorphism. A distinctive "melange dyke" (see Fig. 3.1f), previously attributed to the migration of a thixotropic melange "bed" (Pajari et al., 1979), is also a post lithification feature which Williams (1983) attributes to faulting and metamorphic differentiation.

Gravity and aeromagnetic data obtained in the

Carmanville area- from the east shore of Gander Bay to Aspen Cove and from Gander, Woody, and Green Islands in Hamilton Sound- is included in Miller's (1988) interpretation of gravity and aeromagnetic data from the northeast Gander Zone. The principal result of this study was the delineation of mafic to ultramafic bodies at shallow depths within the Gander Zone east of the GRUB Line. Hence, the GRUB Line is not the most eastward extent of mafic-ultramafic complexes nor is it the sole thrust which transported Dunnage Zone rocks eastward over Gander Zone rocks. This interpretation supports Wonderley and Neuman's (1984) suggestion that Dunnage Zone rocks were thrust eastward over the Gander Zone; this model was invoked to explain the outlier of Dunnage Zone rocks overlying Gander Zone rocks at Indian Bay Big Pond. Others argue that the contact is conformable, requiring that deposition of the Dunnage Zone rocks must have occurred beyond the eastern limits of allochthon transport (eg. Williams and Piasecki, 1988).

The idea of an allochthonous Dunnage Zone above the Gander Zone is supported by other studies in central and southern Newfoundland (Colman-Sadd and Swinden, 1984; Piasecki, 1988; Williams et al., 1989; Piasecki et al., 1990; Williams and Piasecki, 1990 ; Colman-Sadd et al., 1992) and from Lithoprobe seismic results (Keen et al., 1986; Marillier et al., 1989). Williams et al. (1991) advocate both a

structural and stratigraphic break across the contact between the Gander and Davidsville groups southeast of Carmanville.

Noggin Cove Formation\Carmanville Melange

A conceptual link between the Carmanville Ophiolitic Melange and the GRUB Line (Pajari et al., 1979) was challenged by Williams et al. (1991) on the grounds that the Carmanville Melange is a local feature whereas the GRUB Line is a regional feature. In addition, ultramafic blocks are rare or absent in the Carmanville Melange. Williams et al. (1991) proposed a redefinition and changed the name Carmanville Ophiolitic Melange (Pajari et al., 1979) to Carmanville Melange. The volcanic rocks in the Carmanville area were omitted from the melange, considered a separate entity of formational status and assigned to the Noggin Cove Formation. The Carmanville Melange includes only melange that occurs at the periphery of the Noggin Cove Formation. The Noggin Cove Formation was interpreted as structurally overlying the Carmanville Melange and its emplacement may have controlled melange formation.

Williams et al. (1991) also proposed that thin-bedded shales and sandstones with thin manganese-rich layers that occur on the islands north of Carmanville in Hamilton Sound (Noggin Cove Islets, Noggin Cove Island and Green Island) and at Ladle Cove are distinct from, and should not be included with, Davidsville Group sedimentary rocks that occur south of

the Noggin Cove Formation. At low metamorphic grade, coticules (thin strands and nodules of spessartine garnet and quartz) develop in manganese-rich siltstones and shales. Coticules occur stratigraphically with the Carmanville Melange on Woody Island and with the Noggin Cove Formation at Beaver Cove.

Williams (1992) also recognized the distinctive coticule lithology in bedded sedimentary rocks associated with the Dunnage and Dog Bay melanges. In the Dunnage Melange, coticules occur locally in bedded sections or are completely disrupted and form melange matrix (Hibbard and Williams, 1979). Because of the distinct occurrence of the coticule lithology with the Carmanville, Dog Bay and Dunnage melanges, Williams (1992) proposed a correlation of these units across the northeast Exploits Subzone from Ragged Harbour in the east to Lewisporte in the west. Currie (1992) expanded on this correlation and proposed that the Exploits Group could be matched unit by unit to a succession of lithologies in the Hamilton Sound/Gander Bay area. This study also proposes correlation of the Noggin Cove Formation and Carmanville Melange westward to units of the Exploits, Summerford and Wild Bight Groups (see Chapter 6).

1.2 General Geology

Regional tectonic setting

The Noggin Cove Formation and Carmanville Melange are within the Exploits Subzone of the Dunnage Zone (see Figure 1.1; Williams et al., 1988). Rocks of the Dunnage Zone are of oceanic affinity and represent vestiges of a former ocean ("Iapetus") which separated Laurentia from Gondwana during the late Cambrian and early Ordovician. Rocks of the bordering Humber and Gander zones are of continental affinity and are representative of the continental margins of Laurentia and Gondwana that flanked this ocean. The Exploits Subzone of the eastern Dunnage is distinguished from its western counterpart, the Notre Dame Subzone, on the basis of differences in stratigraphy, structure, fauna, plutonism, Pb isotopes in mineral deposits and geophysical anomalies. The subzones are separated by a major fault, the Red Indian Line (Figure 1.1). The favored model at present involves tectonic transport of the subzones over their respective continental margins with the destruction or closure of Iapetus (see Williams et al., 1988).

The Gander Zone is composed of continentally derived metasedimentary rock. Three subzones are distinguished primarily on the basis of geographic separation. The type area is at Gander Lake within the Gander Lake Subzone. The Mount

Cormack and Meelpaeg subzones occur as structural inliers within the Exploits Subzone (see Figure 1.1; Williams et al., 1988).

The Noggin Cove Formation and Carmanville Melange occur at the northeastern margin of the Exploits Subzone just west of the Gander River Complex (O'Neill and Blackwood, 1989), formerly the Gander River ultrabasic belt (Jenness, 1958) or GRUB Line (Blackwood, 1980), the zonal boundary between the Exploits and Gander Lake Subzones (Figure 1.1).

Carmanville area

The Noggin Cove Formation consists almost entirely of mafic volcanic and volcaniclastic rock. Massive conglomerates predominate; lesser amounts of pillow lavas, lava flows, mafic dykes, bedded tuffs, and lapilli breccias also occur. The largest occurrence extends from Middle Arm west-northwest to the town of Frederickton (Figure 1.2). A separate large occurrence of the Noggin Cove Formation occurs along the east side of Gander Bay, from Beaver Cove in the north to Davidsville in the south. Inland exposures are fairly extensive as the volcanic rock is resistant and forms prominent hills, knolls and distinctive rouche moutonnees.

The Carmanville Melange occurs in association with the Noggin Cove Formation and consists of outsized blocks of sandstone, siltstone, mafic volcanic rock, trondhjemite and

limestone in a homogenized, silty, black shale matrix. The best exposures of the melange occur at Rocky Point, Teakettle Point, on Woody Island and in Davidsville (Figure 1.2). Smaller outcrops occur along the shorelines from Carmanville to Frederickton and from Beaver Cove to Lower Island.

The age of the Noggin Cove Formation and Carmanville Melange is poorly constrained. Faunal or radiometric ages are yet to be obtained from either unit. Regional relationships suggest a Middle-Ordovician or older age (Williams 1992; Johnston 1992 and this study).

South of the Noggin Cove Formation, siliceous sedimentary rocks of the Davidsville Group extend southwest to Gander Lake and beyond. In the Carmanville area, the Davidsville Group is dominated by fine- to medium-bedded sandstones, siltstones and shales. Regionally, the Davidsville Group is more heterogeneous and includes all sedimentary rocks which unconformably overlie the Gander Group. The Davidsville Group ranges in age from late-Arenig (Weir's Pond; O'Neill, 1991) to Caradocian. Caradocian graptolites occur in a black shale near Davidsville (Williams, 1964).

On the islands just north of Frederickton and Carmanville (Noggin Cove Islets, Grassy Island and Woody Island) siltstones and shales have distinctive coticule layers and nodules. This unit extends westward to Dog Bay Point and eastward to Ladle Point (Woody Island Siltstone of Currie,

1992). It has been correlated with coticule rocks that occur in the Dunnage Melange and assigned a Middle-Ordovician or older age (Williams, 1992).

Granitoid plutons, interpreted as Silurian (Pajari and Currie, 1978; Currie, 1992), are extensive in the Carmanville area (Figure 1.2). The Aspen Cove pluton consists of biotite-muscovite quartz monzonite and truncates the Noggin Cove Formation east of Rocky Bay. The Rocky Bay and Frederickton plutons consist of quartz-plagioclase-biotite tonalite with large poikilitic biotite (Currie, 1992); these intrusions separate the Noggin Cove Formation into three distinct occurrences: along the east side of Gander Bay, from Frederickton to Rocky Bay, and a small occurrence on the east side of Rocky Bay. The plutonic rocks weather recessively and form shallow bays, tickles, ponds and bogs. Felsic dykes related to these plutons are common in the Noggin Cove Formation.

Rocks in the Carmanville area have a strong northeast trending cleavage which dips steeply to the southeast. Elongate clasts in conglomerates are oriented with this cleavage and bedding is commonly parallel to sub-parallel with cleavage. This cleavage is axial planar to open to isoclinal folds with northeast plunges that vary from 0 to 90°. Granitic rock of the Aspen Cove, Rocky Bay and Frederickton plutons cut the cleaved and folded rocks.

1.3 Purpose and scope of this study

This is a multidisciplinary examination of the sedimentology, structure, petrology, metamorphism, and geochemistry of the Noggin Cove Formation and its relationships to surrounding units. Because the Carmanville Melange is intimately related to the Noggin Cove Formation, it is also described, but in less detail.

The account concludes with a paleotectonic model for the Noggin Cove Formation and Carmanville Melange and regional correlations and comparisons with other volcanic/melange units of the Exploits Subzone. The implications of this study also bear upon Gander Zone/Dunnage Zone interactions.

Chapter 2

Noggin Cove Formation

2.1 Introduction- Nomenclature, distribution and thickness

The name Noggin Cove Formation was introduced for two large discrete areas of mafic volcanic rock which outcrop in the Carmanville area and along the eastern shore of Gander Bay (Williams et al., 1991). The Noggin Cove Formation, known previously as the Carmanville volcanics (Pickerill et al., 1981), consists of pillow lavas, lava flows, mafic dykes, volcaniclastic conglomerates and sandstones, fine- to coarse-grained bedded tuffs, lapilli breccias and minor black shale.

Discrete occurrences of the Noggin Cove Formation, probably once continuous, are now separated by plutons. The largest and most continuous occurrence of the Noggin Cove Formation extends from Middle Arm in the east to Frederickton in the west (Figure 2.1 and accompanying map in the back cover). The Frederickton Pluton omits a large portion of this occurrence of the Noggin Cove Formation southwest of Noggin Cove and isolates a separate occurrence of the Noggin Cove Formation which outcrops along the east side of Gander Bay from Beaver Cove south to Davidsville. Along the southern

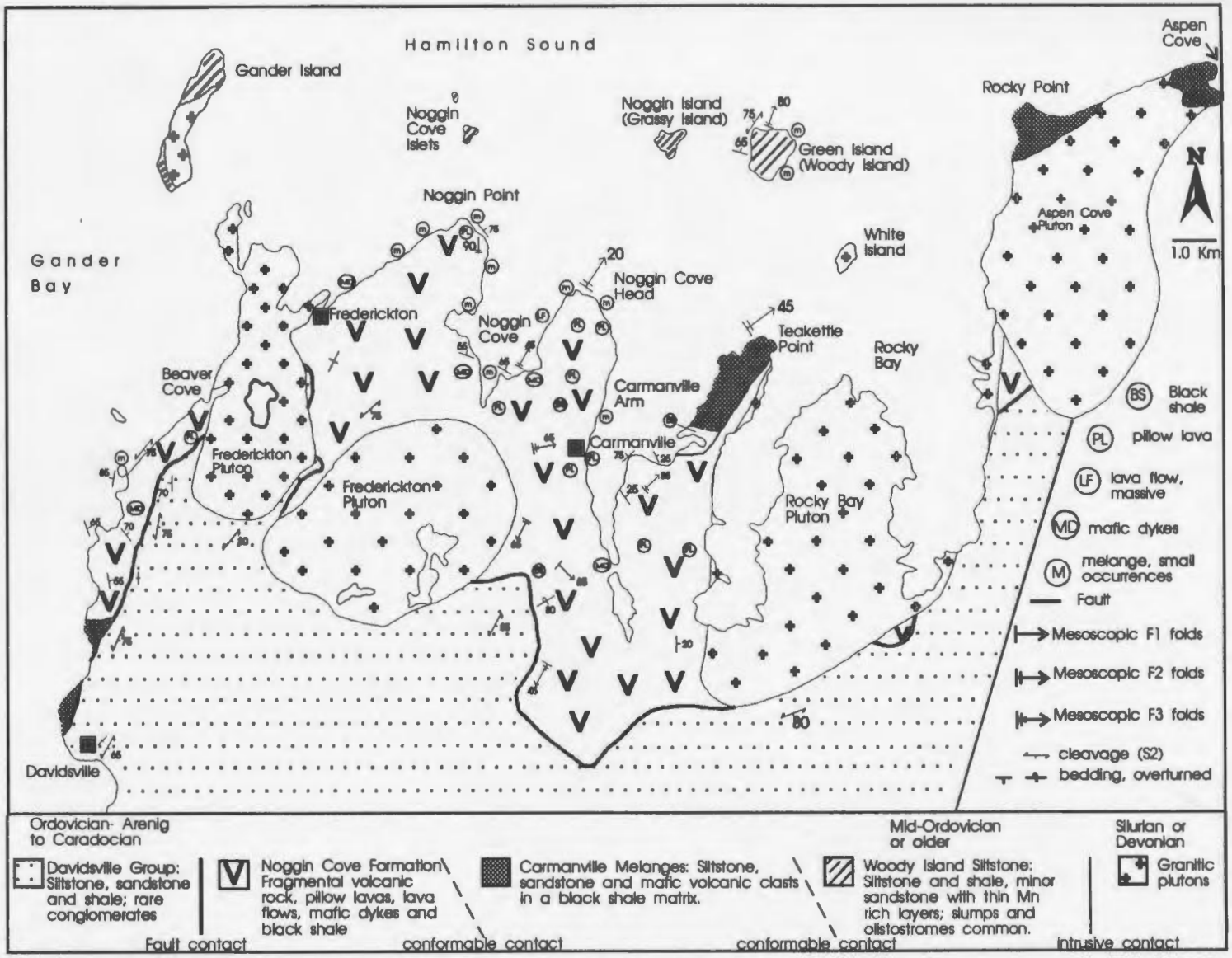

Figure 2.1a: Geological sketch map of the Carmanville area. See Figure 1.1 for location.

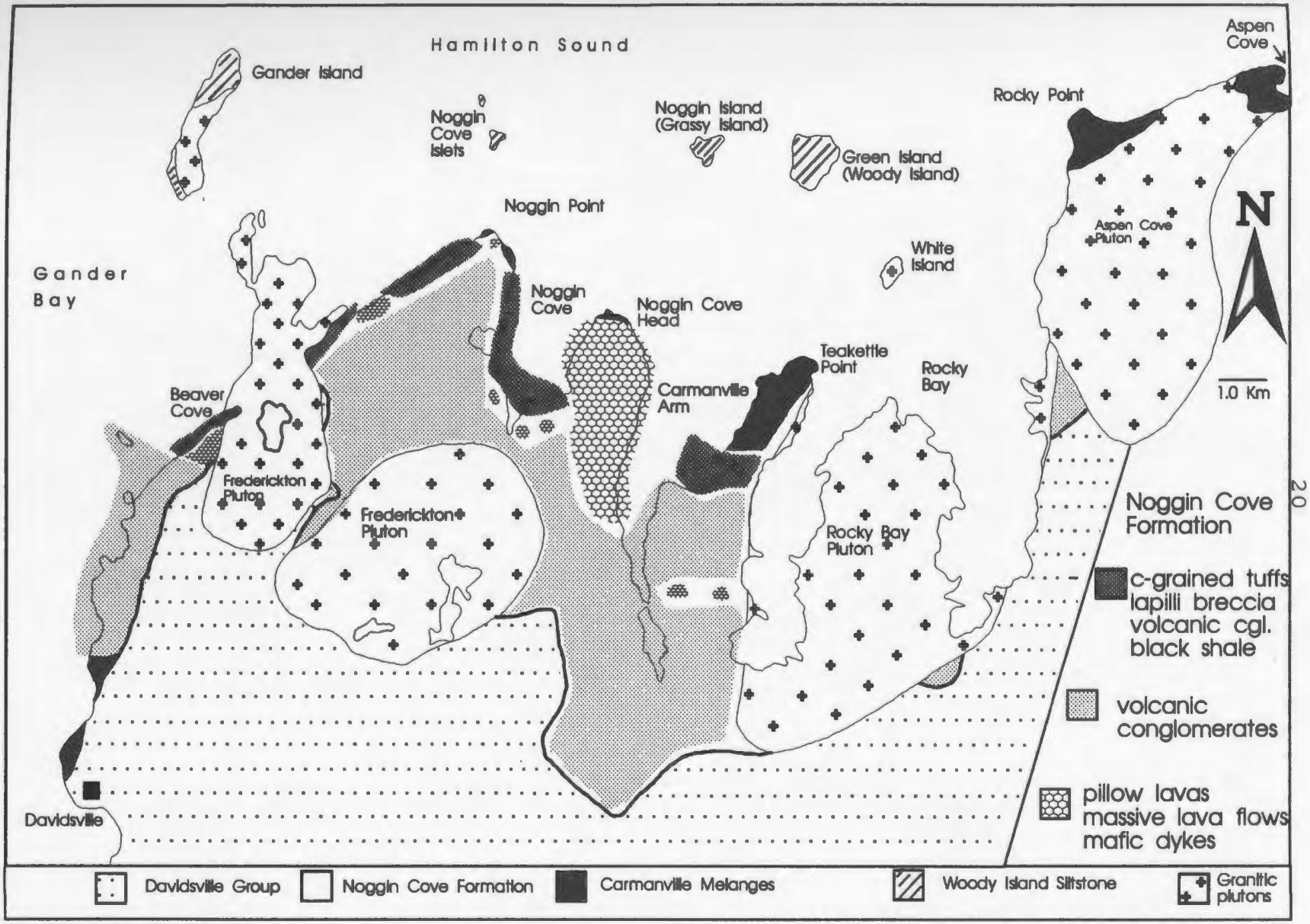

Figure 2.1b: Gross distribution of lithologies of the Noggin Cove Formation. The Carmanville Melange also occurs interbedded with the coarse-grained tuff unit of the Noggin Cove Formation.

margin of these occurrences, the Noggin Cove Formation is in contact with sedimentary rocks of the Davidsville Group; the shorelines of Gander Bay and Hamilton Sound, from Davidsville to Carmanville South, form the northern margin.

The easternmost exposures of the Noggin Cove Formation occur along the east side of Rocky Bay. Here it is cut by the Aspen Cove Pluton to the north and east, cut by the Rocky Bay Pluton to the west, and in contact with sedimentary rocks of the Davidsville Group to the south. This small occurrence, and small isolated occurrences south of Eastern Arm and Middle Arm, indicate the Rocky Bay pluton has omitted a large portion of the Noggin Cove Formation in this area.

The thickness of the Noggin Cove Formation cannot be estimated as neither its base or top is defined. Basal contacts of pillow lavas are not exposed. Beds of the Noggin Cove Formation volcaniclastic rocks are commonly steep and tightly folded. In southern exposures, opposing dip and facing directions in volcanic conglomerates, that do not vary across strike, suggest a shallow enveloping surface for the folded beds. This implies a minimum thickness in the order of 100's of metres. Volcanic conglomerates are interbedded with a variety of lithologies in northern exposures, indicating the thickness of the conglomerates decreases northward.

2.2 Lithologies and stratigraphy

Lithologies

The different lithologies of the Noggin Cove Formation will be discussed in the order of their relative abundance. The conglomerates account for approximately 65-75% of exposures and will therefore be discussed in more detail than other lithologies. Pillow lavas, massive lava flows and basaltic dykes account for approximately 10-15% of exposures, bedded tuffs ≈10%, lapilli breccias ≈5% and black shale < 5%.

Volcanic conglomerates

Conglomerates form almost all of the southern exposures of the Noggin Cove Formation. A basaltic dyke that cuts volcanic conglomerates at Beaver Hill is the only exception. Farther north, conglomerates are subordinate to mafic lavas, bedded tuffs and breccias (Figures 2.1b and 2.5).

Thicknesses of the conglomerate beds range as high as 15 metres, but generally are from 1 to 10 m. Beds are usually unsorted, but in some cases a basal zone of crude reverse grading is capped by a thicker upper zone of normal grading. In the thicker beds, a lower-central, very coarse zone of large, rounded vesicular blocks grades into an upper thicker section of very coarse- to coarse-grained volcanic sandstone. Facings in many of these conglomerate beds were validated by

cross-bedding, scours, and grading in adjoining beds of fine to medium bedded tuffs. Good exposures of thick conglomerate beds with the above features occur 1 Km west, and 1.5 Km southwest, of the head of Carmanville Arm.

The bottom contacts of the beds are commonly planar, even where conglomerate overlies very fine tuffs. This is likely related to coarse-grained sandstones dominating the lowermost portion of the beds. Parallel lamination of coarse-grained sandstones occurs in the upper and lower parts of some conglomerate beds. The long axis of ellipsoidal clasts commonly are oriented parallel to the contacts. In some conglomerates, clasts form crude bed-parallel layers and in rare cases are imbricated.

A salient feature of the volcanic conglomerates is the monomictic basaltic composition of the clasts. Clasts are predominantly vesicular to amygdaloidal; vesicle diameters are highly variable to a maximum of 7 mm. Non-vesicular clasts are less common and are presumed to be derived from basaltic pillow lavas.

Smaller clasts (< 30cm) are the most common and are generally sub-angular to sub-round but larger sub-round blocks, up to .60 m. in diameter, are not uncommon. Large isolated volcanic clasts commonly occur in the coarse-grained volcanic sandstone which dominates the upper portion of the conglomerate beds. Typical volcanic conglomerates of the

Noggin Cove Formation are shown in Figures 2.2a, b, and c. In rare cases, clasts are rimmed by a very fine tuff which resembles the matrix of the conglomerates (Figure 2.2d).

Clasts of bedded tuffs and massive conglomerates are common. Spectacular outsize clasts are more rare. The best example of outsized clasts (to 5 m.) of folded, medium bedded tuffs occur along the east shore of Gander Bay, 1 km. north of Davidsville (Figure 2.2e). A smaller bedded clast (0.3 m. x 1.5 m.) occurs in a volcanic conglomerate 1 km. south-southeast of Frederickton. Chaotic folding and contortion of the beds indicates soft sediment deformation.

Outsized clasts (to 9 m. in diameter!) of massive conglomerates can best be seen at low tide along the Carmanville South shoreline just south of Tucks High Point and on the west slope of the prominent ridge which overlooks this area (Figure 2.2f). Other less spectacular occurrences are along the Carmanville shoreline 1 km. from the head of Carmanville Arm, 0.5 km. southwest of the head of Carmanville Arm, and along the Gander Bay shoreline near Lower Island.

Clasts are supported in a fine to coarse tuffaceous matrix; only rarely are the conglomerates clast supported. In many cases, large, vesicular, sub-rounded blocks are isolated in the fine to coarse tuffaceous matrix. Within some beds (eg. Carmanville South), there is chaotic juxtapositioning of clast-rich conglomerate with more matrix-rich conglomerate.

Figure 2.2a: Clast-rich unsorted volcanic conglomerate of the Noggin Cove Formation, top of prominent knoll, southwest corner of Noggin Cove. The light brown matrix is predominantly very fine- to fine-grained. Note the angularity of the clasts and the size of the volcanic block under the hammer.

Figure 2.2b: Matrix-rich volcanic conglomerate of the Noggin Cove Formation, town of Noggin Cove. As in figure 2.2a, note the light brown colour of the matrix, which contrasts sharply with the light green colour of the clasts.

Figure 2.2c: Volcanic conglomerate of the Noggin Cove Formation, west shoreline of Noggin Cove. Note both the size and abundance of vesicles in the volcanic blocks. The strong S_2 cleavage (parallel to the hammer) appears to have deformed the blocks to the right and left of the hammer into similar shapes. Many of the vesicles are elongate in this strong cleavage; this is most obvious in the elongate clast flattened into the cleavage in the lower right area of the photograph.

Figure 2.2d: Volcanic conglomerate of the Noggin Cove Formation, 250 metres southwest of the town of Noggin Cove. The prominent clast in the centre of the photograph is rimmed by a very fine tuff similar to the matrix of the conglomerate. Note the black pen hiding in the shadow to the right of the clast.

Figure 2.2e: Outsized, medium bedded blocks in a volcanic conglomerate of the Noggin Cove Formation, along the shoreline 2 km north of Davidsville. Note the small block under the hammer in the center of the photo. A much larger block dominates the upper portion of the photograph.

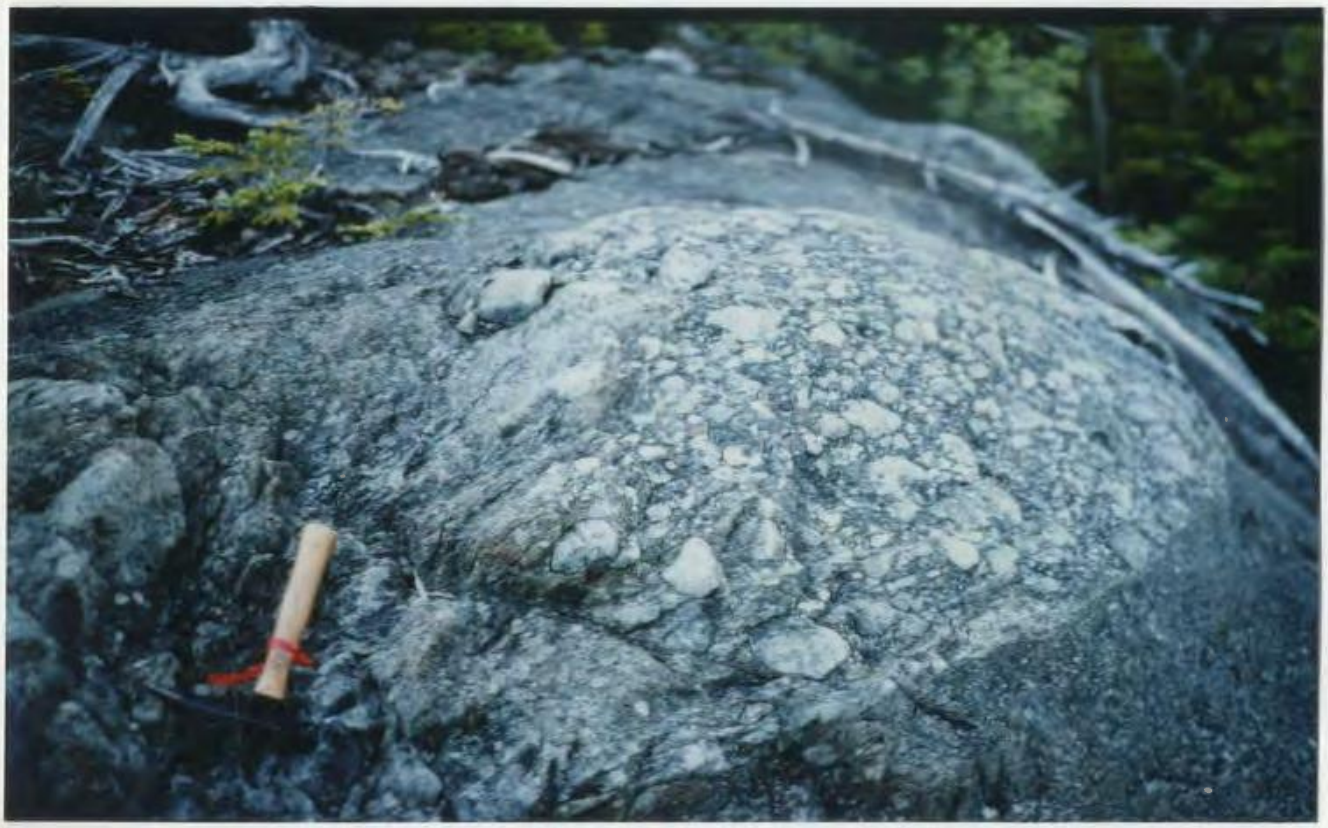

Figure 2.2f: Large block of clast-rich, massive volcanic conglomerate in a more matrix-rich volcanic conglomerate, Noggin Cove Formation. Note the curious teardrop shape of the block. Location: west slope of large hill overlooking Carmanville South.

Figure 2.2g: Highly calcareous medium-bedded tuffs, Noggin Cove Formation, southeast shoreline of Noggin Cove. Cross-bedding nearby indicates beds are right way up. Pitted surface (below coin and at top of photograph) results as limestone erodes from the top of the beds .

Interpretation:

The following features of the coarse conglomerates suggest most were deposited as subaqueous debris flows:

-lack of sorting,
-common occurrence of large isolated blocks,
-clasts rimmed with matrix,
-chaotic juxtapositioning of clast rich and more matrix rich conglomerates in some beds,
-parallel lamination in coarse-grained sandstone,
-outsized clasts of bedded tuff and massive conglomerate,
-high ratio of bed thickness to maximum clast size,
-narrow zone of reverse grading at the base of beds,
-thick cap of sandstone gradational with the underlying conglomerate.

A very viscous matrix with plastic behavior is common for debris flows (Fisher, 1984). The viscosity and plasticity can be likened to that of toothpaste or wet concrete. The plastic behavior of debris flows is a function of the high concentration of particles relative to entrained water and the abundance of fine versus coarse grained sediments. A small percentage (< 10%) of clay-size particles can have a large

effect on reducing turbulence (Hampton, 1972). A highly viscous matrix explains the lack of sorting, the occurrence of large isolated blocks, and clasts rimmed by matrix. Highly viscous debris flows are known to terminate in an abrupt manner ("freeze"; Fisher, 1984). This could explain the chaotic juxtapositioning of clast rich and more matrix rich conglomerates in some beds.

Parallel laminated sandstones at the base and top of some conglomerate beds indicate laminar flow. The massive central portions of debris flows can be transported largely intact (as a "plug") over basal laminar underflow (Hampton, 1972). This could explain the occurrence of outsized clasts in the conglomerates. Non-erosive basal contacts also suggest laminar flow.

The bed thicknesses are commonly 5 to 10 times the maximum fragment size for these debris flows. This suggests the debris flows were subaqueous as opposed to subareal; bed thicknesses of subareal debris flows are only 2 to 4 times the maximum fragment size (Fisher, 1984). Subaqueous debris flow deposits are capped by massive coarse grained sandstone which is gradational with the underlying conglomerate; in high-concentration flows there is inverse grading in a narrow zone at their base (Fisher, 1984). Both these features are common in conglomerate beds of the Noggin Cove Formation.

Pillow lavas, lava flows and mafic dykes.

Basaltic pillow lavas, lava flows, and mafic dykes are largely confined to the northern exposures of the Noggin Cove Formation (Figure 2.1b; Appendix I). The most extensive and largest outcrops of pillow lava occur from Noggin Hill southward into Carmanville and southwest into the town of Noggin Cove. Isolated smaller exposures occur just south of Beaver Cove, at Noggin Point, and in the hills east of Carmanville South.

The dark green basaltic pillows are generally 0.2 to 0.3 m. in diameter but can be as large as 0.5 m. in diameter. Rare, small amygdules were observed in thin section, but in general the pillow lavas are non-amygdaloidal. Most pillows are rimmed by dark selvages. Trondhjemites intrude pillow lava at Noggin Cove Head and along the Carmanville shoreline.

A massive, basaltic lava flow, along the west shore of Noggin Cove Head, is also non-amygdaloidal and is presumably associated with the large pillow lava occurrence just east at Noggin Hill. Trondhjemite also intrudes this lava flow.

Small mafic dykes occur at Beaver Hill, in Frederickton, in Noggin Cove, and at the head of Carmanville Arm. Mafic dykes cut the lava flow, pillow lavas and volcanic conglomerates. A larger dyke of picrite basalt which cuts conglomerates east of Noggin Cove is very distinct from the other mafic dykes both in appearance and mineralogy. The light

green weathered surface of the rock is highly pitted due to the preferential weathering of serpentinized olivine grains and is cross-cut by a network of very light green to white veinlets of antigorite (for petrology and chemical composition, see Chap. 5).

Medium bedded tuffs

Minor, medium bedded, fine- to medium-grained tuffs are largely confined to southern exposures of the Noggin Cove Formation, interbedded with the debris flows. Partial Bouma sequences, variably composed of normally graded, parallel-, and cross-laminated deposits (a-c divisions), indicate deposition by turbidity currents. The lack of intervening mudstone layers (divisions d and\or e) indicates deposition occurred at proximal to medial distances from the source. Reverse grading capped by normal grading in some beds suggests turbidity currents were highly concentrated, similar to the debris flows described above. Massive, pebbly coarse-grained sandstone beds, up to 1 m. thick, may have been deposited as highly concentrated turbidity currents or as small debris flows.

Medium bedded, coarse grained tuffs, that occur only in Noggin Cove (Figure 2.2g) and Noggin Point, are highly calcareous and locally exhibit low to high angle cross-bedding, indicating deposition in a shallow marine setting.

Breccias

Lapilli breccias are confined to northern exposures of the Noggin Cove Formation; small outcrops of the breccia occur in the cove at Frederickton, at Noggin Point, on the southeastern shore of Noggin Cove, at Rocky Point, and in a large roadcut between Carmanville and Noggin Cove. The lapilli breccias consist of very angular, dark basaltic clasts in a limestone matrix. The limestone weathers preferentially resulting in a very jagged, scoria-like surface.

A chaotic breccia of finely bedded siltstone clasts in a limestone matrix is interbedded with lapilli breccia at Noggin Point and on the southeastern shore of Noggin Cove. The angularity of the clasts and the high proportion of limestone matrix in these breccias suggest deposition occurred in a very proximal marine setting.

Black shale

Minor occurrences of black shale are interbedded with volcanic conglomerates at a roadcut near the western turn-off to Carmanville, on the east side of the small pond between Carmanville and Noggin Cove, and along the southeast shoreline of Noggin Cove.

These small occurrences of graphitic, pyritic black shale are strongly deformed. Weathered surfaces have a strong rust stain. This black shale resembles the matrix to the

Carmanville Melange but does not contain any clasts and is not homogenized.

Stratigraphy

A difficult stratigraphic relationship to define is between the pillow lavas and the volcanic conglomerates. Although commonly in contact, the conglomerates are generally massive and the pillow lavas lack reliable way-up indicators.

Massive volcanic conglomerates drape pillow lavas at two separate roadcuts in Noggin Cove and at the top of the hill overlooking the Carmanville South turn-off. Due to limited exposure, facing directions could not be determined in either the pillows or the massive conglomerates and it is possible that the rocks are overturned. On the hilltop overlooking the Carmanville South turn-off, the interfingering of pillow lava and volcanic conglomerate indicate deposition of this conglomerate was contemporaneous with formation of the pillows. Pillow lava exposed 1 km. east of the head of Carmanville Arm is separated from flat-lying, right-way-up, medium-bedded fine-grained tuffs and volcanic conglomerates by 2 to 3 metres of cover. These observations suggest the conglomerates cverlie the pillow lavas.

Non-vesicular clasts and blocks are common in the volcanic conglomerates are almost certainly derived from the fragmentation of pillow lavas and lava flows. In many cases,

large clasts are pillow shaped. Again, this suggests the comglomerates overlie the pillow lavas and lava flows.

Southern exposures of the Noggin Cove Formation are dominated by monotonously similar volcanic conglomerates, in places interbedded with fine-grained, medium-bedded tuffs. The stratigraphy is far more varied in northern exposures, where conglomerates are variably interbedded with coarse-grained medium-bedded tuffs, lappilli breccias, and black shale (eg. shoreline of Noggin Cove; Figure 2.1b). Beds consistently face north on north plunging F_2 folds along the northern shoreline from Frederickton to Carmanville South indicating these lithologies are stratigraphically above the volcanic conglomerates. This is supported by a predominance of north facings in the volcanic conglomerates to the south.

2.3 Provenance

The Noggin Cove Formation is dominated by fragmental volcanic rock. Most evidence indicates a northern source for these sedimentary rocks.

On the southeast shoreline of Noggin Cove, a south to southwest paleo-flow direction is indicated by imbricated clasts in bedded tuffs. Debris flow conglomerates dominate southern exposures of the Noggin Cove Formation but to the north are subordinate to basaltic lavas, mafic dykes, medium

bedded tuffs, and lapilli breccias (Figure 2.1b). Pillow lavas and massive lava flows are found only to the north. The north versus south distribution of debris flow conglomerates and lavas strongly suggest the eroding volcanic edifice was to the north.

The vesicular clasts of the volcanic conglomerates indicate that the volcanic source was subareal to shallow submarine (less than 200 m. below water level; Fisher, 1984). Lapilli breccias, composed of very angular basaltic clasts in a limestone matrix, are found only in northern exposures of the Noggin Cove Formation. These were likely deposited in a shallow marine, relatively proximal setting. Similarly, medium bedded tuffs in Noggin Cove have predominantly angular clasts and are coarse-grained, have low to high angle cross-stratification, and are highly calcareous, suggesting shallow marine deposition.

Further evidence in support of a northerly source include the following points. (1) Clast supported volcanic conglomerates occur only to the north (eg. Noggin Cove). (2) Outsize clasts are more common in conglomerates to the north (eg. Carmanville Arm, Carmanville South, Noggin Cove). (3) A single occurrence of large sub-rounded volcanic blocks, up to 0.6 m x 1.8 m, suspended in a fine grained tuffaceous matrix, outcrops in the town of Noggin Cove; this "conglomerate" suggests mass wastage in a very proximal setting.

2.4 Structure

The dominant structural feature of the Noggin Cove Formation is a regional northeast trending cleavage. This strong cleavage commonly dips steeply to the southeast. Beds are generally steeply dipping and subparallel to the regional cleavage. Three stages of folding are defined: an early phase which predates the regional cleavage, a second phase for which the regional cleavage is axial planar, and a third phase which folds the regional cleavage.

F_1 folds

Mesoscopic F_1 folds are commonly tight to isoclinal, intrafolial, and in many cases are attenuated or disrupted in the strong northeast cleavage that cross-cuts them. F_1 folds are defined as those which are cross-cut in a non-axial planar manner by the regional cleavage. A faint bed parallel cleavage associated with F_1 occurs only very rarely.

Several F_1 intrafolial folds were identified in the Noggin Cove Formation with fold limbs ranging to 15 metres in length but commonly less than 1 metre. The largest and most notable example is located 1.50 km southwest of the head of Carmanville Arm. Here a 0.60 metre thick bed of coarse-grained volcanic sandstone is isoclinally folded within a volcanic conglomerate. The axial plane of this fold trends NW-SE and

dips moderately to the NE; the regional cleavage trends SW-NE and dips steeply to the SE. Smaller silt layers with attenuated limbs are similarly folded within volcanic conglomerate at this same location. Intrafolial, attenuated beds of silt in coarse-grained volcanic sandstones are tightly folded and cross-cut by the regional cleavage 0.4 km due east and 0.3 km due north of the previous location.

Coaxial F_1/F_2 fold interference patterns (type III of Ramsay, 1967) occur in the Noggin Cove Formation along the shoreline from Frederickton to Noggin Point, on the southeast side of Noggin Cove and in the crags overlooking the highway south of Carmanville; also, a well defined coaxial (type III) refold of a fine silt bed occurs within a black shale interbedded with the volcanics in Noggin Cove. Mushroom and coaxial F_1/F_2 fold interference patterns- Ramsay (1967) type II and type III refolds- have been reported in nearby units (eastern shore of Gander Bay, Noggin and Green Islands; Karlstrom et al, 1982). These interference patterns indicate the F_1 axial planes were at a high angle to the F_2 axial plane before F_2 folding. Because S_2 is steep, the F_1 axial plane must have been horizontal to sub-horizontal prior to F_2 folding, suggesting F_1 folds were recumbent.

A large, open, downward facing anticline, cross-cut by S_2, occurs in volcanic conglomerates south of Carmanville in the rocky bluffs 1 km due west of the head of Carmanville Arm

(Figure 2.3). Several examples of overturned beds, cut by a steeper S_2, were identified in the volcanic rocks of the Noggin Cove Formation. These observations support F_1 recumbent folding.

F_2 folds

These folds are defined as those for which the dominant regional cleavage is axial planar. This strong cleavage commonly rotates the long axis of ellipsoidal clasts into the plane of cleavage and in many cases vesicles are stretched into elongate shapes parallel to the cleavage (eg. Figure 2.2c). F_2 folds are asymmetric with cleavage and axial surfaces predominantly dipping steeply to the southeast (Figure 2.4a). F_2 fold axes have variable plunges but collectively form a girdle that matches the average orientation of S_2 (Figure 2.4b). Most F_2 folds plunge north to northeast, except west of Carmanville, where south plunges occur. East-plunging F_3 fold axes in this area strongly suggest F_2 folds are largely controlled by F_3 folding about east-west axes. The F_2 fold axial plane is also defined by bedding/S_2 cleavage lineations (L_2); this plane matches the axial plane defined by F_2 fold axes and by S_2 (Figure 2.4c). Mesoscopic F_2 folds are the most obvious and most common folds in the Noggin Cove Formation; these folds are open to isoclinal, although predominantly isoclinal, with bedding

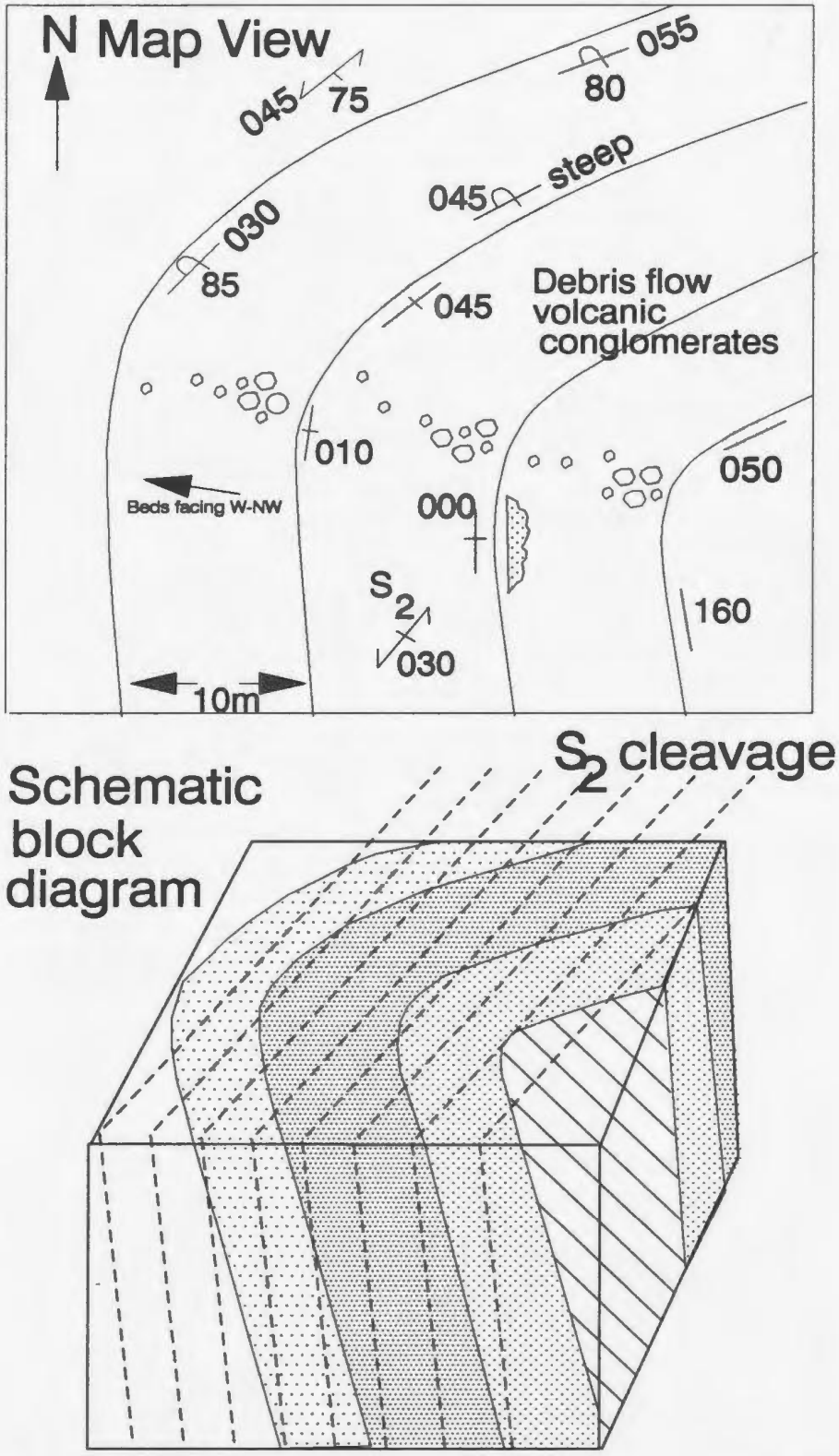

Figure 2.3: Overturned anticline, Noggin Cove Formation, south of Carmanville 1 km due west of the head of Carmanville Arm.

Figure 2.4: Structural data, Noggin Cove Formation

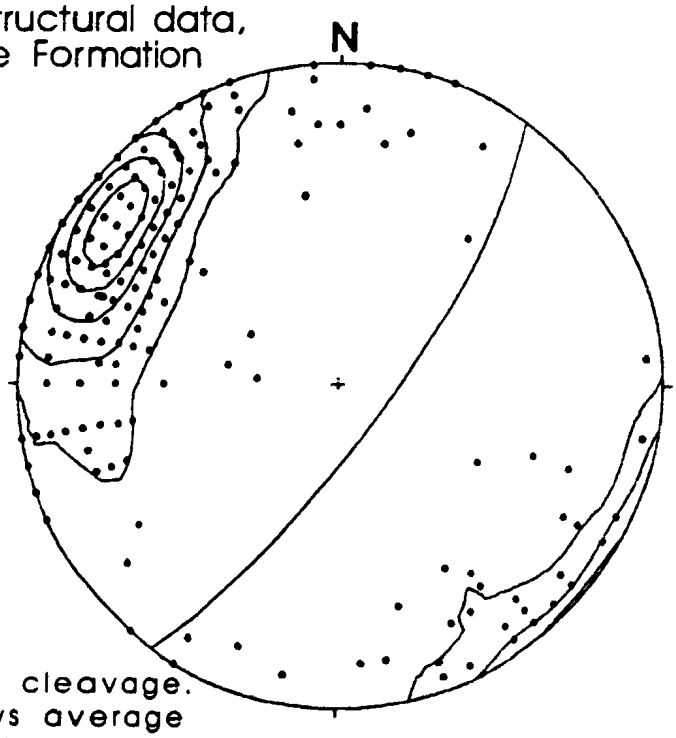

2.4a:
Poles to S2 cleavage. Girdle shows average northeast cleavage. Contours: 1 3 6 9 12. n = 382

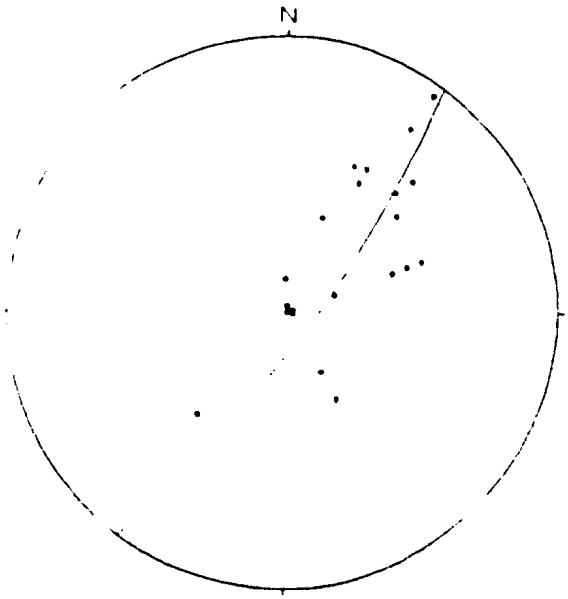

2.4b:
F2 fold axes. Girdle defines F2 axial plane. n = 23

Figure 2.4 (cont'd): Structural data, Noggin Cove Formation

2.4c:
Bedding/cleavage (S2) lineations. Girdle defines F2 axial plane.

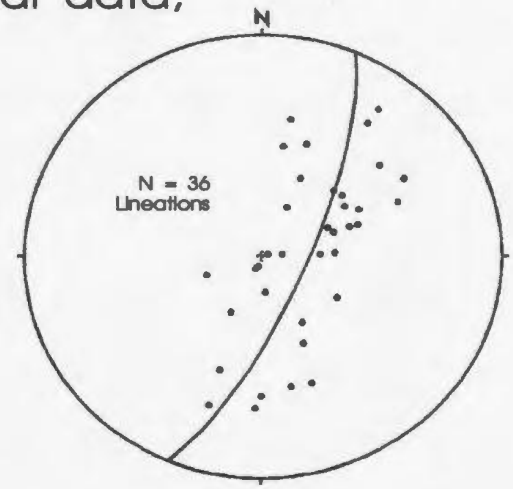

2.4d:
Poles to Bedding. Girdle is 90 degrees to highest contour.

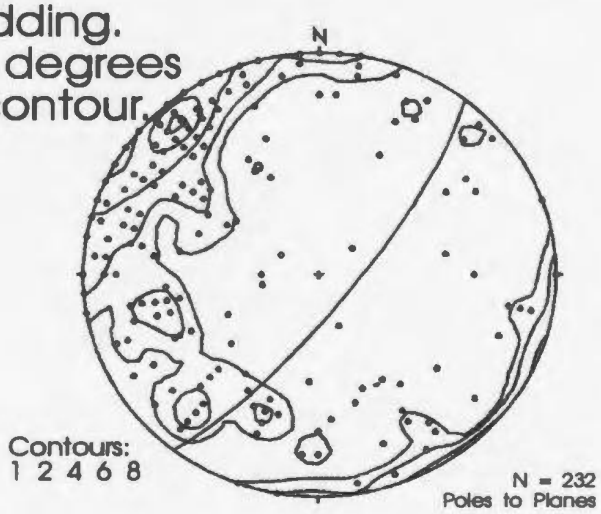

2.4e:
F3 Fold axes.

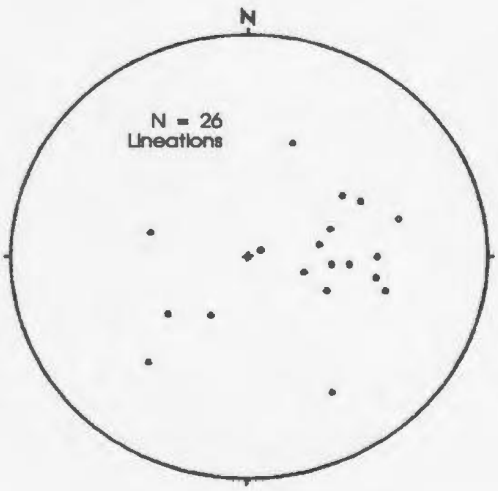

commonly rotated into the strong S_2 cleavage (Figure 2.4d).

Fold hinges could only be traced short distances and appear to terminate parallel to S_2, suggesting the variable plunges are part of a tight system of doubly plunging en echelon folds (for an illustration see p.313, Ramsay and Huber, 1987). Because of this tight en echelon folding of the Noggin Cove Formation volcanic rocks, coupled with limited lateral continuity of beds and lack of marker horizons, macroscopic F_2 folds could not be delineated. Detailed structural analysis of rocks to the west, that have undergone a similar deformational history (Karlstrom et al., 1982), indicate a sub-horizontal enveloping surface for macroscopic F_2 folds.

F_3 folds

These structures kink and fold the regional northeast cleavage (S_2). Kinking of the cleavage is more common than folding. Gentle to tight folding about moderate to steep fold axes results in the S_2 cleavage varying substantially from its northeast trend (Figure 2.4e). S, Z and M/W folds occur; hinge interference of the folded S_2 cleavage occurs in an M fold of coarse grained volcanic sandstone 0.5 km northeast of the west turn-off to Carmanville. More than one generation of post F_2 folding may be present. In addition to the northeast-southwest trend, a more dominant east-west trend is suggested by the

preponderance of F_3 fold axes with moderate to steep plunges to the east and west (Figure 2.4e). This trend is likely associated with a late, east-west, weak, open fracture cleavage.

Faults

No major faults are clearly expressed in the research area (eg. topographic expression, fault breccia). An inferred fault contact between volcanic rocks of the Noggin Cove Formation and sandstones, siltstones and shales of the Davidsville Group is based on the following: (1) A sharp contact between mafic volcanic conglomerates of the Noggin Cove Formation and siliceous sandstones, siltstones and shales of the Davidsville Group can be seen 1 km south of Beaver Cove just west of the road. Farther south, the contact can be placed within 5 m in many locations and is linear. South of Frederickton the same contact can be placed within 5-10m in many locations. (2) The siliceous sediments are invariably disrupted or sheared near the contact whereas the volcanic rocks seem unaffected. This could be due to the competency contrast between the two units and\or may indicate the volcanic rock rode over the siliceous sediments. (3) Contoured gravity data (Miller, 1988) show a pronounced east-west break along the southern margin of the Noggin Cove Formation. (4) Regionally, the contact has a sinuous trace, suggesting it is

an early fault folded by F_2. The most likely scenario is that this is a thrust fault of southward polarity related to F_1 recumbent folding.

No other major faults were delineated. The general competency of the volcanic rock commonly produces brittle failure during folding. Hence the volcanic rocks are commonly brecciated and small brittle offsets locally disrupt folds.

2.5 Relationships to surrounding units

Noggin Cove Formation - Davidsville Group

As outlined above, an inferred fault contact between the Noggin Cove Formation and the Davidsville Group may be an early southward thrust which put the Noggin Cove Formation above the Davidsville Group.

Noggin Cove Formation - Plutons

The Noggin Cove Formation is cut by the Silurian (Pajari and Currie, 1978) Frederickton, Rocky Bay and Aspen Cove plutons. The plutonic rocks are massive, cutting all earlier structures of the Noggin Cove Formation (namely F_2 and F_3).

Noggin Cove Formation - Carmanville Melange - Woody Island Siltstone

No continuous stratigraphic sections are exposed.

Stratigraphic relationships are based on a variety of observations at different locations. To the north, the Noggin Cove Formation is interbedded with melanges (see Chapter 3), siliceous breccias (finely bedded angular siltstone clasts in a limestone matrix) and bedded siltstones. There is a transition from the mafic volcanic rock of the Noggin Cove Formation to these siliceous units; interbedding of the two occur at Noggin Point and in Noggin Cove.

Relations between the volcanic conglomerates of Carmanville South and the large occurrence of melange just north at Teakettle Point, imply the Carmanville Melange is above the Noggin Cove Formation. Blocks of volcanic rock are common in the melange at Teakettle Point; the monomictic volcanic conglomerates do not contain melange clasts. Intervening strongly deformed black shale obscures this relationship such that a tectonic contact cannot be ruled out. In general, the monomictic volcanic conglomerates do not contain melange clasts; volcanic and volcaniclastic blocks occur in the melanges, suggesting the Carmanville melanges overlie the Noggin Cove Formation.

In other locations, volcanic conglomerates of the Noggin Cove Formation may be directly overlain by siltstone of the Woody Island Siltstone. Siltstone, similar to that of the Woody Island Siltstone, is in contact with volcanic conglomerates along the Frederickton to Noggin Point shoreline

and with coarse-grained tuffs in Noggin Cove. Cross-bedding in the tuffs in Noggin Cove indicate they are overlain by the siltstone. Coticules, common in the siltstone and sandstone beds of the Woody Island Siltstone, also occur in siltstone and sandstones interbedded with volcaniclastics of the Noggin Cove Formation at Beaver Cove.

F_2 folds with low to moderate northeast plunges and consistent north facings cut by S_2 cleavage along the northern shorelines indicate the siliceous units (melanges, siltstones, breccia) are stratigraphically above the Noggin Cove Formation. This is supported by a predominance of north facings within beds of the Noggin Cove Formation. Gravity data (Miller, 1988) and bathymetric charts show no major breaks north of the Noggin Cove Formation, suggesting the volcanic rocks extend northward at depth.

Noggin Cove Formation - Carmanville Melange (Davidsville)

The melange that occurs at Davidsville is interpreted here as olistostromal and above the Noggin Cove Formation. This interpretation is based on the following. (1) The melange is similar to the melanges north of the Noggin Cove Formation with respect to its matrix and clasts. (2) Rare folded beds of siltstone occur within the black shale of the melange and the predominance of siliceous clasts (versus mafic volcanic clasts) suggest a transition to a more siliceous source. (3)

Coticules in a medium bedded siltstone occur as a large block in black shale along the shoreline at Davidsville, indicating the same transition from the volcanic rocks to melange to the coticule bearing siltstone and sandstone that occurs northward of the Noggin Cove Formation. The subhorizontal enveloping surface of F_2 folds suggests horizontal layering prior to F_2 folding. Because F_2 folds are doubly plunging (see also Wu, 1979), the melange at Davidsville may be equivalent to melanges north of the Noggin Cove Formation.

Figure 2.5 shows the gross distribution of rock types within the Noggin Cove Formation and the proposed stratigraphy in which the Carmanville Melange and Woody Island Siltstone form a stratigraphic succession above the Noggin Cove Formation.

2.6 Age and correlation

There are no faunal or radiometric ages for the Noggin Cove Formation. A highly calcareous medium bedded tuff from Noggin Cove was processed for conodonts, but proved to be barren. Black shales were checked for graptolites but were also barren. The strong D_2 deformation is likely responsible for the lack of preserved fossils.

Melanges and coticule bearing lithologies like those at Woody Island are stratigraphically overlain by the Silurian

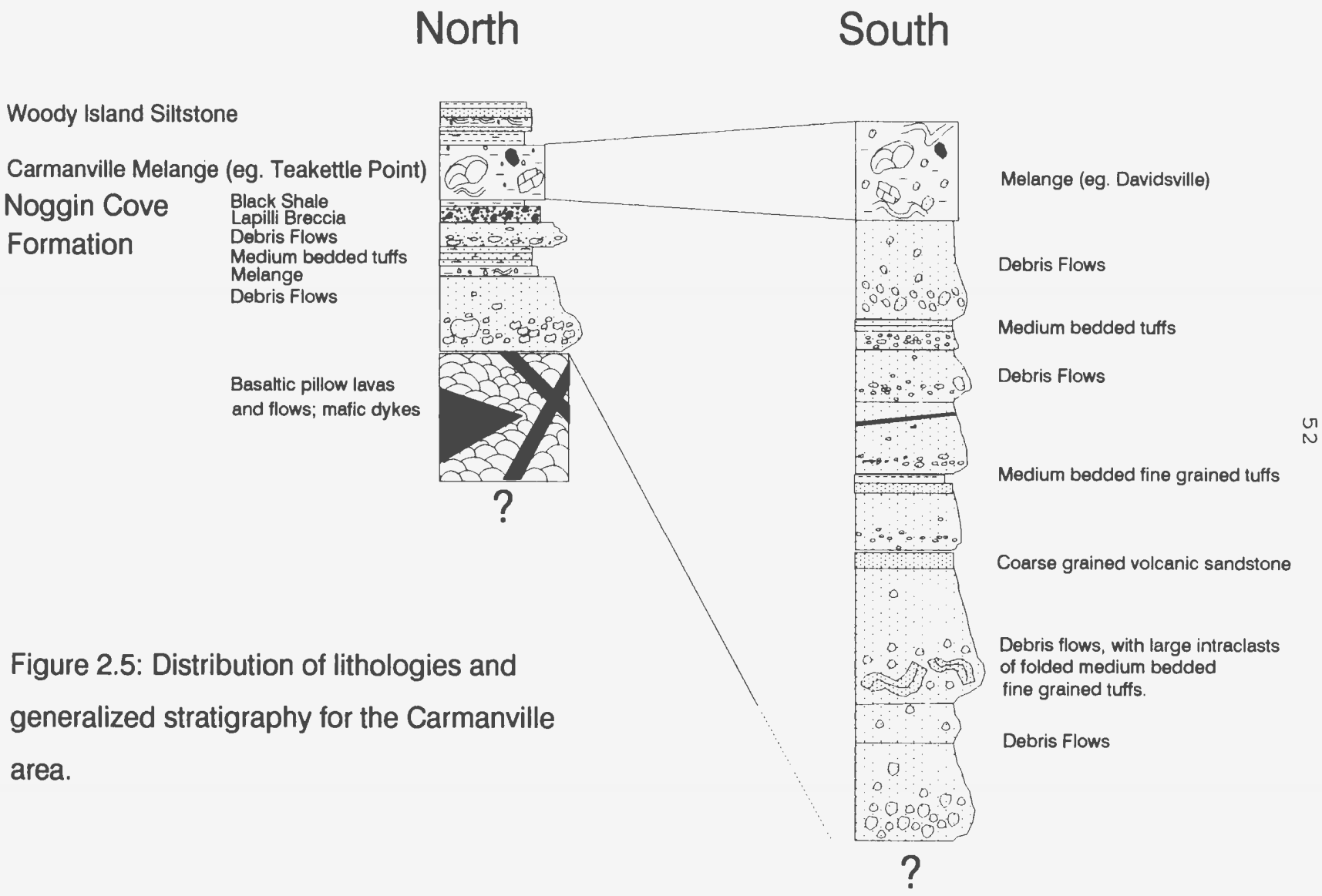

Figure 2.5: Distribution of lithologies and generalized stratigraphy for the Carmanville area.

Indian Islands Group west of Gander Bay (H. Williams, pers comm 1992). The underlying rocks and correlatives are therefore Ordovician. Based on regional correlations that include the Dunnage Melange, the Carmanville Melange and Woody Island coticule rock are considered Middle Ordovician or older (Williams, 1992). The Noggin Cove Formation underlies these units and is interpreted here as Middle Ordovician or older. This age is supported by a proposed correlation of the Noggin Cove Formation with the Tea Arm Volcanics of the Exploits Group (see chapter 6). The Tea Arm Volcanics are conformably overlain by the Strong Island Chert which contains early Llanvirn graptolites (Dec et al., 1992; Williams et al., 1992). Geochemical analyses of lavas from the Tea Arm Volcanics and from lavas interbedded with the Strong Island Chert indicate an arc to back-arc succession (Dec et al., 1992). A coeval arc to back-arc transition is suggested from similar geochemical results from samples of the Noggin Cove Formation (see Chapters 4 and 6).

Chapter 3

Carmanville Melange

3.1 Introduction

The Carmanville Melange (Williams et al., 1991), formerly the Carmanville Ophiolitic Melange (Pajari et al., 1979), is intimately associated with the Noggin Cove Formation. The purpose of this chapter is to briefly describe the Carmanville Melange and present observations which indicate the melange is olistostromal. Previous workers have emphasized the tectonic features of the Carmanville Melange (Pajari et al., 1979; Williams et al., 1991). This has tended to overshadow stratigraphic relationships between the Noggin Cove Formation and the Carmanville Melange.

3.2 Definition and Distribution

Carmanville Melange is the name applied to melanges that occur at the periphery of the two large discrete occurrences of the Noggin Cove Formation between Gander Bay and Aspen Cove (Williams et al., 1991). Occurrences of the Carmanville Melange are largely confined to the northern periphery of the Noggin Cove Formation, from Gander Bay in the west to Aspen Cove in the east (see Figure 2.1a and thesis map). Melange also occurs interbedded with fine-grained sedimentary rocks on

Woody Island and Noggin Cove Islets. The exception is at Davidsville, where the melange occurs south of the Noggin Cove Formation.

3.3 Lithology and stratigraphy

The Carmanville melanges are chaotic mixtures of siliceous and mafic clasts in a shale matrix. The melange matrix is predominantly silty to sandy homogenized black shale. Less commonly, the matrix is more tuffaceous and is lime green. The very heterogeneous assemblage of clasts incorporated into the melange range from millimeters to tens of meters. Pebbles and cobbles of sandstone and siltstone are the most common constituents of the melanges (Figure 3.1a). More conspicuous, but less common, are outsized blocks of siltstone, sandstone, pillow lavas, gabbro, volcanic conglomerates, bedded tuffs, limestone, trondhjemite, and ultramafic rock. Clasts of previously formed melange occur in melanges on the east side of Noggin Cove Head and on Woody Island. At Aspen Cove, an ultramafic block occurs along strike of bedded melange at Rocky Point that contains both mafic volcanic blocks and fine-grained altered ultramafic detritus (talc).

In many cases, folded beds of siltstone can be seen within the black shale matrix of the melange (eg. shorelines

Figure 3.1a: Carmanville Melange, Woody Island. As well as the obvious preponderance of sandstone clasts, note the abundance of pelitic clasts; these pelitic clasts are very similar to the black shale matrix of the melange (eg. just below fractured clast and in the top left portion of the photograph).

Figure 3.1b: Interbedding of melange with a black shale matrix (center of photograph) and melange with a light green, tuffaceous shale matrix (left and right of photograph). Hammer for scale is on the contact to the right. View is from the west shoreline of Noggin Cove looking north to Woody and Grassy Islands on the hazy horizon.

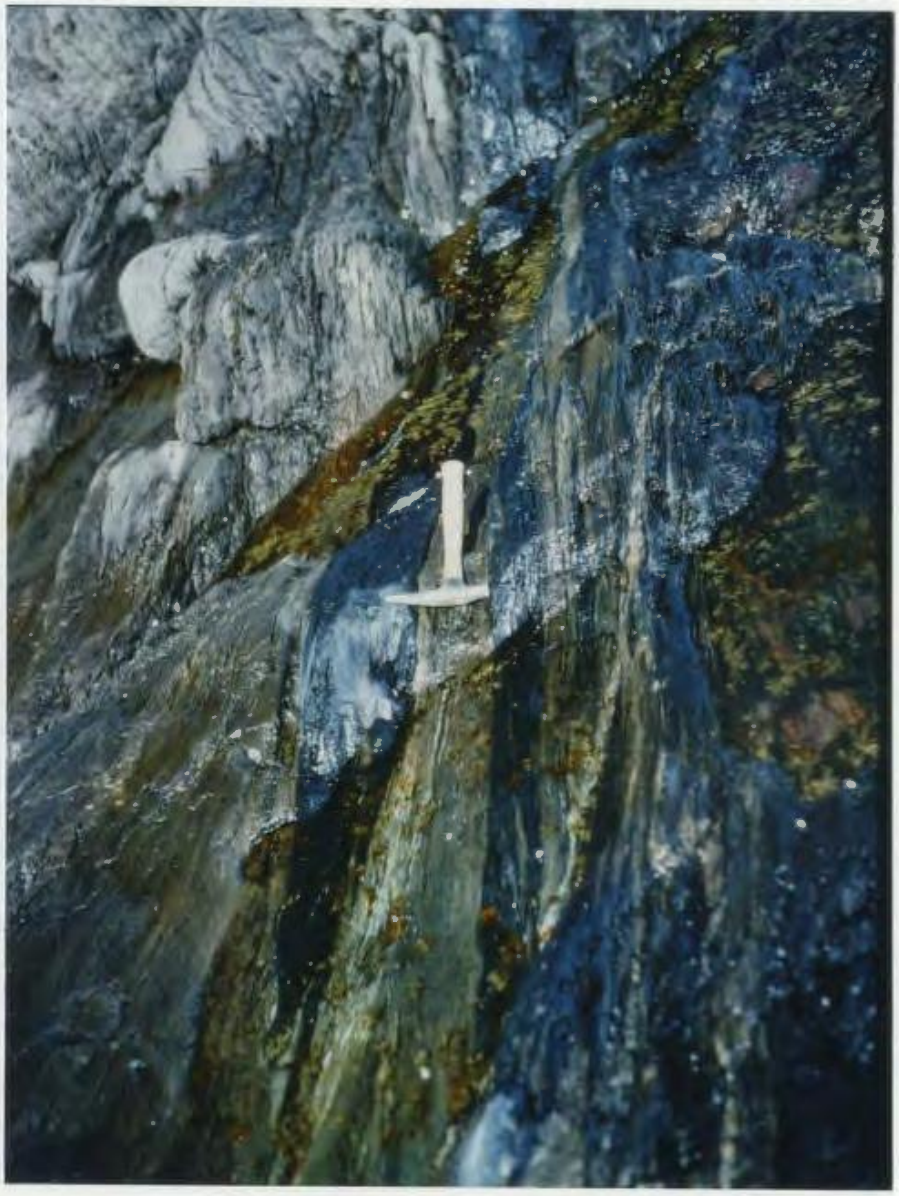

Figure 3.1c: Interfingering of melange with a black shale matrix and melange with a light green, tuffaceous shale matrix. The interfingering of the two units is parallel to sub-parallel with the strong S_2 cleavage (parallel to hammer) and is likely the result of isoclinal F_2 folding. Same location as figure 3.1b.

Figure 3.1d: Contact between melange with a black shale matrix and melange with a light green tuffaceous shale matrix, east side of Noggin Cove Head. Contact is just behind the heel of the boot and runs towards the viewer.

Figure 3.1e: Black shale matrix injected through blocks of light green, tuffaceous shale, east side of Noggin Cove Head. The difficult question is whether this is a soft-rock or hard-rock phenomenon.

Figure 3.1f: "Melange dyke" cutting bedded sediments of the Woody Island Siltstone, Woody Island. The melange dyke is an offshoot of a melange bed that lies to the right of the photograph interbedded with sediments of the Woody Island Siltstone. Bedding is parallel to the hammer handle. The dyke is perpendicular to bedding and parallel to the strong S_2 cleavage. Note how the quartz vein is boudinaged and the clasts highly elongated in this strong cleavage.

in Noggin Cove and north of Davidsville). Olistostromal "beds" of melange also occur which are unsorted and have very strong fabrics (eg. Noggin Cove, Rocky Point, Woody Island). Melange occurs interbedded with coticule bearing siltstones and silty shales on Woody Island and in Beaver Cove. Melange is interbedded with volcanic rocks in Noggin Cove and in Beaver Cove. At Noggin Point, and along the northwest side of Noggin Cove, melange with a homogenized fine-tuffaceous lime green matrix is interbedded and gradational with melange with homogenized black shale matrix (Figure 3.1b and c). A small occurrence of this green melange matrix is in contact with homogenized black shale on the east side of Noggin Cove Head (Figure 3.1d).

From the observations above, two important features of the Carmanville Melange need to be emphasized. First, the Carmanville Melange forms a stratigraphic link between the underlying Noggin Cove Formation and the overlying Woody Island Siltstone; melange is interbedded with these units and lithologically related to each locally. North facings in melange beds at Teakettle Point and Rocky Point agree with a predominance of north facings on northly plunging F_2 folds in the Noggin Cove Formation and Woody Island Siltstone. Second, the melanges are predominantly siliceous. Mafic blocks are conspicuous but volumetrically subordinate to the siliceous

shale matrix and siltstone/sandstone clasts.

Large areas of intensely deformed melange are in sharp contact with less deformed melange (described above). Intensely deformed melange with large blocks of banded mafic schist, greenschist, attenuated pillow lava and psammitic schist in a black semipelitic to pelitic matrix occurs at Teakettle Point, at Noggin Cove Head and on the west side of Noggin Point ("recycled" melange of Williams, 1992). According to this interpretation, the large areas of intensely deformed melange emphasized by Williams et al. (1991) are blocks within less deformed melange. Their origin, and controls of their deformation and metamorphism, may or may not be related to the controls of the less deformed melange.

3.4 Provenance

Blocks of pillow lava, gabbro, volcanic conglomerate, medium bedded tuff, trondhjemite and limestone all have equivalents in the Noggin Cove Formation. This suggests the olistostromal melanges were derived from the Noggin Cove Formation or a northern source like that proposed for the Noggin Cove Formation.

The shale matrix and siliceous siltstone/sandstone clasts of the melanges are very similar to the shale and fine-grained

sedimentary rocks of the Woody Island Siltstone. This is very obvious on Woody Island, where melange is interbedded with siliceous sedimentary rock of the Woody Island Siltstone. The matrix and clasts can be matched to nearby shale, siltstone, or sandstone beds. There are also transitions between bedded sections and broken beds to melange on the NE corner of Grassy Island. Melange along the shoreline north of Davidsville has conspicuous pillow lava and gabbro blocks but it's siliceous matrix and clasts are very similar to the matrix and clasts of melange on Woody Island. Thus the siliceous matrix and clasts of the Carmanville Melange are likely Woody Island Siltstone equivalents.

The melanges sample only local lithologies. Volcanic clasts occur in melanges that are near volcanic rocks of the Noggin Cove Formation. However, melanges interbedded with the Woody Island Siltstone (eg. Woody Island) contain only shale, siltstone and sandstone clasts which have equivalents in adjoining beds. Melange at Aspen Cove and Rocky Point contains ultramafic rock, presumably derived from the nearby Gander River Complex. This provenance is confirmed by a comparison of the major- and trace-element abundances in a sample of fresh pyroxenite (from under the pier at the north end of the town of Aspen Cove) with the average of abundances in 6 fresh pyroxenites from the Gander River Complex (Table 11, Appendix 2, O'Neill, 1991).

Table 3.1: Comparison of average major- and trace-element abundances in a sample of fresh pyroxenite from Aspen Cove with the average of abundances in six fresh pyroxenites from the Gander River Complex (O'Neill, 1991).

	Aspen Cove	Gander River Complex
SiO2	52.30 %	50.58 %
TiO2	.05	.06
Al2O3	1.54	2.20
FeO	5.15	4.76
MnO	.14	.15
MgO	19.96	20.57
CaO	14.61	17.62
Na2O	.06	.10
K2O	.02	.03
P2O5	.02	.02
Fe2O3	.48	-
LOI	4.77	3.45
Total	99.10 %	99.52 %
Cr (ppm)	2194	2023
Ba (ppm)	2	77
Zr (ppm)	2	23

3.5 Structure

In general, the melanges have undergone the same deformation as the Noggin Cove Formation. The regional northeast trending S_2 cleavage is very intense in the

melanges. Coaxial F_1/F_2 interference patterns (type III of Ramsay, 1967) can be seen in siltstone beds within the melange matrix on the southeast side of Noggin Cove and along the shoreline 0.5 km northeast of Frederickton. F_2 folds, defined by the axial planar, northeast trending regional cleavage, occur in silty beds in the matrix (shoreline, 1.25 km north of Davidsville) and where the melange is interbedded with fragmental volcanic rock (in Noggin Cove) or with siliceous sediments of the Woody Island Siltstone (on Woody Island). Interfingering along the contact between beds of melange with the black shale matrix and melange with the more tuffaceous lime green matrix is likely the result of F_2 isoclinal folding (Figure 3.1b). In some cases, the S_2 regional cleavage trends east-west, indicating F_3 folding of S_2.

Distinctive features in the melanges indicate post-depositional disruption associated with the strong S_2 regional cleavage. The black shale matrix locally pierces ajoining beds of melange with lime green, tuffaceous matrix (western shoreline of Noggin Cove); piercement is parallel to the regional cleavage. On the west side of Noggin Cove and on the east side of Noggin Cove Head, the black shale matrix locally pierces and appears to "bleed" through enclosed blocks of light green fine-grained tuff (Figure 3.1e). This piercement is also parallel to sub-parallel to the regional cleavage. A "melange dyke" cuts across bedding on Woody Island (Figure

3.1f). The strike of this dyke is parallel to the regional cleavage. Thin beds of siltstone in the melange are kinked and offset by the strong regional cleavage.

All of the disruptive features in the melanges noted here, and by others, can be attributed to the strong regional cleavage (see also Pajari et al., 1979; and Williams, 1983). The regional cleavage has a much stronger expression in the melanges than in adjoining units (ie: Noggin Cove Formation, Woody Island Siltstone). Pajari and his co-workers (1979) attributed the strong cleavage and associated folds in the melanges to soft-sediment deformation. Williams (1983) shows the cleavage to be a second generation feature (S_2) and the result of hard-rock deformation. Dyke-like structures (eg. Figure 3.1f), attributed to the migration of thixotropic melange units by Pajari et al. (1979), are post lithification and are the result of faulting and metamorphic differentiation (Williams, 1983). The strong regional cleavage is shown to be S_2 in this study. Hence, remobilization of the melanges is considered post-depositional and attributed to hard-rock deformation (ie: D_2).

The S_2 cleavage is Early Silurian or younger as it cuts fossiliferous sedimentary rocks of the Early Silurian Indian Islands Group (Twenhofel and Schrock, 1937; Karlstrom et al., 1982).

Incompetent, thin bedded tuffs are locally strongly

affected by pre-D_2 deformation and are preferentially strained relative to adjacent thicker volcanic units (eg. pillows, conglomerates). The best example of F_2 folds of this strong pre-D_2 fabric occurs at Noggin Cove Head. This D_1(?) strain partitioning could explain the occurrence of highly strained greenschists at Teakettle Point, Noggin Cove Head and along the shoreline 1 km. northeast of Frederickton. The occurrence of highly strained pillows at these locations is more problematic but may also be the result of strain partitioning. The more competent mafic blocks accumulate strain as they resist deformation, whereas the incompetent matrix has a much lower yield strength and offers far less resistance to deformation. Alternatively, the intensely deformed blocks may be from deep-crustal fault zones exhumed as an arc was rifted apart to form a back-arc basin (see Chapters 4, 6 and 7). Both alternatives are admittedly speculative. For the purposes of this study, it is important only that the deformed blocks be recognized as olistoliths in the less deformed melange.

3.6 Relationship to surrounding units

Is the Carmanville Melange structurally controlled or is it a stratigraphic unit? This first order concern is critical in determining how the Carmanville Melange is related to surrounding units. A number of observations indicate the

Carmanville Melange is olistostromal, rather than tectonic, in origin. (1) Interbedding and interfolding of melange with the Noggin Cove Formation and Woody Island Siltstone. (2) Common occurrence of fine siltstone beds within the matrix of the melange. (3) Matrix has a strong fabric (S_2) but is not scaly. (4) Chaotic melange at Rocky Point is crudely bedded (beds $\leq$ 5m.).

In melange beds and where melange is interbedded with rocks of the Noggin Cove Formation or Woody Island Siltstone (eg. shoreline 1 km northeast of Fredericton, Noggin Cove, Teakettle Point, Rocky Point, Woody Island), a predominance of northerly facings on north to northeast plunging F_2 folds indicate the melanges are above the volcanic rocks of the Noggin Cove Formation and are below the siliceous sedimentary rocks of the Woody Island Siltstone. A north-younging stratigraphic succession is supported by a predominance of north facings in the Noggin Cove Formation and Woody Island Siltstone; rare southeast facings in these units are attributed to F_1 recumbent folding.

The Carmanville Melange is intruded by the Rocky Bay pluton at Teakettle Point and by the Aspen Cove pluton at Rocky Point and Aspen Cove. The melanges are cut by numerous felsic dykes associated with the Frederickton, Rocky Bay and Aspen Cove plutons.

3.7 Age and correlations

No fossil ages or isotopic dates are available for the Carmanville Melange. Three samples from limestone blocks in the melange were processed for conodonts but proved to be barren.

Regional relationships indicate a Middle Ordovician or older age for the Carmanville Melange. The Carmanville Melange and coticule-bearing rocks of the Woody Island Siltstone have been correlated with the Dunnage Melange, which is overlain by Caradocian black shales (Williams, 1991). A correlative of the Carmanville Melange on the west side of Gander Bay at Dog Bay Point is stratigraphically below the Silurian Indian Islands Group (pers. comm. H. Williams, 1993).

Chapter 4

Geochemistry of the Noggin Cove Formation and Carmanville Melange

4.1 Introduction

Comparisons with modern geologic environments are important in the interpretation of ancient deformed and metamorphosed rocks. Volcanic rocks of the Noggin Cove Formation are polydeformed (Chapter 2) and have undergone greenschist-facies and contact metamorphism (Chapter 5). Particularly in such polydeformed and metamorphosed terranes, geochemical analyses provide an important link to modern analogues. Certain elements are generally considered immobile during alteration or metamorphism (Pearce, 1975; Shervais, 1982). It is the geochemical signatures of these key immobile elements, in samples of volcanic rock from the study area, which will be compared to those of volcanic rocks in modern tectonic settings.

Geochemical data were obtained from 18 samples of volcanic rock from the Noggin Cove Formation. Of the 18 samples, 7 are from pillow lavas, 1 is from a massive lava flow, 3 are from mafic dykes, and 7 are from fragmental volcanic rock. A small trondhjemite intrusion, which cuts the massive lava flow, was also sampled. Of the 7 samples of fragmental volcanic rock, 2 are from fine-grained tuffs, 2 are

from coarse- to very coarse-grained volcaniclastic sandstone, and 3 are from vesicular blocks that occur in volcanic conglomerates. Seven samples were analysed from mafic volcanic blocks in the Carmanville Melange. Of the 7 samples, 5 are from blocks of pillow lava and 2 are from blocks of massive gabbro. Mafic volcanic rock that occurs within siliceous sedimentary rock of the Davidsville Group south of the Noggin Cove Formation were also sampled (1 pillow lava, 1 gabbroic dyke). Geochemical results and locations for all samples are given in Appendix I. The 28 samples are displayed together in discrimination diagrams and extended REE plots. The symbols given in Figure 4.1 are used in all diagrams to distinquish samples from each of the three units (Noggin Cove Formation, Carmanville Melange, and Davidsville Group).

4.2 Geochemical characterization of volcanic rocks from the Carmanville area.

4.2.1 Introduction- mobile versus immobile elements

Rocks of the Noggin Cove Formation have undergone greenschist-facies metamorphism and very likely seafloor/hydrothermal alteration. Under these conditions, SiO_2, Na_2O, K_2O and most low field-strength elements (LFSE: Cs, Rb, Ba, Sr) become mobile whereas the high field-strength elements (HFSE: P, Ti, Y, Zr, Nb, Hf, Ta), Th, the transition

metals (Sc, V, Cr, Ni) and REE's are essentially immobile (Swinden et al., 1990). It is also recognized that the molecular proportion of MgO to FeO is not significantly changed in volcanic rocks that have undergone sub-seafloor metamorphism at low water/rock ratios (Swinden et al., 1990).

4.2.2 Discrimination Diagrams

As shown in Figure 4.1, the volcanic rocks are predominantly basaltic; the sample with the relatively high silica content is trondhjemite. Because SiO_2 may be mobile during metamorphism or alteration, a discrimination diagram using only immobile elements is included to confirm the basaltic composition of the volcanic rocks (Figure 4.2a). The basalts range from alkaline to subalkaline, as shown by Figure 4.2a. The subalkaline basalts from the Noggin Cove Formation and Carmanville Melange show increasing TiO_2 with differentiation and are likely tholeiitic (Figure 4.2b). The similarity between the mafic block and pillow lavas in the Carmanville Melange (Figure 4.2b) makes it likely the mafic block is also tholeiitic.

Figure 4.3 shows that basalts have both arc and non-arc affinity. The overlap of geochemical signatures for samples from the Noggin Cove Formation and Carmanville Melange in figures 4.1 - 4.3 suggest that all are from the same volcanic complex. The majority of samples plot within the E-MORB and N-

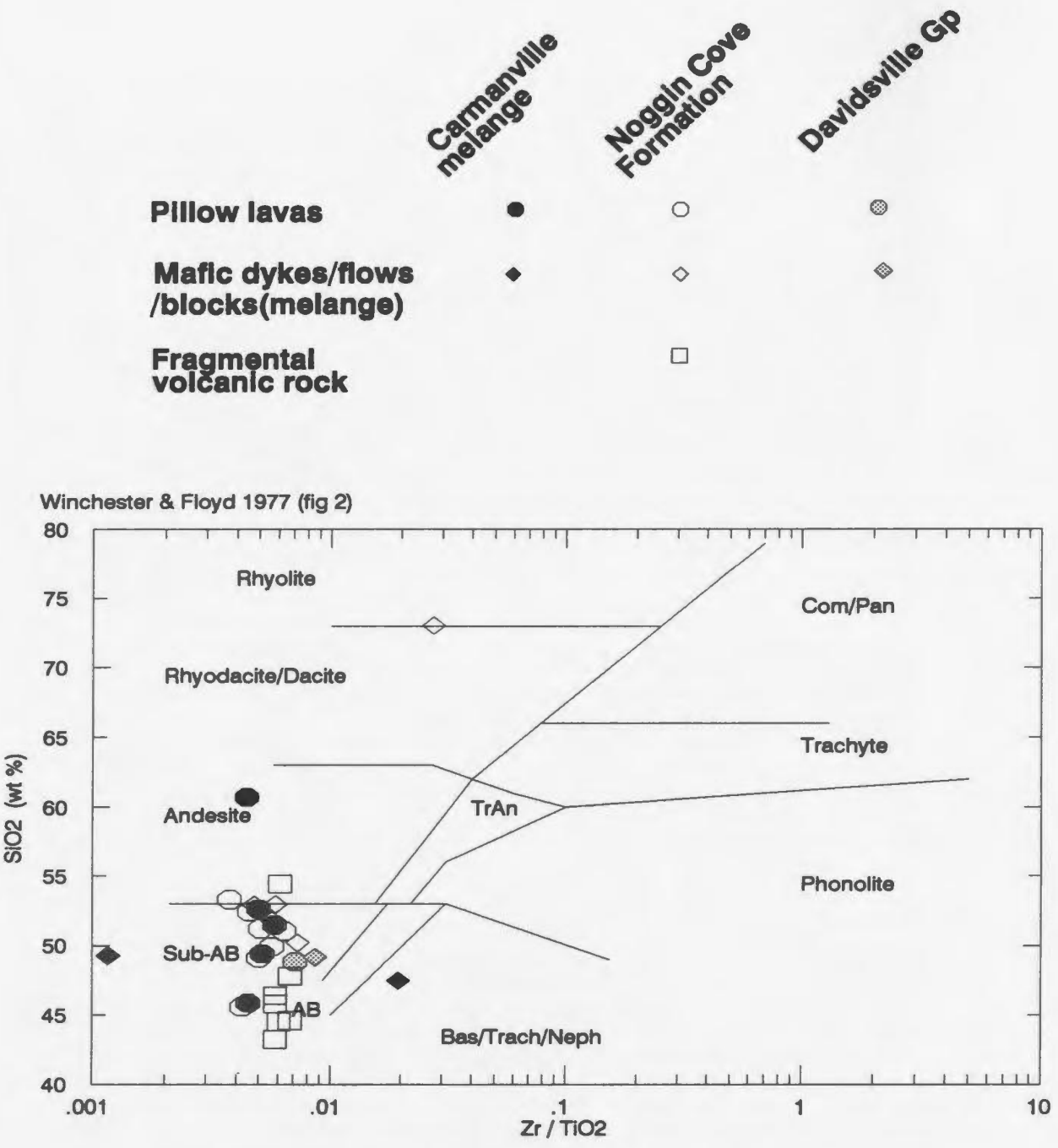

Figure 4.1: Zr/TiO2 vs Nb/Y discrimination diagram for volcanic rocks of the Noggin Cove Formation, Carmanville Melange and Davidsville Group. The one sample with 74% SiO2 is trondhjemite.

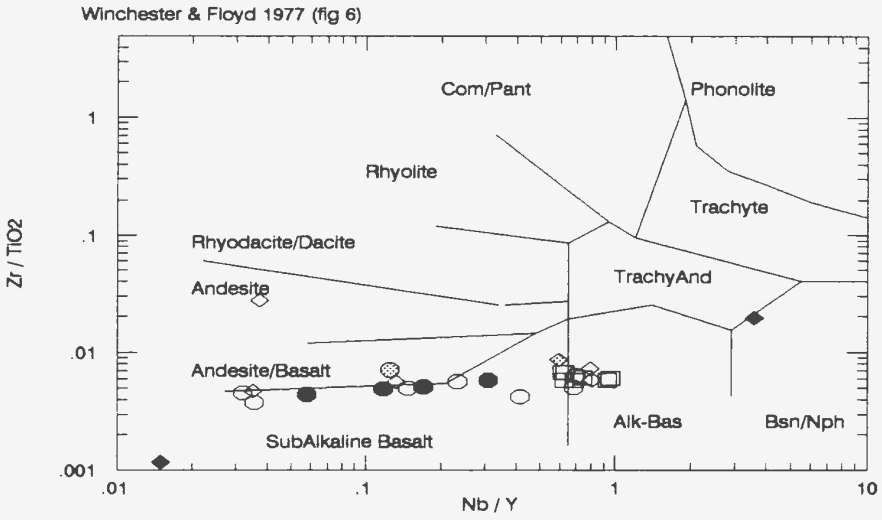

a: Zr/TiO2 vs Nb/Y discrimination diagram (Winchester and Floyd, 1977). Symbols per figure 4.1

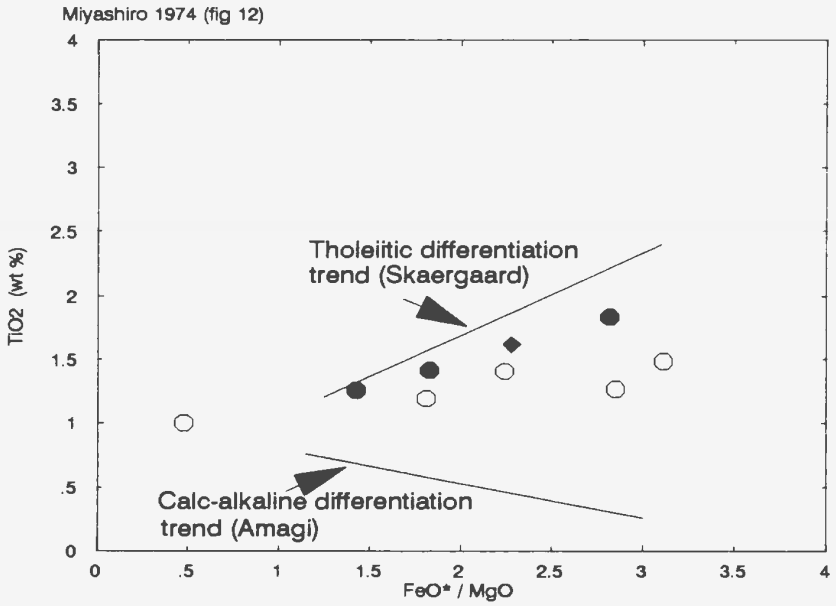

b: TiO2 vs FeO*/MgO discrimination diagram (Miyashiro, 1974) for subalkaline basalts of Figure 4.2a. FeO* not available for sample 2106. Symbols per figure 4.1

Figure 4.2: Discrimination diagrams for volcanic rocks of the Noggin Cove Formation, Carmanville Melange and Davidsville Group.

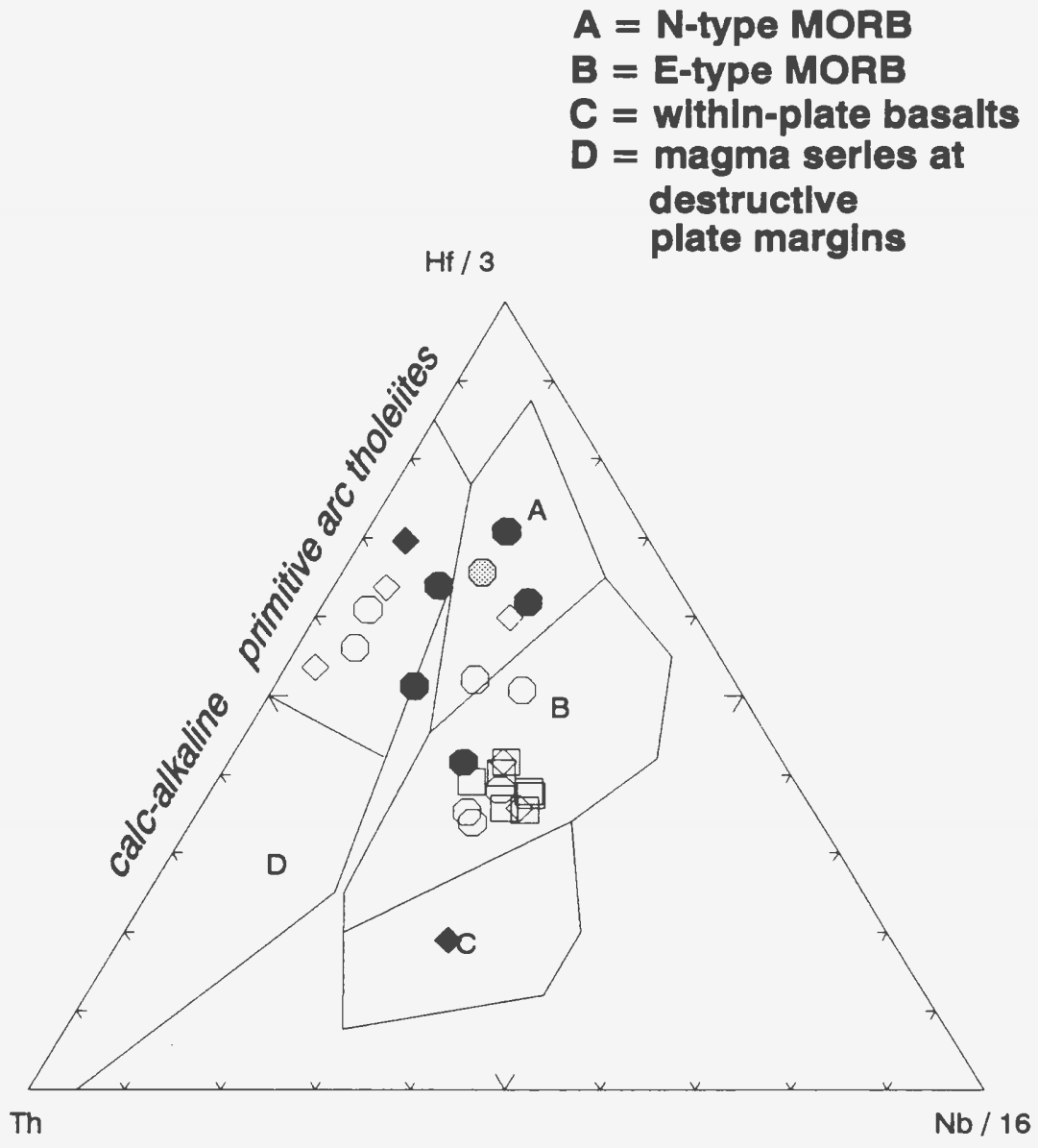

Figure 4.3: Hf-Th-Nb discrimination diagram (Wood, 1980) for volcanic rocks of the Noggin Cove Formation, Carmanville Melange and Davidsville Group. Symbols per Figure 4.1.

MORB fields, indicating a back-arc paleotectonic setting. Arc signatures for some of the samples (field D) support this interpretation. Tight grouping of the fragmental volcanic rocks in the E-MORB field reflects a consistent source.

4.2.3 Extended REE plots

Volcanic rocks from modern island-arcs show a distinctive depletion in certain high field strength elements (HFSE: Nb, Ta) and are enriched in low field strength elements (LFSE: Cs, Rb, Ba, Sr) relative to the light rare earth elements (Wood, 1980; Arculus, 1987). On the normalized extended rare earth element (REE) plots for the Noggin Cove Formation that follow, this relationship is shown by positive Th anomalies and negative Nb anomalies. Volcanic rocks from non-arc settings do not show this relationship (Swinden et al., 1990). A positive Th anomaly and negative Nb anomaly are the primary discriminants between arc and non-arc volcanic rocks and it is this relationship\signature which is used in this study. Ta values are in error because of resident contamination (Ta from previous sample analyses, G. Jenner, pers. comm.).

The extended REE plots and geochemical characterization of the samples are modelled after Swinden et al. (1990) to facilatate correlations westward (see Chapter 6). In their (ibid.) detailed geochemical and Nd-isotope study of the volcanic rocks of the Wild Bight Group, age and stratigraphic

control allow documentation of an early to mid-Ordovician arc to back-arc chemostratigraphic succession. Arc volcanic rocks were subdivided into four geochemical groups (A-I, A-II, A-III, felsic) and non-arc volcanic rocks into three geochemical groups (N-I, N-II, N-III) to record the chemostratigraphic succession. The same classification scheme will be used in this study.

Island arc volcanic rocks

Type A-I, LREE-enriched arc rocks

No samples have this geochemical signature.

Type A-II, LREE-depleted arc rocks

The largest occurrence of mafic lavas of the Noggin Cove Formation is in the immediate Carmanville area. Pillow lavas, massive lava flows, and mafic and trondhjemitic dykes, occur at Noggin Cove Head and Noggin Hill. A large occurrence of pillow lava forms a prominent knoll behind the Carmanville school. Smaller occurrences of pillow lava are exposed along the Carmanville shoreline. Pillow lava samples from Noggin Hill and from behind the Carmanville school, and a sample from a massive lava flow along the west side of Noggin Cove Head, all have a similar distinctive arc signature (Figure 4.4). Trondhjemite that intrudes the massive lava flow also has an arc signature (Figure 4.4).

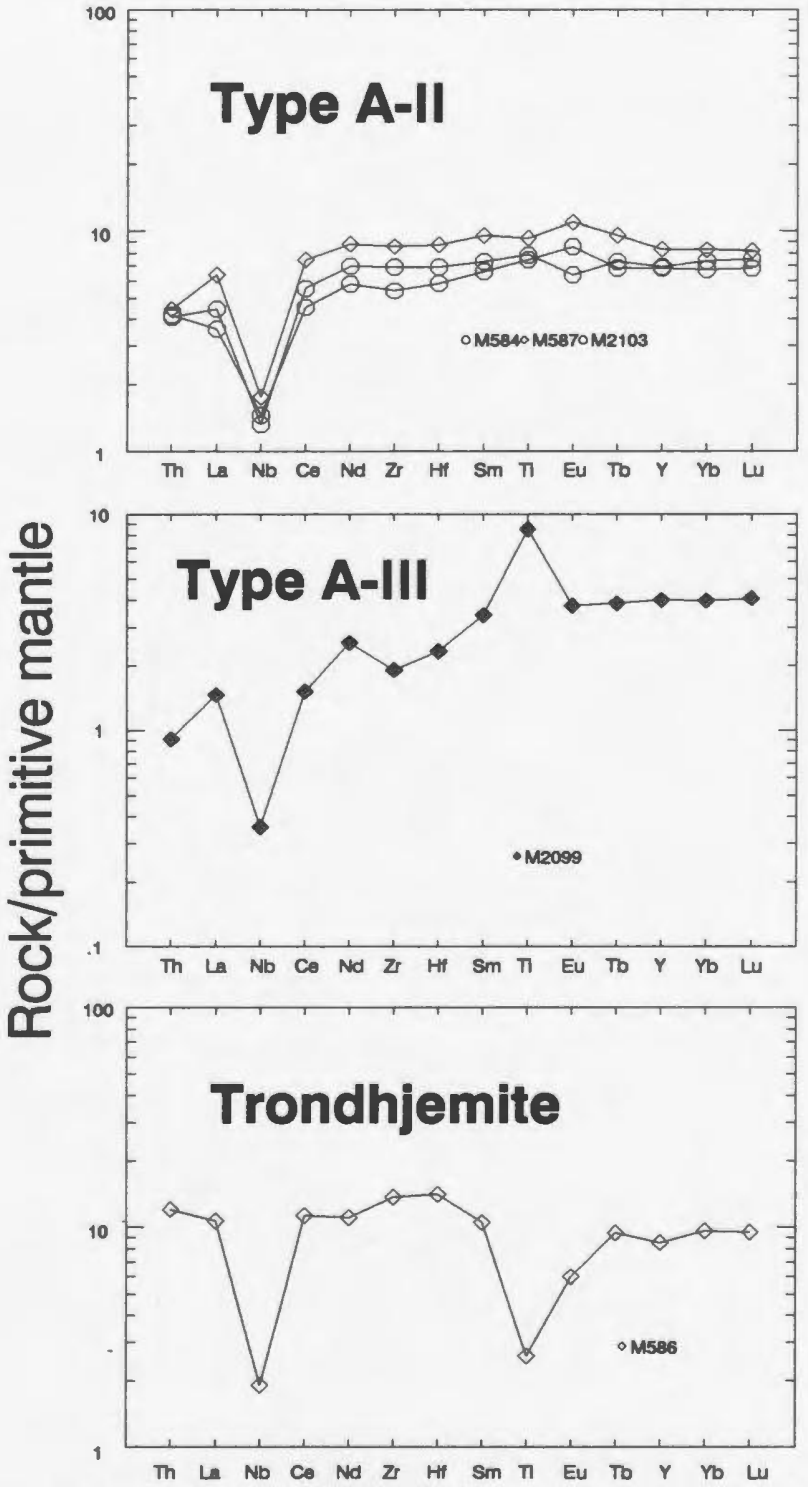

Figure 4.4: Extended REE plots for samples of volcanic rock from the Carmanville area with arc signatures. Symbols as per figure 4.1. Normalizing values from Swinden et al., 1990.

Type A-III, strongly depleted arc rocks

Only one sample has this distinctive geochemical signature (Figure 4.4); the sample is from a block of massive gabbro in the Carmanville Melange at Rocky Point.

Non-arc volcanic rocks

Type N-I, alkalic basalts

Again, only one sample has this geochemical signature (Figure 4.5). The sample is from a block of massive gabbro that occurs in the Carmanville Melange along the shoreline just north of Davidsville.

Type N-II, strongly LREE-enriched basalts

Nearly half of the samples (13 of 28), including all of the fragmental volcanic rocks (7 samples) are type II non-arc tholeiites (Figure 4.5). None of the samples from mafic blocks in the Carmanville Melange have this geochemical signature. Two samples are from mafic dykes that cut volcanic conglomerates in Noggin Cove. Three samples are from pillow lavas that occur with fragmental volcanic rock. At a roadcut just east of the large church in Noggin Cove, pillow basalts are in contact with volcanic conglomerates. Spatially, the conglomerates overlie the pillow basalts but a reliable facing direction could not be determined. At the top of a large hill overlooking the Carmanville South turn-off, pillow lava

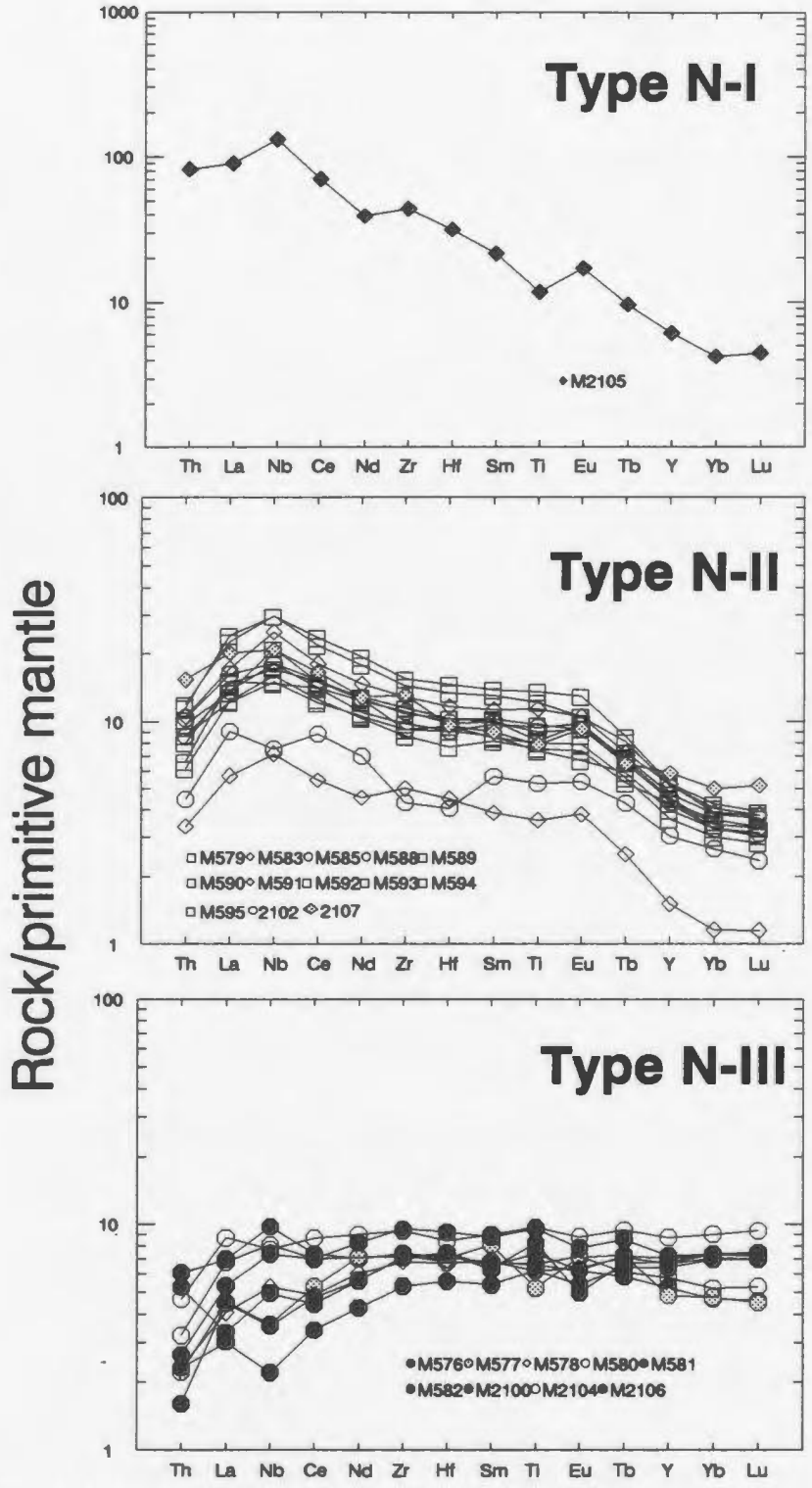

Figure 4.5: Extended REE plots for samples of volcanic rock from the Carmanville area with non-arc signatures. Symbols as per figure 4.1. Normalizing values from Swinden et al., 1990.

appears to intrude into volcanic conglomerates. Another occurrence of pillow lava is exposed 1 km to the east; it is separated from an outcrop of medium bedded, fine grained tuff by 2-3 metres of cover. Finally, one sample is from a gabbroic dyke which intrudes banded shale and chert of the Davidsville Group in a small quarry 4.5 km southeast of Carmanville.

Ocean island basalts (eg. Kilauean tholeiites) are the best modern equivalent of type N-II basalts. Basalts with REE patterns similar to the N-II pattern are also found in some modern back-arc basins (eg. Lau Basin; Gill, 1976).

Type N-III, weakly LREE-enriched non-arc basalts (Figure 4.5)

A large proportion of the samples in this group (5 of 9) are from blocks of pillow lava in the Carmanville Melange; these occur at Rocky Point, Teakettle Point (2 separate blocks), Noggin Point and along the shoreline just north of Davidsville. Pillow lavas of the Noggin Cove Formation with the N-III signature occur in a roadcut 1 km south of Beaver Cove and in a large roadcut between Carmanville and Noggin Cove. A mafic dyke that cuts the pillow lavas at this large roadcut is also a N-III basalt. N-III pillow basalts occur with Davidsville Group sedimentary rocks at Round Pond.

N-III basalts are the most MORB-like, indicating little or no influence of a subducting slab on the source magmas. Modern equivalents of N-III basalts occur in back-arc basins

(eg. Scotia Sea; Hawkesworth et al., 1977) and at transitional spreading portions of mid-ocean ridges ("T-MORB"; Schilling et al., 1983).

4.3 Discussion

As can be seen in Figure 4.3, the geochemical signatures do not indicate a specific tectonic environment for the volcanic rocks in the Carmanville area. The close association of arc and MORB volcanic rocks suggests an arc/back-arc tectonic setting. From a comparison of the Hf-Th-Nb discrimination diagrams (Figures 4.6), it can be seen that the Noggin Cove Formation basalts have geochemical signatures very similar to those of the Lau Basin, Valu Fa Ridge and Ata Island (see sketch map of Tonga-Lau region, Figure 7.2). There is an excellent match in the extended REE plots between arc basalts from the immediate Carmanville area and samples dredged from the Valu Fa Ridge (Figure 4.7). The Valu Fa Ridge is an active back-arc spreading centre in the Lau Basin; it is approximately 200 km long and is located 40-50 km west of the active Tofua Volcanic Arc. The narrow ridge separates the active Tofua Volcanic Arc from the Lau Ridge (remnant arc); it rises to 1800m below sea level in places and is about 150 km above the seismic Waditi-Benioff Zone. Ata Island is part of the active Tofua Volcanic Arc and is the closest arc volcano

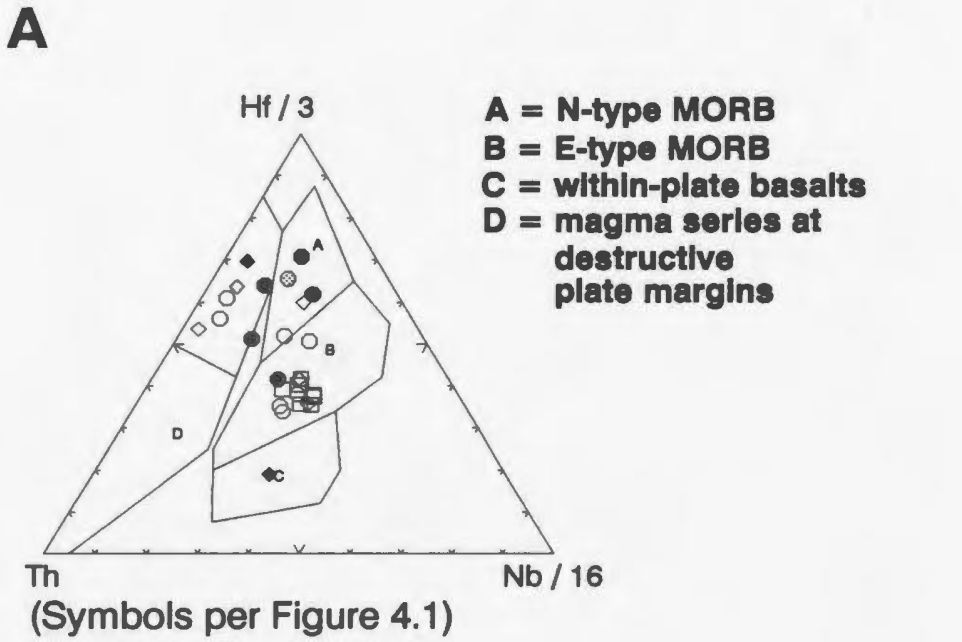

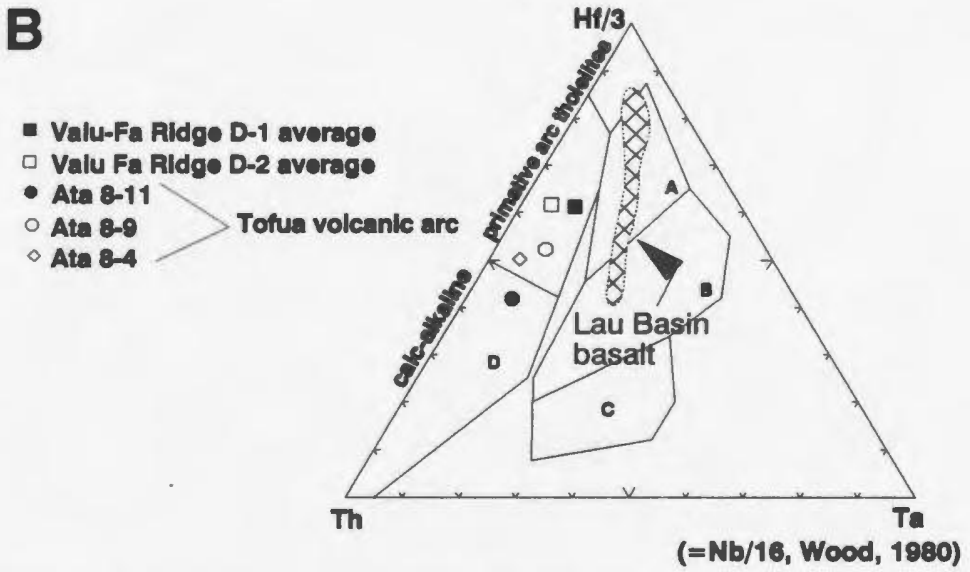

Figure 4.6: Comparitive Hf/3-Th-Nb/16 discrimination diagrams to illustrate the similarities in geochemistry between volcanic rocks from the Carmanville area (A) and from the Valu-Fa Ridge and Tofua volcanic arc (B; from Vallier et al., 1991).

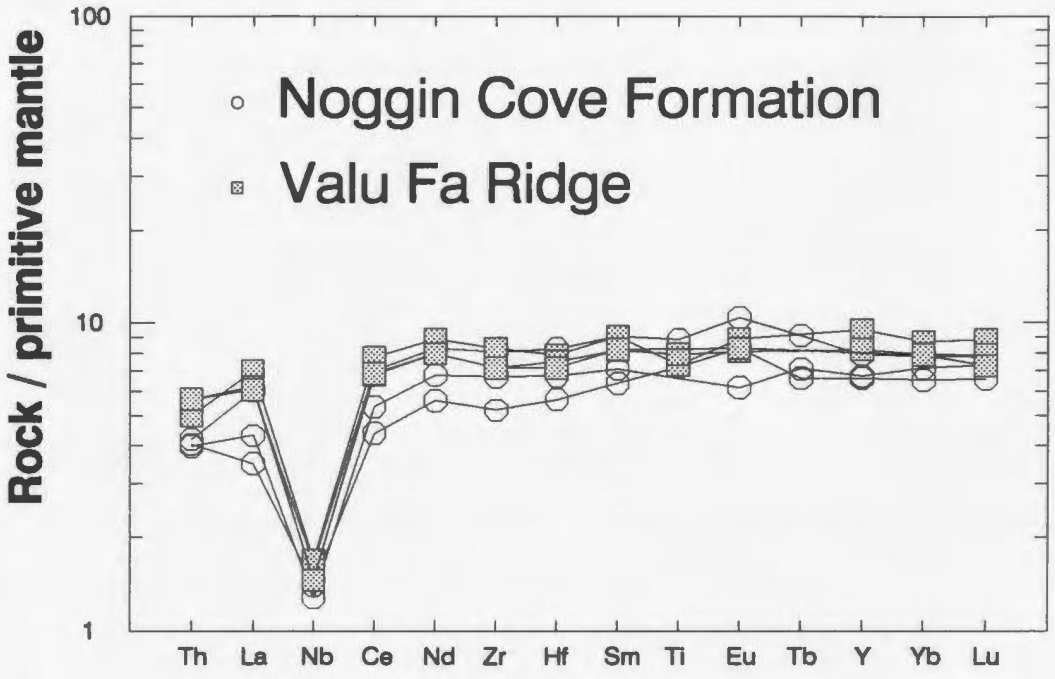

Figure 4.7: Comparitive extended REE plots for samples from the Carmanville area and Valu Fa Ridge that plot in field D of figure 4.6a and b. Values for Valu Fa Ridge samples from Vallier et al., 1991. Normalizing values from Swinden et al., 1990.

to the Valu Fa Ridge (Vallier et al., 1991;). The geochemical results from the Noggin Cove Formation strongly suggest a similar back-arc basin paleotectonic setting.

The spread in geochemical signatures on the ternary diagrams may represent the transition from arc to mantle derived magmas as an arc is rifted to form a back-arc basin (eg. Lau Basin). Ideally, one would like to match the geochemical results to a detailed stratigraphic succession showing the same arc to back-arc basin transition. However, the stratigraphy of volcanic terranes such as the Noggin Cove Formation is invariably complex. In addition, the volcanic rocks of the Noggin Cove Formation have undergone three stages of folding in which D_2 deformation was very intense. The general stratigraphy established is from mafic lavas to successively overlying fragmental volcanic rock, olistostromal Carmanville Melange, and the Woody Island Siltstone (Chapters 3 and 4). The geochemical results and stratigraphic succession support an interpretation of an arc to back-arc basin transition.

The bulk of the samples from the Noggin Cove Formation and from mafic blocks in the Carmanville Melange are A-II, N-II and N-III type basalts. The rock types which dominate these groups match the general stratigraphic succession proposed for the Noggin Cove Formation and the Carmanville Melange. Mafic lavas (A-II) are overlain by fragmental rock (N-II) which are

in turn overlain by the olistostromal Carmanville Melange (N-III; Table 4.1). The corresponding geochemical and stratigraphic successions are summarized in the following table.

Table 4.2: Chemostratigraphic succession proposed for rocks of the Noggin Cove Formation (NCF), Carmanville Melange and Woody Island Siltstone.

Proposed Stratigraphy	Geochemical Succession
Woody Island Siltstone	
Carmanville Melange	N-III
Fragmental Volcanics, NCF	N-II
Mafic lavas,NCF	A-II

Figure 4 .8 shows the magma sources and tectonic setting of the arc and non-arc groups. Samples from the Noggin Cove Formation and from mafic blocks in the Carmanville Melange are predominantly of non-arc affinity, suggesting arc rifting and volcanism were waning and a more mature back-arc basin was developing. The deeper water sedimentary rocks of the Woody Island Siltstone overlie the Carmanville Melange and may represent deposition into the developing back-arc basin.

Formation	Arc-trondhj.	A-II	A-III	N-I	N-II	N-III
Noggin Cove Fm.	M586-dyke (cuts M587)	**M584-pillow lava** **M587-lava flow** **2103-pillow lava**			**M579-fragmental** **M589-fragmental** **M590-fragmental** **M592-fragmental** **M593-fragmental** **M594-fragmental** **M595-fragmental** M583-mafic dyke (cuts volc. cgl.) M591-mafic dyke (cuts volc. cgl.) M585-pillow lava M588-pillow lava 2102-pillow lava	M578-mafic dyke (cuts M580) M580-pillow lava 2104-pillow lava
Carmanville Melange			2099-gabbro block	2105-gabbro block		**M576-pillow block** **M581-pillow block** **M582-pillow block** **2100-pillow block** **2106-pillow block**
Davidsville Group					2107-mafic dyke	M577-pillow lava

Table 4.1: Summary of geochemical characterizations per extended REE plots (see figures 4.5 and 4.6). Dominant rock types are highlighted in larger, bold type and indicate a succession from arc lavas to non-arc fragmental volcanic rock to non-arc pillow basalts of the Carmanville Melange.

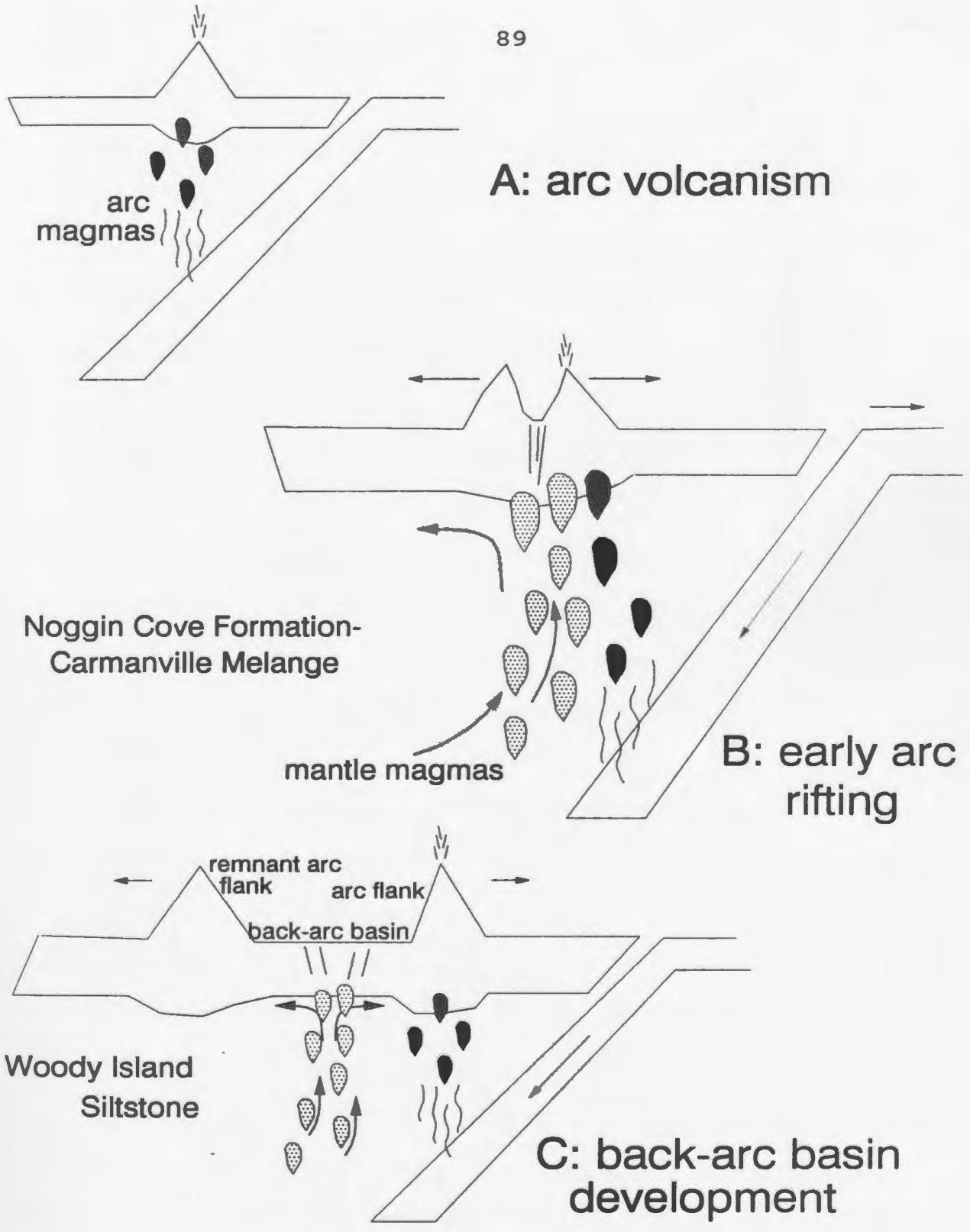

Figure 4.8: Schematic diagram to illustrate arc to back-arc transition.

Chapter 5

Petrology and metamorphism of the Noggin Cove Formation

5.1 Introduction

Regional metamorphism increases eastward in the Carmanville area from greenschist facies in the Noggin Cove Formation to middle amphibolite (sillaminite grade) in pelites of the Davidsville Group near the Dunnage/Gander boundary (Pajari and Currie, 1978). East of the Dunnage/Gander boundary, the Gander Zone consists of amphibolite facies psammites and pelites, megacrystic granite of the Ragged Harbour Pluton, and high grade polymetamorphosed gneisses (central gneissic complex; Pajari and Currie, 1979).

Rocks of the Noggin Cove Formation, Carmanville Melange, and Davidsville Group are hornfelsed in the contact aureoles of the Frederickton, Rocky Bay and Aspen Cove plutons. At Teakettle Point for example, garnet and andalusite are abundant in graphitic schists and metasiltstone of the Carmanville Melange near the contact with the Rocky Bay Pluton.

The focus of this chapter is on the petrology and metamorphism of the Noggin Cove Formation; rocks from the Carmanville Melange or from the contact aureoles of the plutons are not discussed. Petrographic observations are based on the examination of 35 thin sections cut from mafic volcanic

rocks of the Noggin Cove Formation. A wavelength dispersive electron microprobe and scanning electron microscope with an energy dispersive detector were used to determine mineral compositions.

5.2 Mineral Assemblages

Metabasalts of the Noggin Cove Formation consist of calcic fibrous amphiboles and subordinate chlorite, epidote, albite, sphene, calcite and biotite. Fe(Ti) oxides are abundant. X-ray diffraction results from two representative samples of fragmental volcanic rock, show that amphibole is the dominant mineral present (Appendix II).

Two different Ca-amphiboles can be identified and characterized in thin section. Edenite occurs as "clean" blades, has light brown to bright green pleochroism and has a 3rd order yellow birefringence. Tremolite has a more fibrous habit and the grains are more irregular in outline (Figure 5.1). It has weaker pleochroism (very light brown to light green) and a higher birefringence (3rd order yellowish red to red). Based on textural criteria, the edenitic amphiboles are considered to post-date those of tremolitic composition.

Pillow lavas and massive lava flows are predominantly fine- to medium-grained; mafic dykes are coarse grained; an ophitic texture is commonly well preserved. Plagioclase

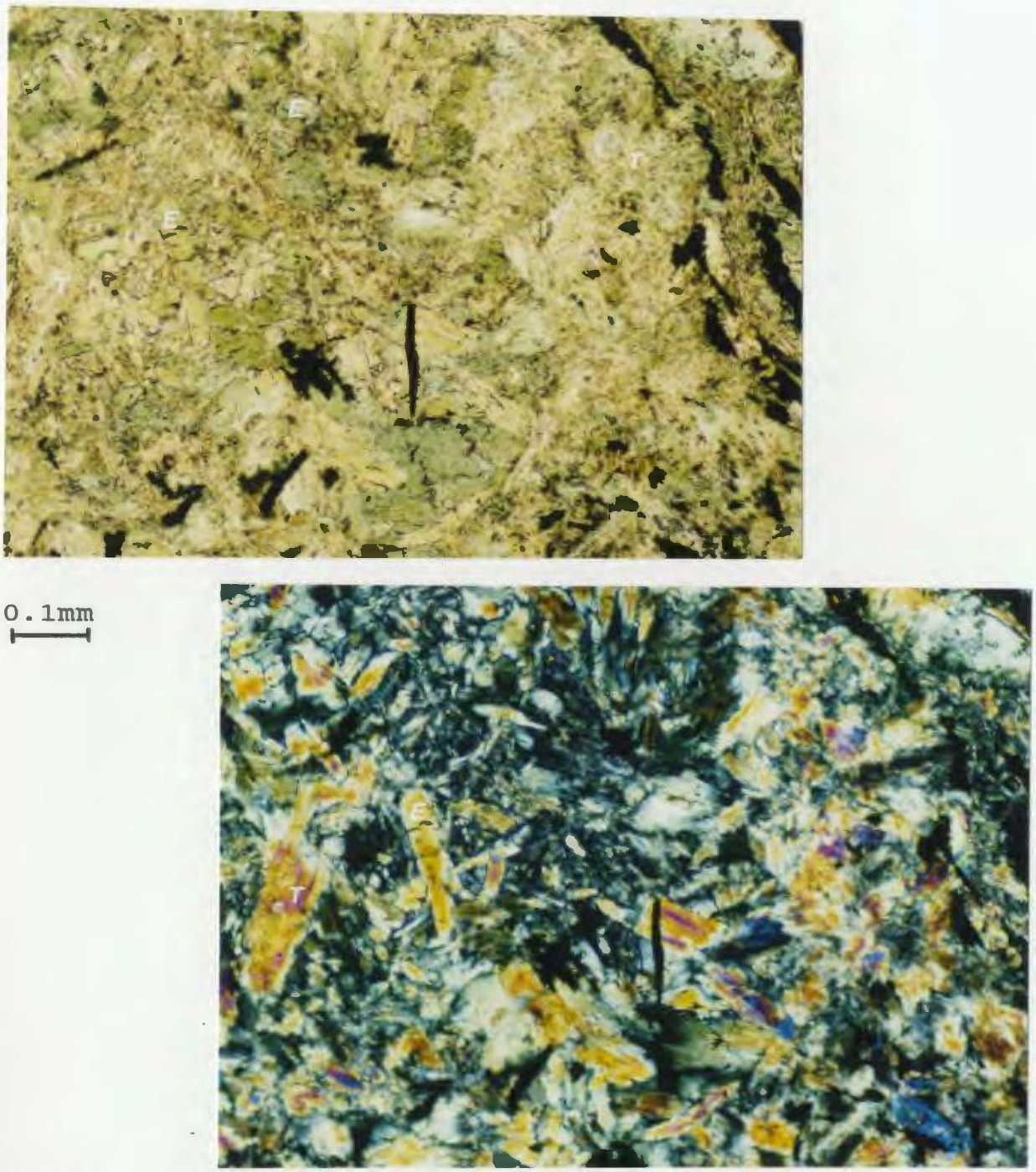

Figure 5.1: Plane-polarized (top) and cross-polarized (bottom) photomicrographs (10X) of a sample of fragmental volcanic rock from the Noggin Cove Formation (3107-9). Metamorphic amphiboles dominate the field of view. Representative edenite (E) and tremolite (T) grains are labelled.

grains, which retain their igneous shape, are albite in composition (eg. see Appendix IV). Relict pyroxenes are entirely replaced by fibrous amphiboles and chlorite. Very small amygdules in the pillow lavas are filled with chlorite and calcic amphiboles.

A small mafic intrusion which cuts volcanic conglomerates just east of Noggin Cove is distinctly different from other mafic volcanic rocks of the Noggin Cove Formation and warrants special mention. In outcrop, the light green surface of the rock is pitted and is cut by a network of small light green to white veinlets. In thin section, fractured grains of relict olivine are clearly discernible and locally serpentine can be seen to preserve pseudomorphically the form of the earlier olivine crystals. These serpentinized olivine grains weather preferentially to give the rock its pitted appearance. The white veinlets are composed of antigorite. The rock has a high modal percentage of olivine (50-65%), approximately 20-35% pyroxene and 10% Fe(Ti) oxides. This mineralogy, and the lack of plagioclase, suggest that this rock is more mafic than other volcanic rocks of the Noggin Cove Formation. The chemical composition of this rock is comparable to that of a picrite basalt (sample M591, Appendix I, is similar to the picrite basalt analysis, p. 544, Carmichael et al., 1974).

In the fragmental volcanic rocks of the Noggin Cove

Formation, as in the lavas and dykes, very little of the original mineralogy is preserved. Rare igneous pyroxenes occur, but most are entirely replaced by secondary fibrous amphiboles and chlorite. Aggregates of epidote commonly mimic the lath shapes of the original plagioclase grains. Minor secondary quartz and albite are very fine grained and can only be distinguished at higher magnifications with the scanning electron microscope.

Fragmental textures are well preserved, defined by the contrasting modal proportions and grain size of secondary minerals in the clasts compared to that of the matrix. Fibrous amphiboles are more common than chlorite in the clasts, whereas in the matrix the opposite is true. The fibrous amphiboles are very fine grained in the clasts, medium- to coarse-grained in the matrix and amygdules. Fe-Ti oxides are more common in the matrix than in the clasts.

Bedded tuffs and lapilli breccias have abundant original calcite both as matrix and as small clasts. Clasts observed in thin section are highly amygdaloidal and are generally angular to sub-round. Amygdules are filled with quartz, calcite, chlorite or fibrous amphiboles.

The strong D_2 fabric is evident in all thin sections. This fabric is expressed as a preferred orientation of small clasts and secondary minerals (eg. chlorite and fibrous amphiboles). Vesicles are commonly elongate in the strong

fabric. In many cases, fibrous amphiboles are randomly oriented, indicating they postdate the D_2 metamorphism (eg. Figure 5.1).

5.3 Coexisting amphiboles

5.3.1 Introduction:

An investigation of the amphibole compositions of the metabasalts of the Noggin Cove Formation was prompted by the observation of two coexisting amphiboles with different pleochroism and birefringence.

Amphiboles have the ideal formula:

$$A_{0-1}B_2C_5T_8O_{22}(OH,F,Cl)_2 \ .$$

The A site is commonly occupied by Na or K or is vacant. Ca, Na, Li, Mn, Mg and Fe^{2+} commonly occupy the B site. The C site is generally occupied by Mg, Fe, Mn, Al and Ti and the T site by Si and Al. These are the most common substitutions but many others are possible.

Amphiboles analysed on the microprobe in this study were classified according to the occupancies of the A, B and T sites using a program developed by Currie (1991). Hydroxyl site occupancy was not analysed. Substitutions within the A, B and T sites are independent; given the occupancies of the A, B and T sites, the occupancy of the C site can be fixed by

charge-balance considerations. Figure 5.2 shows the composition space for amphiboles based on substitutions into the A, B and T sites of tremolite ($\square Ca_2Mg_5Si_8O_{22}(OH)_2$, at the origin, $\square$ = vacant). This composition space is subdivided into thirteen domains, each with vertices defined by International Mineralogical Association end-members. The program calculates the mol fractions of each end-member for a given amphibole analysis. The most abundant end-member generally agrees with the International Mineralogical Association name. The advantage of this classification scheme is that it keeps track of less abundant, yet still significant, end-member amphiboles.

5.3.2 Analytical results:

Microprobe results, site occupancies and classification of the amphiboles are given in Appendix III. Table 5.1 summarizes the classification of the amphiboles. An overwhelming proportion (43 of 53 analyses) of the amphiboles are predominantly tremolite, hornblende or edenite. Tschermakite and pargasite also occur. Single analyses of glaucophane, barroisite and taramite rich amphiboles have not been duplicated, despite efforts with the scanning electron microscope, and are not considered further.

Microprobe data for plagioclase grains are listed in Appendix IV. Note that these results are from basaltic lava

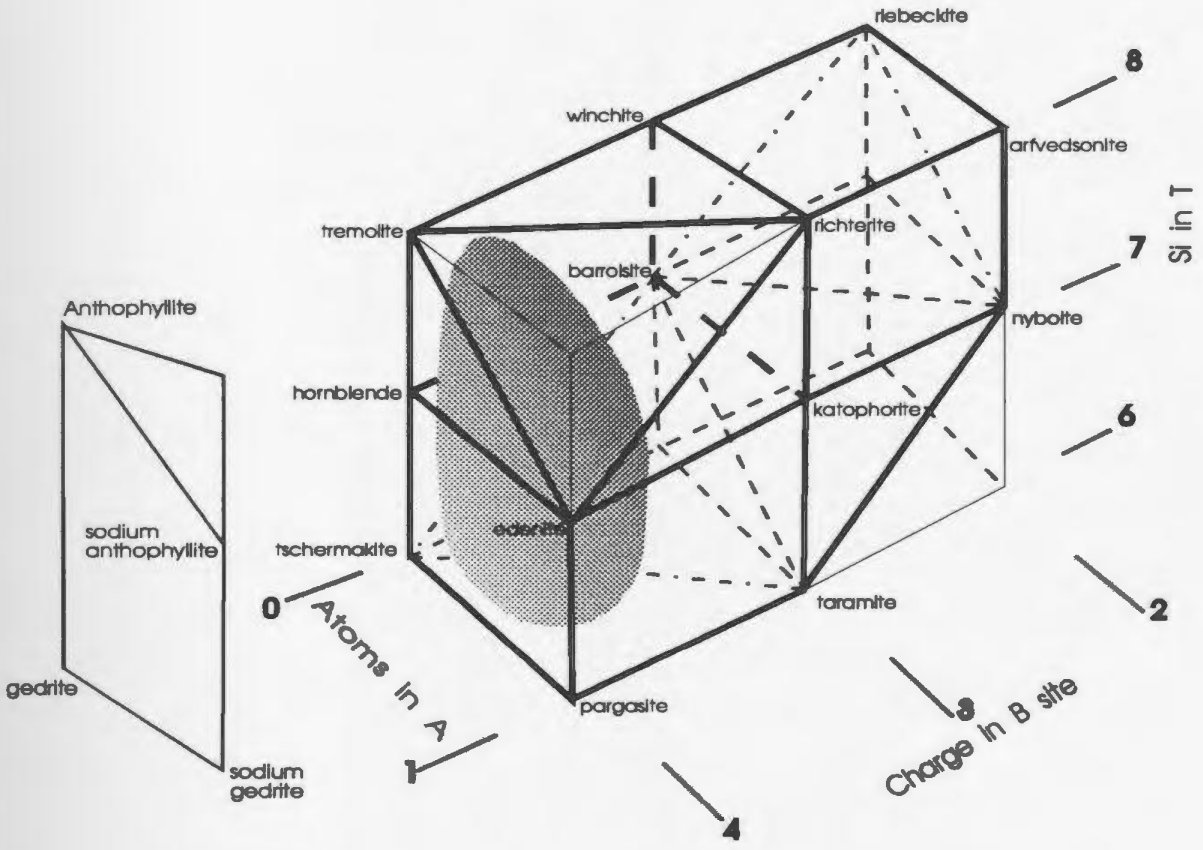

Figure 5.2: Composition space for amphiboles based on the occupancies of the A, B and T sites (from Currie, 1991). End-member amphiboles at the vertices per Currie, 1991. Other end-members occur at these points. For example, magnesio-riebeckite, glaucophane, and ferro-glaucophane occur at the point labelled riebeckite. The planes edenite-tremolite-richterite and riebeckite-barroisite-tschermakite-taramite-nybolite mark the limits of amphibole composition space.

To the left is the composition space for Fe-Mg amphiboles, which lie on the left-hand face of the polyhedron; these end-members are obtained by the substitution of (Fe-Mg) for Ca on this face. Stippled cloud shows where the majority of Noggin Cove Formation amphiboles plot in this composition space.

Table 5.1: Mol fraction of end-member amphiboles for each microprobe analysis. The most abundant end-member is highlighted in larger, bold type and totalled in the last row. Sample 0608-2 is from a basaltic dyke, sample 1108-2 is from a lava flow and the remaining four samples are from fragmental volcanic rock.

Anal #	Fig 5.6 ref	tremol	hbl	barroisite	edenite	tscherm.	glaucoph.	pargasite	kaersutite	anthophyl	taramite	gedrite	other
0608-2-1	1a	**.537**	.150	.177	.136								
-2	b	.084	**.480**	.153	.282								
-3	c	**.398**	.364	.187	.048					.002			
-4	d	.135	**.575**	.124	.164								
-5	e	.141	**.465**	.195	.198								
-6	f	**.663**	.147	.159	.020					.010			
-7	g		**.429**	.245	.197	.128							
-8	h		.156	.214	**.363**	.266							
1108-2-1	2a	**.674**	.143	.124	.024					.031		.003	
-2	b		**.549**	.036	.005	.065				.153		.189	.003(1)
3107-9-1	3a		.141	.213	**.470**	.175							
-2	b			.295	**.396**	.286					.023		
-3	c			.093			**.504**						.368(2) .035(3)
-4	d					.236		**.560**	.077		.086		.041(4)
-5	e				.275	.206		.264	.136		.117		
-6	f			.062	**.557**	.347					.032		
-7	g		.195	.317	.128	**.358**						.001	cont'd

Anal #	Fig 5.6 ref	tremol.	hbl.	barroisite	edenite	tscherm.	glaucoph.	pargasite	kaersutite	anthophyl	taramite	gedrite	other
-8	h			.233	**.450**	.283					.033		
-9	i				.201	**.400**		.238	.071		.089		
-10	j	.224	.144	.293	**.337**								
-11	k				.127	.193		**.444**	.067		.169		
-12	l				**.444**	.347		.012	.054		.142		
0308-3-1	4a	.205	**.308**	.194	.292								
-2	b	.044	**.419**	.208	.327								
-3	c	.063	**.389**	.285	.003					.147		.111	.002(5)
-4	d		.022		.070	**.343**				.014		.459	.091(6)
-5	e			.088	**.469**	.295					.147		
-6	f	.265	**.481**	.079						.118		.056	
-7	g			.250	**.474**	.252					.024		
-8	h	**.680**	.082	.189	.049								
0508-1-1	5a	**.516**	.237	.218	.029								
-2	b	.148	**.408**	.139	.304								
-3	c		.163	**.431**	.110	.295							
-4	d	**.697**	.055	.178	.069								
-5	e	**.627**	.075	.050	.247								
-6	f	**.739**	.105	.134	.021								
-7	g	**.399**	.309	.111	.180								cont'd.

Anal #	Fig 5.6 ref	tremol.	hbl.	barroisite	edenite	tscherm.	glaucoph	pargasite	kaersut.te	anthophyl	taramite	gedrite	other
-8	h	.268	.224	.135	**.374**								
-9	i	**.576**	.184	.167	.072								
-10	j	**.795**	.014	.173	.014					.005			
-11	k	.209	**.356**	.099	.336								
-12	l	**.388**	.206	.176	.229								
0408-4-1	6a			.192	.205						**.405**		.198(6)
-2	b	**.576**	.216	.179	.012					.015		.002	
-3	c				.259	**.323**		.140	.069		.208		
-4	d	.148	**.361**	.170	.320								
-5	e			.034	.329	**.478**					.159		
-6	f			.368	**.470**				.011		.150		
-7	g				**.524**	.273			.041		.161		
-8	h		**.295**	.177	.263	.264							
-9	i	**.666**	.188	.126	.007					.012		.001	
-10	j		**.476**	.177	.398	.008							
-11	k	**.479**	.260	.171	.090								
Totals/53		16/53	14/53	1/53	13/53	5/53	1/53	2/53	0/53	0/53	1/53	0/53	0/53

1.Na-anthopyllite 2.nyboite 3.ATB-4Si5 4.Na-anthopyllite 5.Na-anthopyllite 6.katophorite

and dyke samples only, not from fragmental volcanic rock. The mol fraction of albite (X_{Ab}), for each plagioclase in contact with amphibole, is listed in Table 5.2 matched to mol fraction data for each coexisting amphibole.

Table 5.2: Mol fraction data for co-existing amphibole and plagioclase grains. $X_{Na,A}$ and $X_{\square,A}$ are from Appendix III, X_{Ab} is from Appendix IV. $^{*}X_{Na,A} = X_{Na,A}/(X_{Na,A} + X_{\square,A})$, where $X_{\square,A}$ is computed as $1 - X_{Na,A} - X_{K,A}$. $^{*}X_{Na,A}$ calculated in this way assumes K in the A site does not influence partitioning (Spear,1981). $^{*}X_{Na,A}$ is used in Figure 5.6.

anal#-fsp	X_{Ab}	anal# -amph	$^{*}X_{Na,A}$	$X_{Na,A}$	$X_{\square,A}$
0608-2-3u	.89	0608-2-3	0.023	.018	.955
0608-2-6u	.95	0608-2-2	0.250	.394	.558
0608-2-41	.93	0608-2-5	0.160	.153	.802
0608-2-61	.77	0608-2-8	0.270	.236	.637
1108-2-3u	.98	1108-2-1	0.000	0.00	.975
1108-2-11	.98	1108-2-2	0.000	0.00	.993

An operating breakdown of the JXA-50A electron microprobe at Memorial University of Newfoundland during 1991 precluded further probe analysis of the amphiboles. The same samples were analysed on a Hitachi SEM with an energy dispersive analytical system to further characterize the amphiboles.

Tremolite and edenite grains are readily distinquished on

the SEM. The tremolite grains exhibit a distinctly darker grey tone than those of edenite (Figure 5.3). Semi-quantitative analyses and the E.D. (energy dispersive) spectra of the edenite and tremolite grains in Figure 5.3 are shown in Figure 5.4. Edenite grains have higher Al and Na, and lower Si, relative to tremolite. Appendix V lists the semi-quantitative results of the SEM analyses. These results are presented graphically in Figure 5.5. Amphiboles with compositions intermediate between the tremolite and edenite are probably hornblende. Zoned grains have cores of tremolite (or less commonly of hornblende), which are rimmed by edenite, suggesting that edenitic compositions formed later.

5.3.3 Plagioclase-amphibole equilibria:

The equilibria between plagioclase, calcic amphibole and quartz which exists in these samples can be described by the relation (after Spear 1981):

$$NaAlSi_3O_8 + \square Ca_2Mg_5Si_8O_{22}(OH)_2 = NaCa_2MgAlSi_7O_{22}(OH)_2 + 4SiO_2$$

albite + tremolite = edenite + quartz (1)

This relation governs the partitioning of Na between the A site of the amphiboles and the M site of coexisting plagioclase. The reaction is continuous and predominantly temperature dependent, proceeding to the right with increasing

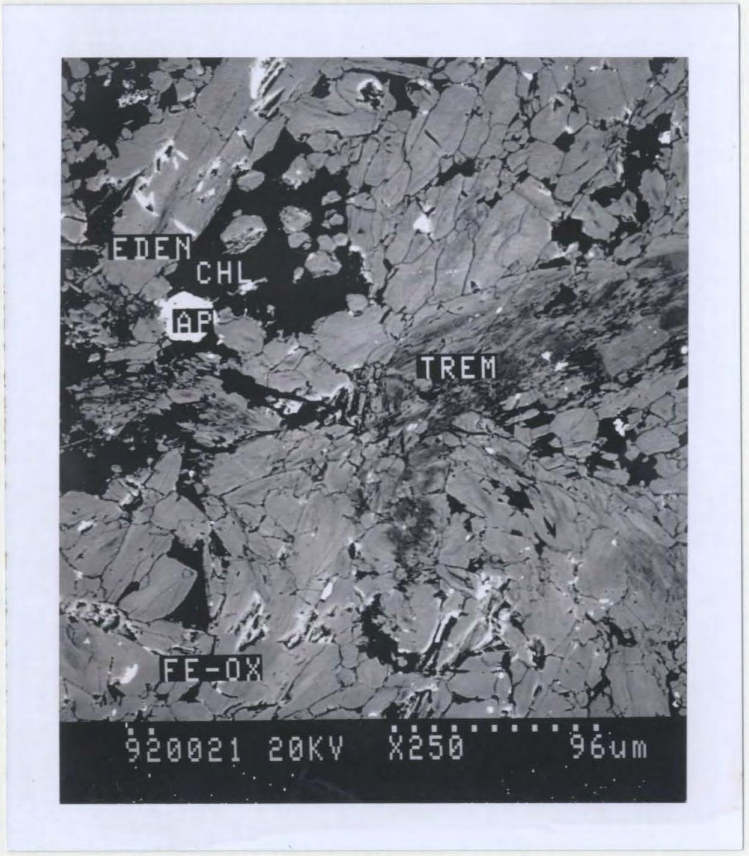

Figure 5.3: Scanning electron microscope (SEM) photograph of a sample of volcanic rock from the Noggin Cove Formation showing the two dominant metamorphic amphibole phases- edenite and tremolite. The edenite has a lighter tone and generally has a more bladed habit. The tremolite is darker and has a more fibrous habit. The white grains scattered throughout are iron oxides. SEM photograph is from the lower left area of the photograph in Figure 5.1a.

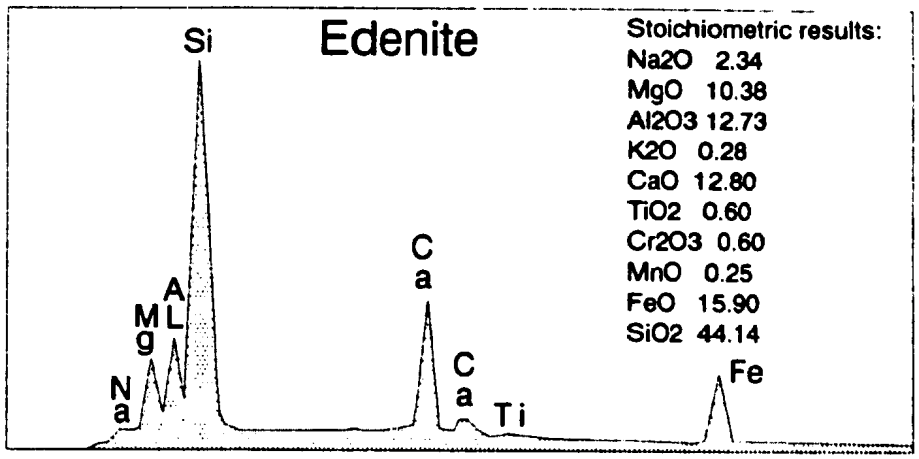

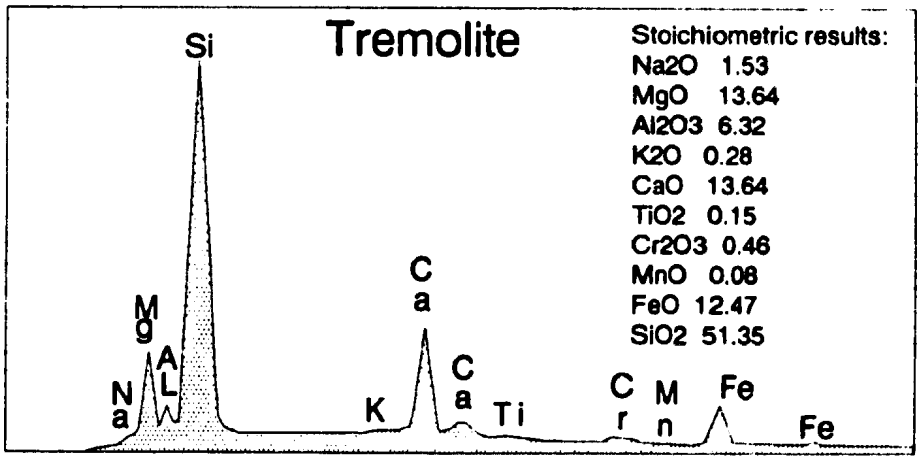

Figure 5.4: Semi-quantitative SEM analyses of the edenite and tremolite shown in Figure 5.3. Note the difference in SiO2, Al2O3 and Na2O content between the two amphiboles.

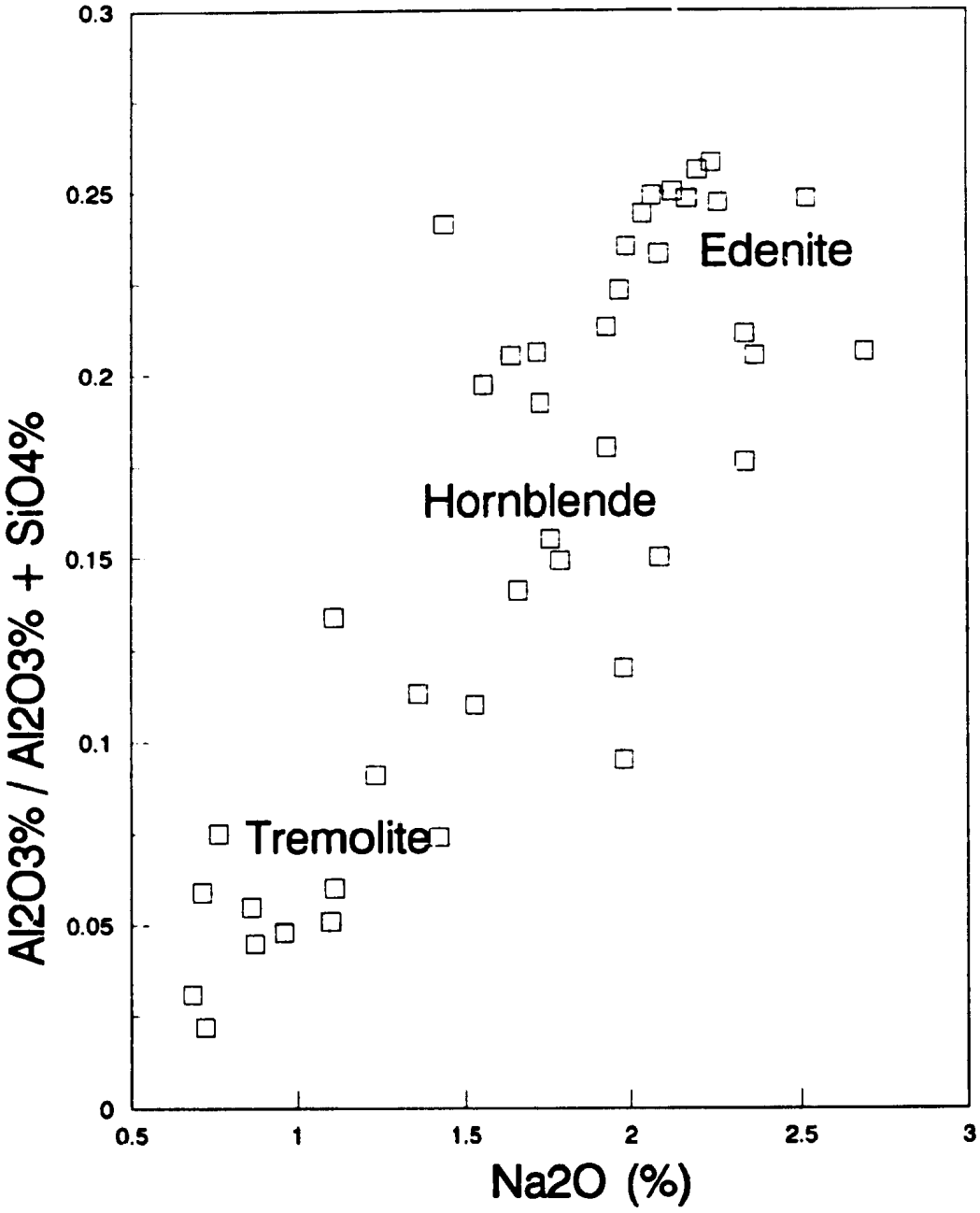

Figure 5.5: Na2O versus Al2O3/Al2O3 + SiO4 plot for amphiboles of the Noggin Cove Formation analysed on the SEM (Appendix V).

temperature. For a given bulk composition, the ideal portion of the equilibrium constant ($K_{id} = X_{Na,A} / X_{\square,A} \quad X_{Ab}$) increases with increasing temperature (Spear, 1981). This reaction explains the abundance of edenite in all samples. Quartz is common in the fragmental rock but is very fine-grained and can only be distinguished at higher magnifications with the SEM.

Both the plagioclase and amphibole solid solutions are distinctly non-ideal: both exhibit miscibility gaps. At temperatures below 700°C, plagioclase solid solutions exhibit immiscibility across the peristerite (Ab100-Ab86), Huttenlocher (Ab40-Ab10), Boggild (Ab55-Ab40) and Voll (Ab60-Ab10) gaps (Spear, 1981). Immiscibility occurs in amphibole solid solutions between calcic and sodic amphiboles and possibly between actinolite and hornblende (Spear, 1980; 1981). To overcome the problem of non-ideality, partitioning of Ca and Na between plagioclase and amphibole is evaluated on an empirical basis by examination of the ideal portion of the equilibrium constant; following Spear (1981).

For comparative purposes, the mol fraction data in Table 5.2 are plotted in Figure 5.6 in a manner consistent with Spear (1981). Tie lines between plagioclase (X_{Ab}) and amphibole ($X_{Na,A}$) steepen with increasing metamorphic grade. If Figure 5.5 is compared to data from naturally occurring amphibolites of known metamorphic grade (Spear, 1981), it can be seen that the maximum metamorphic grade represented by

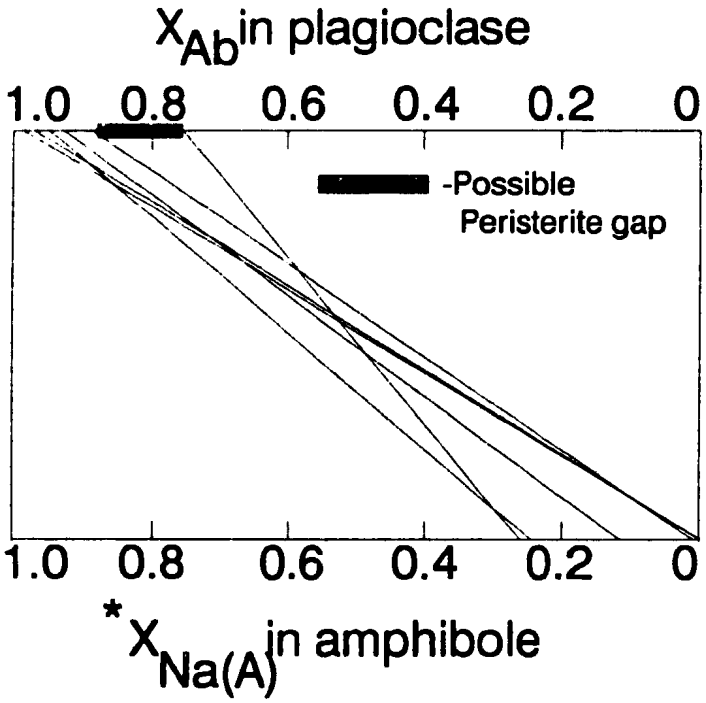

Figure 5.6: Tie lines for data from Table 5.2.
Projection and plot format from Spear, 1981.

these results is middle greenschist facies.

Spear (1981) empirically calibrated a plagioclase-amphibole thermometer based on reaction 1. Assuming ideal mixing in amphibole and plagioclase solutions, an equilibrium constant can be written for reaction 1, for which the ideal portion is;

$$K_{id} = X_{Na,A}/X_{\square,A} \cdot X_{Ab}$$

where $X_{\square,A}$ = mol fraction of the A site vacancy of the amphibole.

Thermodynamic values for reaction 1 are:

$\ln K_{id} = 3.45 - 2{,}914 \cdot 1 / T\ (°K)$

$\Delta H = 7{,}075$ cal/mol

$\Delta S = 6.86$ e.u.

$\Delta V = -0.257$ cal/bar , for P = 5kbar and $X_{Ab} = .75$ (Spear, 1981).

Calculated temperatures may be in error by as much as ±100°C due to the possible error in calculating $X_{Na,A}$ (Spear, 1981). Spear emphasized that these thermodynamic data are valid only for $X_{Ab} = 0.75$. Using the thermodynamic values above, a temperature of 374°C was calculated for the coexisting albite ($X_{Ab} = 0.77$) and tremolite, this feldspar composition closely approximating the required $X_{Ab} = 0.75$. This temperature is an

estimate because of the possible errors in the determination of $^{V}_{Na,A}$ and the assumption of P = 5kbars. It appears realistic and is compatible with other petrologic indicators.

Brown (1977) reported that the crossite or Na_{M4} ($=Na_B$) content of Ca-amphiboles is a useful indicator of the pressure of metamorphism in the greenschist and lower amphibolite facies. At higher temperatures, pressures are indicated by different assemblages of Fe-Mg-Al silicate minerals; higher pressures are indicated by blueschist facies minerals. Brown found that in high pressure amphiboles, Na_{M4} varies inversely with Al in the tetrahedral (T) site. This relationship is best shown graphically, with Na_{M4} on the vertical axis and Al^{IV} on the horizontal axis. For comparative purposes, Na_{M4} versus Al^{IV} for amphiboles analysed on the microprobe was plotted in Figure 5.7a in a manner consistent with Brown (1977). Site allocations (ie: Na_{M4} and Al^{IV}) for each analysis are given in Appendix III. In Figure 5.7a, each sample is given a different symbol and each analysis is given a number which can be referenced back to Table 5.1. Figure 5.7b shows where amphiboles from relatively high pressure/low temperature terranes (Shuksan, Sanbagawa, Otago) and from relative high temperature/low pressure terranes plot in Na_{M4} vs Al^{IV} space.

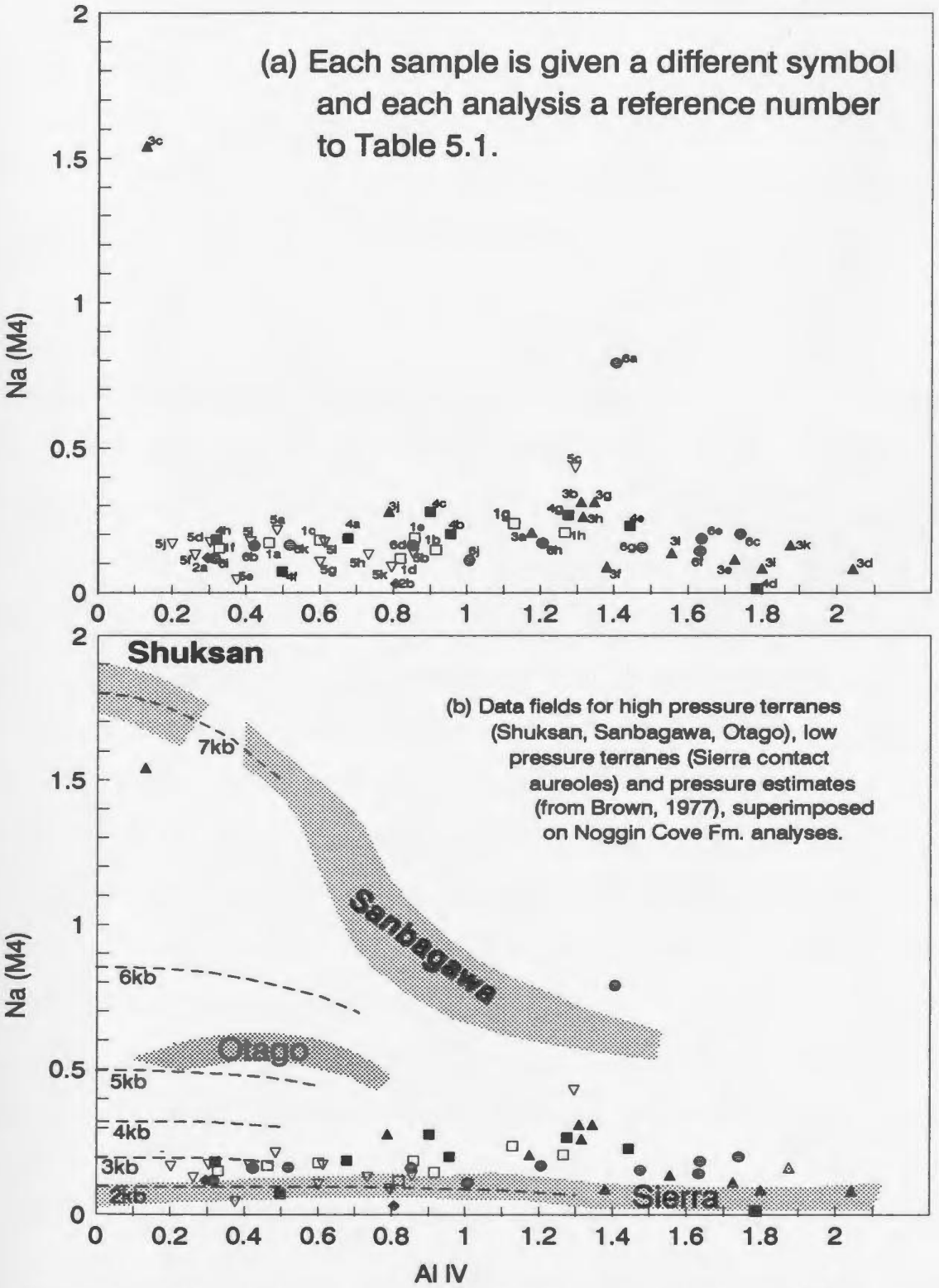

Figure 5.7: Na(M4) versus Al IV plot for amphiboles of the Noggin Cove Formation analysed on the electron microprobe (Table 5.1).

5.4 Interpretation

The assemblage:

albite + tremolite + chlorite + epidote

(+quartz, +sphene, ±calcite, ±biotite),

observed in thin sections, indicates metabasalts of the Noggin Cove Formation have undergone greenschist facies metamorphism. A maximum of middle greenschist facies metamorphic grade is indicated by a comparison of $X_{Ab}/X_{Na,A}$ tie lines (Figure 5.6) to those of Spear (1981), derived from data from naturally occurring amphibolites. Greenschist facies metamorphism is also suggested by a very approximate temperature estimate of 374°C, calculated from microprobe analyses of coexisting tremolite-albite using the thermodynamic data of Spear (1981). Based on the Na_{M4} versus Al_{IV} content in amphiboles, the pressure estimates of Brown (1977) suggest pressure was low during regional metamorphism of the Noggin Cove Formation (less than 4 kbars; Figure 5.7).

Two compositionally distinct coexisting amphiboles in metabasalts of the Noggin Cove Formation can be distinguished in thin section by a contrast in habit, pleochroism and birefringence (eg. Figure 5.1). The two amphiboles were identified as tremolite and edenite using the electron microprobe (Table 5.1) and SEM (Figures 5.3, 5.4, 5.5,

Appendix V). Zoned amphiboles generally have cores of tremolite which are rimmed by edenite (Appendix V).

The reaction albite + tremolite = edenite + 4 quartz proceeds to the right with increasing temperature (Spear, 1981); this equilibrium almost certainly accounts for the high proportion of edenite in metabasalts of the Noggin Cove Formation. Comparison with edenitic amphiboles in the Sierra contact aureole (Figure 5.7) suggests that edenitic amphiboles ($Al^{IV} > 1.0$; $Na_{M4} < 0.25$) of the the volcanic rocks of the Noggin Cove Formation formed during a contact metamorphic event. Zoned amphiboles suggest that the tremolite cores formed first and that edenite developed later. This is compatible with the tremolite forming during regional greenschist facies metamorphism and edenite forming during a later contact metamorphic event. Preservation of the tremolite cores suggests the high temperatures responsible for the formation of edenite rims were relatively short-lived and that low fluid/rock ratios prevailed during the later metamorphism. Prolonged regional metamorphic conditions would likely have resulted in the homogenization of the amphibole compositions.

The earlier greenschist facies regional metamorphism is likely associated D_2. The onset of regional metamorphism may have been the result of tectonic thickening due to thrust faulting- evidence for F_1 recumbent folding and thrusting is presented in Chapter 2. Karlstrom et al. (1982) presented

evidence for a major Silurian F_1 thrusting episode west of the Noggin Cove Formation in the Port Albert Penisula-Notre Dame Bay area. Currie and Pajari (1981), and Currie (1992), suggested that metamorphism and plutonism in the Carmanville area may be the result of tectonic thickening due to southerly directed thrusting.

The later episode of contact metamorphism can be attributed directly to the Frederickton, Rocky Bay and Aspen Cove plutons that postdate D_2. The high proportion of edenite in samples not in close proximity to these plutons suggests that the plutons are more extensive at depth. This conclusion is supported by field evidence: numerous felsic dykes and small intrusions cut volcanic rocks of the Noggin Cove Formation, even at considerable distances from the plutons (eg. Davidsville, Lower Island, Noggin Point, Noggin Cove). The Noggin Cove Formation may be a thin carapace of volcanic rocks overlying plutons which are far more extensive at depth than their surface expression implies.

Chapter 6

Regional correlations and comparisons with other Exploits Subzone units.

6.1 Introduction

An important result of recent work is the recognition that rocks in the Carmanville area are more typical of rocks to the west in the Bay of Exploits than of rocks of the Davidsville Group to the southeast (Williams et al., 1991; Williams, 1992; Currie, 1992; Johnston, 1992). The principal objective of this chapter is to show that the Noggin Cove Formation, the Carmanville Melange, and the Woody Island Siltstone are eastern units that correlate westward with rocks of the Summerford Group, Exploits Group, and Wild Bight Group.

6.2 Noggin Cove Formation/Carmanville Melange versus Summerford Group/Dunnage Melange

The Carmanville Melange has been correlated with the Dunnage Melange (eg. Kennedy and McGonigal, 1972; Pajari et al., 1979; Karlstrom et al., 1982; Williams, 1992 and Currie, 1992). In support of this correlation, many aspects of the Carmanville Melange noted in this account are strikingly similar to aspects of the Dunnage Melange noted by Hibbard and

Williams (1979). Hibbard and Williams state that: (1) "regional tectonic elements... indicate that the (Dunnage) melange formed on the flank of a Lower Ordovician island arc complex"; (2) the melange is a chaotic equivalent of nearby units (ie: matrix and blocks are locally derived); (3) the chaotic aspect is primary and formed as the result of a single, progressive large scale surficial slump (ie: olistostromal origin); (4) the present attitude of the melange is controlled by later, hard rock deformation and (5), the formation of the melange marks a major change from active arc volcanism to arc degradation and basinal infilling.

Each of the five features of the Dunnage Melange noted above can be matched to equivalent features of the Carmanville Melange.

(1) The paleotectonic setting proposed for the succession Noggin Cove Formation→Carmanville Melange→Woody Island Siltstone is along the arc flank of a Lower Ordovician back-arc basin. Hibbard and Williams (1979) state that the Dunnage Melange may have formed in a back-arc basin but proposed no modern analogues.

(2) mafic blocks in the Carmanville Melange can be matched lithologically and geochemically to volcanic rocks of the Noggin Cove Formation. The more common sandstone and siltstone

blocks, and the black shale matrix, have equivalents in the Woody Island Siltstone.

(3) The Carmanville Melange is interpreted in this study as olistostromal in origin and stratigraphically overlying the Noggin Cove Formation (see Chapter 3). The Carmanville Melange is less extensive compared to the Dunnage Melange and olistostromes are interpreted as being triggered by block faulting associated with arc rifting. The thixotropic activation of the Dunnage Melange is attributed to the intrusion of the Coaker Porphyry and associated rocks.

(4) The Carmanville Melange is interfolded with, and has the same strong northeast trending cleavage as, the Noggin Cove Formation and Woody Island Siltstone (see chapter 3). The thixotropic nature of the Carmanville Melange made it susceptible to remobilization during deformation. Locally the melange forms small dykes that pierce adjoining units. Interfingering occurs locally along contacts (see Chapter 3). All such disruptive features are parallel to the strong S_2 cleavage, suggesting they are the result of hard-rock deformation (see also Williams, 1983).

(5) Although mafic blocks are a very striking feature of the Carmanville Melange, volumetrically they are minor. The

melanges record an abrupt cessation of active volcanism and volcaniclastic deposition. However, the olistostromes record continued block faulting as the arc is rifted and the back-arc basin forms (represented by the manganese rich, deeper water sedimentary rocks of the Woody Island Siltstone; see Chap. 7).

Furthermore, both the Carmanville Melange and Dunnage Melange contain large blocks of psammitic schists with pre-entrainment schistosity and metamorphism (H. Williams, pers. comm.).

Jacobi (1984) noted many similarities between the Dunnage Melange and modern submarine sediment slides. Both are internally chaotic. Soft sediment deformational features of the Dunnage Melange similar to those observed in cores from modern submarine sediment slides include pebbly mudstones with no scaly cleavage and isoclinal folds overprinted at high angles by a non-axial-planar cleavage. The Carmanville Melange also exibits these features. It is internally chaotic and generally lacks a scaly cleavage. Isoclinal folds are common but are enigmatic. It is difficult to distinguish isoclinal folds due to F_1 from isoclinal slump folds because of the general lack of F_1 cleavage; most are rotated into the strong regional S_2 cleavage (eg. Woody Island; shoreline 1 km northeast of Frederickton). This strong cleavage would likely obliterate any syn-depositional dewatering cleavage.

Using high resolution seismic records, Jacobi (1984) was able to delineate three depositional facies within giant submarine sediment slides: "hummocky", "blocky", and "debris flow". He interpreted these seismic facies as olistoliths, piles and/or folds of deformed sediment, and debris flow deposits, repectively. Accordingly, the general downslope sequence is hummocky → blocky → debris flow material, all with gradational contacts. Many slides lack hummocky and/or blocky material.

Jacobi's findings have two important implications with regard to the relationship between the Carmanville Melange and the Noggin Cove Formation. First, Jacobi's findings support the assertion of this study that the melanges are olistostromal and are depositionally related to the debris flows of the Noggin Cove Formation. Debris flow conglomerates are the most spectacular and dominant feature of the Noggin Cove Formation. The olistostromes may be upslope depositional equivalents of the debris flows, deposited during the same submarine sediment slide. Piston core studies, and theoretical and experimental considerations, suggest debris flows move as viscous slurries which result in deposits similar to unconsolidated pebbly mudstones (ie: olistostromes; Fisher, 1984; Jacobi, 1984).

The second important implication of Jacobi's findings has to do with the location of the source area for the debris

flows and olistostromes. The Carmanville Melange generally occurs north of the debris flow conglomerates of the Noggin Cove Formation. The only exception is the melange at Davidsville. This distribution is consistent with a northerly source area given Jacobi's downslope sequence of hummocky → blocky → debris flow material. This sequence is similar to that proposed by Fisher (1984) for the deposition of volcaniclastic rocks on the subaqueous slopes of volcanoes (Figure 6.1). Thus, the distribution of melanges with respect to the debris flows suggests a northerly source area, consistent with that proposed for the Noggin Cove Formation (see Chapter 2). The largest occurrence of the Carmanville Melange at Teakettle Point is just north of volcanic conglomerates with spectacular outsized intraclasts which outcrop along the east shore of Carmanville Arm. These chaotic volcanic conglomerates are in turn north of debris flow conglomerates at the head of Carmanville Arm and southward. This southerly succession of melange → outsized blocks → debris flows may be representative of Jacobi's downslope sequence. In the rift environment proposed in this study, high sediment supply and falling sea-levels would cause an off-lapping of this sequence. This would result in the melanges overlying the debris flows, as proposed in chapters 2 and 3.

The foregoing discussion supports the conclusions that the Carmanville Melange is olistostromal and has many features

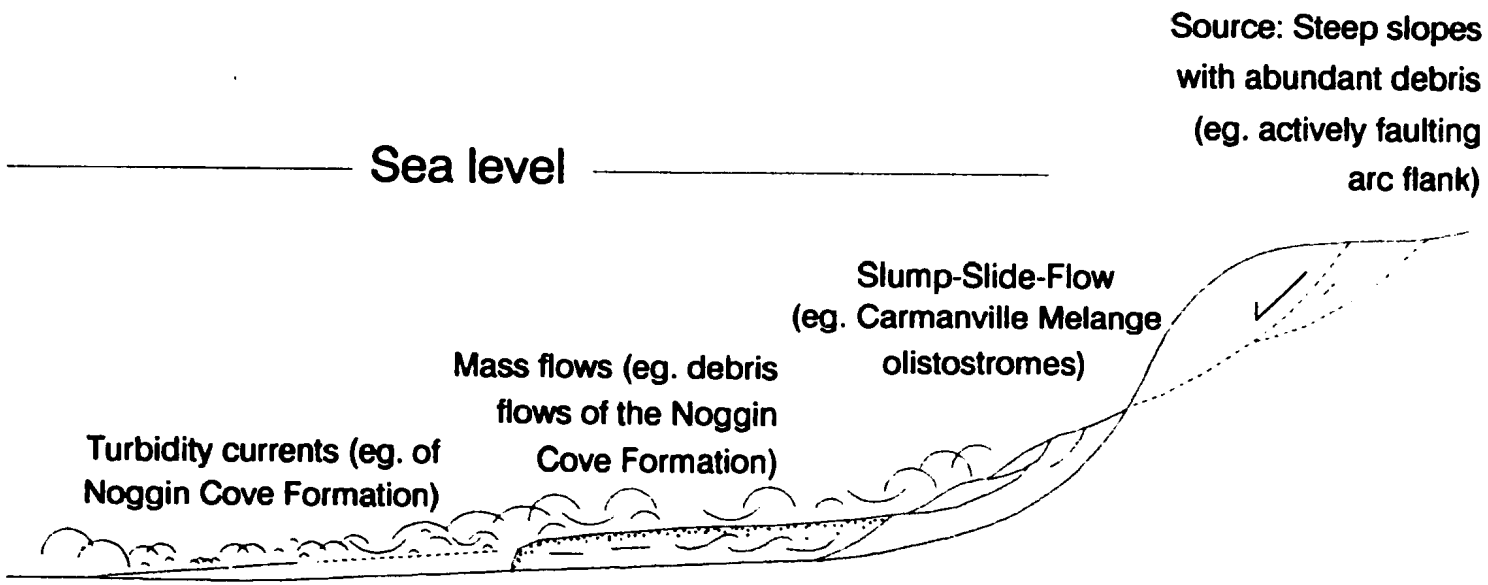

Figure 6.1: Proposed depositional setting and dominant subaqueous transport processes for debris flows and turbidites of the Noggin Cove Formation and olistostromes of the Carmanville Melange. Modified from Fisher (1984) and Jacobi (1984).

in common with the Dunnage Melange. It also implies that the olistostromal Carmanville Melange is depositionally related to the debris flow conglomerates of the Noggin Cove Formation. At a minimum, the olistostromes of the Carmanville Melange represent a continuation of the same depositional process; the lithologies are radically different due to the cessation of active volcanism. If a lithic belt of melange and associated coticule bearing rocks can be correlated across the northeast Exploits Subzone (Williams 1992), the Noggin Cove Formation should have equivalent units to the west associated with this lithic belt.

The geochemistry and lithology of the mafic blocks in the Carmanville Melange strongly suggest they are derived from the same source as the volcanic rocks of the Noggin Cove Formation or are derived directly from the Noggin Cove Formation (see Chapters 3 and 4). Based on geochemistry and lithology, Wasowski and Jacobi (1985) propose a similar kinship between mafic blocks in the Dunnage Melange and volcanic rocks of the Summerford Group. The Summerford Group is a sequence of mafic volcanic rock and interbedded carbonate rocks, arkosic sandstone, pebbly mudstone and argillite. The volcanic rocks are mafic pillow lavas, lapilli tuffs, and tuff breccias as well as isolated pillow and broken pillow tuff breccias (Horne, 1970; Williams, 1963). Ages obtained from carbonates associated with the volcanic rocks range from

Tremadocian to Llandeilian/Caradocian (Williams, 1963; Kay, 1967; Neuman, 1968; Horne, 1970; Dean, 1971; Bergstrom et al., 1974; McKerrow and Cocks, 1978). The Summerford Group occurs north of the Dunnage Melange. The Noggin Cove Formation occurs south of the Carmanville Melange. It is beyond the scope of the present study to rationalize this difference in distribution. However, the Noggin Cove Formation is comparible in age and lithology to volcanic rocks of the Summerford Group and both units are intimately associated with correlative melanges.

Geochemical data generally support a Noggin Cove Formation/Carmanville Melange-Summerford Group/Dunnage Melange correlation. The basalts of both volcanic units are predominantly ocean island or E-type midocean-ridge tholeiites (Chapter 4; Jacobi and Wasowski, 1985). An important difference in the geochemistry of the two units is the presence of early arc basalts in the Noggin Cove Formation. Other units with which the Summerford Group may be correlative, the lower Expoits Group and Wild Bight Group (Dean, 1978), also had an early stage of arc volcanism (Dec et al., 1992; Swinden et al., 1990). It is problematic that no early arc volcanism is reported for the Summerford Group.

6.3 Noggin Cove Formation/Carmanville Melange/Woody Island Siltstone - Tea Arm Volcanics/Strong Island Chert (Lower Exploits Group)

Lithologically and geochemically, the rocks of the Noggin Cove Formation, Carmanville Melange and Woody Island Siltstone record an Early Ordovician transition from arc to back-arc basin magmatism and deposition (Chapters 2, 3, 4 and 7). A similar Early Ordovician volcano-sedimentary succession is seen in the rocks of the upper Tea Arm Volcanics and Strong Island Chert of the Exploits Group (Dec et al., 1992).

Lithologically, the Tea Arm Volcanics are similar to the volcanic rocks of the Noggin Cove Formation. As defined by Horne and Helwig (1969), the Tea Arm Volcanics are basaltic and consist of pillow lava, volcanic breccia, lava flows, agglomerate, intrusive lava, and minor tuff, chert and limestone. The extended rare earth plot for a sample of pillow lava from the Tea Arm Volcanics (Dec et al., 1992) has an arc signature very similar to samples of arc basalts from the Noggin Cove Formation (Figure 6.2). The overlap in extended REE plots strongly supports the correlation of these two units. And the overlap of extended REE plots of the Tea Arm Volcanics' sample and Valu-Fa Ridge dredge samples supports the back-arc basin paleotectonic setting proposed by Dec et al., (1990) for the overlying Strong Island Chert. The Valu-Fa

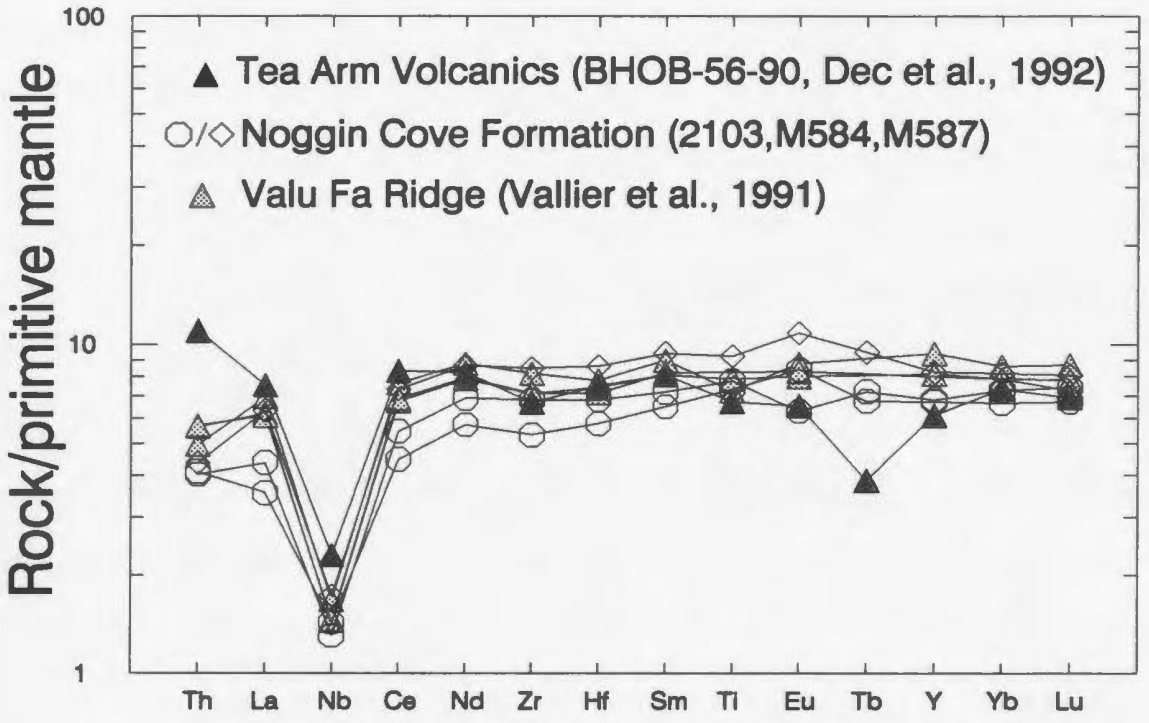

Figure 6.2: Comparative extended REE plots for samples from the Tea Arm Volcanics, Noggin Cove Formation and Valu Fa Ridge. Normalizing values from Swinden et al., 1990.

ridge is an active back-arc spreading ridge in the Lau Basin; the Lau Basin separates the active Tofua volcanic arc from the Lau Ridge remnant arc (Vallier et al., 1991).

The Tea Arm Volcanics are conformably overlain by rocks of the Strong Island Chert. This formation consists of radiolarian cherts, siliceous shales, felsic tuffs and epiclastic sandstones and conglomerates; interbedded with these varied lithologies are basaltic lava flows and pillows (Dec et al., 1992). Graptolites in black shales are early Llanvirn in age (Williams et al., 1992). The Strong Island Chert is in turn conformably overlain by Caradocian black shales (O'Brien, 1990).

A back-arc basin depositional setting has been proposed for the sedimentary rocks of the Strong Island Chert formation. This is based largely on the high proportion of ribbon radiolarites, which are interpreted as deep marine deposits that accumulated in small, arc-related, marginal basins (Jenkyns and Winterer, 1982; Hein and Karl, 1983; Jones and Murchey, 1986). The non-arc, extended REE signature of a sample of pillow lava intercalated with these ribbon radiolarites is very similar to that of Type N-I lavas of the Wild Bight Group (Figure 6.3). Type N-I lavas are modelled by Swinden et al. (1990) as low to moderate partial melts of an ocean island basalt (OIB)-like source in a back-arc setting. A sample from a gabbro block in the Carmanville Melange has an

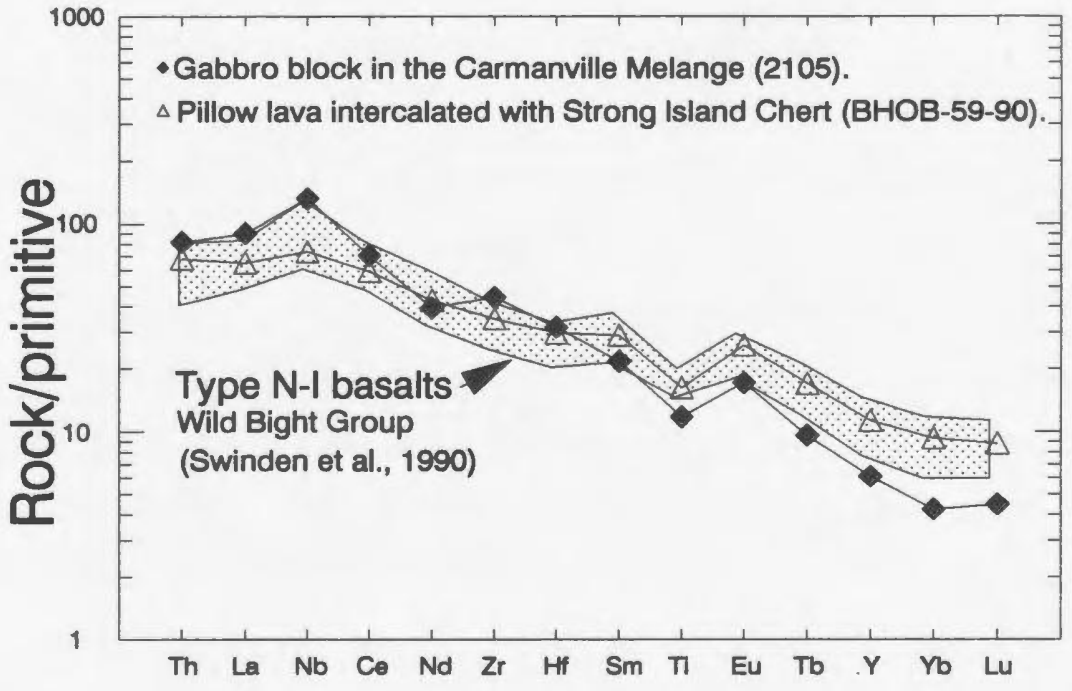

Figure 6.3: Comparative extended REE plots for samples of volcanic rock from the Strong Island Chert and Carmanville Melange. Normalizing values from Swinden et al., 1990.

extended REE signature very similar to the pillow lava sample from the Strong Island Chert and to N-I lavas of the Wild Bight Group (Figure 6.3)

The arc to back-arc transition recorded in the geochemical and stratigraphic successions support a chemostratigraphic correlation of the Tea Arm Volcanics/Strong Island Chert with the Noggin Cove Formation/Carmanville Melange/Woody Island Siltstone. A similar chemostratigraphic correlation has recently been proposed between the Tea Arm Volcanics/Strong Island Chert and the Wild Bight Group (Dec et al., 1992). Thus, the Noggin Cove Formation, Carmanville Melange and Woody Island Siltstone may be the easternmost units of broadly correlative, early to mid Ordovician units that extend west to include rocks of the Exploits and Wild Bight Groups.

6.4 Noggin Cove Formation/Carmanville Melange/ Woody Island Siltstone - Wild Bight Group

Geochemically, the volcanic rocks of the Noggin Cove Formation and Carmanville Melange are remarkably similar to volcanic rocks of the Wild Bight Group. A comparison of the extended REE plots highlights the striking similarity in the geochemical evolution of the Wild Bight Group and the Noggin Cove Formation/Carmanville Melange (Figures 6.4 and 6.5).

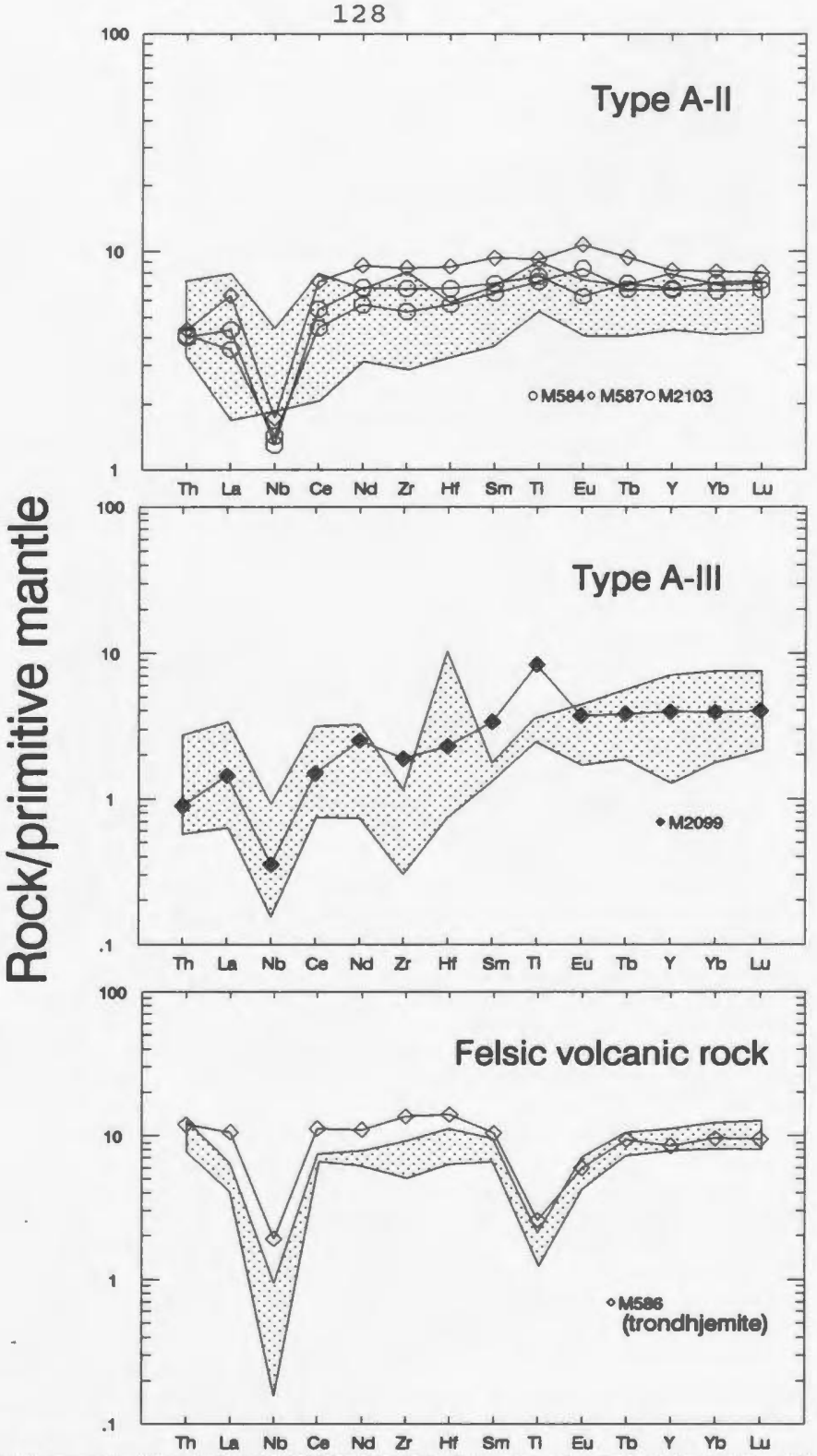

Figure 6.4: Comparative extended REE plots for samples of volcanic rock from the Noggin Cove formation, Carmanville Melange and Wild Bight Group. Data for Wild Bight Group (stippled) and normalizing values from Swinden et al., 1990. Symbols for Noggin Cove Formation and Carmanville Melange as per Fig. 4.1.

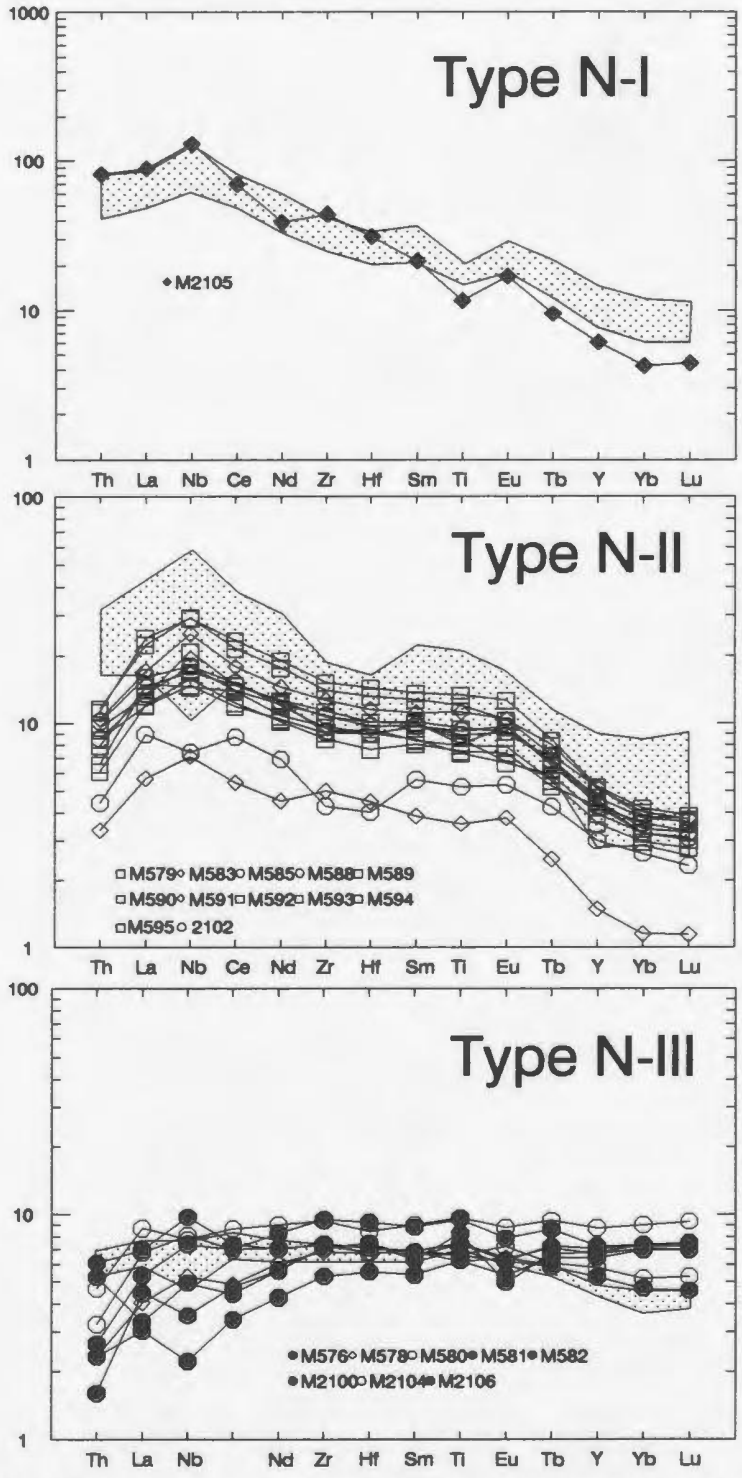

Figure 6-5: Comparative extended REE plots for samples of volcanic rock from the Noggin Cove Formation, Carmanville Melange and Wild Bight Group. Data for Wild Bight Group (stippled) and normalizing values from Swinden et al., 1990. Symbols for Noggin Cove Formation and Carmanville Melange as per Fig. 4.1.

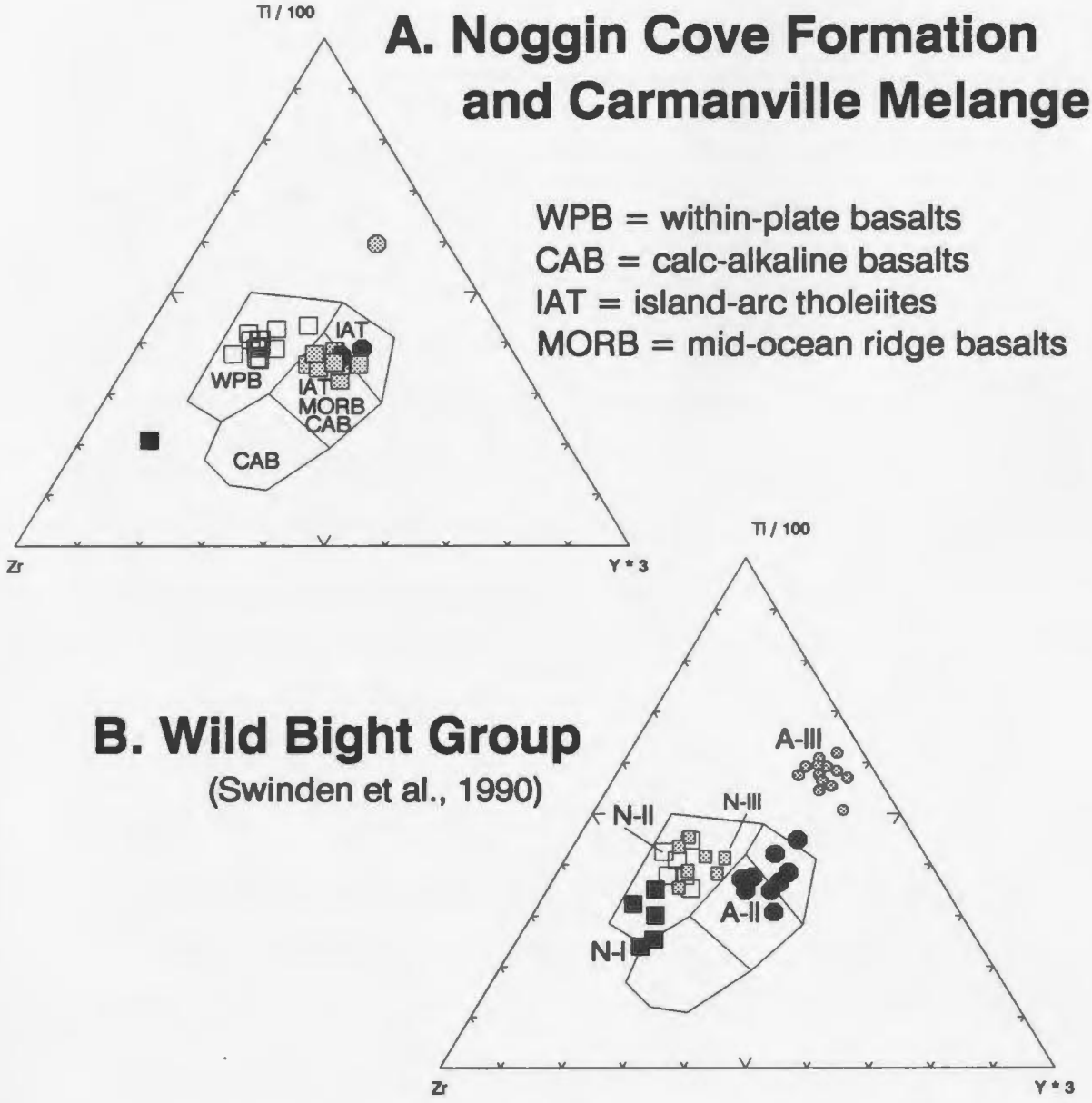

Figure 6.6: Comparative Ti-Zr-Y discrimination diagrams for samples of volcanic rock from the Noggin Cove Formation, Carmanville Melange and Wild Bight Group. Note the stronger MORB component for type N-III volcanic rocks of the Noggin Cove Formation and Carmanville Melange. The one sample of type N-I volcanic rock from the Carmanville Melange appears to have anomolously high Zr.

Plots of the different mafic lava types (A-II to N-III) on a Ti-Zr-Y discrimination diagram correspond to those of the Wild Bight Group (Figure 6.6a versus 6.6b). Type N-III lavas of the Noggin Cove Formation/Carmanville Melange are generally more MORB-like, less LREE enriched, than the Wild Bight Group, indicating a stronger component of normal depleted mantle and a weaker component of OIB partial melting in the magma source.

An important aspect of the arc to back-arc geochemical evolution is that an active arc is rifted to form the back-arc basin. The geochemical evolution must correspond to a stratigraphic succession which records the rifting of the arc and subsequent basin development. The spectacular debris flows of the Noggin Cove Formation and the chaotic olistostromes of the Carmanville Melange record a very dramatic rifting event. The siltstones and shales which dominate the overlying Woody Island Siltstone represent deposition into the back-arc basin formed by arc rifting. Thus, in general terms, the stratigraphic succession proposed in this study matches the geochemical evolution. The arc to back-arc chemostratigraphic succession is correlative to similar coeval successions proposed for the Wild Bight Group (Swinden et al., 1990) and for the Tea Arm Volcanics/Strong Island Chert. A summary of the proposed chemostratigraphic correlations are given in Table 6.1.

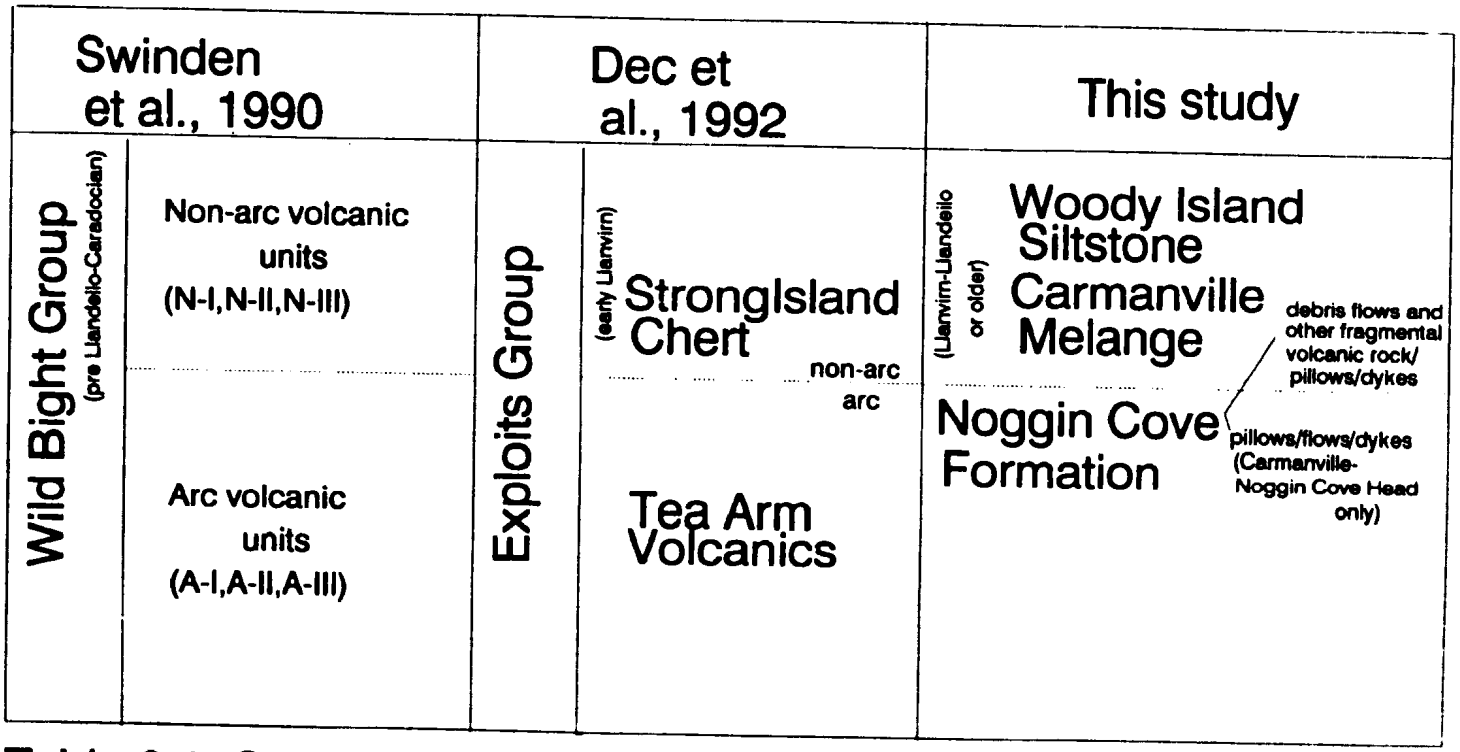

Table 6.1: Summary of proposed chemostratigraphic correlations across the northeast Exploits Subzone.

Chapter 7

Summary, Interpretation, and Significance

7.1 Summary and Interpretation

7.1.1 Noggin Cove Formation

The Noggin Cove Formation is dominated by fragmental volcanic rocks. The fragmental rocks were largely deposited as debris flows, some of which are spectacular in terms of their thickness and the size of massive and bedded intraclasts. Southern exposures of the Noggin Cove Formation are almost entirely debris flow conglomerates and sandstones. Pillow lavas, massive lava flows and basaltic dykes are common in northern exposures of the Noggin Cove Formation. This north-south increase in abundance of debris flow conglomerates relative to basaltic lavas suggests the eroding volcanic edifice was to the north. This is supported by imbricated clasts in medium bedded tuffs at Noggin Cove that indicate a south to southwest paleo-flow direction.

Large intraclasts of massive conglomerate are common in northern exposures of volcanic conglomerates (eg. Noggin Cove, Carmanville South) but are rare in conglomerates to the south. A single occurrence of large sub-rounded blocks of massive lava (up to 0.6m x 1.8m in size), suspended in a fine-grained

tuffaceous matrix, outcrops in the town of Noggin Cove; this "conglomerate" suggests mass wastage in a very proximal setting.

The vesicular clasts of the debris flow conglomerates indicate a subareal to shallow marine source (less than 200m below water level; Fisher, 1984). Medium bedded cross-stratified calcareous tuffs, and a lapilli breccia with a calcite matrix, are found only to the north; these are interpreted as shallow marine deposits fringing a volcanic island.

The Noggin Cove Formation is interpreted as a volcaniclastic apron shed from a northern subareal to shallow submarine explosive volcanic source. A large volume of fragmental volcanic rock was deposited onto and south of basaltic pillow lavas, dykes and flows, which presumably formed part of the pedestal of an island volcano (Figure 7-1).

A back-arc basin paleotectonic setting for the Noggin Cove Formation, and an island arc source for some magmas, is indicated by geochemical results (Chapter 4). The high proportion of fragmental volcanic rocks relative to the primary volcanic rocks of the Noggin Cove Formation, the preponderance of vesicular clasts, the monomictic nature of the conglomerates and exclusion of foreign clasts, and the sheer volume of the fragmental volcanic rock all suggest a

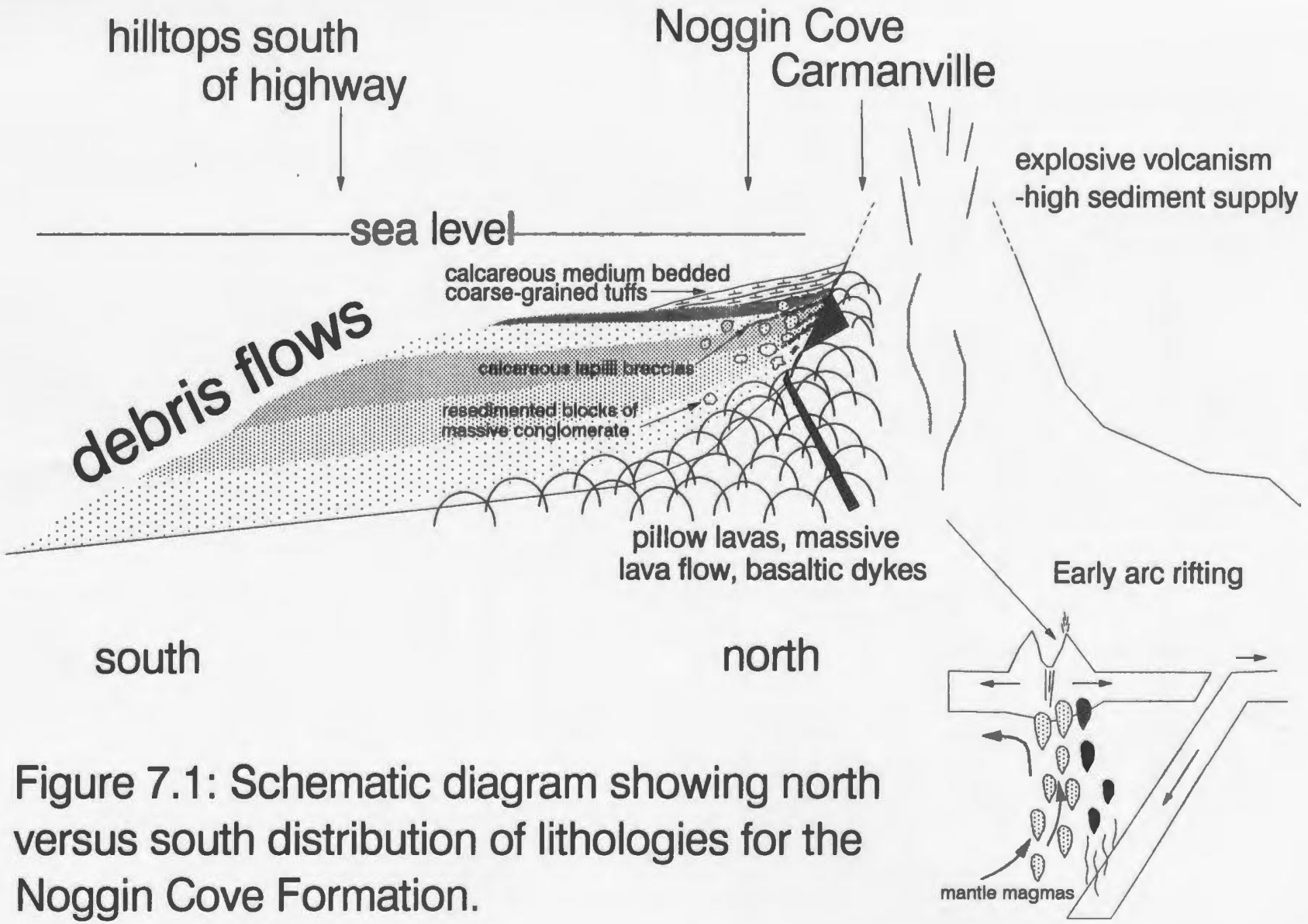

Figure 7.1: Schematic diagram showing north versus south distribution of lithologies for the Noggin Cove Formation.

highly explosive volcanic origin (ie: island arc; Garcia, 1978). To reconcile these interpretations, the Noggin Cove Formation may represent a volcanic complex on the arc flank of a back-arc basin.

Slumping occurs more frequently on the arc flank of back-arc basins than in any other tectonic setting due to the combination of several factors: steep regional gradients, high seismicity, rapid sediment accumulation, unstable sediment structure (eg. thixotropic properties of montmorillonite), and shallow level intrusions into the sediments on steep slopes (Lonsdale, 1975; Busby-Spera, 1988). The thicknesses of many debris flows of the Noggin Cove Formation is likely the result of storage of the fragmental volcanic rock on the slopes of a volcano; the release of the stored debris is triggered by earthquakes and/or gravitational instability. Bedded and massive intraclasts in volcanic conglomerates of the Noggin Cove Formation attest to lithification prior to disruption and resedimentation. The same is true for a chaotic conglomerate that occurs at Noggin Point and in Noggin Cove; this conglomerate consists of angular clasts of finely bedded siltstone in a limestone matrix and is interbedded with a lapilli breccia. Strong earthquake activity is presumed necessary for disruption of the previously lithified rock incorporated in these conglomerates.

Basaltic intra-plate volcanism (ie: OIB and MORB) that

accompanied deposition of the Noggin Cove Formation volcaniclastic apron also suggests an arc flank paleotectonic setting. Intra-plate volcanism is more common along the "hotter" arc flank than along the "colder" remnant-arc flank of a back-arc basin (Weissel, 1981; Busby-Spera, 1988). OIB, MORB and arc volcanic rocks have been obtained from the arc flank of the Lau Basin (G. Jenner, pers. comm., 1992).

7.1.2 Carmanville Melange

Most features of the Carmanville Melange indicate an olistostromal origin. These include; bedded melange (eg. Beaver Cove, Noggin Cove, Teakettle Point, Rocky Point), interbedding and interfolding of melange with rocks of the Noggin Cove Formation or Woody Island Siltstone (eg. Noggin Cove, Woody Island), and the presence of thin siltstone beds within the matrix of the melange.

Other distinctive features indicate hard-rock remobilization of the melanges <u>after</u> olistostrome deposition.

(1) Thin siltstone beds in the melanges are kinked and offset by the strong regional S_2 cleavage.

(2) Black shale matrix locally pierces adjoining beds of melange with a light green, tuffaceous matrix; piercement is parallel to the regional cleavage.

(3) Black shale matrix penetrates blocks of light green very-fine grained tuff (eg. Figure 3.1e); this penetration is

parallel to sub-parallel to the regional cleavage.

(4) A "melange dyke" cuts bedded sediments of the Woody Island Siltstone parallel to the regional cleavage. This "dyke" is an offshoot of melange which is interbedded with sediments of the Woody Island Siltstone (Figure 3.1f; see also Figure 10 of Pajari et al., 1979).

The hard-rock deformational features can all be related to S_2, which has a much stronger expression in the melanges than in adjoining units (ie: Noggin Cove Formation, Woody Island Siltstone). These D_2 features obscure the original olistostromal nature of the Carmanville Melange.

The transition from monomictic mafic conglomerates of the Noggin Cove Formation to the predominantly siliceous rocks of the Carmanville Melange and Woody Island Siltstone marks an abrupt cessation of volcanism. However, the olistostromal Carmanville melanges and slumped beds of the Woody Island Siltstone indicate continued instability. Like the debris flows of the Noggin Cove Formation, olistostrome formation and slumping in the Carmanville Melange, and "melange beds" of the Woody Island Siltstone, may be the result of gravitational instability and/or earthquakes. Clasts of previously formed melange within these units indicates disruption and resedimentation of lithified material.

7.1.3 Woody Island Siltstone

The Woody Island Siltstone consists of alternating beds of dark grey very fine-grained sandstone, dark grey siltstone, and dark grey to black shale. Thin (1-2cm) dark blue to black manganese-rich beds, and distinctive light pink coticule layers (fine-grained spessartine garnet and quartz), are a distinctive feature of the Woody Island Siltstone.

The Mn enrichment of sedimentary rocks of the Woody Island Siltstone and correlative units westward (see Williams, 1992) may be hydrothermal in origin and may be associated with sulphide deposition. Cronan et al. (1984), analysed over 180 samples from the Tonga-Kermadec Ridge and adjacent marginal basins (eg. Lau Basin). Manganese concentrations were low throughout much of the study area but were enriched up to 10-times in the sediments of the Lau Basin. Accumulation rates of Mn, 50 km west of the Lau Basin spreading ridge, approach those from hydrothermally active mid-ocean ridge crests; hydrothermal Mn enrichment occurs in sediments near spreading ridges which also exhibit sulphide deposition (eg. East Pacific Rise and Galapagos Rift; Cronan et al., 1984).

7.1.4 Arc rifting

Geochemical analyses indicate an evolution from arc to non-arc magmas for mafic rocks of the Noggin Cove Formation and Carmanville Melange (A-II → N-II → N-III; Table 4.2). This

transition may record rifting of an arc to form a back-arc basin (Figure 4.8). The spectacular debris flows of the Noggin Cove Formation, and chaotic olistostromes of the Carmanville Melange, also record this rifting event (Figure 6.1). Deposition of these units is attributed to earthquake activity which could be the result of block faulting as an arc is rifted. The enhanced relief provided by block faulting could explain the deposition of thick debris flows (Carey and Sigurdsson, 1984) of the Noggin Cove Formation and olistostromes of the Carmanville Melange. Block faulting may also expose ultramafic rock for incorporation into the melanges (eg. Rocky Point, Aspen Cove). Intensely deformed blocks in the melanges ("recycled" blocks and matrix of Williams et al., 1991) may be from deep-crustal fault zones exhumed by block faulting.

Shales, siltstones, and very fine grained sandstone of the Woody Island Siltstone represent deposition into the developing back-arc basin. Coticules are very common in the Woody Island Siltstone, indicating high levels of Mn; sediments near spreading ridges in modern back-arc basins also have high levels of Mn (eg. Lau Basin; Cronan et al., 1984).

7.2 Regional Tectonic Significance

7.2.1 Noggin Cove Formation - Gander River Complex

The ultramafic block at Aspen Cove, presumably derived from the Gander River Complex, and a "bedded melange" at Rocky Point that contains both volcanic rocks of the Noggin Cove Formation and altered ultramafic detritus (talc), may link the Noggin Cove Formation to the Gander River Complex. Mafic lavas of the Gander River Complex are of island arc affinity and are cut by trondhjemites, also with island arc geochemical signatures (O'Neill, 1991). Similarly, basaltic lavas in the immediate Carmanville area have island arc geochemical signatures and are cut by trondhjemite, which also has an island arc geochemical signature (Figure 4.4). Possibly, the Noggin Cove Formation is the upper portion of a dismembered ophiolite suite (Williams et al., 1991).

Many back-arc basins in the western Pacific have been partly subducted since their formation. Preferential preservation of oceanic crust adjacent to the thick, less easily subducted, arc flank, relative to oceanic crust towards the centre of the basin, has been predicted from studies of back-arc basin volcanic assemblages (see Busby-Spera, 1988; Vallier et al.,1991). The proximity of the Gander River Complex to the Noggin Cove Formation (arc flank) may explain its "preferential preservation".

7.2.2 Noggin Cove Formation - Davidsville Group

South of the Noggin Cove Formation, acid volcanic rocks, pillow basalts and gabbroic dykes occur with sedimentary rocks of the Davidsville Group (see Currie et al., 1980b). These sedimentary rocks range in age from late Arenig - early Llanvirn (Weirs Pond; O'Neill, 1991) to Caradoc (Williams, 1964). The volcanic rock associated with these sedimentary rocks may represent Mid- to Late-Ordovician, post ophiolite-emergence volcanism similar to that of the Twillick Brook Member of the Baie d'Espoir Group in the Mt. Cormack area (see Colman-Sadd et al., 1992). The REE signatures of the two samples of volcanic rock collected from the Davidsville Group are similar to the REE signatures of volcanic rock from modern back-arc basins (eg. Lau Basin, Scotia Sea; see chapter 4). The sample from the gabbroic dyke which cuts distinctive ribbon radiolarites at a small quarry on the north side of the road 3 km southwest of Carmanville is type N-II (Fig. 4.5). The ribbon radiolarites are interpreted as deep marine deposits that accumulated in a small arc-related marginal basin. The other sample of pillow lava from the Davidsville Group at Round Pond is type N-III (Fig 4.5).

In a model proposed by O'Neill (1991), based on work in the Weir's Pond area, Davidsville Group sedimentary rocks were originally deposited into a back-arc basin flanked on one side by an island arc (with exhumed ophiolitic substrate) and on

the other side by a continental source. This model agrees with the geochemical and stratigraphic arc to back-arc basin succession represented by the Noggin Cove Formation, Carmanville Melange and Woody Island Siltstone; presumably, the Davidsville Group was deposited in the same back-arc basin thus formed.

7.2.3 Noggin Cove Formation/Carmanville Melange -Summerford Group/Dunnage Melange -Exploits Group -Wild Bight Group

Correlation of the Noggin Cove Formation and Carmanville Melange across the northeast Exploits Subzone provides the necessary scale for meaningful comparisons to modern analogues (eg. Tonga-Lau region of the SW Pacific Ocean; Figure 7.2). The proposed paleotectonic setting for the Noggin Cove Formation and the Carmanville Melange is along the arc flank of a back-arc basin. The Noggin Cove Formation is correlated with the Summerford Group and both units are intimately associated with correlative melanges (Chapter 6). The Dunnage Melange may have formed in a back-arc basin (Hibbard and Williams, 1979), or more specifically, on the arc flank of a back-arc basin (Jacobi, 1984).

The back-arc basin paleotectonic setting proposed for the Noggin Cove Formation and Carmanville Melange is interpreted to have formed by rifting of an island arc. An arc to back-arc

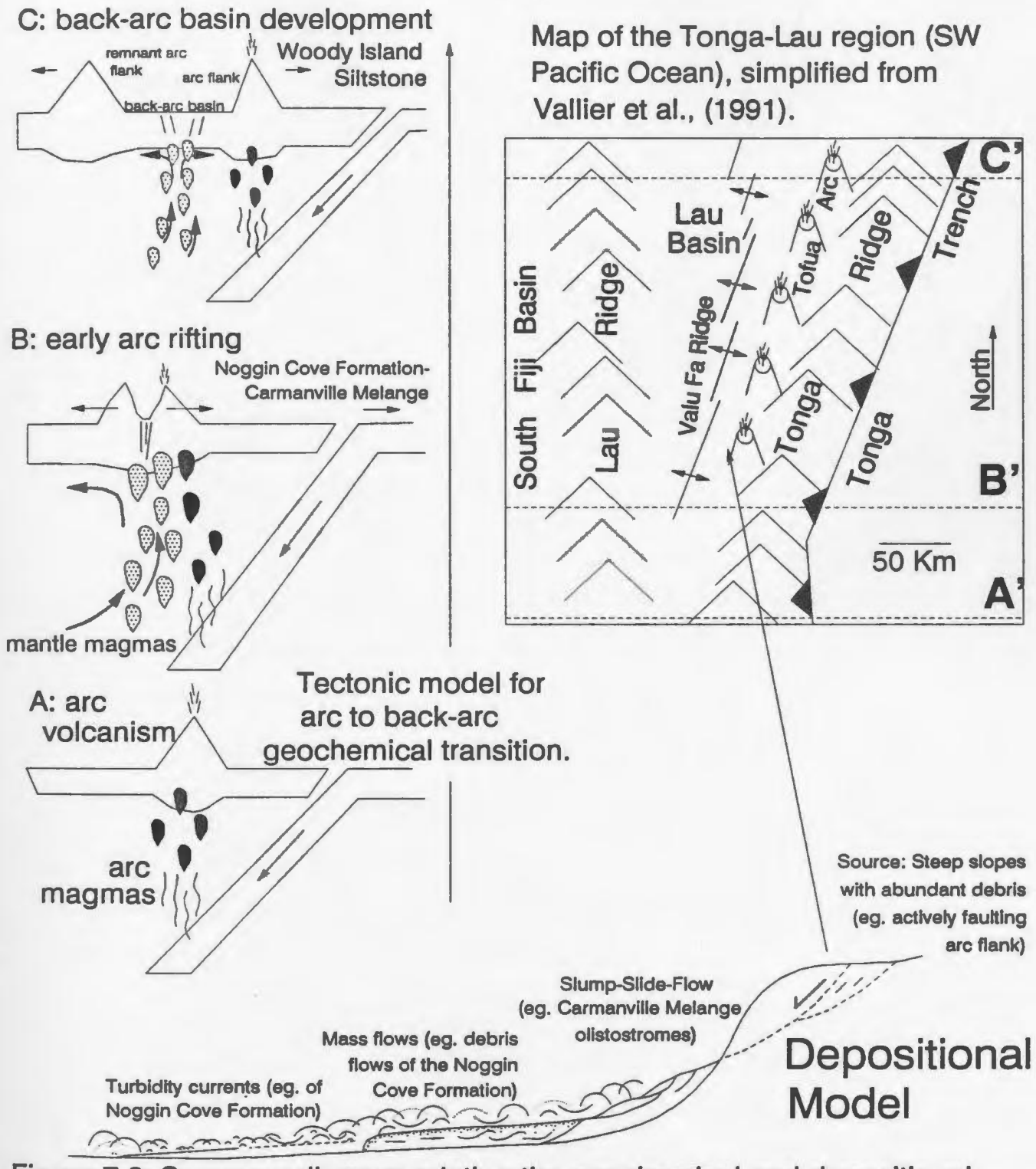

Figure 7.2: Summary diagram relating the geochemical and depositional models proposed for the Noggin Cove Formation and Carmanville Melange to the Tonga-Lau region (SW Pacific Ocean). The arc rifting model proposed (A to C) matches the formation of the Lau Basin as the Tonga-Lau Ridge is progressively "unzipped" (A' to C').

transition is also recorded in the geochemistry and stratigraphy of the Exploits (Dec et al., 1992) and Wild Bight (Swinden et al., 1990) groups. Correlation of the Noggin Cove Formation and Carmanville Melange with coeval chemostratigraphic successions in the Exploits and Wild Bight groups (Chapter 6), indicates the formation of an Early to Middle Ordovician back-arc basin that extended across the Exploits Subzone.

7.3 Recommendations for future work

An age determination is needed for the Noggin Cove Formation. Trondhjemite that occurs in the immediate Carmanville area should be sampled for U-Pb dating.

More analyses of coexisting amphibole and plagioclase in metabasalts of the Noggin Cove Formation are recommended to firmly establish metamorphic temperatures. Also, the possibility that rare high pressure Na-amphiboles are present warrants further microprobe investigation.

Field relations between volcanic and sedimentary rocks of the Davidsville Group need to be determined (eg. acid volcanic rock 4.5 km southwest of Carmanville Arm; pillow lava at Round Pond). Are the volcanics that occur with the Davidsville Group sedimentary rocks structurally emplaced or was volcanism contemporaneous with sedimentation?

References

Arculus, R.J.
1987: The significance of source versus process in the tectonic controls of magma genesis; Journal of Volcanology and Geothermal Research, v. 32, p. 1-12.

Bergstrom, S.M., Riva, J., and Kay, M.
1974: Significance of conodonts, graptolites, and shelly faunas from the Ordovician of north-central Newfoundland; Canadian Journal of Earth Sciences, v. 11, p. 1625-1660.

Blackwood, R.F.
1980: Geology of the Gander (west) area (2D/15), Newfoundland; in Current Research, (eds) C.F. O'Driscoll and R.V. Gibbons; Newfoundland Department of Mines and Energy, Mineral Development Division, Report 81-10, p. 50-56.

Blackwood, R.F. and Kennedy, M.J.
1975: The Dover Fault: Western boundary of the Avalon Zone, in northeastern Newfoundland; Canadian Journal of Earth Science, v. 12, p. 320-325.

Brown, E.H.
1977: The crossite content of Ca-amphibole as a guide to pressure of metamorphism; Journal of Petrology, v. 18, Part 1, p. 53-72.

Bruckner, W.D.
1972: The Gander Lake and Davidsville groups of northeastern Newfoundland: New data and geotectonic implications; Discussion, Canadian Journal of Earth Sciences, v. 9, p. 1778-1779.

Buckley, D.E., and Cranston, R.E.
1968: Atomic absorption analysis of 18 elements from a single decomposition of alumosilica; Marine Geology Atlantic Oceanographic Laboratory, Bedford Institute, Dartmouth, Nova Scotia.

Busby-Spera, C.J.
1988: Evolution of a Middle Jurassic back-arc basin, Cedros Island, Baja California: Evidence from a marine volcaniclastic apron; Geological Society of America Bulletin, v 100, p. 218-233.

Carey, S., and Sigurdsson, H.
1984: A model of volcanogenic sedimentation in marginal basins; in Marginal Basin Geology, (eds) B.P. Kokelaar and M.F. Howells; Geological Society of London Special Publication 16, p. 37-58.

Carmichael, I.S.E., Turner, F.J., and Verhoogen, J.
1974: Igneous Petrology; McGraw-Hill Inc, New York, p. 543.

Colman-Sadd, S.P., Dunning, G.R. and Dec, T.
1992: Dunnage-Gander relationships and Ordovician Orogeny in central Newfoundland: A sediment provenance and U/Pb age study; American Journal of Science, v 292, p. 317-355.

Colman-Sadd, S.P. and Swinden, H.S.
1984: A tectonic window in central Newfoundland? Geological evidence that the Appalachian Dunnage Zone may be allochthonous; Canadian Journal of Earth Sciences, v. 21, p. 1349-1367.

Cronan, D.S., Moorby, S.A., Glasby, G.P., Knedler, K., Thomson, J. and Hodkinson, R.
1984: Hydrothermal and volcaniclastic sedimentation on the Tonga-Kermadec Ridge and in its adjacent marginal basins; in Marginal Basin Geology, (eds) B.P. Kokelar and M.F. Howells; Geological Society of London Special Publication no. 16, p. 137-149.

Currie, K.L.
1992: Carmanville map area (2E-8): - a new look at Gander-Dunnage relations in Newfoundland; in Current Research, Part D; Geological Survey of Canada, Paper-1D, p. 27-33.

1991: A simple quantitative calculation of mol fractions of amphibole end-members; Canadian Mineralogist, v.29, p. 287-299.

Currie, K.L. and Pajari, G.E.
1977: Igneous and metamorphic rocks between Rocky Bay and Ragged Harbour, northeastern Newfoundland; in Report of Activities, Part A; Geological Survey of Canada, Paper 77-1A, p. 341-346.

1980b: Geological map of Carmanville map area (2E/8), Newfoundland; Geological Survey of Canada, Open File 721.

Dean, P.L.
1978: The volcanic stratigraphy and metallogeny of Notre Dame Bay, Newfoundland; Memorial University of Newfoundland, Geology Report 7, 204 pages.

Dean, W.T.
1971: Ordovician trilobites from the central volcanic belt at New World Island, northeastern Newfoundland; Geological Survey of Canada Bulletin 210, 37 pages.

Dec, T., Swinden, S., and Floyd, J.D.
1992: Sedimentological, geochemical and sediment-provenance constraints on stratigraphy and depositional setting of the Strong Island Chert (Exploits subzone, Notre Dame Bay); in Current Research, Newfoundland Department of Mines, Geological Survey of Newfoundland, Report 92-1, p. 85-96.

Fisher, R.V.
1984: Submarine Volcaniclastic Rocks; in Marginal Basin Geology, (eds) B.P. Kokelar and M.F. Howells; Geological Society Special Publication no. 16, Blackwell Scientific Publications, London, p. 5-27.

Garcia, M.O.
1978: Criteria for the identification of ancient volcanic arcs; Earth Science Review 14, p 147-65.

Gill, J.B.
1976: Composition and age of Lau Basin and Ridge volcanic rocks: Implications for evolution of an interarc basin and remnant arc; Geological Society of America, Bulletin, v. 87, p. 1384-1395.

Hampton, M.A.
1972: The role of subaqueous debris flows in generating turbidity currents; Journal of Sedimentary Petrology 42, p. 775-93.

Hawkesworth, C.J., O'Nions, R.K., Pankhurst, R.J., Hamilton, P.J., and Evenson, N.M.
1977: A geochemical study of island arc and back-arc tholeiites from the Scotia Sea; Earth and Planetary Science Letters, v. 36, p. 253-262.

Hein, J.R. and Karl, S.M.
1983: Comparisons between open-ocean and continental margin chert sequences; in Siliceous Deposits in the Pacific Region, (eds) A. Iijama and J.R. Hein; Elsevier Publishing Company, Amsterdam, p. 25-43.

Hibbard, J.P. and Williams, H.
1979: The regional setting of the Dunnage Melange in the Newfoundland Appalachians; American Journal of Science, v. 279, p. 993-1021.

Horne, G.S.
1970: Early Ordovician chaotic deposits in the Central Volcanic Belt of northeastern Newfoundland; Geological Society of America Bulletin, v. 81, p. 1767-1788.

Horne, G.S., and Helwig, J.
1969: Ordovician stratigraphy of Notre Dame Bay; in North Atlantic geology and continental drift, (eds) M. Kay; American Association of Petroleum Geologist, Memoir 12, p. 388-407.

Jacobi, R,D.
1984: Modern submarine sediment slides, melange and the Dunnage Formation in north-central Newfoundland; in Melanges: Their nature, origin, and significance. (eds) L. Raymond; Geological Society of America, Special Paper 13, p. 126-130.

Jacobi, R.D. and Wasowski, J.J.
1985: Geochemistry and plate tectonic significance of the volcanic rocks of the Summerford Group, north-central Newfoundland; Geology, v. 13, p. 126-130.

Jenkyns, H.C. and Winterer, E.L.
1982: Palaeoceanography of Mesozoic ribbon radiolarites; Earth and Planetary Science Letters, v. 60, p. 351-375.

Jenness, S.E.
1958: Geology of the Gander River Ultrabasic Belt, Newfoundland; Geological Survey of Newfoundland, Report 11, 58 pages.

1963: Terra Nova and Bonavista Bay map areas, Newfoundland; Geological Survey of Canada, Memoir 327, 184 pages.

Johnston, D.H.
1992: The Noggin Cove Formation, Carmanville map area, northeast Newfoundland; a back-arc basin volcanic complex; in Current Research, Part E; Geological Survey of Canada, Paper 92-1E, p. 249-257.

Jones, D.L. and Murchey, B.
1986: Geological significance of Paleozoic and mesozoic radiolarian cherts; Annual Reviews of Earth and Planetary Science, v. 14, p. 455-492.

Jukes, J.B.
1843: General Report of the Geological Survey of Newfoundland during the years 1839 and 1840; London, Murray (pub.), 160 pages.

Karlstrom, K.E., van der Pluijm, B.A. and Williams, P.F.
1982: Structural interpretation of the eastern Notre Dame Bay, Newfoundland: regional post-Middle Silurian thrusting and asymmetrical folding; Canadian Journal of Earth Sciences, v. 19, p. 2325-2341.

Kay, M.
1967: Stratigraphy and structure of northeastern Newfoundland bearing on drift in North Atlantic; American Association of Petroleum Geologist Bulletin, v. 51, p. 579-600.

Keen, C.E., Keen, M.J., Nichols, B., Reid, I., Stockmal, G.S., Colman-Sadd, S.P., O'Brien, S.J., Miller, H., Quinlan, G., Williams, H., and Wright, J.
1986: Deep seismic reflection profile across the northern Appalachians; Geology, v. 14, p. 141-145.

Kennedy, M.J.
1975: Repetitive orogeny in the northeastern Appalachians- new plate models based upon Newfoundland examples; Tectonophysics, v. 28, p. 39-87.

Kennedy, M.J. and McGonigal, M.H.
1972: The Gander Lake and Davidsville groups of northeastern Newfoundland: new data and geotectonic implications; Canadian Journal of Earth Sciences, v. 9, p. 452-459.

Langmyhyr, F.J. and Paus, P.E.
1968: Analysis of silicate rocks; Analytical Chemica Acta, 43, p. 397-408.

Lonsdale,P.F.
1975: Sedimentation and tectonic modification of the Samoan archipelagic apron; American Society of Petroleum Geologists Bulletin, v. 59, p. 780-798.

Longerich, H.P., Jenner, G.A., Fryer, B.J., and Jackson, S.E.
1990: Inductively coupled plasma- mass spectrometric analysis of geological samples: A critical evaluation based on case studies; in Microanalytical Methods in Mineralogy and Geochemistry, (eds) P.J. Potts, C. Dupuy, and J.F.W. Bowles; Chemical Geology, 83, p. 105-118.

Marillier, F., Keen, C.E., Stockmal, G.S., Quinlan, G., Williams, H., Colman-Sadd, S.P. and O'Brien, S.J.
1989: Deep structure and zonal subdivisions of the Canadian Appalachians: New seismic reflection data from the Gulf of St. Lawrence; Canadian Journal of Earth Sciences, v. 26, p. 305-321.

McGonigal, M.H.
1973: The Gander and Davidsville Groups: major tectono-stratigraphic units in the Gander Lake area, Newfoundland; unpublished M.Sc. thesis, Memorial University of Newfoundland, St. John's, 121 p.

McKerrow, W.S. and Cocks, L.R.M.
1978: A lower Paleozoic trench-fill sequence, New World Island, Newfoundland; Geological Society of America Bulletin, v. 89, p. 121-1132.

Miller, H.G.
1988: Geophysical interpretation of the geology of the northeast Gander Terrane, Newfoundland; Canadian Journal of Earth Sciences, v. 25, p. 1161-1174.

Miyashiro, A.
1974: Volcanic rock series in island arcs and active continental margins; American Journal of Science, v. 274, p. 321-355.

Murray, A. and Howley, J.P.
1881: Reports of the Geological Survey of Newfoundland for 1866- 1880; London Edward Standard, 536 pages.

Neuman, R.B.
1968: Paleogeographic implications of Ordovician shelly fossils in the Magog Belt of the northern Appalachian region; in Studies in Appalachian Geology: Northern and maritime, (eds) E. Zen, W.S. White, J.B. Hadley, and J.B. Thompson Jr.; New York, John Wiley & Sons, p. 35-48.

O'Brien, B.H.
1990: Geology of the New Bay area (parts of 2E/6 and 2E/11), Notre Dame Bay, Newfoundland; Newfoundland Department of Mines and Energy, Geological Survey Branch, Open File Map 90-124, scale 1:50,000.

O'Neill, P.P.
1991: Geology of the Weir's Pond area, Newfoundland (NTS 2E/1). Newfoundland Department of Mines and Energy, Geological Survey Branch, Report 91-3.

O'Neill, P.P. and Blackwood, R.F
1989: A proposal for revised stratigraphic nomenclature of the Gander and Davidsville Groups and the Gander River ultrabasic belt, of northeast Newfoundland; in Current Research, (eds) C.P.G. Pereira, D. Walsh and R.F. Blackwood; Newfoundland Department of Mines, Mineral Development Division, Report 89-1, p. 127-130.

Pajari, G.E., Pickerill, R.K., and Currie, K.L.
1979: The nature, origin and significance of the Carmanville Ophiolitic Melange, Northeastern Newfoundland; Canadian Journal of Earth Sciences, v. 15, p. 1439-1451.

Pajari, G.E. and Currie, K.L.
1978: The Gander Lake and Davidsville Groups of northeastern Newfoundland: a reexamination; Canadian Journal of Earth Sciences, v. 15, p. 708-714.

Pearce, J.A.
1975: Basalt geochemistry used to investigate past tectonic environments on Cyprus; Tectonophysics v. 25, p. 41-67

Piasecki, M.A.J.
1988: A major ductile shear zone in the Bay d'Espoir area, Gander Terrane, southeastern Newfoundland; in Current Research, Newfoundland Department of Mines, Mineral Development Division, Report 88-1, p. 135-144.

Piasecki, M.A.J., Williams, H. and Colman-Sadd, S.P.
1990: Tectonic relationships along the Meelpaeg, Burgeo and Burlington lithoprobe transects in Newfoundland; in Current Research, Newfoundland Department of Mines and Energy, Geological Survey Branch, Report 90-1, p. 327-339.

Pickerill, R.K., Pajari, G.E. and Currie, K.L.
1981: Resedimented volcaniclastics in the Carmanville area, northeastern Newfoundland- depositional remnants of Early Paleozoic oceanic islands; Canadian Journal of Earth Science, v. 18. p. 55-70.

Pickerill, R.K., Pajari, G.E., Currie, K.L., and Berger, A.R.
1978: Carmanville map area, Newfoundland; the northeastern end of the Appalachians; in Current Research, Part A; Geological Survey of Canada, Paper 78-1A, p. 209-216.

Ramsay, J.G.
1967: Folding and Fracturing of Rocks; McGraw-Hill Book Co., New York, 568 p.

Ramsey, J.G. and Huber, M.I.
1987: The techniques of modern structural geology; vol 2, Folds and Fractures; Academic Press, London. p. 313.

Schilling, J-G., Zajac, M., Evans, R., Johnston, T., White, W., Devine, J.D., and Kingsley, R.
1983: Petrologic and geochemical variations along the mid- Atlantic Ridge from 29N to 73N; American Journal of Science, v. 283, p. 510-586.

Shervais, J.W.
1982: Ti-V plots and the petrogenesis of modern and ophiolitic lavas; Earth and Planetary Science Letters v. 59, p. 101-118.

Spear, F.S.
1981: Amphibole-plagioclase equilibria: an empirical model for the relation albite + tremolite = edenite + 4 quartz; Contributions to Mineralogy and Petrology, v. 77, p. 355-364.

Swinden, H.C., Jenner, G.A., Fryer, B.J., Hertogen, J., and Roddick, J.C.
1990: Petrogenesis and paleotectonic history of the Wild Bight Group, an Ordovician rifted island arc in central Newfoundland; Contributions to Mineralogy and Petrology, v. 105, p. 219-241.

Twenhofel, W.H.
1947: The Silurian of eastern Newfoundland with some data relating to the physiography and Wisconsin glaciation of Newfoundland; American Journal of Science, v. 245, p. 65-122.

Twenhofel, W.H. and Shrock, R.R.
1937: Silurian srata of Notre Dame Bay and Exploits Valley, Newfoundland; Geological Society of America, Bulletin, v. 48, p. 1743-1772.

Vallier, T.L., Jenner, G.A., Frey, F.A., Gill, J.B., Davis, A.S., Volpe, A.M., Hawkins, J.W., Morris, J.D., Cawood, P.A., Moreton, J.L., Scholl, D.W., Rautenschlein, M., White, W.M., Williams, R.W., Stevenson, A.J. and White, L.D.
1991: Subalkaline andesite from Valu Fa Ridge, a back-arc spreading center in southern Lau Basin: petrogenesis, comparitive chemistry, and tectonic implications; Chemical Geology, v. 91, p.227-256.

Wasowski, J.J. and Jacobi, R.D.
1985: Geochemistry and tectonic significance of the mafic blocks in the Dunnage melange, north-central Newfoundland; Canadian Journal of Earth Science, v. 22, p. 1248-1256.

Weissel, J.K.
1981: Magnetic lineations in marginal basins of the western Pacific. Royal Society of London Philosophical Transactions, Series A, v. 300, p. 223-247.

Williams, H.
1963: Twillingate map-area, Newfoundland; Geological Survey of Canada map and report, 33-1963, 30p.

1964: Botwood, Newfoundland; Geological Survey of Canada, Map 60-1963.

1968: Wesleyville, Newfoundland; Geological Survey of Canada, Map 1227A.

1992: Melanges and coticule occurences in the northeast Exploits Subzone, Newfoundland; in Current Research, Part D; Geological Survey of Canada, Paper 92-1D, p. 121-127.

Williams, H., Colman-Sadd, S.P., and Swinden, H.S.
1988: Tectonic-stratigraphic subdivisions of Central Newfoundland; in Current Research, Part B; Geological Survey of Canada, Paper 88-1B, p. 91-98.

Williams, H. and Piasecki, M.A.J.
1990: The Cold Spring Melange and its significance in central Newfoundland; Canadian Journal of Earth Sciences, v. 27, p. 268-272.

Williams, H., Piasecki, M.A.J., and Colman-Sadd, S.P.
1989: Tectonic relationships along the proposed central Newfoundland lithoprobe transect and regional correlations; in Current Research, Part B; Geological Survey of Canada, Paper 89-1B, p. 55-66.

Williams, H., Piasecki, M.A.J., and Johnston, D.
1991: The Carmanville Melange and Dunnage-Gander relationships in northeast Newfoundland; in Current Research, Part D; Geological Survey of Canada, Paper 91-1D, p.15-23.

Williams, P.F.
1983: Timing of deformation and the mechanism of cleavage development in a Newfoundland melange; Maritime Sediments and Atlantic Geology, v. 19, p. 31-48.

Williams, S.H., O'Brien, B.H., Colman-Sadd, S.P., and O'Brien, F.H.C.
1992: Dunnage Zone graptolites- an extension of the age range and distribution of certain Ordovician formations of the Exploits Subzone; in Current Research, Newfoundland Department of Mines, Geological Survey of Newfoundland, Report 92-1, p. 203-210.

Winchester, J.A. and Floyd, P.A.
1977: Geochemical discrimination of different magma series and their differentiation products using immobile elements; Chemical Geology, v. 20, p. 325-343.

Wonderley, P.R. and Neuman, R.B.
1984: The Indian Bay Formation: fossiliferous Early Ordovician volcanogenic rocks in the northern Gander Terrane, Newfoundland, and their regional significance; Canadian Journal of Earth Science, v. 21, p. 525-532.

Wood, D.A.
1980: The application of a Th-Hf-Ta diagram to problems of tectonomagmatic classification and to establishing the nature of crustal contamination of basaltic lavas of the British Tertiary Volcanic Province; Earth and Planetary Science Letters, v. 50, p. 11-30.

Wu, T.W.
1979: Structural, stratigraphic and geochemical studies of the Horwood Peninsula - Gander Bay area, northeast Newfoundland; M.Sc. Thesis, Brock University, St. Catherines, Ontario, 185 p.

Appendices

Appendix I

Geochemical Data

1.1 Description and location of samples

M576 -Pillow lava block, Carmanville Melange; eastern shoreline of Carmanville Arm, 1.75 km. SW of Twillick Point, known locally as Teakettle Point.

M577 -Pillow lava with Davidsville Group sediments; shoreline, NE corner of Round Pond.

M578 -Mafic dyke cutting pillow lava (M580), Noggin Cove Formation; large roadcut between the towns of Carmanville and Noggin Cove (north side of road).

M579 -Fine grained tuff, Noggin Cove Formation; east shoreline of Gander Bay, 0.5 km NW of Beaver Hill.

M580 -Pillow lava, Noggin Cove Formation; large roadcut between the towns of Noggin Cove and Carmanville.

M581 -Pillow lava block, Carmanville Melange; west side of Teakettle Point, 0.75 km from Point.

M582 -Pillow lava block, Carmanville Melange; Noggin Point

M583 -Mafic dyke, cutting volcanic conglomerates, Noggin Cove Formation; shoreline, SE corner of Noggin Cove.

M584 -Pillow lava, Noggin Cove Formation; beside Carmanville School.

M585 -Pillow lava, Noggin Cove Formation; south end of prominent ridge overlooking the town of Carmanville South, 0.3 km east of the head of Carmanville Arm.

M586 -Trondhjemite, cutting a lava flow (M587), Noggin Cove Formation; east shoreline of Noggin Cove, 1 km south of Noggin Cove Head.

M587 -Lava flow, Noggin Cove Formation; east shoreline of Noggin Cove, 1 km south of Noggin Cove Head.

M588 -Pillow lava, Noggin Cove Formation; roadcut, south side of road, in town of Noggin Cove, just east of the head of Noggin Cove.

M589 -Vesicular clast from volcanic conglomerate, Noggin Cove Formation; top of prominent hill overlooking SW corner of Noggin Cove.

M590 -Vesicular clast from volcanic conglomerate, Noggin Cove Formation; Frederickton, behind (south of) houses 0.25 km south of Noggin Cove road T junction.

M591 -Mafic dyke, cutting volcanic conglomerates, Noggin Cove Formation; behind sawmill, Noggin Cove (known locally as "Suicide Run"- when the spring-water on this slope freezes over in the winter it provides a treacherous, high speed toboggan run!)

M592 -Coarse grained volcanic sandstone, Noggin Cove Formation; behind prominent church at the head of Noggin Cove.

M593 -Vesicular clast from volcanic conglomerate, Noggin Cove Formation; entrance to abandoned Fox Farm, just east of Frederickton.

M594 -Fine grained tuff, Noggin Cove Formation; S-SE shoreline of Noggin Cove.

M595 -Pebbly coarse grained volcanic sandstone, Noggin Cove Formation; Frederickton to Noggin Point shoreline, approximately 100 m beyond the last house.

M2099-Block of massive gabbro, Carmanville Melange; shoreline, 0.5 km S-SW of Rocky Point.

M2100-Pillow block, Carmanville Melange; shoreline, 0.30 km east of Rocky Point.

M2102-Pillow lava, Noggin Cove Formation; 1 km east of the head of Carmanville Arm.

M2103-Pillow lava, Noggin Cove Formation; Communication Tower, Noggin Hill.

M2104-Pillow lava, Noggin Cove Formation; roadcut, 0.4 km south of Beaver Cove.

M2105-Block of massive gabbro, Carmanville Melange; shoreline, 1 km north of Davidsville.

M2106-Pillow lava block, Carmanville Melange; shoreline, 0.7 km north of Davidsville.

M2107-Mafic dyke cutting Davidsville Group sediments; small gravel pit on the west side of the road to Gander, 3 km SW of Carmanville.

1.2 Geochemical data

Major elements were analyzed using atomic absorption at Memorial University (M576-M595) and Newfoundland Department of Mines and Energy (M2099-M2107). The method is adapted from Langmyhyr and Paus (1968) and Buckley and Cranston (1968). Trace elements were determined by ICP-MS, using a Na_2O_2 sinter technique (Longerich et al., 1990). In the following presentation of geochemical data, oxides are given in percent, trace elements in ppm.

Sample	M576	M577	M578	M579	M580	M581
SiO2	50.80	44.10	49.60	40.00	46.70	48.00
TiO2	1.24	0.90	1.14	1.32	1.18	1.78
Al2O3	15.40	16.60	13.50	8.74	15.10	15.70
FeO	7.69	9.82	10.93	7.58	5.39	13.28
Fe2O3	1.40	0.56	1.83	1.57	3.80	1.50
MnO	0.16	0.24	0.19	0.14	0.12	0.25
MgO	6.28	3.35	6.94	12.60	3.09	5.19
CaO	10.83	8.72	6.99	18.50	13.08	5.04
Na2O	4.62	5.76	4.37	1.65	4.64	4.09
K2O	0.17	0.16	0.22	0.12	0.29	2.19
P2O5	0.13	0.10	0.09	0.15	0.13	0.15
LOI	1.52	10.04	3.08	7.40	5.57	2.00
Total	100.1	100.35	98.88	99.77	99.09	99.17
K	1411	1328	1826	996	2407	18180
Ba	85	151	89	12	101	364
Sr	261	264	158	267	220	217
Nb	6.3	2.1	3.3	9.6	4.9	4.7
Hf	1.98	1.79	1.82	1.99	1.78	2.55
Zr	72	64	65	78	67	92
Ti	7434	5396	6834	7913	7074	10671
Y	20	17	25	15	21	28
Th	0.53	0.18	0.20	0.50	0.27	0.23
La	4.36	2.59	2.47	7.16	4.02	3.31
Ce	11.66	7.66	7.52	18.32	10.46	10.94
Pr	1.72	1.42	1.29	2.60	1.62	1.86
Nd	8.43	7.89	7.11	11.56	8.06	9.82
Sm	2.69	2.96	2.64	3.01	2.55	3.46
Eu	0.93	0.97	0.93	1.02	1.01	1.16
Gd	3.36	3.77	3.67	3.11	3.41	4.79
Tb	0.57	0.65	0.67	0.48	0.56	0.82
Dy	3.80	4.14	4.64	3.00	3.82	5.42
Ho	0.79	0.80	1.01	0.58	0.82	1.12
Er	2.21	2.17	3.07	1.57	2.35	3.20
Tm	0.32	0.31	0.44	0.21	0.33	0.47
Yb	2.01	1.88	2.94	1.31	2.11	3.09
Lu	0.30	0.27	0.45	0.19	0.33	0.47

Sample	M582	M583	M584	M585	M586	M587
SiO2	50.60	50.80	51.60	49.60	71.60	50.00
TiO2	1.36	2.06	1.36	1.72	0.48	1.67
Al2O3	14.00	11.70	14.70	11.20	10.90	13.20
FeO	10.97	6.80	11.44	8.26	4.79	10.89
Fe2O3	0.80	2.02	1.09	2.83	0.37	2.82
MnO	0.18	0.15	0.19	0.19	0.10	0.23
MgO	6.40	8.09	5.54	9.49	3.06	5.97
CaO	7.91	8.97	6.15	9.52	1.74	4.30
Na2O	3.18	5.00	4.47	3.68	4.89	5.21
K2O	0.66	0.23	0.19	0.18	0.06	0.11
P2O5	0.10	0.17	0.10	0.17	0.05	0.10
LOI	2.55	2.97	2.57	1.91	2.42	4.33
Total	98.71	98.96	99.40	98.75	100.56	98.83
K	5479	1909	1577	1494	498	913
Ba	83	62	50	109	19	31
Sr	192	187	210	330	51	113
Nb	3.1	15.7	0.9	11.4	1.2	1.1
Hf	2.03	3.12	1.58	2.46	3.86	2.30
Zr	67	121	51	87	131	79
Ti	8153	12350	8153	10311	2878	10012
Y	27	20	26	17	33	31
Th	0.45	0.89	0.36	0.88	1.04	0.37
La	2.03	10.43	2.20	9.92	6.59	3.80
Ce	6.84	27.60	6.98	23.53	17.60	11.16
Pr	1.21	3.74	1.21	3.22	2.71	1.83
Nd	6.61	17.05	6.78	14.66	13.11	10.02
Sm	2.53	4.31	2.54	3.77	4.10	3.60
Eu	0.91	1.51	1.24	1.42	0.88	1.55
Gd	3.57	4.55	3.64	3.64	4.68	4.92
Tb	0.68	0.68	0.64	0.61	0.90	0.88
Dy	4.68	4.05	4.53	3.63	5.84	5.89
Ho	1.05	0.78	1.00	0.70	1.31	1.28
Er	3.24	2.01	2.93	1.84	4.06	3.72
Tm	0.46	0.27	0.43	0.24	0.61	0.55
Yb	3.05	1.60	2.82	1.37	4.08	3.38
Lu	0.47	0.24	0.43	0.20	0.61	0.51

Sample	M588	M589	M590	M591	M592	M593
SiO2	50.00	42.20	53.30	47.40	43.40	45.80
TiO2	1.66	1.32	1.78	0.64	1.44	1.48
Al2O3	11.90	9.85	13.30	5.09	9.64	9.91
FeO	9.15	6.58	7.24	5.71	9.48	8.25
Fe2O3	1.80	5.86	1.77	3.82	2.26	3.07
MnO	0.17	0.16	0.12	0.15	0.17	0.18
MgO	10.98	18.65	8.09	22.69	17.08	14.59
CaO	8.76	8.14	6.24	8.69	9.69	9.88
Na2O	3.24	1.43	5.27	0.14	1.27	2.16
K2O	0.18	0.20	0.56	0.02	0.08	0.22
P2O5	0.15	0.09	0.15	0.06	0.14	0.14
LOI	2.51	5.21	1.56	5.39	3.88	3.39
Total	100.50	99.69	99.38	99.80	99.53	99.07
K	1494	1660	4649	166	664	1826
Ba	26	15	134	3	29	73
Sr	219	62	186	46	123	233
Nb	11.5	9.0	13.4	4.4	9.2	10.7
Hf	2.70	2.41	2.82	1.19	2.52	2.74
Zr	106	90	110	46	85	101
Ti	9952	7913	10671	3837	8633	8873
Y	17	15	18	6	13	17
Th	0.74	0.55	0.83	0.28	0.72	0.68
La	8.46	8.99	8.29	3.39	7.28	8.91
Ce	22.10	21.15	23.25	8.22	18.18	22.74
Pr	3.14	2.83	3.29	1.10	2.55	3.18
Nd	14.64	12.46	15.15	5.20	12.07	14.64
Sm	3.88	3.22	3.99	1.46	3.19	3.86
Eu	1.35	0.95	1.36	0.54	1.12	1.39
Gd	3.98	3.39	4.04	1.48	3.26	3.89
Tb	0.65	0.55	0.66	0.23	0.52	0.63
Dy	3.83	3.18	3.88	1.37	3.06	3.76
Ho	0.73	0.63	0.76	0.25	0.58	0.72
Er	1.89	1.65	2.15	0.64	1.60	1.90
Tm	0.25	0.22	0.29	0.08	0.20	0.24
Yb	1.53	1.33	1.61	0.47	1.22	1.41
Lu	0.21	0.19	0.24	0.07	0.18	0.21

Sample	M594	M595	M2099	M2100	M2102	M2103
SiO2	44.20	41.60	48.20	44.50	42.95	50.90
TiO2	2.44	2.14	1.58	1.53	0.94	1.44
Al2O3	11.40	10.80	13.06	16.53	6.50	16.16
FeO	10.14	10.56	14.34	12.37	9.78	12.10
Fe2O3	2.00	1.42	1.91	1.57	2.62	1.60
MnO	0.18	0.18	0.21	0.27	0.17	0.18
MgO	11.49	11.15	7.04	9.32	25.43	4.35
CaO	10.34	12.08	8.86	6.61	5.49	4.63
Na2O	2.39	2.34	2.44	2.68	0.19	5.32
K2O	0.34	0.89	0.19	1.52	0.04	0.33
P2O5	0.20	0.18	0.05	0.14	0.13	0.10
LOI	4.24	6.29	2.04	3.49	5.12	3.22
Total	99.36	99.63	99.92	100.53	99.36	100.33
K	2822	7388	1577	12618	332	2739
Ba	85	108	20	247	5	40
Sr	141	166	140	220	109	134
Nb	18.3	18.0	0.2	2.3	4.6	0.8
Hf	3.90	3.50	0.64	2.04	1.08	1.88
Zr	144	131	18	69	40	66
Ti	14628	12829	9472	9172	5635	8633
Y	20	19	15	26	11	26
Th	0.96	0.98	0.08	0.14	0.37	0.35
La	14.54	13.41	0.90	2.76	5.35	2.72
Ce	35.92	32.51	2.36	7.41	13.16	8.53
Pr	4.93	4.48	0.47	1.25	1.73	1.42
Nd	22.30	20.24	3.02	6.68	7.97	8.19
Sm	5.26	4.84	1.33	2.47	2.13	2.82
Eu	1.84	1.47	0.55	0.73	0.76	0.93
Gd	4.83	4.33	2.06	3.80	2.63	4.08
Tb	0.79	0.74	0.37	0.64	0.39	0.69
Dy	4.61	4.26	2.64	4.43	2.29	4.76
Ho	0.88	0.77	0.59	1.01	0.45	1.06
Er	2.25	2.07	1.77	3.06	1.22	3.23
Tm	0.31	0.28	0.26	0.46	0.16	0.45
Yb	1.74	1.64	1.68	3.11	1.08	3.09
Lu	0.25	0.23	0.26	0.49	0.15	0.48

Sample	M2104	M2105	M2106	M2107
SiO2	48.90	44.70	52.65	46.80
TiO2	1.85	2.10	1.02	1.42
Al2O3	13.30	14.72	15.39	15.51
FeO	13.20	9.89	11.53	8.75
Fe2O3	2.62	0.88	0.00	0.79
MnO	0.25	0.52	0.62	0.19
MgO	5.69	12.92	4.93	11.47
CaO	9.31	5.66	8.33	5.95
Na2O	3.89	1.35	3.52	2.96
K2O	0.39	0.68	0.20	1.17
P2O5	0.19	0.68	0.09	0.21
LOI	1.61	5.51	1.79	3.95
Total	101.20	99.61	100.07	99.17
K	3238	5645	1660	9713
Ba	95	251	77	2941
Sr	161	343	200	306
Nb	5.1	80.7	1.2	12.9
Hf	2.38	8.33	1.35	2.55
Zr	92	409	45	123
Ti	11091	12589	6115	8513
Y	34	22	22	22
Th	0.41	6.80	0.18	1.29
La	5.52	53.43	1.65	12.13
Ce	13.87	105.77	4.67	25.06
Pr	2.09	11.85	0.79	3.41
Nd	10.96	44.78	4.47	14.74
Sm	3.62	8.15	1.87	3.41
Eu	1.32	2.42	0.70	1.33
Gd	5.26	6.81	2.93	4.06
Tb	0.92	0.88	0.54	0.60
Dy	6.25	4.67	3.80	3.90
Ho	1.38	0.85	0.87	0.81
Er	4.18	2.31	2.62	2.38
Tm	0.61	0.31	0.38	0.33
Yb	3.93	1.73	2.61	2.05
Lu	0.62	0.28	0.40	0.32

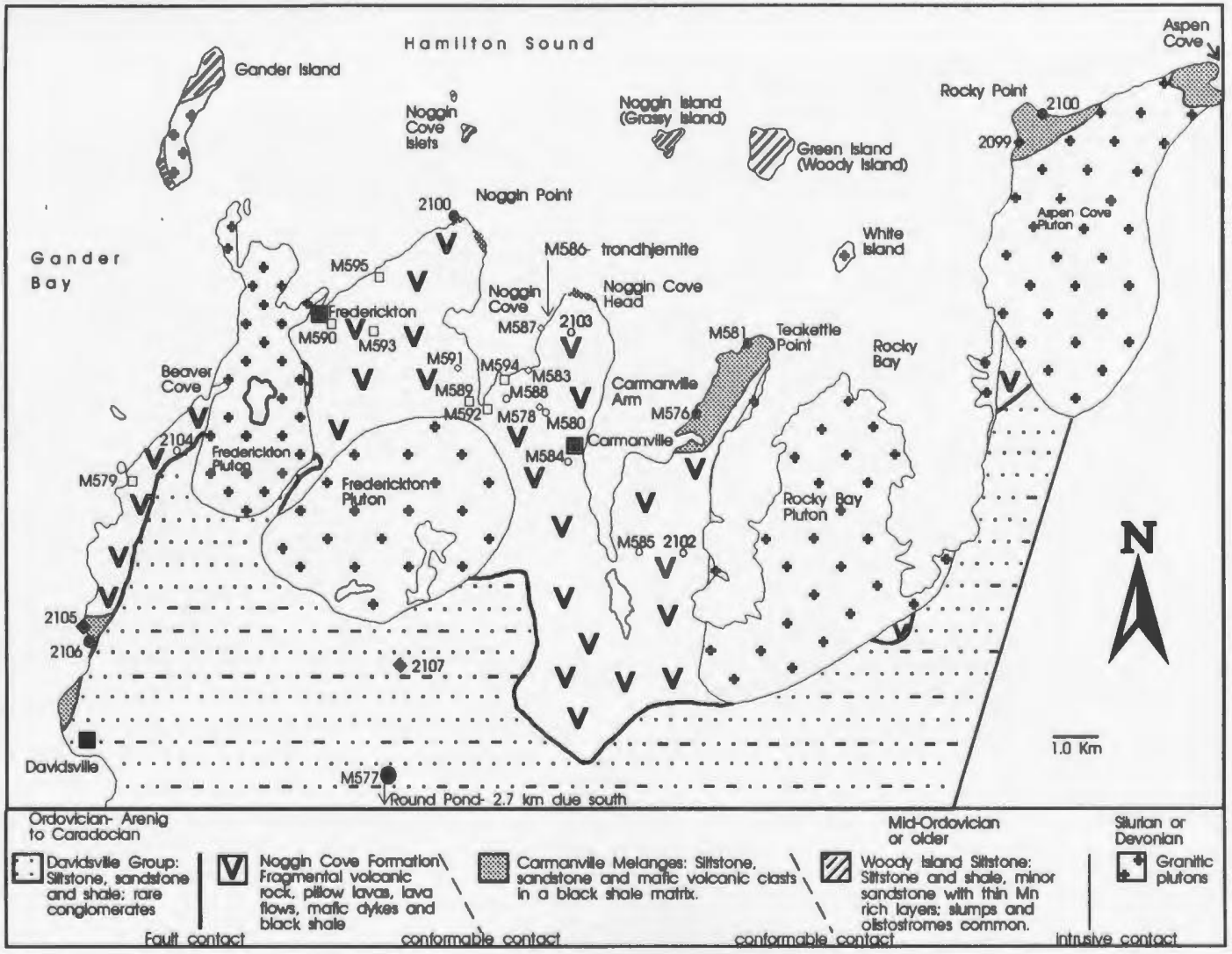

Appendix 1.3: Locations of geochemistry samples from the Noggin Cove Formation, Carmanville Melange and Davidsville Group. Symbols per Figure 4.1.

Appendix II

X-Ray Diffraction Data-
Noggin Cove Formation

Sample 3107-9-1 (Matrix of volcanic conglomerate)

Mineral Name	JCPDS #	OP*	PDF/Match
Magnesiohornblende	21,149	2.06	24/24
Ferro-pargasite	26,1372	2.32	15/15
Pargasite	23,1406	2.52	23/22
Ferro-actinolite	23,118	2.68	23/22
Riebeckite	19,1061	3.29	31/29
Crossite	31,1312	4.40	25/13
Clinoclore	29,701	5.08	22/22
Magnesioadanagait(!)	38,359	5.13	37/33
Edenite	23,1405	5.29	23/21
Magnesioriebeckite	20,656	5.43	35/30
Tremolite	13,437	5.81	39/32
Edenite, sodian	31,1282	5.81	23/20

Sample 3107-9-2 (Matrix of volcanic conglomerate)

Mineral Name	JCPDS #	OP	PDF/Match
Ferro-actinolite	23,118	8.51	23/19
Ferro-pargasite	26,1372	9.54	15/13
Pargasite	23,1406	9.89	23/19
Edenite, sodian	31,1282	9.92	23/19
Crossite	31,1312	10.11	25/22
Tremolite	13,437	10.33	39/29
Montanite	38,417	10.42	8/7
Pecoraite (!)	22,754	11.72	5/5
Richterite, calcian	31,1284	12.03	23/20
Riebeckite	19,1061	12.80	31/23
Burtite, syn	9,30	13.11	12/11
Elpasolite, syn	22,1235	13.69	9/8

* -order parameter; this is a ranking of the identifications based primarily on d-spacing and to a lesser extent on peak intensities.

Sample 3107-9-3 (Clast of volcanic conglomerate)

Mineral Name	JCPDS #	OP	PDF/Match
Magnesiohornblende	21,149	0.92	24/24
Crossite	31,1312	2.10	25/24
Ferro-actinolite	23,118	2.91	23/23
Pargasite	23,1406	3.02	23/23
Edenite	23,1405	3.53	23/22
Ferro-pargasite	26,1372	4.19	15/15
Riebeckite	19,1061	4.33	31/28
Tirodi	23,603	5.44	21/18
Ferro-hornblende	29,1258	5.86	32/29
Edenite, sodian	31,1282	6.34	23/21
Kozulite	25,850	6.47	21/18
Tremolite, sodian	31,1285	6.47	29/24

Sample 0308-3-1 (whole rock-matrix and clasts)

Mineral Name	JCPDS #	OP	PDF/Match
Ferro-actinolite	23,118	3.00	23/23
Ferro-pargasite	26,1372	3.28	15/15
Hastingsite, magn	20,469	3.35	39/35
Tremolite	13,437	3.37	39/35
Magnesiohornblende	21,149	3.40	24/24
Magnesioadanagait (!)	38,359	4.27	37/34
Arfedsonite	14,633	4.31	22/21
Riebeckite	19.1061	4.47	31/29
Edenite, sodian	31,1282	4.78	23/21
Pargasite	23,1406	5.01	23/22
Crossite	31,1312	5.17	25/24
Hastingsite, chlor	20,378	5.67	31/28

Note: X-ray diffraction is not a reliable analytical technique for the identification of amphibole species; it is only reliable for the identification of amphiboles in general (ie: versus pyroxenes, chlorite, etc.; pers. comm. T. Rivers).

Appendix III

Microprobe Data

Note: Presentation format following Currie (1991) to agree with classification scheme used in chapter 5. Site assignment scheme follows presentation of data.

0608-2-1

	Oxide		Cell
SiO2	52.020	Si	7.538
TiO2	0.240	Ti	0.026
Al2O3	4.700	Al	0.803
Fe2O3	1.020	Fe3	0.111
Cr2O3	0.020	Cr	0.002
FeO	13.770	Fe2	1.669
MnO	0.290	Mn	0.036
NiO	0.130	Ni	0.015
MgO	12.970	Mg	2.802
CaO	11.740	Ca	1.823
Na2O	1.020	Na	0.287
K2O	0.140	K	0.026

Total 98.060 Ions 15.136
(O+OH+F+Cl) 23.001 Normalised 0.000

Classification of 0608-2-1
T site: 7.538 Si 0.462 Al
C site: 0.340 Al 0.114 Fe3 0.026 Ti 4.520 FM
B site: 0.001 FM 1.823 Ca 0.177 Na
A site: 0.110 Na 0.026 K 0.000 Li

A site: Full 0.136 Empty 0.864
B site: FeMg 0.000 Ca2 0.823 CaNa 0.177
T site: Si8 0.538 Si7 0.462

0.537	AOB4Si8	0.333	tremolite	0.198	ferro-actinolite
0.150	hornblende	0.070	magnesio-alumino	0.041	ferro-alumino
		0.023	magnesio-ferri	0.014	ferro-ferri
0.177	barroisite	0.082	magnesio-alumino	0.049	ferro-alumino
		0.027	magnesio-ferri	0.016	ferro-ferri
0.136	edenite	0.084	magnesio	0.050	ferro

Fe/FM = 0.369 Mg/FM = 0.620 Mn/FM = 0.002
Al/M3 = 0.750 Fe3/M3 = 0.250 Cr/M3 = 0.005
K/A = 0.190 Li = 0.000

0608-2-2

	Oxide		Cell
SiO2	48.850	Si	7.583
TiO2	0.330	Ti	0.039
Al2O3	0.140	Al	0.026
Cr2O3	0.070	Cr	0.009
FeO	18.610	Fe2	2.416
MnO	0.190	Mn	0.025
MgO	10.180	Mg	2.356
CaO	11.880	Ca	1.976

Na2O	1.390	Na	0.418
K2O	0.240	K	0.048

Total 91.880 Ions 14.893
(O+OH+F+Cl) 22.299 Normalised 13.000

Classification of 0608-2-2
T site: 7.583 Si 0.026 Al 0.039 Ti 0.353 Vacant
C site: 0.000 Al 0.009 Fe3 0.000 Ti 4.796 FM 0.195 Vacant
B site: 0.000 FM 1.976 Ca 0.024 Na
A site: 0.394 Na 0.048 K 0.000 Li

A site: Full 0.442 Empty 0.558
B site: Ca2 0.976 CaNa 0.024
T site: Si8 0.583 Si7 0.417

0.558 AOB4Si8	0.274 tremolite	0.281 ferro-actinolite
0.024 richterite	0.012 magnesio	0.012 ferro
0.417 edenite	0.205 magnesio	0.210 ferro

Fe/FM = 0.504 Mg/FM = 0.491 Mn/FM = 0.001
Al/M3 = 0.000 Fe3/M3 = 1.000 Cr/M3 = 1.000
K/A = 0.108 Li = 0.000

0608-2-3

Oxide		Cell	
SiO2	52.870	Si	7.406
TiO2	0.200	Ti	0.021
Al2O3	4.890	Al	0.807
Fe2O3	4.400	Fe3	0.464
Cr2O3	0.200	Cr	0.022
FeO	11.820	Fe2	1.385
MnO	0.270	Mn	0.032
MgO	13.710	Mg	2.863
CaO	12.050	Ca	1.809
Na2O	0.770	Na	0.209
K2O	0.150	K	0.027

Total 101.330 Ions 15.045
(O+OH+F+Cl) 23.001 Normalised 0.000

Classification of 0608-2-3
T site: 7.406 Si 0.594 Al
C site: 0.214 Al 0.486 Fe3 0.021 Ti 4.279 FM
B site: 0.001 FM 1.809 Ca 0.191 Na
A site: 0.018 Na 0.027 K 0.000 Li

A site: Full 0.045 Empty 0.955
B site: FeMg 0.000 Ca2 0.809 CaNa 0.191
T site: Si8 0.406 Si7 0.594

0.406 AOB4Si8	0.272 tremolite	0.131 ferro-actinolite
0.358 hornblende	0.073 magnesio-alumino	0.035 ferro-alumino
	0.166 magnesio-ferri	0.080 ferro-ferri
0.191 barroisite	0.039 magnesio-alumino	0.019 ferro-alumino
	0.089 magnesio-ferri	0.043 ferro-ferri
0.045 edenite	0.030 magnesio	0.015 ferro

Fe/FM = 0.324 Mg/FM = 0.669 Mn/FM = 0.002
Al/M3 = 0.305 Fe3/M3 = 0.695 Cr/M3 = 0.032
K/A = 0.594 Li = 0.000

0608-2-4

Oxide		Cell	
SiO2	46.950	Si	7.136
TiO2	0.810	Ti	0.093
Al2O3	4.570	Al	0.819
Fe2O3	5.830	Fe3	0.667
Cr2O3	0.240	Cr	0.029
FeO	10.130	Fe2	1.288
MnO	0.250	Mn	0.032
NiO	0.020	Ni	0.002
MgO	12.970	Mg	2.939
CaO	11.500	Ca	1.873
Na2O	0.900	Na	0.265
K2O	0.120	K	0.023

Total 94.290 Ions 15.164
(O+OH+F+Cl) 23.005 Normalised 0.000

Classification of A608-2-4
T site: 7.136 Si 0.819 Al 0.046 Fe3
C site: 0.000 Al 0.650 Fe3 0.093 Ti 4.258 FM
B site: 0.003 FM 1.873 Ca 0.124 Na
A site: 0.141 Na 0.023 K 0.000 Li

A site: Full 0.164 Empty 0.836
B site: FeMg 0.002 Ca2 0.874 CaNa 0.124
T site: Si8 0.136 Si7 0.864

0.135	A0B4Si8	0.093	tremolite	0.041	ferro-actinolite
0.575	hornblende	0.000	magnesio-alumino	0.000	ferro-alumino
		0.397	magnesio-ferri	0.174	ferro-ferri
0.124	barroisite	0.000	magnesio-alumino	0.000	ferro-alumino
		0.086	magnesio-ferri	0.038	ferro-ferri
0.164	edenite	0.113	magnesio	0.050	ferro

Fe/FM = 0.302 Mg/FM = 0.690 Mn/FM = 0.002
Al/M3 = 0.000 Fe3/M3 = 1.000 Cr/M3 = 0.044
K/A = 0.142 Li = 0.000

0608-2-5

Oxide		Cell	
SiO2	47.220	Si	7.141
TiO2	0.330	Ti	0.038
Al2O3	6.450	Al	1.150
Fe2O3	4.310	Fe3	0.490
Cr2O3	0.040	Cr	0.005
FeO	13.580	Fe2	1.717
MnO	0.180	Mn	0.023
NiO	0.040	Ni	0.005
MgO	10.790	Mg	2.433
CaO	11.130	Ca	1.803

Na2O	1.190	Na	0.349
K2O	0.230	K	0.044

Total 95.490 Ions 15.198
(O+OH+F+Cl) 23.002 Normalised 0.000

Classification of 0608-2- 5
T site: 7.141 Si 0.859 Al
C site: 0.291 Al 0.495 Fe3 0.038 Ti 4.177 FM
B site: 0.001 FM 1.803 Ca 0.195 Na
A site: 0.153 Na 0.044 K 0.000 Li

A site: Full 0.198 Empty 0.802
B site: FeMg 0.001 Ca2 0.804 CaNa 0.195
T site: Si8 0.141 Si7 0.859

0.141 AOB4Si8	0.082 tremolite	0.058 ferro-actinolite
0.465 hornblende	0.100 magnesio-alumino	0.071 ferro-alumino
	0.171 magnesio-ferri	0.121 ferro-ferri
0.195 barroisite	0.042 magnesio-alumino	0.030 ferro-alumino
	0.072 magnesio-ferri	0.051 ferro-ferri
0.198 edenite	0.115 magnesio	0.081 ferro

Fe/FM = 0.411 Mg/FM = 0.582 Mn/FM = 0.001
Al/M3 = 0.370 Fe3/M3 = 0.630 Cr/M3 = 0.006
K/A = 0.224 Li = 0.000

0608-2- 6

Oxide		Cell	
SiO2	54.350	Si	7.672
TiO2	0.260	Ti	0.028
Al2O3	2.700	Al	0.449
Fe2O3	2.930	Fe3	0.311
Cr2O3	0.220	Cr	0.025
FeO	12.820	Fe2	1.513
MnO	0.280	Mn	0.033
MgO	14.110	Mg	2.969
CaO	12.030	Ca	1.819
Na2O	0.580	Na	0.159
K2O	0.110	K	0.020

Total 100.390 Ions 14.999
(O+OH+F+Cl) 23.002 Normalised 0.000

Classification of 0608-2- 6
T site: 7.672 Si 0.328 Al
C site: 0.121 Al 0.336 Fe3 0.028 Ti 4.494 FM 0.021 Vacant
B site: 0.022 FM 1.819 Ca 0.159 Na
A site: 0.000 Na 0.020 K 0.000 Li

A site: Full 0.020 Empty 0.980
B site: FeMg 0.011 Ca2 0.830 CaNa 0.159
T site: Si8 0.672 Si7 0.328

0.663 AOB4Si8	0.436 tremolite	0.222 ferro-actinolite
0.147 hornblende	0.026 magnesio-alumino	0.013 ferro-alumino
	0.071 magnesio-ferri	0.036 ferro-ferri

0.159	barroisite	0.028	magnesio-alumino	0.014	ferro-alumino
		0.077	magnesio-ferri	0.039	ferro-ferri
0.020	edenite	0.013	magnesio	0.007	ferro
0.010	anthophyllite	0.006	magnesio	0.003	ferro

Fe/FM = 0.335 Mg/FM = 0.657 Mn/FM = 0.002
Al/M3 = 0.265 Fe3/M3 = 0.735 Cr/M3 = 0.054
K/A = 1.000 Li = 0.000

0608-2-7

Oxide		Cell	
SiO2	47.290	Si	6.871
TiO2	0.550	Ti	0.060
Al2O3	8.460	Al	1.449
Fe2O3	6.550	Fe3	0.716
Cr2O3	0.230	Cr	0.026
FeO	12.370	Fe2	1.503
MnO	0.230	Mn	0.028
NiO	0.070	Ni	0.008
MgO	10.800	Mg	2.339
CaO	11.260	Ca	1.753
Na2O	1.320	Na	0.372
K2O	0.380	K	0.070

Total 99.510 Ions 15.197
(O+OH+F+Cl) 23.003 Normalised 0.000

Classification of 0608-2-7
T site: 6.871 Si 1.129 Al
C site: 0.320 Al 0.743 Fe3 0.060 Ti 3.877 FM
B site: 0.002 FM 1.753 Ca 0.245 Na
A site: 0.127 Na 0.070 K 0.000 Li

A site: Full 0.197 Empty 0.803
B site: FeMg 0.001 Ca2 0.754 CaNa 0.245
T site: Si7 0.871 Si6 0.129

0.429	hornblende	0.078	magnesio-alumino	0.050	ferro-alumino
		0.181	magnesio-ferri	0.116	ferro-ferri
0.245	barroisite	0.045	magnesio-alumino	0.029	ferro-alumino
		0.103	magnesio-ferri	0.066	ferro-ferri
0.128	tschermakite	0.023	magnesio-alumino	0.015	ferro-alumino
		0.054	magnesio-ferri	0.035	ferro-ferri
0.197	edenite	0.119	magnesio	0.076	ferro

Fe/FM = 0.388 Mg/FM = 0.603 Mn/FM = 0.002
Al/M3 = 0.301 Fe3/M3 = 0.699 Cr/M3 = 0.025
K/A = 0.357 Li = 0.000

0608-2-8

Oxide		Cell	
SiO2	44.640	Si	6.733
TiO2	0.530	Ti	0.060
Al2O3	10.360	Al	1.842
Fe2O3	3.680	Fe3	0.418
Cr2O3	0.090	Cr	0.011

FeO	16.170	Fe2	2.040
MnO	0.170	Mn	0.022
NiO	0.010	Ni	0.001
MgO	8.340	Mg	1.875
CaO	11.040	Ca	1.784
Na2O	1.540	Na	0.450
K2O	0.660	K	0.127

Total 97.230 Ions 15.363
(O+OH+F+Cl) 23.003 Normalised 0.000

Classification of 0608-2-8
T site: 6.733 Si 1.267 Al
C site: 0.575 Al 0.428 Fe3 0.060 Ti 3.936 FM
B site: 0.002 FM 1.784 Ca 0.214 Na
A site: 0.236 Na 0.127 K 0.000 Li

A site: Full 0.363 Empty 0.637
B site: FeMg 0.001 Ca2 0.785 CaNa 0.214
T site: Si7 0.733 Si6 0.267

0.156 hornblende	0.043 magnesio-alumino	0.046 ferro-alumino
	0.032 magnesio-ferri	0.034 ferro-ferri
0.214 barroisite	0.058 magnesio-alumino	0.064 ferro-alumino
	0.044 magnesio-ferri	0.047 ferro-ferri
0.266 tschermakite	0.073 magnesio-alumino	0.079 ferro-alumino
	0.054 magnesio-ferri	0.059 ferro-ferri
0.363 edenite	0.173 magnesio	0.188 ferro

Fe/FM = 0.518 Mg/FM = 0.476 Mn/FM = 0.001
Al/M3 = 0.573 Fe3/M3 = 0.427 Cr/M3 = 0.011
K/A = 0.350 Li = 0.000

1108-2-1

Oxide		Cell	
SiO2	51.840	Si	7.702
TiO2	0.240	Ti	0.027
Al2O3	1.680	Al	0.294
Fe2O3	4.350	Fe3	0.486
Cr2O3	0.010	Cr	0.001
FeO	13.420	Fe2	1.667
MnO	0.700	Mn	0.088
NiO	0.010	Ni	0.001
MgO	12.340	Mg	2.733
CaO	11.350	Ca	1.807
Na2O	0.430	Na	0.124
K2O	0.130	K	0.025

Total 96.500 Ions 14.956
(O+OH+F+Cl) 23.001 Normalised 0.000

Classification of 1108-2-1
T site: 7.702 Si 0.294 Al 0.004 Fe3
C site: 0.000 Al 0.484 Fe3 0.027 Ti 4.421 FM 0.069 Vacant
B site: 0.069 FM 1.807 Ca 0.124 Na
A site: 0.000 Na 0.025 K 0.000 Li

```
A site:  Full  0.025  Empty 0.975
B site:  FeMg  0.035  Ca2   0.841  CaNa  0.124
T site:  Si8   0.702  Si7   0.298

0.674 A0B4Si8        0.411 tremolite              0.250 ferro-actinolite
0.143 hornblende     0.000 magnesio-alumino       0.000 ferro-alumino
                     0.087 magnesio-ferri         0.053 ferro-ferri
0.124 barroisite     0.000 magnesio-alumino       0.000 ferro-alumino
                     0.075 magnesio-ferri         0.046 ferro-ferri
0.024 edenite        0.014 magnesio               0.009 ferro
0.031 anthophyllite  0.019 magnesio               0.011 ferro
0.003 gedrite        0.002 magnesio               0.001 ferro

Fe/FM = 0.371  Mg/FM  = 0.609  Mn/FM = 0.004
Al/M3 = 0.000  Fe3/M3 = 1.000  Cr/M3 = 0.002
K/A   = 1.000  Li     = 0.000


1108-2-2
        Oxide         Cell
SiO2    48.400  Si    6.899
TiO2     0.230  Ti    0.025
Al2O3    4.790  Al    0.805
Fe2O3   23.140  Fe3   2.482
Cr2O3    0.010  Cr    0.001
MnO      0.510  Mn    0.062
NiO      0.020  Ni    0.002
MgO     13.480  Mg    2.864
CaO      8.340  Ca    1.274
Na2O     0.130  Na    0.036
K2O      0.040  K     0.007

Total  99.090 Ions 14.456
(O+OH+F+Cl) 23.001 Normalised  0.000

Classification of 1108-2-2
T site: 6.899 Si  0.805 Al   0.297 Fe3
C site: 0.000 Al  2.186 Fe3  0.025 Ti  2.238 FM  0.551 Vacant
B site: 0.690 FM  1.274 Ca   0.036 Na
A site: 0.000 Na  0.007 K    0.000 Li

A site:  Full  0.007  Empty 0.993
B site:  FeMg  0.345  Ca2   0.619  CaNa  0.036
T site:  Si7   0.899  Si6   0.101

0.549 hornblende        0.000 magnesio-alumino     0.000 ferro-alumino
                        0.537 magnesio-ferri       0.000 ferro-ferri
0.036 barroisite        0.000 magnesio-alumino     0.000 ferro-alumino
                        0.035 magnesio-ferri       0.000 ferro-ferri
0.065 tschermakite      0.000 magnesio-alumino     0.000 ferro-alumino
                        0.064 magnesio-ferri       0.000 ferro-ferri
0.005 edenite           0.005 magnesio             0.000 ferro
0.153 anthophyllite     0.150 magnesio             0.000 ferro
0.189 gedrite           0.185 magnesio             0.000 ferro
0.003 Na-anthophyllite  0.003 magnesio             0.000 ferro

Fe/FM = 0.000  Mg/FM  = 0.978  Mn/FM = 0.007
Al/M3 = 0.000  Fe3/M3 = 1.000  Cr/M3 = 0.001
```

K/A = 1.000 Li = 0.000

3107-9-1

Oxide		Cell	
SiO2	47.510	Si	6.825
TiO2	0.440	Ti	0.048
Al2O3	9.800	Al	1.659
Fe2O3	3.020	Fe3	0.326
Cr2O3	0.150	Cr	0.017
FeO	9.510	Fe2	1.143
MnO	0.150	Mn	0.018
NiO	0.030	Ni	0.003
MgO	13.830	Mg	2.962
CaO	11.600	Ca	1.785
Na2O	2.290	Na	0.638
K2O	0.250	K	0.046

Total 98.580 Ions 15.471
(O+OH+F+Cl) 23.003 Normalised 0.000

Classification of 3107-9-1
T site: 6.825 Si 1.175 Al
C site: 0.484 Al 0.344 Fe3 0.048 Ti 4.125 FM
B site: 0.001 FM 1.785 Ca 0.213 Na
A site: 0.425 Na 0.046 K 0.000 Li

A site: Full 0.471 Empty 0.529
B site: FeMg 0.001 Ca2 0.786 CaNa 0.213
T site: Si7 0.825 Si6 0.175

0.141 hornblende	0.059 magnesio-alumino	0.023 ferro-alumino
	0.042 magnesio-ferri	0.016 ferro-ferri
0.213 barroisite	0.090 magnesio-alumino	0.035 ferro-alumino
	0.063 magnesio-ferri	0.024 ferro-ferri
0.175 tschermakite	0.073 magnesio-alumino	0.028 ferro-alumino
	0.052 magnesio-ferri	0.020 ferro-ferri
0.470 edenite	0.337 magnesio	0.130 ferro

Fe/FM = 0.277 Mg/FM = 0.718 Mn/FM = 0.001
Al/M3 = 0.585 Fe3/M3 = 0.415 Cr/M3 = 0.021
K/A = 0.097 Li = 0.000

3107-9-2

Oxide		Cell	
SiO2	45.670	Si	6.691
TiO2	0.480	Ti	0.053
Al2O3	9.750	Al	1.683
Fe2O3	6.370	Fe3	0.702
Cr2O3	0.270	Cr	0.031
FeO	6.460	Fe2	0.791
MnO	0.100	Mn	0.012
NiO	0.160	Ni	0.019
MgO	13.820	Mg	3.018
CaO	10.710	Ca	1.681
Na2O	2.480	Na	0.704
K2O	0.170	K	0.032

Total 96.440 Ions 15.419
(O+OH+F+Cl) 23.003 Normalised 0.000

Classification of 3107-9-2
T site: 6.691 Si 1.309 Al
C site: 0.374 Al 0.734 Fe3 0.053 Ti 3.839 FM
B site: 0.002 FM 1.681 Ca 0.317 Na
A site: 0.387 Na 0.032 K 0.000 Li

A site: Full 0.419 Empty 0.581
B site: FeMg 0.001 Ca2 0.682 CaNa 0.317
T site: Si7 0.691 Si6 0.309

0.295 barroisite	0.078 magnesio-alumino	0.021 ferro-alumino
	0.153 magnesio-ferri	0.040 ferro-ferri
0.286 tschermakite	0.076 magnesio-alumino	0.020 ferro-alumino
	0.149 magnesio-ferri	0.039 ferro-ferri
0.396 edenite	0.311 magnesio	0.082 ferro
0.023 taramite	0.006 magnesio-alumino	0.002 ferro-alumino
	0.012 magnesio-ferri	0.003 ferro-ferri

Fe/FM = 0.206 Mg/FM = 0.786 Mn/FM = 0.001
Al/M3 = 0.338 Fe3/M3 = 0.662 Cr/M3 = 0.028
K/A = 0.076 Li = 0.000

3107-9-3

Oxide		Cell	
SiO2	58.000	Si	7.872
TiO2	0.240	Ti	0.024
Al2O3	16.270	Al	2.603
Cr2O3	0.060	Cr	0.006
FeO	5.020	Fe2	0.570
MnO	0.090	Mn	0.010
NiO	0.100	Ni	0.011
MgO	6.280	Mg	1.271
CaO	3.170	Ca	0.461
Na2O	7.360	Na	1.937
K2O	0.030	K	0.005

Total 96.620 Ions 14.771
(O+OH+F+Cl) 23.002 Normalised 13.000

Classification of 3107-9-3
T site: 7.872 Si 0.128 Al
C site: 2.475 Al 0.006 Fe3 0.024 Ti 1.862 FM 0.632 Vacant
B site: 0.000 FM 0.461 Ca 1.539 Na
A site: 0.398 Na 0.005 K 0.000 Li

A site: Full 0.403 Empty 0.597
B site: CaNa 0.461 Na2 0.539
T site: Si8 0.872 Si7 0.128

0.504 AOB2Si8	0.343 glaucophane	0.154 Fe glaucophane
	0.001 Mg riebeckite	0.000 riebeckite
0.093 barroisite	0.063 magnesio-alumino	0.028 ferro-alumino
	0.000 magnesio-ferri	0.000 ferro-ferri
0.368 richterite	0.251 magnesio	0.113 ferro

0.035 nyboite 0.024 magnesio-alumino 0.011 ferro-alumino
0.000 magnesio-ferri 0.000 ferro-ferri

Fe/FM = 0.306 Mg/FM = 0.683 Mn/FM = 0.003
Al/M3 = 0.997 Fe3/M3 = 0.003 Cr/M3 = 0.003
K/A = 0.013 Li = 0.000

3107-9-4

	Oxide		Cell
SiO2	38.640	Si	5.959
TiO2	0.660	Ti	0.077
Al2O3	12.930	Al	2.350
Fe2O3	7.520	Fe3	0.873
Cr2O3	0.290	Cr	0.035
FeO	5.990	Fe2	0.773
MnO	0.110	Mn	0.014
NiO	0.100	Ni	0.012
MgO	12.650	Mg	2.908
CaO	11.570	Ca	1.912
Na2O	2.710	Na	0.810
K2O	0.200	K	0.039

Total 93.370 Ions 15.764
(O+OH+F+Cl) 23.004 Normalised 0.000

Classification of 3107-9-4
T site: 5.959 Si 2.041 Al
C site: 0.310 Al 0.908 Fe3 0.077 Ti 3.706 FM
B site: 0.002 FM 1.912 Ca 0.086 Na
A site: 0.724 Na 0.039 K 0.000 Li

A site: Full 0.764 Empty 0.236
B site: FeMg 0.001 Ca2 0.913 CaNa 0.086
T site: Si6 0.959 Si5 0.041

0.236 tschermakite	0.047 magnesio-alumino	0.012 ferro-alumino
	0.138 magnesio-ferri	0.037 ferro-ferri
0.560 A1B4Si6	0.112 pargasite	0.030 Fe pargasite
	0.328 Mg hastingsite	0.087 hastingsite
0.086 taramite	0.017 magnesio-alumino	0.005 ferro-alumino
	0.050 magnesio-ferri	0.013 ferro-ferri
0.077 kaersutite	0.060 magnesio-alumino	0.016 ferro-alumino
0.041 A1B4Si5	0.032 magnesio-alumino	0.008 ferro-alumino

Fe/FM = 0.208 Mg/FM = 0.784 Mn/FM = 0.001
Al/M3 = 0.254 Fe3/M3 = 0.746 Cr/M3 = 0.029
K/A = 0.052 Li = 0.000

3107-9-5

	Oxide		Cell
SiO2	42.450	Si	6.275
TiO2	1.220	Ti	0.136
Al2O3	12.110	Al	2.110
Fe2O3	3.610	Fe3	0.402
Cr2O3	0.050	Cr	0.006
FeO	9.430	Fe2	1.166

MnO	0.140	Mn	0.018
NiO	0.140	Ni	0.017
MgO	13.050	Mg	2.876
CaO	11.860	Ca	1.878
Na2O	3.090	Na	0.886
K2O	0.130	K	0.025

Total 97.280 Ions 15.793
(O+OH+F+Cl) 23.008 Normalised 0.000

Classification of 3107-9-5
T site: 6.275 Si 1.725 Al
C site: 0.385 Al 0.407 Fe3 0.136 Ti 4.072 FM
B site: 0.004 FM 1.878 Ca 0.117 Na
A site: 0.769 Na 0.025 K 0.000 Li

A site: Full 0.793 Empty 0.207
B site: FeMg 0.002 Ca2 0.881 CaNa 0.117
T site: Si7 0.275 Si6 0.725

0.206 tschermakite	0.071 magnesio-alumino	0.029 ferro-alumino
	0.075 magnesio-ferri	0.030 ferro-ferri
0.275 edenite	0.194 magnesio	0.079 ferro
0.264 A1B4Si6	0.090 pargasite	0.037 Fe pargasite
	0.096 Mg hastingsite	0.039 hastingsite
0.117 taramite	0.040 magnesio-alumino	0.016 ferro-alumino
	0.042 magnesio-ferri	0.017 ferro-ferri
0.136 kaersutite	0.096 magnesio-alumino	0.039 ferro-alumino

Fe/FM = 0.286 Mg/FM = 0.706 Mn/FM = 0.001
Al/M3 = 0.486 Fe3/M3 = 0.514 Cr/M3 = 0.007
K/A = 0.031 Li = 0.000

3107-9-6

Oxide		Cell	
SiO2	43.100	Si	6.620
TiO2	0.820	Ti	0.095
Al2O3	8.350	Al	1.512
Fe2O3	4.780	Fe3	0.553
Cr2O3	0.170	Cr	0.021
FeO	7.450	Fe2	0.957
MnO	0.030	Mn	0.004
NiO	0.110	Ni	0.014
MgO	14.100	Mg	3.229
CaO	11.560	Ca	1.902
Na2O	2.180	Na	0.649
K2O	0.180	K	0.035

Total 92.830 Ions 15.590
(O+OH+F+Cl) 23.005 Normalised 0.000

Classification of 3107-9-6
T site: 6.620 Si 1.380 Al
C site: 0.132 Al 0.573 Fe3 0.095 Ti 4.200 FM
B site: 0.003 FM 1.902 Ca 0.095 Na
A site: 0.555 Na 0.035 K 0.000 Li

```
A site:  Full  0.590  Empty 0.410
B site:  FeMg  0.001  Ca2   0.904  CaNa  0.095
T site:  Si7   0.620  Si6   0.380

0.062 barroisite          0.009 magnesio-alumino     0.003 ferro-alumino
                          0.039 magnesio-ferri       0.012 ferro-ferri
0.347 tschermakite        0.050 magnesio-alumino     0.015 ferro-alumino
                          0.217 magnesio-ferri       0.064 ferro-ferri
0.557 edenite             0.428 magnesio               0.127 ferro
0.032 taramite            0.005 magnesio-alumino     0.001 ferro-alumino
                          0.020 magnesio-ferri       0.006 ferro-ferri

Fe/FM = 0.228  Mg/FM  = 0.768  Mn/FM = 0.000
Al/M3 = 0.187  Fe3/M3 = 0.813  Cr/M3 = 0.029
K/A   = 0.060  Li     = 0.000


3107-9-7
        Oxide         Cell
SiO2    45.290  Si    6.641
TiO2     0.310  Ti    0.034
Al2O3    7.780  Al    1.345
Fe2O3   13.350  Fe3   1.473
Cr2O3    0.210  Cr    0.024
MnO      0.120  Mn    0.015
NiO      0.070  Ni    0.008
MgO     15.840  Mg    3.463
CaO     10.690  Ca    1.679
Na2O     1.490  Na    0.424
K2O      0.120  K     0.022

Total   95.270 Ions 15.129
(O+OH+F+Cl) 23.002 Normalised  0.000

Classification of 3107-9-7
T site: 6.641 Si  1.345 Al   0.014 Fe3
C site: 0.000 Al  1.483 Fe3  0.034 Ti  3.483 FM
B site: 0.003 FM  1.679 Ca   0.317 Na
A site: 0.106 Na  0.022 K    0.000 Li

A site:  Full  0.129  Empty 0.871
B site:  FeMg  0.002  Ca2   0.681  CaNa  0.317
T site:  Si7   0.641  Si6   0.359

0.195 hornblende          0.000 magnesio-alumino     0.000 ferro-alumino
                          0.193 magnesio-ferri       0.000 ferro-ferri
0.317 barroisite          0.000 magnesio-alumino     0.000 ferro-alumino
                          0.315 magnesio-ferri       0.000 ferro-ferri
0.358 tschermakite        0.000 magnesio-alumino     0.000 ferro-alumino
                          0.356 magnesio-ferri       0.000 ferro-ferri
0.128 edenite             0.128 magnesio               0.000 ferro
0.001 gedrite             0.001 magnesio               0.000 ferro

Fe/FM = 0.000  Mg/FM  = 0.993  Mn/FM = 0.001
Al/M3 = 0.000  Fe3/M3 = 1.000  Cr/M3 = 0.016
K/A   = 0.174  Li     = 0.000
```

3107-9-8

Oxide		Cell	
SiO2	47.610	Si	6.684
TiO2	0.350	Ti	0.037
Al2O3	11.670	Al	1.931
Fe2O3	3.720	Fe3	0.393
Cr2O3	0.190	Cr	0.021
FeO	9.580	Fe2	1.125
MnO	0.190	Mn	0.023
NiO	0.130	Ni	0.015
MgO	13.250	Mg	2.773
CaO	11.520	Ca	1.733
Na2O	2.660	Na	0.724
K2O	0.140	K	0.025

Total 101.010 Ions 15.483
(O+OH+F+Cl) 23.002 Normalised 0.000

Classification of 3107-9-8
T site: 6.684 Si 1.316 Al
C site: 0.615 Al 0.414 Fe3 0.037 Ti 3.934 FM
B site: 0.001 FM 1.733 Ca 0.266 Na
A site: 0.458 Na 0.025 K 0.000 Li

A site: Full 0.483 Empty 0.517
B site: FeMg 0.001 Ca2 0.733 CaNa 0.266
T site: Si7 0.684 Si6 0.316

0.233 barroisite	0.098 magnesio-alumino	0.040 ferro-alumino
	0.066 magnesio-ferri	0.027 ferro-ferri
0.283 tschermakite	0.119 magnesio-alumino	0.048 ferro-alumino
	0.080 magnesio-ferri	0.033 ferro-ferri
0.450 edenite	0.317 magnesio	0.129 ferro
0.033 taramite	0.014 magnesio-alumino	0.006 ferro-alumino
	0.009 magnesio-ferri	0.004 ferro-ferri

Fe/FM = 0.286 Mg/FM = 0.705 Mn/FM = 0.001
Al/M3 = 0.598 Fe3/M3 = 0.402 Cr/M3 = 0.020
K/A = 0.052 Li = 0.000

3107-9-9

Oxide		Cell	
SiO2	40.440	Si	6.201
TiO2	0.620	Ti	0.071
Al2O3	11.860	Al	2.143
Fe2O3	6.600	Fe3	0.762
Cr2O3	0.380	Cr	0.046
FeO	5.740	Fe2	0.736
MnO	0.200	Mn	0.026
NiO	0.120	Ni	0.015
MgO	13.130	Mg	3.002
CaO	11.620	Ca	1.909
Na2O	2.210	Na	0.657
K2O	0.160	K	0.031

Total 93.080 Ions 15.600
(O+OH+F+Cl) 23.004 Normalised 0.000

Classification of 3107-9-9
T site: 6.201 Si 1.799 Al
C site: 0.345 Al 0.808 Fe3 0.071 Ti 3.776 FM
B site: 0.002 FM 1.909 Ca 0.089 Na
A site: 0.568 Na 0.031 K 0.000 Li

A site: Full 0.600 Empty 0.400
B site: FeMg 0.001 Ca2 0.910 CaNa 0.089
T site: Si7 0.201 Si6 0.799

0.400 tschermakite	0.095 magnesio-alumino	0.023 ferro-alumino
	0.223 magnesio-ferri	0.055 ferro-ferri
0.201 edenite	0.160 magnesio	0.039 ferro
0.238 A1B4Si6	0.057 pargasite	0.014 Fe pargasite
	0.133 Mg hastingsite	0.032 hastingsite
0.089 taramite	0.021 magnesic-alumino	0.005 ferro-alumino
	0.049 magnesio-ferri	0.012 ferro-ferri
0.071 kaersutite	0.057 magnesio-alumino	0.014 ferro-alumino

Fe/FM = 0.195 Mg/FM = 0.794 Mn/FM = 0.002
Al/M3 = 0.299 Fe3/M3 = 0.701 Cr/M3 = 0.040
K/A = 0.052 Li = 0.000

3107-9-10

Oxide		Cell	
SiO2	51.260	Si	7.225
TiO2	0.460	Ti	0.049
Al2O3	7.200	Al	1.196
Fe2O3	1.980	Fe3	0.210
Cr2O3	0.080	Cr	0.009
FeO	9.460	Fe2	1.115
MnO	0.070	Mn	0.008
NiO	0.040	Ni	0.005
MgO	15.160	Mg	3.185
CaO	11.290	Ca	1.705
Na2O	2.210	Na	0.604
K2O	0.150	K	0.027

Total 99.360 Ions 15.337
(O+OH+F+Cl) 23.003 Normalised 0.000

Classification of 3107-9-10
T site: 7.225 Si 0.775 Al
C site: 0.421 Al 0.219 Fe3 0.049 Ti 4.312 FM
B site: 0.002 FM 1.705 Ca 0.293 Na
A site: 0.310 Na 0.027 K 0.000 Li

A site: Full 0.337 Empty 0.663
B site: FeMg 0.001 Ca2 0.706 CaNa 0.293
T site: Si8 0.225 Si7 0.775

0.224 A0B4Si8	0.166 tremolite	0.058 ferro-actinolite
0.144 hornblende	0.070 magnesio-alumino	0.025 ferro-alumino
	0.036 magnesio-ferri	0.013 ferro-ferri
0.293 barroisite	0.143 magnesio-alumino	0.050 ferro-alumino
	0.074 magnesio-ferri	0.026 ferro-ferri
0.337 edenite	0.249 magnesio	0.087 ferro

Fe/FM = 0.259 Mg/FM = 0.738 Mn/FM = 0.000
Al/M3 = 0.658 Fe3/M3 = 0.342 Cr/M3 = 0.014
K/A = 0.080 Li = 0.000

3107-9-11

	Oxide		Cell
SiO2	40.770	Si	6.127
TiO2	0.590	Ti	0.067
Al2O3	12.270	Al	2.173
Fe2O3	6.690	Fe3	0.757
Cr2O3	0.430	Cr	0.051
FeO	7.620	Fe2	0.958
MnO	0.110	Mn	0.014
NiO	0.100	Ni	0.012
MgO	12.690	Mg	2.843
CaO	11.360	Ca	1.829
Na2O	3.250	Na	0.947
K2O	0.150	K	0.029

Total 96.030 Ions 15.807
(O+OH+F+Cl) 23.004 Normalised 0.000

Classification of 3107-9-11
T site: 6.127 Si 1.873 Al
C site: 0.301 Al 0.808 Fe3 0.067 Ti 3.825 FM
B site: 0.002 FM 1.829 Ca 0.169 Na
A site: 0.778 Na 0.029 K 0.000 Li

A site: Full 0.807 Empty 0.193
B site: FeMg 0.001 Ca2 0.830 CaNa 0.169
T site: Si7 0.127 Si6 0.873

0.193 tschermakite	0.039 magnesio-alumino	0.013 ferro-alumino
	0.104 magnesio-ferri	0.035 ferro-ferri
0.127 edenite	0.094 magnesio	0.032 ferro
0.444 A1B4Si6	0.089 pargasite	0.030 Fe pargasite
	0.240 Mg hastingsite	0.081 hastingsite
0.169 taramite	0.034 magnesio-alumino	0.011 ferro-alumino
	0.091 magnesio-ferri	0.031 ferro-ferri
0.067 kaersutite	0.050 magnesio-alumino	0.017 ferro-alumino

Fe/FM = 0.250 Mg/FM = 0.743 Mn/FM = 0.001
Al/M3 = 0.271 Fe3/M3 = 0.729 Cr/M3 = 0.046
K/A = 0.036 Li = 0.000

3107-9-12

	Oxide		Cell
SiO2	43.100	Si	6.445
TiO2	0.480	Ti	0.054
Al2O3	10.650	Al	1.877
Fe2O3	5.400	Fe3	0.608
Cr2O3	0.110	Cr	0.013
FeO	7.940	Fe2	0.993
MnO	0.140	Mn	0.018
NiO	0.080	Ni	0.010
MgO	13.390	Mg	2.985

CaO	11.590	Ca	1.857
Na2O	2.620	Na	0.760
K2O	0.180	K	0.034

Total 95.680 Ions 15.652
(O+OH+F+Cl) 23.003 Normalised 0.000

Classification of 3107-9-12
T site: 6.445 Si 1.555 Al
C site: 0.322 Al 0.621 Fe3 0.054 Ti 4.004 FM
B site: 0.002 FM 1.857 Ca 0.142 Na
A site: 0.618 Na 0.034 K 0.000 Li

A site: Full 0.652 Empty 0.348
B site: FeMg 0.001 Ca2 0.858 CaNa 0.142
T site: Si7 0.445 Si6 0.555

0.347 tschermakite	0.088 magnesio-alumino	0.029 ferro-alumino
	0.170 magnesio-ferri	0.057 ferro-ferri
0.444 edenite	0.331 magnesio	0.110 ferro
0.012 A1B4Si6	0.003 pargasite	0.001 Fe pargasite
	0.006 Mg hastingsite	0.002 hastingsite
0.142 taramite	0.036 magnesio-alumino	0.012 ferro-alumino
	0.069 magnesio-ferri	0.023 ferro-ferri
0.054 kaersutite	0.040 magnesio-alumino	0.013 ferro-alumino

Fe/FM = 0.248 Mg/FM = 0.745 Mn/FM = 0.001
Al/M3 = 0.341 Fe3/M3 = 0.659 Cr/M3 = 0.014
K/A = 0.073 Li = 0.000

0308-3-1

	Oxide		Cell
SiO2	50.330	Si	7.205
TiO2	0.230	Ti	0.025
Al2O3	4.010	Al	0.677
Fe2O3	7.070	Fe3	0.762
Cr2O3	0.060	Cr	0.007
FeO	1.000	Fe2	0.120
MnO	0.140	Mn	0.017
NiO	0.020	Ni	0.002
MgO	19.620	Mg	4.187
CaO	11.770	Ca	1.805
Na2O	1.680	Na	0.466
K2O	0.110	K	0.020

Total 96.040 Ions 15.292
(O+OH+F+Cl) 23.001 Normalised 0.000

Classification of 0308-3-1
T site: 7.205 Si 0.677 Al 0.118 Fe3
C site: 0.000 Al 0.650 Fe3 0.025 Ti 4.325 FM
B site: 0.001 FM 1.805 Ca 0.194 Na
A site: 0.272 Na 0.020 K 0.000 Li

A site: Full 0.292 Empty 0.708
B site: FeMg 0.000 Ca2 0.806 CaNa 0.194
T site: Si8 0.205 Si7 0.795

0.205 A0B4Si8	0.198 tremolite	0.006 ferro-actinolite
0.308 hornblende	0.000 magnesio-alumino	0.000 ferro-alumino
	0.299 magnesio-ferri	0.009 ferro-ferri
0.194 barroisite	0.000 magnesio-alumino	0.000 ferro-alumino
	0.188 magnesio-ferri	0.005 ferro-ferri
0.292 edenite	0.283 magnesio	0.008 ferro

Fe/FM = 0.028 Mg/FM = 0.968 Mn/FM = 0.001
Al/M3 = 0.000 Fe3/M3 = 1.000 Cr/M3 = 0.010
K/A = 0.069 Li = 0.000

0308-3-2

Oxide		Cell	
SiO2	49.150	Si	7.044
TiO2	0.320	Ti	0.034
Al2O3	5.800	Al	0.980
Fe2O3	6.930	Fe3	0.747
FeO	2.680	Fe2	0.321
MnO	0.130	Mn	0.016
NiO	0.160	Ni	0.018
MgO	17.970	Mg	3.840
CaO	11.660	Ca	1.791
Na2O	1.850	Na	0.514
K2O	0.120	K	0.022

Total 96.770 Ions 15.328
(O+OH+F+Cl) 23.002 Normalised 0.000

Classification of 0308-3-2
T site: 7.044 Si 0.956 Al
C site: 0.024 Al 0.747 Fe3 0.034 Ti 4.194 FM
B site: 0.001 FM 1.791 Ca 0.208 Na
A site: 0.306 Na 0.022 K 0.000 Li

A site: Full 0.328 Empty 0.672
B site: FeMg 0.001 Ca2 0.791 CaNa 0.208
T site: Si8 0.044 Si7 0.956

0.044 A0B4Si8	0.041 tremolite	0.003 ferro-actinolite
0.419 hornblende	0.012 magnesio-alumino	0.001 ferro-alumino
	0.372 magnesio-ferri	0.031 ferro-ferri
0.208 barroisite	0.006 magnesio-alumino	0.000 ferro-alumino
	0.185 magnesio-ferri	0.015 ferro-ferri
0.327 edenite	0.300 magnesio	0.025 ferro

Fe/FM = 0.077 Mg/FM = 0.915 Mn/FM = 0.001
Al/M3 = 0.031 Fe3/M3 = 0.969 Cr/M3 = 0.000
K/A = 0.067 Li = 0.000

0308-3-3

Oxide		Cell	
SiO2	50.770	Si	7.099
TiO2	0.160	Ti	0.017
Al2O3	5.800	Al	0.956
Fe2O3	10.650	Fe3	1.121
Cr2O3	0.040	Cr	0.004

MnO	0.120	Mn	0.014
NiO	0.170	Ni	0.019
MgO	20.520	Mg	4.277
CaO	7.970	Ca	1.194
Na2O	1.050	Na	0.285
K2O	0.030	K	0.005

Total 97.280 Ions 14.990
(O+OH+F+Cl) 23.001 Normalised 0.000

Classification of 0308-3-3
T site: 7.099 Si 0.901 Al
C site: 0.054 Al 1.125 Fe3 0.017 Ti 3.789 FM 0.015 Vacant
B site: 0.521 FM 1.194 Ca 0.285 Na
A site: 0.000 Na 0.005 K 0.000 Li

A site: Full 0.005 Empty 0.995
B site: FeMg 0.261 Ca2 0.455 CaNa 0.285
T site: Si8 0.099 Si7 0.901

0.063 A0B4Si8	0.062 tremolite		0.000 ferro-actinolite
0.389 hornblende	0.018 magnesio-alumino		0.000 ferro-alumino
	0.368 magnesio-ferri		0.000 ferro-ferri
0.285 barroisite	0.013 magnesio-alumino		0.000 ferro-alumino
	0.269 magnesio-ferri		0.000 ferro-ferri
0.003 edenite	0.003 magnesio		0.000 ferro
0.147 anthophyllite	0.146 magnesio		0.000 ferro
0.111 gedrite	0.111 magnesio		0.000 ferro
0.002 Na-anthophyllite	0.002 magnesio		0.000 ferro

Fe/FM = 0.000 Mg/FM = 0.992 Mn/FM = 0.001
Al/M3 = 0.046 Fe3/M3 = 0.954 Cr/M3 = 0.004
K/A = 1.000 Li = 0.000

0308-3-4

Oxide		Cell	
SiO2	41.690	Si	6.213
TiO2	0.180	Ti	0.020
Al2O3	10.170	Al	1.786
Fe2O3	11.600	Fe3	1.301
MnO	0.220	Mn	0.028
NiO	0.110	Ni	0.013
MgO	21.460	Mg	4.767
CaO	5.460	Ca	0.872
Na2O	0.540	Na	0.156
K2O	0.030	K	0.006

Total 91.460 Ions 15.162
(O+OH+F+Cl) 22.857 Normalised 0.000

Classification of 0308-3-4
T site: 6.213 Si 1.786 Al 0.001 Fe3
C site: 0.000 Al 1.300 Fe3 0.020 Ti 3.680 FM
B site: 1.128 FM 0.872 Ca 0.000 Na
A site: 0.156 Na 0.006 K 0.000 Li

A site: Full 0.162 Empty 0.838

```
B site:  FeMg  0.564  Ca2   0.436
T site:  Si7   0.213  Si6   0.787

0.022 hornblende          0.000 magnesio-alumino     0.000 ferro-alumino
                          0.022 magnesio-ferri       0.000 ferro-ferri
0.343 tschermakite        0.000 magnesio-alumino     0.000 ferro-alumino
                          0.340 magnesio-ferri       0.000 ferro-ferri
0.070 edenite             0.070 magnesio             0.000 ferro
0.014 anthophyllite       0.014 magnesio             0.000 ferro
0.459 gedrite             0.455 magnesio             0.000 ferro
0.091 Na-anthophyllite    0.090 magnesio             0.000 ferro

Fe/FM = 0.000  Mg/FM  = 0.991  Mn/FM = 0.001
Al/M3 = 0.000  Fe3/M3 = 1.000  Cr/M3 = 0.000
K/A   = 0.035  Li     = 0.000
```

0308-3-5

	Oxide		Cell
SiO2	45.040	Si	6.557
TiO2	0.480	Ti	0.053
Al2O3	9.390	Al	1.611
Fe2O3	7.080	Fe3	0.776
Cr2O3	0.160	Cr	0.018
FeO	4.660	Fe2	0.567
MnO	0.180	Mn	0.022
MgO	15.650	Mg	3.397
CaO	11.300	Ca	1.763
Na2O	2.880	Na	0.813
K2O	0.210	K	0.039

```
Total  97.030 Ions 15.616
(O+OH+F+Cl) 23.003 Normalised  0.000

Classification of 0308-3-5
T site: 6.557 Si  1.443 Al
C site: 0.169 Al  0.794 Fe3  0.053 Ti  3.985 FM
B site: 0.002 FM  1.763 Ca   0.236 Na
A site: 0.577 Na  0.039 K    0.000 Li

A site:  Full  0.616  Empty 0.384
B site:  FeMg  0.001  Ca2   0.764  CaNa  0.236
T site:  Si7   0.557  Si6   0.443

0.088 barroisite          0.013 magnesio-alumino     0.002 ferro-alumino
                          0.062 magnesio-ferri       0.010 ferro-ferri
0.295 tschermakite        0.044 magnesio-alumino     0.007 ferro-alumino
                          0.207 magnesio-ferri       0.035 ferro-ferri
0.469 edenite             0.399 magnesio             0.067 ferro
0.147 taramite            0.022 magnesio-alumino     0.004 ferro-alumino
                          0.103 magnesio-ferri       0.017 ferro-ferri

Fe/FM = 0.142  Mg/FM  = 0.852  Mn/FM = 0.001
Al/M3 = 0.175  Fe3/M3 = 0.825  Cr/M3 = 0.019
K/A   = 0.063  Li     = 0.000
```

0308-3-6

	Oxide		Cell
SiO2	51.860	Si	7.327
TiO2	0.140	Ti	0.015
Al2O3	2.990	Al	0.498
Fe2O3	9.240	Fe3	0.982
Cr2O3	0.060	Cr	0.007
MnO	0.180	Mn	0.022
NiO	0.070	Ni	0.008
MgO	21.100	Mg	4.444
CaO	10.390	Ca	1.573
Na2O	0.290	Na	0.079

Total 96.320 Ions 14.955
(O+OH+F+Cl) 23.001 Normalised 0.000

Classification of 0308-3-6
T site: 7.327 Si 0.498 Al 0.175 Fe3
C site: 0.000 Al 0.814 Fe3 0.015 Ti 4.126 FM 0.045 Vacant
B site: 0.348 FM 1.573 Ca 0.079 Na
A site: 0.000 Na 0.000 K 0.000 Li

A site: Full 0.000 Empty 1.000
B site: FeMg 0.174 Ca2 0.747 CaNa 0.079
T site: Si8 0.327 Si7 0.673

0.265 A0B4Si8	0.264 tremolite		0.000 ferro-actinolite
0.481 hornblende	0.000 magnesio-alumino		0.000 ferro-alumino
	0.478 magnesio-ferri		0.000 ferro-ferri
0.079 barroisite	0.000 magnesio-alumino		0.000 ferro-alumino
	0.079 magnesio-ferri		0.000 ferro-ferri
0.118 anthophyllite	0.117 magnesio		0.000 ferro
0.056 gedrite	0.056 magnesio		0.000 ferro

Fe/FM = 0.000 Mg/FM = 0.993 Mn/FM = 0.001
Al/M3 = 0.000 Fe3/M3 = 1.000 Cr/M3 = 0.008
K/A = 0.000 Li = 0.000

0308-3-7

	Oxide		Cell
SiO2	48.810	Si	6.724
TiO2	0.350	Ti	0.036
Al2O3	9.820	Al	1.594
Fe2O3	5.550	Fe3	0.575
Cr2O3	0.830	Cr	0.090
FeO	4.580	Fe2	0.528
MnO	0.210	Mn	0.025
NiO	0.030	Ni	0.003
MgO	16.680	Mg	3.425
CaO	11.690	Ca	1.725
Na2O	2.770	Na	0.740
K2O	0.180	K	0.032

Total 101.500 Ions 15.498
(O+OH+F+Cl) 23.002 Normalised 0.000

Classification of 0308-3-7
T site: 6.724 Si 1.276 Al

C site: 0.318 Al 0.666 Fe3 0.036 Ti 3.980 FM
B site: 0.001 FM 1.725 Ca 0.274 Na
A site: 0.466 Na 0.032 K 0.000 Li

A site: Full 0.498 Empty 0.502
B site: FeMg 0.000 Ca2 0.726 CaNa 0.274
T site: Si7 0.724 Si6 0.276

0.250 barroisite	0.070 magnesio-alumino	0.011 ferro-alumino
	0.145 magnesio-ferri	0.022 ferro-ferri
0.252 tschermakite	0.070 magnesio-alumino	0.011 ferro-alumino
	0.147 magnesio-ferri	0.023 ferro-ferri
0.474 edenite	0.408 magnesio	0.063 ferro
0.024 taramite	0.007 magnesio-alumino	0.001 ferro-alumino
	0.014 magnesio-ferri	0.002 ferro-ferri

Fe/FM = 0.133 Mg/FM = 0.860 Mn/FM = 0.002
Al/M3 = 0.323 Fe3/M3 = 0.677 Cr/M3 = 0.092
K/A = 0.064 Li = 0.000

0308-3-8

Oxide		Cell	
SiO2	54.790	Si	7.680
TiO2	0.230	Ti	0.024
Al2O3	3.190	Al	0.527
Fe2O3	1.850	Fe3	0.195
Cr2O3	0.120	Cr	0.013
FeO	5.570	Fe2	0.653
MnO	0.110	Mn	0.013
NiO	0.040	Ni	0.005
MgO	18.620	Mg	3.891
CaO	12.050	Ca	1.810
Na2O	0.810	Na	0.220
K2O	0.100	K	0.018

Total 97.480 Ions 15.049
(O+OH+F+Cl) 23.001 Normalised 0.000

Classification of 0308-3-8
T site: 7.680 Si 0.320 Al
C site: 0.207 Al 0.208 Fe3 0.024 Ti 4.560 FM
B site: 0.001 FM 1.810 Ca 0.189 Na
A site: 0.031 Na 0.018 K 0.000 Li

A site: Full 0.049 Empty 0.951
B site: FeMg 0.000 Ca2 0.810 CaNa 0.189
T site: Si8 0.680 Si7 0.320

0.680 A0B4Si8	0.580 tremolite	0.097 ferro-actinolite
0.082 hornblende	0.035 magnesio-alumino	0.006 ferro-alumino
	0.035 magnesio-ferri	0.006 ferro-ferri
0.189 barroisite	0.080 magnesio-alumino	0.014 ferro-alumino
	0.081 magnesio-ferri	0.014 ferro-ferri
0.049 edenite	0.041 magnesio	0.007 ferro

Fe/FM = 0.143 Mg/FM = 0.853 Mn/FM = 0.001
Al/M3 = 0.498 Fe3/M3 = 0.502 Cr/M3 = 0.032

K/A = 0.368 Li = 0.000

05C8-1-1

	Oxide		Cell
SiO2	54.420	Si	7.516
TiO2	0.180	Ti	0.019
Al2O3	4.200	Al	0.684
Fe2O3	3.900	Fe3	0.405
Cr2O3	0.300	Cr	0.033
FeO	7.450	Fe2	0.860
MnO	0.210	Mn	0.025
NiO	0.130	Ni	0.014
MgO	16.730	Mg	3.445
CaO	12.040	Ca	1.782
Na2O	0.850	Na	0.228
K2O	0.110	K	0.019

Total 100.520 Ions 15.029
(O+OH+F+Cl) 23.001 Normalised 0.000

Classification of 0508-1-1
T site: 7.516 Si 0.484 Al
C site: 0.200 Al 0.438 Fe3 0.019 Ti 4.344 FM
B site: 0.000 FM 1.782 Ca 0.218 Na
A site: 0.010 Na 0.019 K 0.000 Li

A site: Full 0.029 Empty 0.971
B site: FeMg 0.000 Ca2 0.782 CaNa 0.218
T site: Si8 0.516 Si7 0.484

0.516 A0B4Si8	0.409 tremolite		0.102 ferro-actinolite
0.237 hornblende	0.059 magnesio-alumino		0.015 ferro-alumino
	0.129 magnesio-ferri		0.032 ferro-ferri
0.218 barroisite	0.054 magnesio-alumino		0.014 ferro-alumino
	0.119 magnesio-ferri		0.030 ferro-ferri
0.029 edenite	0.023 magnesio		0.006 ferro

Fe/FM = 0.198 Mg/FM = 0.793 Mn/FM = 0.001
Al/M3 = 0.313 Fe3/M3 = 0.687 Cr/M3 = 0.051
K/A = 0.667 Li = 0.000

0508-1-2

	Oxide		Cell
SiO2	47.720	Si	7.148
TiO2	0.240	Ti	0.027
Al2O3	5.840	Al	1.031
Fe2O3	4.030	Fe3	0.454
Cr2O3	0.010	Cr	0.001
FeO	6.950	Fe2	0.871
MnO	0.140	Mn	0.018
NiO	0.080	Ni	0.010
MgO	15.410	Mg	3.441
CaO	11.590	Ca	1.860
Na2O	1.500	Na	0.436
K2O	0.040	K	0.008

Total 93.550 Ions 15.305
(O+OH+F+Cl) 23.001 Normalised 0.000

Classification of 0508-1-2
T site: 7.148 Si 0.852 Al
C site: 0.179 Al 0.455 Fe3 0.027 Ti 4.338 FM
B site: 0.001 FM 1.860 Ca 0.139 Na
A site: 0.207 Na 0.008 K 0.000 Li

A site: Full 0.305 Empty 0.695
B site: FeMg 0.001 Ca2 0.861 CaNa 0.139
T site: Si8 0.148 Si7 0.852

0.148 AOB4Si8	0.118 tremolite	0.030 ferro-actinolite
0.408 hornblende	0.091 magnesio-alumino	0.023 ferro-alumino
	0.232 magnesio-ferri	0.059 ferro-ferri
0.139 barroisite	0.031 magnesio-alumino	0.008 ferro-alumino
	0.079 magnesio-ferri	0.020 ferro-ferri
0.304 edenite	0.241 magnesio	0.061 ferro

Fe/FM = 0.201 Mg/FM = 0.793 Mn/FM = 0.001
Al/M3 = 0.283 Fe3/M3 = 0.717 Cr/M3 = 0.002
K/A = 0.025 Li = 0.000

0508-1-3

Oxide		Cell	
SiO2	48.110	Si	6.704
TiO2	0.360	Ti	0.038
Al2O3	9.410	Al	1.545
Fe2O3	12.150	Fe3	1.274
Cr2O3	0.200	Cr	0.022
FeO	1.780	Fe2	0.207
MnO	0.110	Mn	0.013
NiO	0.170	Ni	0.019
MgO	15.300	Mg	3.178
CaO	10.500	Ca	1.568
Na2O	1.890	Na	0.511
K2O	0.170	K	0.030

Total 100.150 Ions 15.110
(O+OH+F+Cl) 23.002 Normalised 0.000

Classification of 0508-1-3
T site: 6.704 Si 1.296 Al
C site: 0.250 Al 1.296 Fe3 0.038 Ti 3.417 FM
B site: 0.001 FM 1.568 Ca 0.431 Na
A site: 0.080 Na 0.030 K 0.000 Li

A site: Full 0.110 Empty 0.890
B site: FeMg 0.001 Ca2 0.568 CaNa 0.431
T site: Si7 0.704 Si6 0.296

0.163 hornblende	0.025 magnesio-alumino	0.002 ferro-alumino
	0.127 magnesio-ferri	0.008 ferro-ferri
0.431 barroisite	0.065 magnesio-alumino	0.004 ferro-alumino
	0.336 magnesio-ferri	0.022 ferro-ferri
0.295 tschermakite	0.044 magnesio-alumino	0.003 ferro-alumino

0.110 edenite

0.230 magnesio-ferri
0.102 magnesio

0.015 ferro-ferri
0.007 ferro

Fe/FM = 0.061 Mg/FM = 0.930 Mn/FM = 0.001
Al/M3 = 0.162 Fe3/M3 = 0.838 Cr/M3 = 0.014
K/A = 0.275 Li = 0.000

0508-1-4

	Oxide		Cell
SiO2	55.410	Si	7.697
TiO2	0.240	Ti	0.025
Al2O3	4.140	Al	0.678
Cr2O3	0.420	Cr	0.046
FeO	9.510	Fe2	1.105
MnO	0.150	Mn	0.018
MgO	16.430	Mg	3.403
CaO	12.240	Ca	1.822
Na2O	0.840	Na	0.226
K2O	0.120	K	0.021

Total 99.500 Ions 15.041
(O+OH+F+Cl) 23.002 Normalised 13.000

Classification of 0508-1-4
T site: 7.697 Si 0.303 Al
C site: 0.375 Al 0.046 Fe3 0.025 Ti 4.525 FM 0.029 Vacant
B site: 0.000 FM 1.822 Ca 0.178 Na
A site: 0.048 Na 0.021 K 0.000 Li

A site: Full 0.069 Empty 0.931
B site: Ca2 0.822 CaNa 0.178
T site: Si8 0.697 Si7 0.303

0.697 A0B4Si8
0.055 hornblende
0.178 barroisite
0.069 edenite

0.524 tremolite
0.037 magnesio-alumino
0.005 magnesio-ferri
0.119 magnesio-alumino
0.015 magnesio-ferri
0.052 magnesio

0.170 ferro-actinolite
0.012 ferro-alumino
0.001 ferro-ferri
0.039 ferro-alumino
0.005 ferro-ferri
0.017 ferro

Fe/FM = 0.244 Mg/FM = 0.752 Mn/FM = 0.001
Al/M3 = 0.891 Fe3/M3 = 0.109 Cr/M3 = 0.109
K/A = 0.307 Li = 0.000

0508-1-5

	Oxide		Cell
SiO2	50.800	Si	7.627
TiO2	0.130	Ti	0.015
Al2O3	4.430	Al	0.784
Cr2O3	0.130	Cr	0.015
FeO	6.440	Fe2	0.809
MnO	0.090	Mn	0.011
NiO	0.070	Ni	0.008
MgO	16.040	Mg	3.590
CaO	12.120	Ca	1.950
Na2O	0.950	Na	0.277

```
K2O      0.110  K     0.021

Total   91.310 Ions 15.108
(O+OH+F+Cl) 23.001 Normalised 13.000

Classification of 0508-1-5
T site: 7.627 Si  0.373 Al
C site: 0.411 Al  0.015 Fe3  0.015 Ti  4.419 FM  0.140 Vacant
B site: 0.000 FM  1.950 Ca   0.050 Na
A site: 0.226 Na  0.021 K    0.000 Li

A site:  Full  0.247  Empty 0.753
B site:  Ca2   0.950  CaNa  0.050
T site:  Si8   0.627  Si7   0.373

0.627 A0B4Si8        0.510 tremolite             0.115 ferro-actinolite
0.075 hornblende      0.059 magnesio-alumino      0.013 ferro-alumino
                      0.002 magnesio-ferri        0.000 ferro-ferri
0.050 barroisite      0.039 magnesio-alumino      0.009 ferro-alumino
                      0.001 magnesio-ferri        0.000 ferro-ferri
0.247 edenite         0.201 magnesio              0.045 ferro

Fe/FM = 0.183  Mg/FM  = 0.812  Mn/FM = 0.001
Al/M3 = 0.964  Fe3/M3 = 0.036  Cr/M3 = 0.036
K/A   = 0.085  Li     = 0.000


0508-1-6
         Oxide          Cell
SiO2    56.270  Si    7.739
TiO2     0.110  Ti    0.011
Al2O3    2.380  Al    0.386
Fe2O3    2.170  Fe3   0.225
Cr2O3    0.000  Cr    0.003
FeO      5.610  Fe2   0.645
MnO      0.070  Mn    0.008
NiO      0.100  Ni    0.011
MgO     19.370  Mg    3.972
CaO     12.660  Ca    1.866
Na2O     0.550  Na    0.147
K2O      0.050  K     0.009

Total   99.370 Ions 15.021
(O+OH+F+Cl) 23.001 Normalised  0.000

Classification of 0508-1-6
T site: 7.739 Si  0.261 Al
C site: 0.125 Al  0.228 Fe3  0.011 Ti  4.636 FM
B site: 0.000 FM  1.866 Ca   0.134 Na
A site: 0.012 Na  0.009 K    0.000 Li

A site:  Full  0.021  Empty 0.979
B site:  Ca2   0.866  CaNa  0.134
T site:  Si8   0.739  Si7   0.261

0.739 A0B4Si8        0.633 tremolite             0.103 ferro-actinolite
0.105 hornblende      0.032 magnesio-alumino      0.005 ferro-alumino
                      0.058 magnesio-ferri        0.009 ferro-ferri
```

0.134 barroisite 0.041 magnesio-alumino 0.007 ferro-alumino
0.074 magnesio-ferri 0.012 ferro-ferri
0.021 edenite 0.018 magnesio 0.003 ferro

Fe/FM = 0.139 Mg/FM = 0.857 Mn/FM = 0.000
Al/M3 = 0.354 Fe3/M3 = 0.646 Cr/M3 = 0.009
K/A = 0.416 Li = 0.000

0508-1-7

Oxide		Cell	
SiO2	52.360	Si	7.400
TiO2	0.250	Ti	0.027
Al2O3	3.900	Al	0.650
Fe2O3	4.010	Fe3	0.426
Cr2O3	0.050	Cr	0.006
FeO	4.730	Fe2	0.559
MnO	0.100	Mn	0.012
NiO	0.160	Ni	0.018
MgO	18.530	Mg	3.904
CaO	12.470	Ca	1.888
Na2O	1.030	Na	0.282
K2O	0.050	K	0.009

Total 97.640 Ions 15.180
(O+OH+F+Cl) 23.002 Normalised 0.000

Classification of 0508-1-7
T site: 7.400 Si 0.600 Al
C site: 0.049 Al 0.432 Fe3 0.027 Ti 4.492 FM
B site: 0.001 FM 1.888 Ca 0.111 Na
A site: 0.171 Na 0.009 K 0.000 Li

A site: Full 0.180 Empty 0.820
B site: FeMg 0.000 Ca2 0.889 CaNa 0.111
T site: Si8 0.400 Si7 0.600

0.399 AOB4Si8 0.347 tremolite 0.050 ferro-actinolite
0.309 hornblende 0.027 magnesio-alumino 0.004 ferro-alumino
0.241 magnesio-ferri 0.035 ferro-ferri

0.111 barroisite 0.010 magnesio-alumino 0.001 ferro-alumino
0.087 magnesio-ferri 0.012 ferro-ferri
0.180 edenite 0.157 magnesio 0.022 ferro

Fe/FM = 0.124 Mg/FM = 0.869 Mn/FM = 0.001
Al/M3 = 0.102 Fe3/M3 = 0.898 Cr/M3 = 0.012
K/A = 0.050 Li = 0.000

0508-1-8

Oxide		Cell	
SiO2	50.220	Si	7.268
TiO2	0.230	Ti	0.025
Al2O3	6.930	Al	1.182
Cr2O3	0.330	Cr	0.038
FeO	9.630	Fe2	1.166
NiO	0.090	Ni	0.010

MgO	15.250	Mg	3.290
CaO	12.030	Ca	1.865
Na2O	1.680	Na	0.471
K2O	0.200	K	0.037

Total 96.590 Ions 15.353
(O+OH+F+Cl) 23.001 Normalised 13.000

Classification of 0508-1-8
T site: 7.268 Si 0.732 Al
C site: 0.450 Al 0.038 Fe3 0.025 Ti 4.466 FM 0.021 Vacant
B site: 0.000 FM 1.865 Ca 0.135 Na
A site: 0.337 Na 0.037 K 0.000 Li

A site: Full 0.374 Empty 0.626
B site: Ca2 0.865 CaNa 0.135
T site: Si8 0.268 Si7 0.732

0.268 AOB4Si8		0.197 tremolite		0.070 ferro-actinolite	
0.224 hornblende		0.152 magnesio-alumino		0.054 ferro-alumino	
		0.013 magnesio-ferri		0.005 ferro-ferri	
0.135 barroisite		0.092 magnesio-alumino		0.032 ferro-alumino	
		0.008 magnesio-ferri		0.003 ferro-ferri	
0.374 edenite		0.275 magnesio		0.098 ferro	

Fe/FM = 0.261 Mg/FM = 0.737 Mn/FM = 0.000
Al/M3 = 0.923 Fe3/M3 = 0.077 Cr/M3 = 0.077
K/A = 0.099 Li = 0.000

0508-1-9

Oxide		Cell	
SiO2	55.520	Si	7.577
TiO2	0.340	Ti	0.035
Al2O3	4.230	Al	0.680
Fe2O3	1.790	Fe3	0.184
Cr2O3	0.110	Cr	0.012
FeO	7.250	Fe2	0.827
MnO	0.130	Mn	0.015
NiO	0.050	Ni	0.005
MgO	18.020	Mg	3.666
CaO	12.530	Ca	1.832
Na2O	0.870	Na	0.230
K2O	0.050	K	0.009

Total 100.890 Ions 15.072
(O+OH+F+Cl) 23.002 Normalised 0.000

Classification of 0508-1-9
T site: 7.577 Si 0.423 Al
C site: 0.257 Al 0.196 Fe3 0.035 Ti 4.513 FM
B site: 0.001 FM 1.832 Ca 0.167 Na
A site: 0.063 Na 0.009 K 0.000 Li

A site: Full 0.072 Empty 0.928
B site: FeMg 0.001 Ca2 0.833 CaNa 0.167
T site: Si8 0.577 Si7 0.423

0.576	A0B4Si8	0.468	tremolite	0.106 ferro-actinolite
0.184	hornblende	0.085	magnesio-alumino	0.019 ferro-alumino
		0.065	magnesio-ferri	0.015 ferro-ferri
0.167	barroisite	0.077	magnesio-alumino	0.017 ferro-alumino
		0.059	magnesio-ferri	0.013 ferro-ferri
0.072	edenite	0.059	magnesio	0.013 ferro

Fe/FM = 0.183 Mg/FM = 0.812 Mn/FM = 0.001
Al/M3 = 0.568 Fe3/M3 = 0.432 Cr/M3 = 0.026
K/A = 0.121 Li = 0.000

0508-1-10

Oxide		Cell	
SiO2	56.950	Si	7.799
TiO2	0.030	Ti	0.003
Al2O3	2.230	Al	0.360
Fe2O3	2.040	Fe3	0.210
Cr2O3	0.020	Cr	0.002
FeO	7.350	Fe2	0.842
MnO	0.070	Mn	0.008
NiO	0.080	Ni	0.009
MgO	18.450	Mg	3.767
CaO	12.390	Ca	1.818
Na2O	0.650	Na	0.173
K2O	0.080	K	0.014

Total 100.340 Ions 15.005
(O+OH+F+Cl) 23.000 Normalised 0.000

Classification of 0508-1-10
T site: 7.799 Si 0.201 Al
C site: 0.159 Al 0.212 Fe3 0.003 Ti 4.616 FM 0.009 Vacant
B site: 0.009 FM 1.818 Ca 0.173 Na
A site: 0.000 Na 0.014 K 0.000 Li

A site: Full 0.014 Empty 0.986
B site: FeMg 0.005 Ca2 0.823 CaNa 0.173
T site: Si8 0.799 Si7 0.201

0.795	A0B4Si8	0.647	tremolite	0.145 ferro-actinolite
0.014	hornblende	0.005	magnesio-alumino	0.001 ferro-alumino
		0.007	magnesio-ferri	0.001 ferro-ferri
0.173	barroisite	0.060	magnesio-alumino	0.013 ferro-alumino
		0.080	magnesio-ferri	0.018 ferro-ferri
0.014	edenite	0.011	magnesio	0.003 ferro
0.005	anthophyllite	0.004	magnesio	0.001 ferro

Fe/FM = 0.182 Mg/FM = 0.814 Mn/FM = 0.000
Al/M3 = 0.429 Fe3/M3 = 0.571 Cr/M3 = 0.006
K/A = 1.000 Li = 0.000

0508-1-11

Oxide		Cell	
SiO2	49.380	Si	7.209
TiO2	0.200	Ti	0.022
Al2O3	6.340	Al	1.091

Fe2O3	1.860	Fe3	0.204
Cr2O3	0.060	Cr	0.007
FeO	9.510	Fe2	1.161
MnO	0.140	Mn	0.017
NiO	0.130	Ni	0.015
MgO	15.040	Mg	3.273
CaO	12.150	Ca	1.901
Na2O	1.450	Na	0.410
K2O	0.130	K	0.024

Total 96.390 Ions 15.336
(O+OH+F+Cl) 23.001 Normalised 0.000

Classification of 0508-1-11
T site: 7.209 Si 0.791 Al
C site: 0.300 Al 0.211 Fe3 0.022 Ti 4.466 FM
B site: 0.001 FM 1.901 Ca 0.099 Na
A site: 0.312 Na 0.024 K 0.000 Li

A site: Full 0.336 Empty 0.664
B site: FeMg 0.000 Ca2 0.901 CaNa 0.099
T site: Si8 0.209 Si7 0.791

0.209 AOB4Si8	0.153 tremolite	0.054 ferro-actinolite
0.356 hornblende	0.153 magnesio-alumino	0.054 ferro-alumino
	0.108 magnesio-ferri	0.038 ferro-ferri
0.099 barroisite	0.042 magnesio-alumino	0.015 ferro-alumino
	0.030 magnesio-ferri	0.011 ferro-ferri
0.336 edenite	0.246 magnesio	0.087 ferro

Fe/FM = 0.260 Mg/FM = 0.733 Mn/FM = 0.001
Al/M3 = 0.587 Fe3/M3 = 0.413 Cr/M3 = 0.014
K/A = 0.072 Li = 0.000

0508-1-12

Oxide		Cell	
SiO2	51.100	Si	7.389
TiO2	0.230	Ti	0.025
Al2O3	4.390	Al	0.748
Fe2O3	3.410	Fe3	0.371
Cr2O3	0.030	Cr	0.003
FeO	6.510	Fe2	0.787
MnO	0.040	Mn	0.005
NiO	0.070	Ni	0.008
MgO	17.000	Mg	3.664
CaO	11.770	Ca	1.823
Na2O	1.050	Na	0.294
K2O	0.600	K	0.111

Total 96.200 Ions 15.229
(O+OH+F+Cl) 23.001 Normalised 0.000

Classification of 0508-1-12
T site: 7.389 Si 0.611 Al
C site: 0.137 Al 0.374 Fe3 0.025 Ti 4.464 FM
B site: 0.001 FM 1.823 Ca 0.176 Na
A site: 0.118 Na 0.111 K 0.000 Li

A site: Full 0.229 Empty 0.771
B site: FeMg 0.000 Ca2 0.824 CaNa 0.176
T site: Si8 0.389 Si7 0.611

0.388 A0B4Si8	0.319 tremolite		0.068 ferro-actinolite
0.206 hornblende	0.045 magnesio-alumino		0.010 ferro-alumino
	0.124 magnesio-ferri		0.027 ferro-ferri
0.175 barroisite	0.039 magnesio-alumino		0.008 ferro-alumino
	0.106 magnesio-ferri		0.023 ferro-ferri
0.229 edenite	0.188 magnesio		0.040 ferro

Fe/FM = 0.176 Mg/FM = 0.821 Mn/FM = 0.000
Al/M3 = 0.267 Fe3/M3 = 0.733 Cr/M3 = 0.007
K/A = 0.483 Li = 0.000

0408-4-1

Oxide		Cell	
SiO2	43.890	Si	6.595
TiO2	0.370	Ti	0.042
Al2O3	14.650	Al	2.594
Fe2O3	1.050	Fe3	0.119
Cr2O3	0.040	Cr	0.005
FeO	10.680	Fe2	1.342
MnO	0.110	Mn	0.014
NiO	0.030	Ni	0.004
MgO	10.210	Mg	2.287
CaO	7.480	Ca	1.204
Na2O	5.430	Na	1.582
K2O	0.110	K	0.021

Total 94.050 Ions 15.808
(O+OH+F+Cl) 23.002 Normalised 0.000

Classification of 0408-4-1
T site: 6.595 Si 1.405 Al
C site: 1.189 Al 0.123 Fe3 0.042 Ti 3.646 FM
B site: 0.001 FM 1.204 Ca 0.795 Na
A site: 0.787 Na 0.021 K 0.000 Li

A site: Full 0.808 Empty 0.192
B site: FeMg 0.001 Ca2 0.205 CaNa 0.795
T site: Si7 0.595 Si6 0.405

0.192 barroisite	0.109 magnesio-alumino	0.064 ferro-alumino
	0.011 magnesio-ferri	0.007 ferro-ferri
0.205 edenite	0.128 magnesio	0.075 ferro
0.198 kataphorite	0.112 magnesio-alumino	0.066 ferro-alumino
	0.012 magnesio-ferri	0.007 ferro-ferri
0.405 taramite	0.230 magnesio-alumino	0.135 ferro-alumino
	0.024 magnesio-ferri	0.014 ferro-ferri

Fe/FM = 0.368 Mg/FM = 0.627 Mn/FM = 0.001
Al/M3 = 0.906 Fe3/M3 = 0.094 Cr/M3 = 0.004
K/A = 0.026 Li = 0.000

0408-4-2

	Oxide		Cell
SiO2	54.330	Si	7.588
TiO2	0.140	Ti	0.015
Al2O3	3.800	Al	0.639
Fe2O3	3.660	Fe3	0.385
Cr2O3	0.090	Cr	0.010
FeO	11.180	Fe2	1.306
MnO	0.230	Mn	0.027
NiO	0.010	Ni	0.001
MgO	14.550	Mg	3.030
CaO	11.930	Ca	1.785
Na2O	0.660	Na	0.179
K2O	0.070	K	0.012

Total 100.730 Ions 14.977
(O+OH+F+Cl) 23.001 Normalised 0.000

Classification of 0408-4-2
T site: 7.588 Si 0.412 Al
C site: 0.227 Al 0.395 Fe3 0.015 Ti 4.328 FM 0.036 Vacant
B site: 0.036 FM 1.785 Ca 0.179 Na
A site: 0.000 Na 0.012 K 0.000 Li

A site: Full 0.012 Empty 0.988
B site: FeMg 0.018 Ca2 0.803 CaNa 0.179
T site: Si8 0.588 Si7 0.412

0.576 A0B4Si8	0.400 tremolite		0.172 ferro-actinolite
0.216 hornblende	0.055 magnesio-alumino		0.024 ferro-alumino
	0.095 magnesio-ferri		0.041 ferro-ferri
0.179 barroisite	0.045 magnesio-alumino		0.020 ferro-alumino
	0.079 magnesio-ferri		0.034 ferro-ferri
0.012 edenite	0.008 magnesio		0.004 ferro
0.015 anthophyllite	0.011 magnesio		0.005 ferro
0.002 gedrite	0.002 magnesio		0.001 ferro

Fe/FM = 0.299 Mg/FM = 0.694 Mn/FM = 0.001
Al/M3 = 0.365 Fe3/M3 = 0.635 Cr/M3 = 0.016
K/A = 1.000 Li = 0.000

0408-4-3

	Oxide		Cell
SiO2	43.390	Si	6.259
TiO2	0.640	Ti	0.069
Al2O3	14.210	Al	2.416
Fe2O3	4.120	Fe3	0.447
Cr2O3	0.170	Cr	0.019
FeO	11.650	Fe2	1.405
MnO	0.140	Mn	0.017
NiO	0.030	Ni	0.003
MgO	11.000	Mg	2.365
CaO	11.580	Ca	1.790
Na2O	3.000	Na	0.839
K2O	0.250	K	0.046

Total 100.180 Ions 15.677

(O+OH+F+Cl) 23.004 Normalised 0.000

Classification of 0408-4-3
T site: 6.259 Si 1.741 Al
C site: 0.675 Al 0.467 Fe3 0.069 Ti 3.789 FM
B site: 0.002 FM 1.790 Ca 0.208 Na
A site: 0.631 Na 0.046 K 0.000 Li

A site: Full 0.677 Empty 0.323
B site: FeMg 0.001 Ca2 0.791 CaNa 0.208
T site: Si7 0.259 Si6 0.741

0.323 tschermakite	0.119 magnesio-alumino	0.071 ferro-alumino
	0.082 magnesio-ferri	0.049 ferro-ferri
0.259 edenite	0.161 magnesio	0.096 ferro
0.140 A1B4Si6	0.052 pargasite	0.031 Fe pargasite
	0.036 Mg hastingsite	0.021 hastingsite
0.208 taramite	0.077 magnesio-alumino	0.046 ferro-alumino
	0.053 magnesio-ferri	0.032 ferro-ferri
0.069 kaersutite	0.043 magnesio-alumino	0.026 ferro-alumino

Fe/FM = 0.371 Mg/FM = 0.624 Mn/FM = 0.001
Al/M3 = 0.591 Fe3/M3 = 0.409 Cr/M3 = 0.017
K/A = 0.068 Li = 0.000

0408-4-4

Oxide		Cell	
SiO2	50.380	Si	7.148
TiO2	0.350	Ti	0.037
Al2O3	8.400	Al	1.405
Fe2O3	0.470	Fe3	0.050
Cr2O3	0.250	Cr	0.028
FeO	15.350	Fe2	1.821
MnO	0.240	Mn	0.029
NiO	0.050	Ni	0.006
MgO	11.710	Mg	2.477
CaO	12.030	Ca	1.829
Na2O	1.710	Na	0.470
K2O	0.110	K	0.020

Total 101.050 Ions 15.320
(O+OH+F+Cl) 23.002 Normalised 0.000

Classification of 0408-4-4
T site: 7.148 Si 0.852 Al
C site: 0.553 Al 0.078 Fe3 0.037 Ti 4.332 FM
B site: 0.001 FM 1.829 Ca 0.170 Na
A site: 0.300 Na 0.020 K 0.000 Li

A site: Full 0.320 Empty 0.680
B site: FeMg 0.001 Ca2 0.829 CaNa 0.170
T site: Si8 0.148 Si7 0.852

0.148 A0B4Si8	0.085 tremolite	0.062 ferro-actinolite
0.361 hornblende	0.181 magnesio-alumino	0.133 ferro-alumino
	0.026 magnesio-ferri	0.019 ferro-ferri
0.170 barroisite	0.085 magnesio-alumino	0.063 ferro-alumino

	0.012 magnesio-ferri	0.009 ferro-ferri
0.320 edenite	0.183 magnesio	0.135 ferro

Fe/FM = 0.420 Mg/FM = 0.572 Mn/FM = 0.002
Al/M3 = 0.876 Fe3/M3 = 0.124 Cr/M3 = 0.044
K/A = 0.062 Li = 0.000

0408-4-5

Oxide		Cell	
SiO2	43.390	Si	6.363
TiO2	0.370	Ti	0.041
Al2O3	12.200	Al	2.108
Fe2O3	7.140	Fe3	0.788
Cr2O3	0.050	Cr	0.006
FeO	10.790	Fe2	1.323
MnO	0.240	Mn	0.030
NiO	0.140	Ni	0.017
MgO	10.640	Mg	2.326
CaO	11.500	Ca	1.807
Na2O	2.260	Na	0.643
K2O	0.200	K	0.037

Total 98.920 Ions 15.488
(O+OH+F+Cl) 23.002 Normalised 0.000

Classification of 0408-4-5
T site: 6.363 Si 1.637 Al
C site: 0.471 Al 0.794 Fe3 0.041 Ti 3.694 FM
B site: 0.001 FM 1.807 Ca 0.192 Na
A site: 0.450 Na 0.037 K 0.000 Li

A site: Full 0.488 Empty 0.512
B site: FeMg 0.001 Ca2 0.807 CaNa 0.192
T site: Si7 0.363 Si6 0.637

0.034 barroisite	0.008 magnesio-alumino	0.004 ferro-alumino
	0.013 magnesio-ferri	0.008 ferro-ferri
0.478 tschermakite	0.112 magnesio-alumino	0.064 ferro-alumino
	0.189 magnesio-ferri	0.107 ferro-ferri
0.329 edenite	0.207 magnesio	0.118 ferro
0.159 taramite	0.037 magnesio-alumino	0.021 ferro-alumino
	0.063 magnesio-ferri	0.036 ferro-ferri

Fe/FM = 0.358 Mg/FM = 0.629 Mn/FM = 0.002
Al/M3 = 0.372 Fe3/M3 = 0.628 Cr/M3 = 0.005
K/A = 0.077 Li = 0.000

0408-4-6

Oxide		Cell	
SiO2	43.090	Si	6.369
TiO2	0.460	Ti	0.051
Al2O3	12.160	Al	2.119
Fe2O3	5.820	Fe3	0.647
Cr2O3	0.180	Cr	0.021
FeO	8.910	Fe2	1.102
MnO	0.100	Mn	0.013

NiO	0.010	Ni	0.001
MgO	12.160	Mg	2.680
CaO	11.670	Ca	1.848
Na2O	2.250	Na	0.645
K2O	0.180	K	0.034

Total 96.980 Ions 15.529
(O+OH+F+Cl) 23.003 Normalised 0.000

Classification of 0408-4-6
T site: 6.369 Si 1.631 Al
C site: 0.487 Al 0.668 Fe3 0.051 Ti 3.793 FM
B site: 0.002 FM 1.848 Ca 0.150 Na
A site: 0.495 Na 0.034 K 0.000 Li

A site: Full 0.529 Empty 0.471
B site: FeMg 0.001 Ca2 0.849 CaNa 0.150
T site: Si7 0.369 Si6 0.631

0.470 tschermakite	0.140 magnesio-alumino	0.058 ferro-alumino
	0.192 magnesio-ferri	0.079 ferro-ferri
0.368 edenite	0.260 magnesio	0.107 ferro
0.150 taramite	0.045 magnesio-alumino	0.018 ferro-alumino
	0.061 magnesio-ferri	0.025 ferro-ferri
0.011 kaersutite	0.008 magnesio-alumino	0.003 ferro-alumino

Fe/FM = 0.290 Mg/FM = 0.706 Mn/FM = 0.001
Al/M3 = 0.422 Fe3/M3 = 0.578 Cr/M3 = 0.018
K/A = 0.064 Li = 0.000

0408-4-7

Oxide		Cell	
SiO2	44.460	Si	6.525
TiO2	0.610	Ti	0.067
Al2O3	12.420	Al	2.148
Fe2O3	0.760	Fe3	0.084
Cr2O3	0.220	Cr	0.026
FeO	13.170	Fe2	1.616
MnO	0.130	Mn	0.016
NiO	0.110	Ni	0.013
MgO	11.460	Mg	2.507
CaO	11.680	Ca	1.837
Na2O	2.990	Na	0.851
K2O	0.200	K	0.037

Total 98.210 Ions 15.727
(O+OH+F+Cl) 23.004 Normalised 0.000

Classification of 0408-4-7
T site: 6.525 Si 1.475 Al
C site: 0.673 Al 0.109 Fe3 0.067 Ti 4.150 FM
B site: 0.002 FM 1.837 Ca 0.161 Na
A site: 0.690 Na 0.037 K 0.000 Li

A site: Full 0.727 Empty 0.273
B site: FeMg 0.001 Ca2 0.838 CaNa 0.161
T site: Si7 0.525 Si6 0.475

0.273 tschermakite	0.142 magnesio-alumino	0.091 ferro-alumino
	0.023 magnesio-ferri	0.015 ferro-ferri
0.524 edenite	0.316 magnesio	0.204 ferro
0.161 taramite	0.084 magnesio-alumino	0.054 ferro-alumino
	0.014 magnesio-ferri	0.009 ferro-ferri
0.041 kaersutite	0.025 magnesio-alumino	0.016 ferro-alumino

Fe/FM = 0.389 Mg/FM = 0.604 Mn/FM = 0.001
Al/M3 = 0.860 Fe3/M3 = 0.140 Cr/M3 = 0.033
K/A = 0.051 Li = 0.000

0408-4-8

Oxide		Cell	
SiO2	45.150	Si	6.736
TiO2	0.280	Ti	0.031
Al2O3	6.860	Al	1.206
Fe2O3	10.330	Fe3	1.160
Cr2O3	0.150	Cr	0.018
FeO	3.840	Fe2	0.479
MnO	0.150	Mn	0.019
NiO	0.100	Ni	0.012
MgO	15.020	Mg	3.340
CaO	11.400	Ca	1.822
Na2O	1.450	Na	0.419
K2O	0.110	K	0.021

Total 94.840 Ions 15.263
(O+OH+F+Cl) 23.002 Normalised 0.000

Classification of 0408-4-8
T site: 6.736 Si 1.206 Al 0.058 Fe3
C site: 0.000 Al 1.119 Fe3 0.031 Ti 3.850 FM
B site: 0.001 FM 1.822 Ca 0.177 Na
A site: 0.242 Na 0.021 K 0.000 Li

A site: Full 0.263 Empty 0.737
B site: FeMg 0.000 Ca2 0.823 CaNa 0.177
T site: Si7 0.736 Si6 0.264

0.295 hornblende	0.000 magnesio-alumino	0.000 ferro-alumino
	0.256 magnesio-ferri	0.037 ferro-ferri
0.177 barroisite	0.000 magnesio-alumino	0.000 ferro-alumino
	0.154 magnesio-ferri	0.022 ferro-ferri
0.264 tschermakite	0.000 magnesio-alumino	0.000 ferro-alumino
	0.229 magnesio-ferri	0.033 ferro-ferri
0.263 edenite	0.228 magnesio	0.033 ferro

Fe/FM = 0.124 Mg/FM = 0.868 Mn/FM = 0.001
Al/M3 = 0.000 Fe3/M3 = 1.000 Cr/M3 = 0.016
K/A = 0.080 Li = 0.000

0408-4-9

Oxide		Cell	
SiO2	53.360	Si	7.676
TiO2	0.130	Ti	0.014
Al2O3	1.860	Al	0.315

Fe2O3	4.350	Fe3	0.471
Cr2O3	0.050	Cr	0.006
FeO	7.230	Fe2	0.870
MnO	0.220	Mn	0.027
NiO	0.050	Ni	0.006
MgO	16.860	Mg	3.616
CaO	11.990	Ca	1.848
Na2O	0.450	Na	0.126
K2O	0.040	K	0.007

Total 96.590 Ions 14.981
(O+OH+F+Cl) 23.001 Normalised 0.000

Classification of C408-4-9
T site: 7.676 Si 0.315 Al 0.009 Fe3
C site: 0.000 Al 0.468 Fe3 0.014 Ti 4.492 FM 0.026 Vacant
B site: 0.026 FM 1.848 Ca 0.126 Na
A site: 0.000 Na 0.007 K 0.000 Li

A site: Full 0.007 Empty 0.993
B site: FeMg 0.013 Ca2 0.861 CaNa 0.126
T site: Si8 0.676 Si7 0.324

0.666 A0B4S:8	0.533 tremolite	0.128 ferro-actinolite	
0.188 hornblende	0.000 magnesio-alumino	0.000 ferro-alumino	
	0.151 magnesio-ferri	0.036 ferro-ferri	
0.126 barroisite	0.000 magnesio-alumino	0.000 ferro-alumino	
	0.100 magnesio-ferri	0.024 ferro-ferri	
0.007 edenite	0.006 magnesio	0.001 ferro	
0.012 anthophyllite	0.009 magnesio	0.002 ferro	
0.001 gedrite	0.001 magnesio	0.000 ferro	

Fe/FM = 0.193 Mg/FM = 0.800 Mn/FM = 0.001
Al/M3 = 0.000 Fe3/M3 = 1.000 Cr/M3 = 0.012
K/A = 1.000 Li = 0.000

0408-4-10

Oxide		Cell	
SiO2	47.950	Si	6.992
TiO2	0.350	Ti	0.038
Al2O3	8.120	Al	1.396
Fe2O3	2.290	Fe3	0.251
Cr2O3	0.130	Cr	0.015
FeO	11.010	Fe2	1.343
MnO	0.120	Mn	0.015
NiO	0.030	Ni	0.004
MgO	13.560	Mg	2.948
CaO	12.040	Ca	1.881
Na2O	1.740	Na	0.492
K2O	0.130	K	0.024

Total 97.470 Ions 15.399
(O+OH+F+Cl) 23.002 Normalised 0.000

Classification of 0408-4-10
T site: 6.992 Si 1.008 Al
C site: 0.388 Al 0.266 Fe3 0.038 Ti 4.307 FM

B site: 0.001 FM 1.881 Ca 0.117 Na
A site: 0.374 Na 0.024 K 0.000 Li

A site: Full 0.399 Empty 0.601
B site: FeMg 0.001 Ca2 0.882 CaNa 0.117
T site: Si7 0.992 Si6 0.008

0.476 hornblende	0.193 magnesio-alumino	0.088 ferro-alumino
	0.133 magnesio-ferri	0.060 ferro-ferri
0.117 barroisite	0.048 magnesio-alumino	0.022 ferro-alumino
	0.033 magnesio-ferri	0.015 ferro-ferri
0.008 tschermakite	0.003 magnesio-alumino	0.001 ferro-alumino
	0.002 magnesio-ferri	0.001 ferro-ferri
0.398 edenite	0.273 magnesio	0.124 ferro

Fe/FM = 0.312 Mg/FM = 0.684 Mn/FM = 0.001
Al/M3 = 0.593 Fe3/M3 = 0.407 Cr/M3 = 0.023
K/A = 0.061 Li = 0.000

0408-4-11

Oxide		Cell	
SiO2	51.410	Si	7.479
TiO2	0.200	Ti	0.022
Al2O3	3.300	Al	0.566
Fe2O3	4.580	Fe3	0.501
Cr2O3	0.130	Cr	0.015
FeO	8.320	Fe2	1.012
MnO	0.220	Mn	0.027
NiO	0.090	Ni	0.011
MgO	15.530	Mg	3.368
CaO	11.730	Ca	1.828
Na2O	0.740	Na	0.209
K2O	0.280	K	0.052

Total 96.530 Ions 15.090
(O+OH+F+Cl) 23.001 Normalised 0.000

Classification of 0408-4-11
T site: 7.479 Si 0.521 Al
C site: 0.045 Al 0.516 Fe3 0.022 Ti 4.417 FM
B site: 0.001 FM 1.828 Ca 0.171 Na
A site: 0.038 Na 0.052 K 0.000 Li

A site: Full 0.090 Empty 0.910
B site: FeMg 0.000 Ca2 0.829 CaNa 0.171
T site: Si8 0.479 Si7 0.521

0.479 A0B4Si8	0.365 tremolite	0.110 ferro-actinolite
0.260 hornblende	0.016 magnesio-alumino	0.005 ferro-alumino
	0.183 magnesio-ferri	0.055 ferro-ferri
0.171 barroisite	0.010 magnesio-alumino	0.003 ferro-alumino
	0.120 magnesio-ferri	0.036 ferro-ferri
0.090 edenite	0.068 magnesio	0.021 ferro

Fe/FM = 0.229 Mg/FM = 0.762 Mn/FM = 0.001
Al/M3 = 0.080 Fe3/M3 = 0.920 Cr/M3 = 0.027
K/A = 0.579 Li = 0.000

Site Assignments (after Currie, 1991):

The sum of (O + OH + F + Cl) is reduced to 24 where data are available for Fe^{3+}, OH, F and Cl. If microprobe analyses lack H_2O and Fe^{3+} determinations, microprobe data are normalized to 46 + Ti charges, where Ti is the number of Ti atoms in the calculated cell. Fe^{2+}/Fe^{3+} is then adjusted to reduce the sum of cations less Ca + Na + K to 13 for analyses in which Na + Ca exceeds 1.34, and the sum of cations less Na + K to 15 for analyses in which Na + K is less than 1.34.

Sites are filled in the order T, C, B, A to a maximum of 8, 5, 2, and 1 atoms, respectively. This site assignment order assumes: (1) Ca cannot be accommodated in the C or A sites, and (2) the B site must contain 2 atoms, even if this demands a vacancy in C.

Appendix IV

Microprobe data for plagioclase grains, Noggin Cove Formation.

sample	0608-2-3u	0608-2-6u	0608-2-4L	0608-2-6L	1108-2-3u
Na+1	7.83	7.97	7.89	6.52	8.12
Mg+2	0.74	0.09	0.10	0.05	0.04
Al+3	10.39	10.11	10.22	10.65	9.30
Si+4	31.21	30.18	30.51	29.10	33.80
K+1	0.59	0.10	0.08	0.13	0.09
Ca+2	1.12	0.69	0.99	3.21	0.20
Ti+4	0.08	0.07	0.07	0.10	0.04
Cr+3	-	0.01	-	0.01	-
Mn+2	0.01	-	-	0.02	-
Fe+2	1.75	0.32	0.30	0.37	0.25
Ni+2	0.01	-	0.03	0.06	-
#Na+1	3.55	3.80	3.72	3.13	3.63
#Mg+2	0.32	0.04	0.05	0.02	0.02
#Al+3	4.01	4.11	4.11	4.35	3.54
#Si+4	11.58	11.79	11.78	11.42	12.37
#K+1	0.16	0.03	0.02	0.04	0.02
#Ca+2	0.29	0.09	0.27	0.88	0.05
#Ti+4	0.02	0.02	0.01	0.02	0.01
#Cr+3	-	0.00	-	0.00	-
#Mn+2	0.00	-	-	0.00	-
#Fe+2	0.33	0.06	0.06	0.07	0.05
#Ni+2	0.00	-	0.01	0.01	-
#Total	20.25	20.05	20.02	19.96	19.68
#O-2	32.00	32.00	32.00	32.00	32.00
alk	4.00	4.02	4.01	4.05	3.70
An	0.07	0.05	0.07	0.22	0.01
Or	0.04	0.01	0.01	0.01	0.01
Ab	.89	0.95	0.93	0.77	0.98

Appendix IV (continued)

sample	1108-2-1L	1108-2-6L	1108-2-7L	1108-2-9L	1108-2-4u
Na+1	8.21	7.00	5.60	2.15	8.80
Mg+2	0.01	0.01	-	0.01	0.07
Al+3	9.68	7.34	6.22	3.54	9.55
Si+4	29.59	37.61	36.46	42.09	29.96
K+1	0.07	0.07	0.03	0.04	0.08
Ca+2	0.19	0.07	0.06	0.11	0.11
Ti+4	0.08	0.10	0.05	0.17	0.03
Cr+3	-	-	0.02	0.01	0.02
Mn+2	0.14	0.02	0.02	0.03	-
Fe+2	-	0.09	0.06	0.10	0.08
Ni+2	-	0.03	0.04	0.05	0.04
#Na+1	4.03	3.00	2.54	0.92	4.28
#Mg+2	0.01	0.00	-	0.00	0.03
#Al+3	4.05	2.68	2.40	1.29	3.96
#Si+4	11.88	13.19	13.53	14.73	11.90
#K+1	0.02	0.02	0.01	0.01	0.02
#Ca+2	0.05	0.02	0.02	0.03	0.03
#Ti+4	0.02	0.02	0.01	0.03	0.01
#Cr+3	-	-	0.00	0.00	0.00
#Mn+2	0.01	0.00	0.00	0.01	-
#Fe+2	0.03	0.02	0.01	0.02	0.02
#Ni+2	-	0.01	0.01	0.01	0.01
#Total	20.10	18.05	18.53	17.05	20.96
#O-2	32.00	32.00	32.00	32.00	32.00
alk	4.11	3.03	2.56	0.96	4.34
An	0.01	0.01	0.01	0.03	0.01
Or	0.01	0.01	0.00	0.01	0.01
Ab	0.98	0.99	0.99	0.96	0.99

Plagioclase in contact with amphibole is highlighted in bold.

Ab = X_{Ab} = #Na+1 / #Na+1 + #Ca+2 + #K+1

Appendix V: SEM semi-quantitative amphibole analyses. Distinctive edenite characteristics highlighted in bold type.

Sample #	comments	Na2O	MgO	Al2O3	K2O	CaO	TiO2	Cr2O3	MnO	FeO	SiO2	name
3107-9-1	**bladed, light**	**2.34**	10.38	**12.73**	0.28	12.80	0.60	0.61	0.25	15.90	**44.14**	eden
-2	**bladed, light**	**2.26**	9.81	**13.93**	0.34	12.90	0.60	0.63	0.15	16.89	**42.57**	eden
-3	**fibrous, dark**	1.53	13.64	6.32	0.25	13.64	0.15	0.46	0.08	12.47	51.35	trem
-4	**fibrous, dark**	1.11	14.79	3.51	0.14	14.17	0.16	0.28	0.15	10.67	54.85	trem
-5	**light area of dark grain(3,4)**	**1.93**	11.55	**10.08**	0.30	13.28	0.37	0.62	0.08	15.23	**46.66**	eden
-6	**bladed, light**	1.76	12.68	8.82	0.23	12.90	0.43	0.65	0.00	14.27	48.21	hbl
-7	**fibrous, dark**	1.10	14.69	2.99	0.14	14.11	0.01	0.41	0.17	11.11	55.13	trem
-8	**bladed, light**	**2.52**	9.84	**13.98**	0.24	12.79	0.64	0.63	0.07	16.82	**42.49**	eden
-9a	**rim**	**1.56**	8.95	**10.18**	0.32	15.40	0.75		0.37	20.82	**41.35**	eden
-9b	core	0.86	12.18	3.00	0.15	16.69	0.30		0.27	14.88	51.55	trem
-10a	rim	1.72	9.00	10.69	0.27	15.81	0.73		0.30	20.44	41.11	eden
-10b	core	1.64	8.61	10.35	0.38	15.56	0.73		0.60	22.03	40.10	eden
-11a	**rim**	**1.73**	8.60	**9.60**	0.34	16.51	0.95		0.46	21.69	**40.15**	eden
-11b	core	0.76	10.15	3.77	0.27	17.50	0.20		0.57	19.81	46.80	trem
-12	**bladed, light**	**1.99**	9.77	**13.10**	0.17	13.62	0.40	0.45	0.10	17.65	**42.76**	eden
-13	**darker**	1.66	11.95	7.98	0.21	14.06	0.25	0.25	0.03	14.84	48.61	hbl
-14	**light**	**2.17**	8.87	**13.53**	0.32	13.28	0.65	0.42	0.14	19.60	**41.05**	eden

continued...

Appendix V

sample #	comments	Na2O	MgO	Al2O3	K2O	CaO	TiO2	Cr2O3	MnO	FeO	SiO2	name
0608-1-1a	rim	1.44	5.88	12.95	0.50	12.95	0.29		0.24	24.90	40.85	eden
-1b	core	1.11	8.40	7.12	0.20	13.35	0.11		0.30	22.71	46.58	hbl
0308-3-1a	rim	0.68	15.00	1.86	0.02	14.47	0.00		0.21	11.11	57.34	trem
-1b	core	0.72	14.39	1.29	0.06	13.68	0.02		0.04	12.45	57.34	trem
-2a	rim	2.09	13.34	8.75	0.16	13.26	0.20		0.16	12.58	49.48	hbl
-2b	core	1.79	13.28	8.53	0.22	13.67	0.25		0.21	13.33	48.69	hbl
-3a	rim	2.69	11.89	11.91	0.15	12.79	0.48		0.16	14.16	45.81	eden
-3b	core	2.34	13.09	10.24	0.16	13.16	0.32		0.16	12.55	47.82	eden
-4a	rim	1.98	16.29	5.49	0.05	10.74	0.12		0.04	12.77	52.42	hbl
-4b	core	1.98	14.24	7.01	0.07	13.54	0.25		0.20	11.21	51.42	hbl
0508-1-1a	rim	2.24	10.96	15.14	0.15	12.73	0.77		0.08	14.35	43.57	eden
-1b	core	2.13	9.85	14.20	0.20	12.78	0.72		0.06	17.44	42.59	eden
-2a	rim	2.37	11.27	12.33	0.10	13.48	0.31		0.04	12.03	47.90	eden
-2b	core	2.07	11.23	14.62	0.24	13.57	0.70		0.19	13.20	44.13	eden
-3	light, bladed	2.04	9.94	13.63	0.25	13.71	0.56	0.42	0.23	16.99	42.20	eden
-4	light, bladed	1.93	10.78	11.96	0.21	12.25	0.43	0.24	0.21	17.72	44.20	eden
-5	light, bladed	2.20	10.14	14.73	0.14	14.11	0.68	0.24	0.00	14.76	42.84	eden
	continued...											

sample #	comments	Na2O	MgO	Al2O3	K2O	CaO	TiO2	Cr2O3	MnO	FeO	SiO2	name
0408-4-1a	rim	1.97	9.57	12.96	0.22	12.48	0.54		0.07	17.13	45.87	eden
-1b	core	1.36	11.58	6.48	0.10	12.93	0.09		0.08	16.42	50.85	hbl
-2a	rim	1.42	13.00	4.35	0.01	12.90	0.00		0.16	13.18	54.80	trem
-2b	core	0.96	13.40	2.78	0.00	13.70	0.02		0.17	13.72	55.09	trem
-3a	rim	1.23	13.37	5.31	0.19	13.52	0.01		0.02	13.16	53.19	trem
3b	core	0.87	12.00	2.54	0.04	13.31	0.00		0.18	17.11	53.93	trem
-4a	light	2.09	9.14	13.14	0.26	13.38	0.68	0.17	0.04	17.96	43.11	eden
-4b	darker	0.71	12.99	3.35	0.16	14.15	0.07	0.00	0.05	14.83	53.52	trem

Appendix V

Geological Map of the Noggin Cove Formation and surrounding units

Dennis Johnston

MSc Thesis

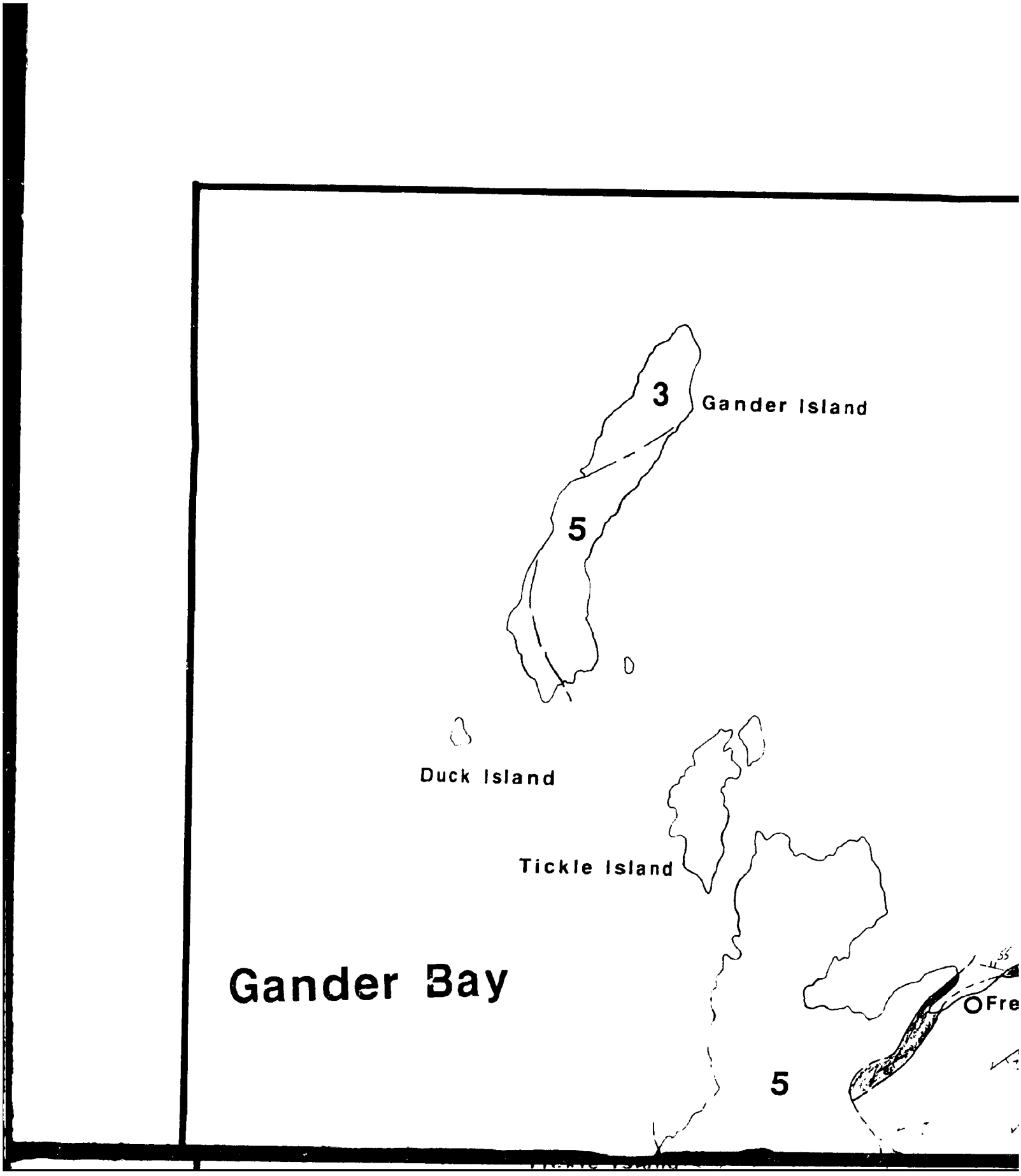
3
Gander Island
5
Duck Island
Tickle Island
Gander Bay
5

Hamilton S


Noggin Cove Islets
3

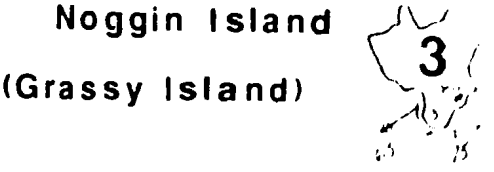
Noggin Island
(Grassy Island)
3

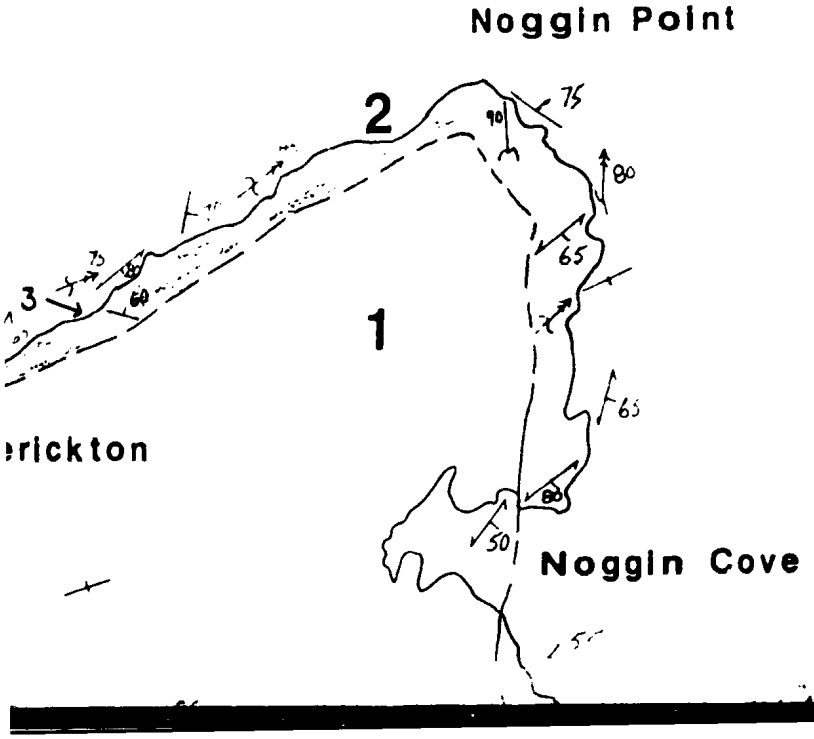
Noggin Point
2
1
3
Noggin Cove
erickton

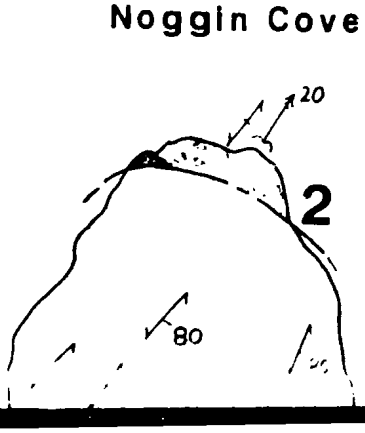
Noggin Cove Head
2

Hamilton Sound

Noggin Island

(Grassy Island)

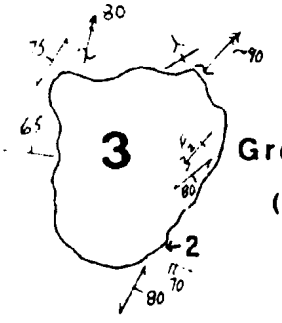

Green Island

(Woody Island)

White Island

Cove Head

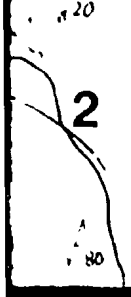

Teakettle Point

Rocky Bay

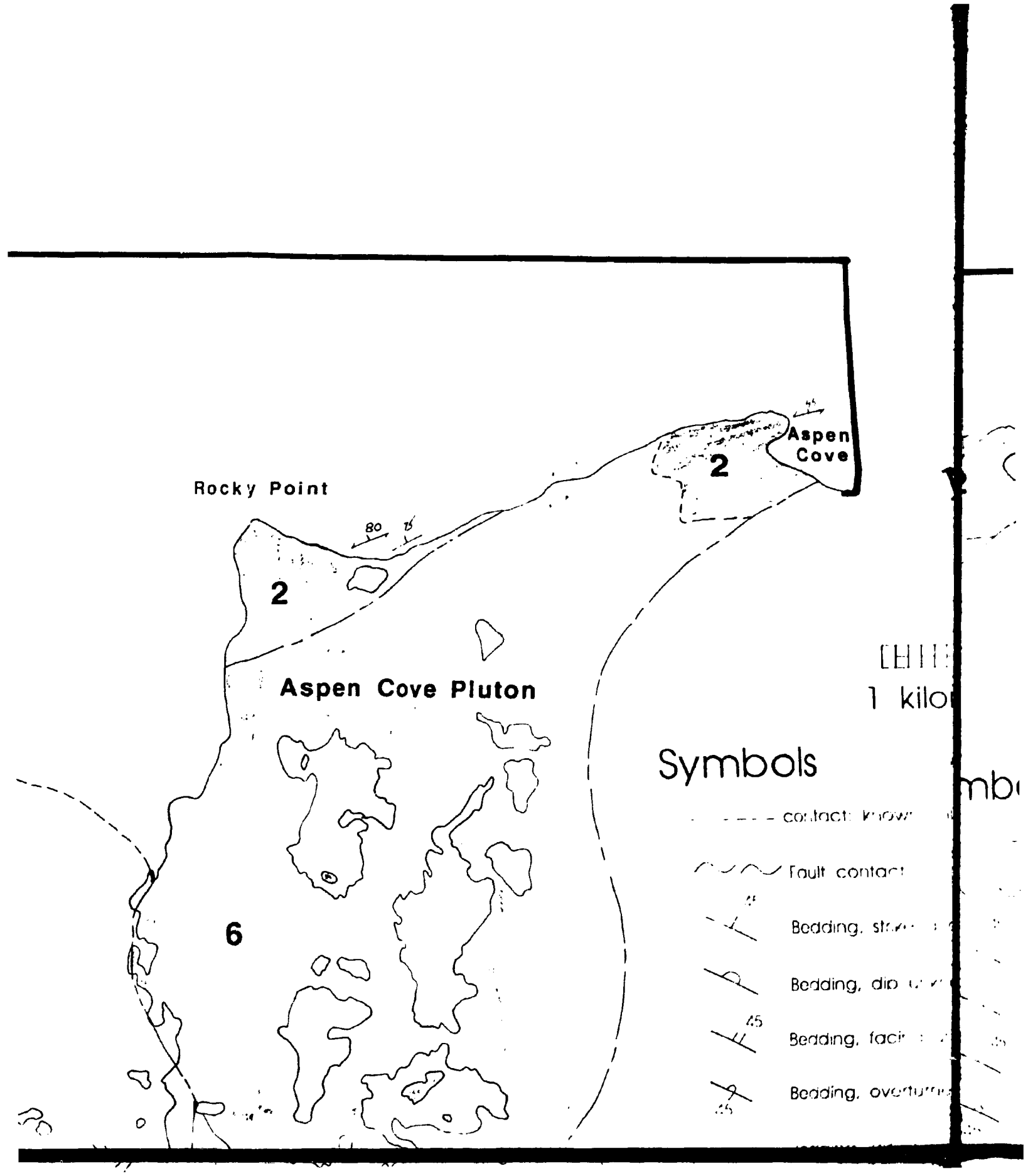
Aspen Cove
2
Rocky Point
80
2
Aspen Cove Pluton
6
Symbols
Fault contact
45
45

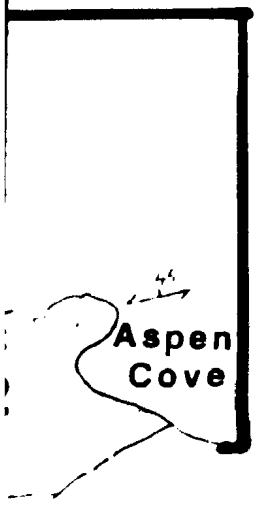

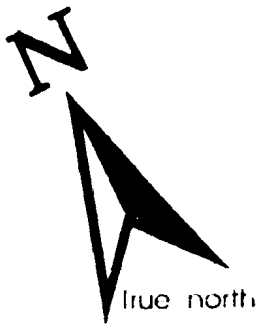

1 kilometre

nbols

- contact: known, in... ed

Fault contact

Bedding, strike and dip

Bedding, dip unknown

Bedding, facing unknown

Bedding, overturned

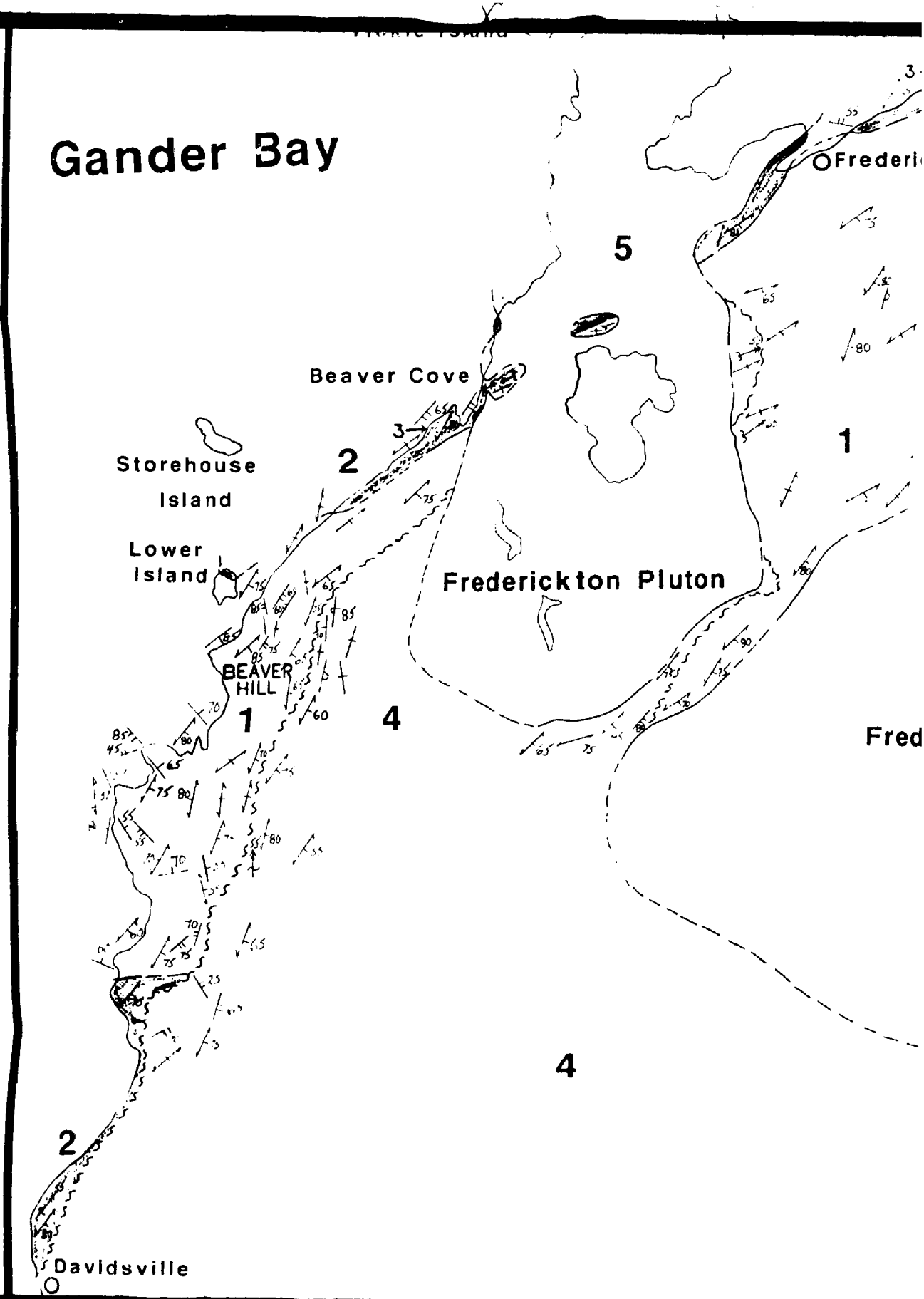
Gander Bay
Beaver Cove
Storehouse
Island
Lower
Island
BEAVER
HILL
Frederickton Pluton
Davidsville
1
2
3
4
5

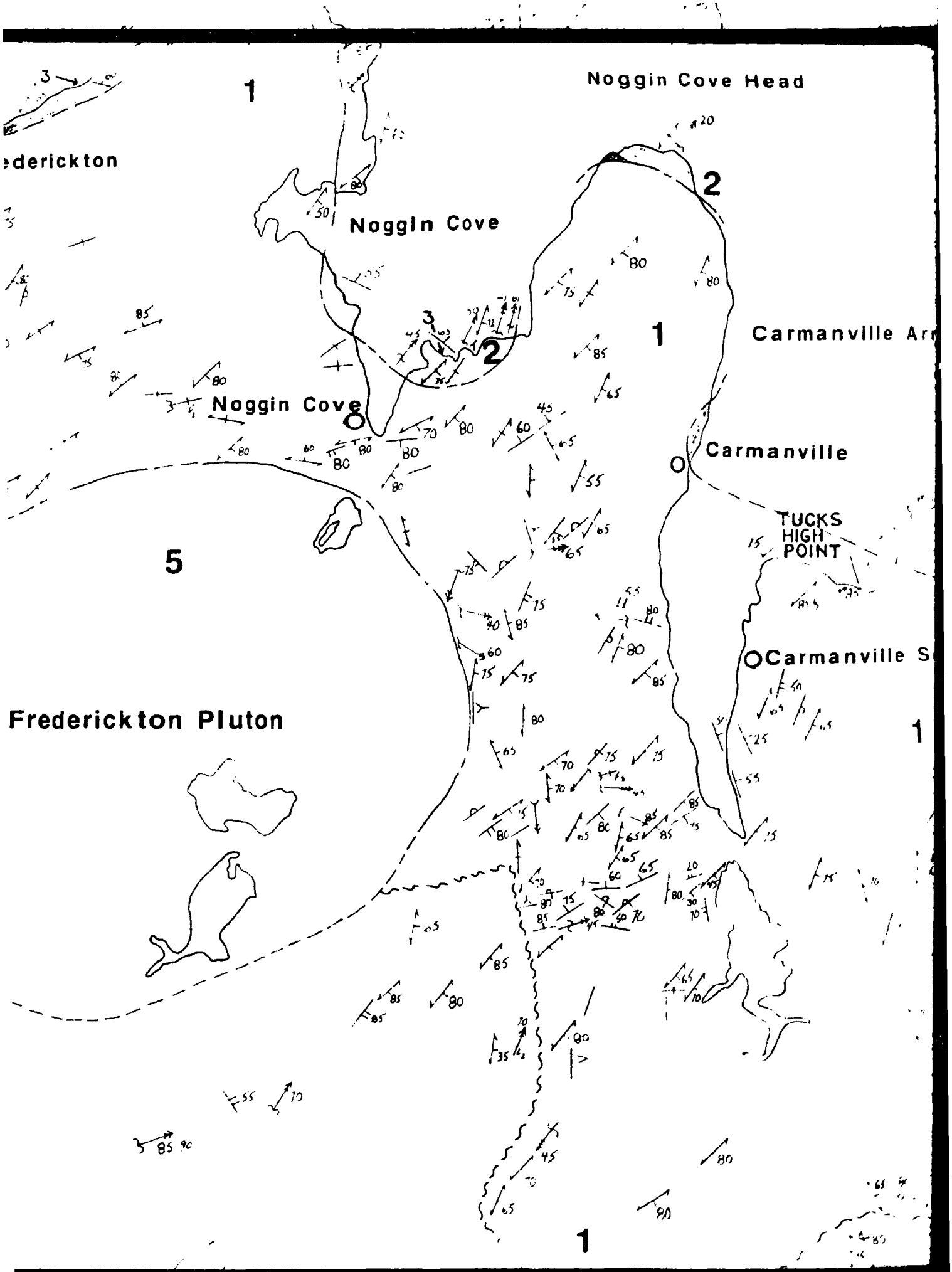
Noggin Cove Head
ederickton
Noggin Cove
Noggin Cove
Carmanville
Carmanville Ar
TUCKS
HIGH
POINT
Carmanville S
Fredericton Pluton
1
2
3
5

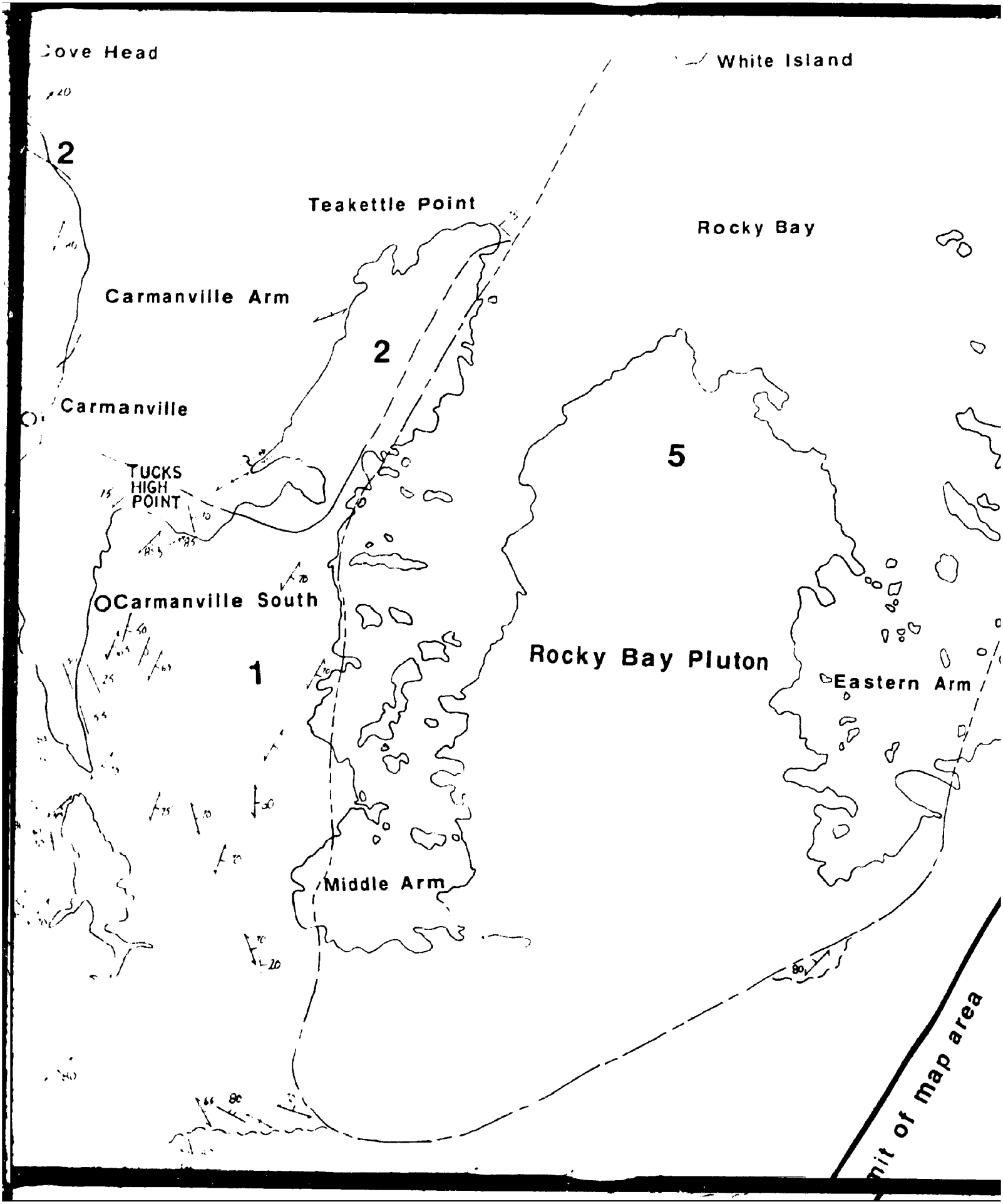
Cove Head
White Island
2
Teakettle Point
Rocky Bay
Carmanville Arm
2
Carmanville
5
TUCKS
HIGH
POINT
Carmanville South
1
Rocky Bay Pluton
Eastern Arm
Middle Arm
nit of map area

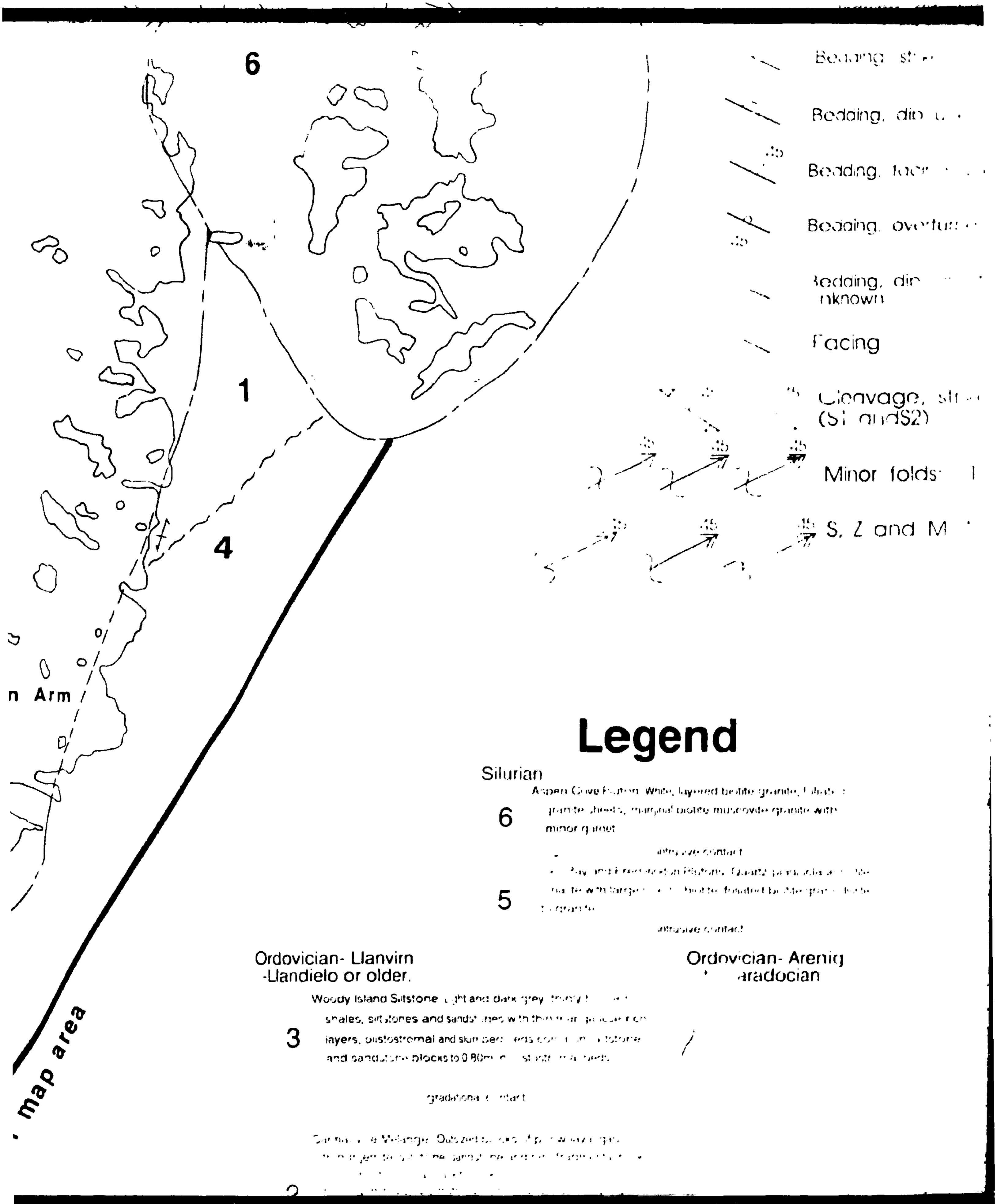

6
1
4
Arm
map area
Bedding,
Bedding,
Bedding,
Facing
Minor folds
Legend
Silurian
Aspen Cove Pluton. White, layered biotite granite,
6
minor garnet
intrusive contact
5
intrusive contact
Ordovician- Llanvirn
-Llandielo or older.
Woody Island Siltstone
shales, siltstones and sandstones
3
gradational contact
Ordovician- Arenig

Bedding, strike and dip known

Bedding, dip unknown

Bedding, facing unknown

Bedding, overturned

Bedding, dip direction unknown

Facing

Cleavage, strike and dip (S1 and S2)

Minor folds: F1, F2, F3

S, Z and M/W folds (eg. F2)

Arenig
ocian

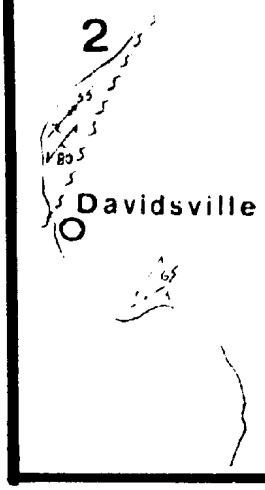

Geological Map of the

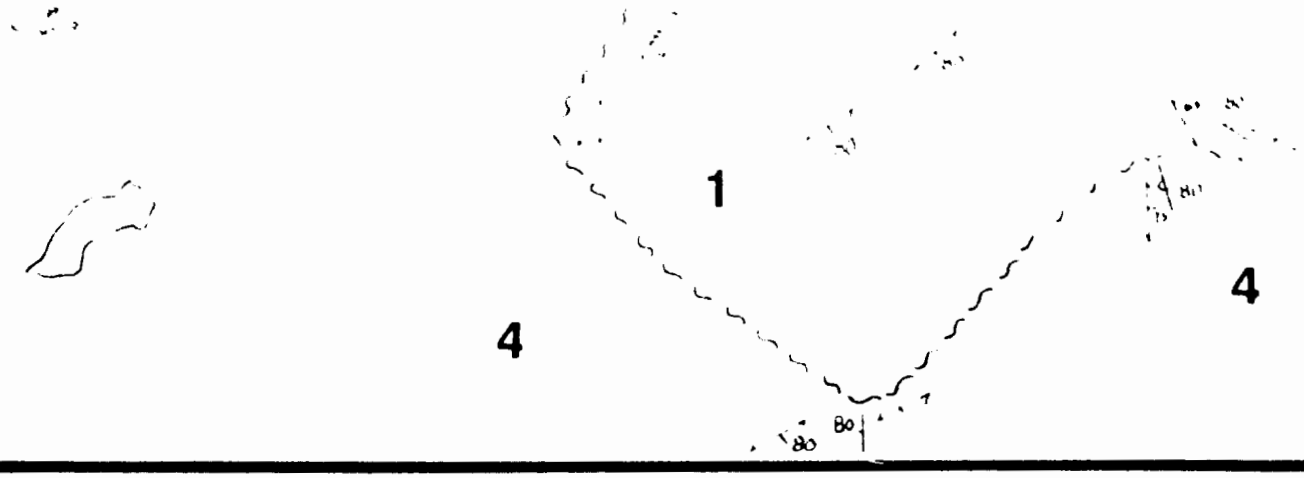

the Noggin Cove Formation and surrou

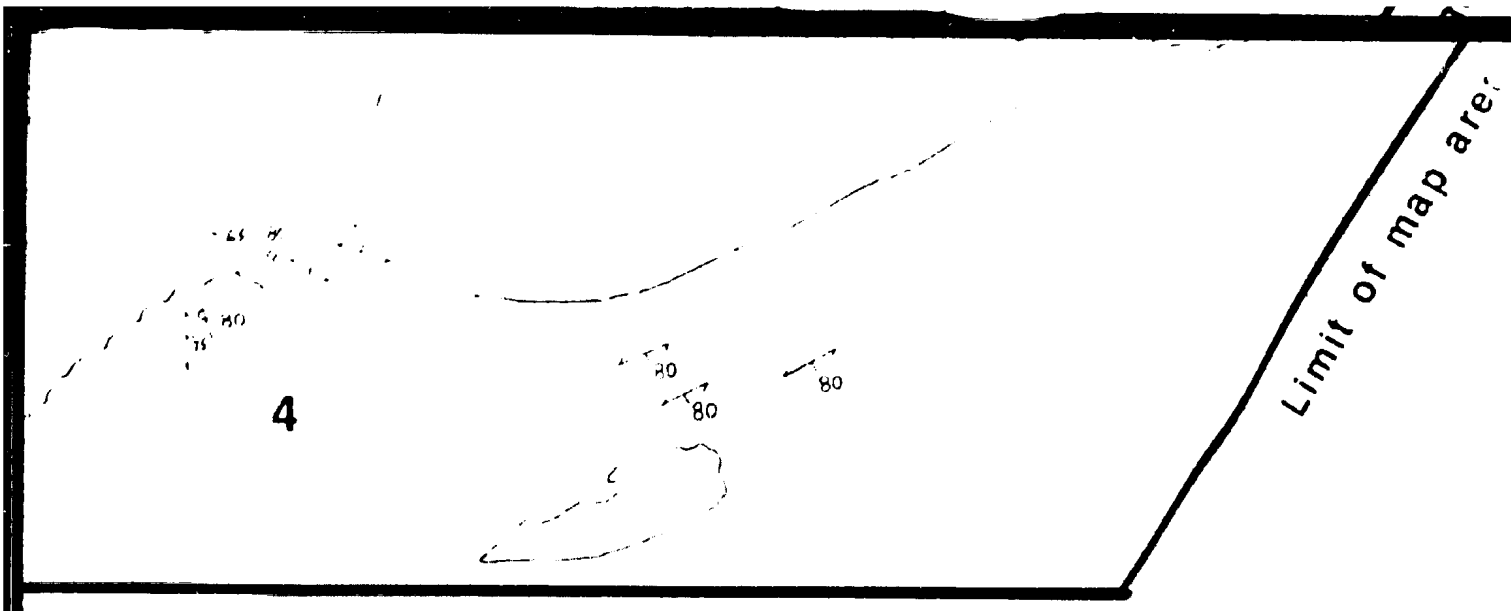

nd surrounding units

3

2

1

4

Geological Map of the Noggin Cove Formation and surrounding units

Dennis Johnston

MSc Thesis